Formation of Ovarian Follicular Fluid

Thesis submitted for the degree Doctor of Philosophy

Hannah Clarke BSc (Hons)

Department of Obstetrics and Gynaecology, School of Medicine,

The University of Adelaide

Adelaide

South Australia, Australia

June 2005

Dedication

In Memory of my Grandmother Margaret Crowley-Smith

(1916 – 2005)

Acknowledgements

I would like to extend my deepest gratitude to all who have contributed to the production of this thesis. It is your support, encouragement and friendship that have enabled me to fulfil one of the most rewarding and enjoyable experiences of my life.

To my supervisors Assoc. Prof. Raymond Rodgers (The University of Adelaide), Dr Sharon Byers (The Women and Children's Hospital Adelaide) and Dr Chris Hardy (CSIRO, Division of Sustainable Ecosystems), I gratefully acknowledge the opportunity you have given me and for your guidance, intellectual input and motivation throughout the course of this doctorate degree. I look forward to your continued support throughout my scientific career.

To the Department of Obstetrics and Gynaecology at The University of Adelaide, the Department of Pathophysiology, The Women and Children's Hospital Adelaide and the National Health and Medical Research Council (NHMRC) and the Pest Animal Control Co-operative research Centre (PACRC), thank-you for providing me with the opportunity to undertake this doctorate degree and for the financial support.

To my numerous laboratory colleagues: Karla Hutt, Sandra Beaton, Nigel French, Helen Irving-Rodgers, Lyn Harland, Stephanie Morris, Malgosia Krupa I am very grateful for the assistance you have provided and for your moral support and friendship.

Special thanks are extended to those who helped me through the long periods away from home Helen, Kathy, Damien, Esther, Margaret, Frances, Lenny and Graham.

To my parents and family, thank-you for your love and for believing in me. Finally to my husband Zaid, without your love and understanding none of this would have been possible. I am forever in your debt.

Table of Contents

List of Tables

List of Figures

List of Commonly used Abbreviations

The abbreviations used are:

PG	Proteoglycan
GAG	Glycosaminoglycan
ITI	Inter-alpha trypsin inhibitor
HA	Hyaluronan
HAS	Hyaluronan synthase
CS	Chondroitin sulphate
DS	Dermatan sulphate
KS	Keratan sulphate
HS	Heparan sulphate
MW	Molecular weight
PAGE	Polyacrylamide gel electrophoresis
ELISA	Enzyme-Linked Immunosorbent Assays
HABP	Hyaluronic acid binding protein
DEPC	Diethylpyrocarbonate
ECM	Extracellular matrix
PCR	Polymerase chain reaction

Abstract

The formation of a fluid filled antrum is a key feature of folliculogenesis. The oocyte is expelled in the fluid in the event of ovulation, making follicular fluid necessary for unassisted reproduction. The mechanism(s) by which follicular fluid is formed is not understood. The studies described in this thesis were the basis of a project designed to investigate the hypothesis that an osmotic gradient exists between follicular fluid and serum. This osmotic gradient drives the recruitment of fluid from the vascularised theca layer surrounding the follicle. The aim of this study was to identify potential osmotically active molecules within follicular fluid of bovine follicles and advance existing data in this area.

The osmotic potential created by follicular fluid changes during folliculogenesis and that the constitution of the fluid was subtly different between healthy and atretic follicles. By specific enzyme digestion of chondroitin sulphate, dermatan sulphate, heparan sulphate, keratan sulphate and hyaluronan glycosaminoglycan chains, proteins and collagen the classes of molecule responsible for the potential were distinguished.

Using a combined physical, immunological and molecular approach hyaluronan, and the chondroitin sulphate proteoglycans versican and inter-alpha trypsin inhibitor (ITI) were identified as potential contributors to the colloid osmotic pressure of the fluid and that of these hyaluronan was the most osmotically active. Both hyaluronan and versican exist in high molecular weight forms and could contribute to colloid osmotic pressure as discrete molecules. However, ITI may contribute via its potential to form very large molecular weight aggregates with hyaluronan and versican. It is proposed that a fluid matrix consisting of these molecules provides versatility of the fluid osmotic potential, in addition to the variations in permeability of the follicular basal lamina and vasculature, and hence the follicles ability to recruit fluid in to the antrum from the follicles vascular surrounds.

To examine the hypothesis further three specific enzymes synthesise hyaluronan, hyaluronan synthases 1, 2 and 3 (HAS 1, HAS 2 and HAS 3) were made. RT PCR, Northern analysis and in situ hybridisation identified which cells were expressing these enzymes in the follicle during devlopment. Expression of HAS 1 and HAS 3 could not be correlated with antrum expansion but may contribute in a secondary manner to fluid osmotic potential. Expression of HAS 2 by the mural granulosa cells could be temporally linked to the visualisation of a follicular antrum and hence could be responsible in part for antrum formation. The regulation of transcription of HAS 2 is probably tightly controlled by differential signalling or receptor activity of any number of growth factors and gonadotrophins and that the turnover of hyaluronan in the fluid at any time is tempered by

differential expression of HAS enzymes and the hyaluronidases responsible for its degradation.

Macromolecules have been identified in follicular fluid, which have an osmotic effect as hyaluronan and the chondroitin sulphate proteoglycans versican and inter-alpha trypsin inhibitor. Hyaluronan was the most osmotically active of these molecules and its synthesis by the HAS 2 enzyme could be correlated with the timing of antrum formation.

Declaration

This work contains no material, which has been accepted for the award of any other degree or diploma in any university or other tertiary institution and, to the best of my knowledge and belief, contains no material previously published or written by another person, except where due reference has been made in the text.

I give my consent to this copy of my thesis, when deposited in the University Library, being available for loan and photocopying

(Hannah Clarke)

Chapter 1 Literature Review

1.1. Introduction

Survival of a species relies on the replacement of individuals. In mammals successful propagation is achieved by sexual reproduction, whereby a female gamete (oocyte) and a male gamete (sperm) fuse to form a genetically new individual ensuring propagation and increased rigor of the species by genetic recombination. General characteristics of cyclic reproductive activity, seasonality, and triggering of ovulation differ widely among mammals however; common mechanisms underlie ovarian function and these will be outlined in this review.

Female gametes originate from the ovary and are contained within follicles that are in turn situated within the cortical stroma of the ovary (Mossman & Duke, 1973). The mammalian ovarian follicle changes dynamically as it nurtures the growth of its enclosed oocyte. Each day in adult life, a number of primordial follicles are activated, and the oocyte commences growing and the granulosa cells begin to divide (pre-antral stage) (Hirshfield, 1997). As the follicle grows the granulosa cells divide and the number of layers of granulosa cells (termed the membrana granulosa) around the oocyte increases, with concomitant expansion of the basal lamina, which separates the follicle from the stroma. Later in development a fluid-filled cavity or antrum develops at the centre of the follicle (antral stage). At this stage the layers of granulosa cells, in turn surrounded by the basal lamina, surround the antrum. The oocyte is still enclosed by specialised granulosa cells (corona and cumulus cells) and lies adjacent to the antrum to one side of the follicle as the antrum expands. Specialised stromal layers - theca interna and externa develop outside of the basal lamina. These layers are vascularised, unlike the membrana granulosa surrounding the follicular antrum. In cattle only follicles that develop a large antrum (>10 mm) ovulate, by release of the cumulus-oocyte complex in to the follicular fluid and then expulsion of both through the ruptured wall of the follicle to the outside of the ovary. Rapid expansion of the follicular antrum can signal development of a follicle to ovulatory stage and in both veterinary and human medicine follicle growth is monitored by ultrasonography and is representative of the accumulation of follicular fluid (Kemeter & Feichtinger, 1991, Kerin *et al.*, 1981). Despite its importance, there is a dearth of literature on the formation of the follicular antrum and follicular fluid.

This review will focus on the origin of the primordial germ cell, the formation of the oocyte enclosed within the primordial follicle and the maturation processes involved in forming a pre-ovulatory follicle, its ovulation and the formation of the endocrine support gland the corpus luteum, with particular reference to the cow. Within this scope to review of

the structural changes occurring within the follicle and the hormones and growth factors involved in the process of recruitment and selection of the dominant follicle, which will ensure this maturation process. In addition it will review the literature pertaining to antrum formation, and discuss the forces that may drive fluid accumulation and the molecules, which may play a role in this process.

1.2. The Mammalian Ovary

Two primary functions of the ovary are production of oocytes and their support to subsequent ovulation and the production of secreted hormones, which maintain pregnancy and the female form and characteristics (Erickson & Shimasaki, 2001). Structurally, the mammalian ovary is a small ovoid tissue covered by a single layer of cuboidal epithelium termed the germinal epithelium. The ovary is attached to the broad ligament by peritoneal tissue called the mesovarium. The mesovarium supplies a means by which the ovary is sourced with blood and nutrients through the blood vessels, which enter the ovary at the hilus (Erickson, 1978).

Beneath the germinal epithelium the ovary is comprised of fibrous connective tissue, which forms the tunica albuginea (Lunenfeld *et al.*, 1976). Beneath this lies the core of the ovary, which is divided in to the outer cortex, comprised of a very cellular connective tissue stroma made up of laminins, collagens elastins and fibroblasts, where the follicles are situated and the inner medulla composed of loose connective tissue containing blood vessels and nerves (Bjersing *et al.*, 1981). A diagram depicting the structure of the ovary and its enclosed follicles can be seen in (Figure 1)

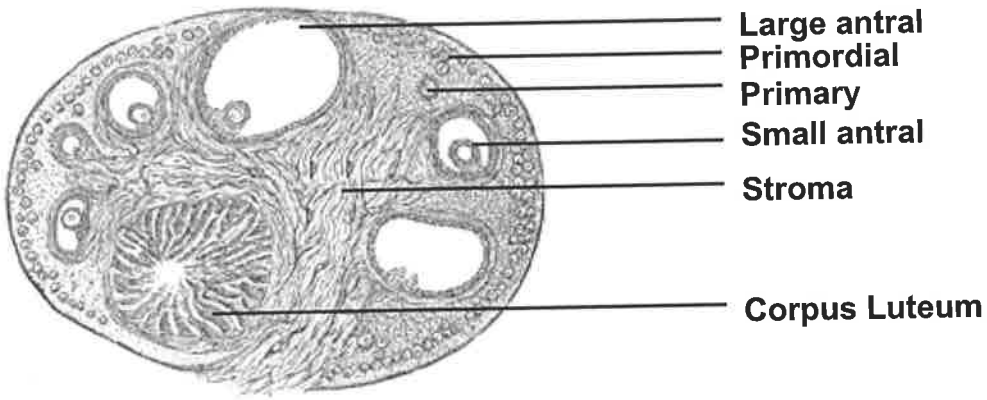

Mammalian ovary

Figure 1 Diagram of the human ovary derived from The Anatomy of the Human Body by Henry Gray 20th Ed.

1.3. The Ovarian Follicle

1.3.1. Oogenesis

Oogenesis is the term used to describe the development and differentiation of the female germ cell from the migrating primordial germ cell to the fertilisable haploid egg (Russe, 1983). The time taken to complete this process is species specific. Russe defined 6 stages of oogenesis 1; the primordial germ cell period, 2; the oogonial period, 3; meiotic prophase, 4; isolation of the oocyte from the germ cell cord, 5; follicle activation, 6, tertiary follicle and completion of meiosis (Russe, 1983).

1.3.1.1. The Primordial Germ Cell (PGC) period

The store of primordial follicles used for folliculogenesis is formed during oogenesis. The size of the store is dependent upon the degree of oogonia multiplication, the time of meiosis and the extent of the loss of germ cells, for review see (Gosden R. & Bownes, 1995). The full compliment of oocytes is derived from the inner cell mass of the developing blastocyst. The PGCs are derived from the PGC "store" in the endoderm of the embryonic yolk sac. Once formed, they migrate to the gonadal ridge where they multiply, for review see (McGee *et al.*, 1998). The PGCs are separated by somatic cells, which surround them, the whole unit surrounded by a basal membrane. It is considered that the somatic cells of the foetal ovary may be precursors of follicular cells (Picton, 2001). The number of accompanying cells is species specific (7-19, Human; 16, sheep; 10, mouse; (Gougeon A., 1996, Lintern-Moore & Moore, 1979, McNatty *et al.*, 1999)). This process is thought to occur six months after birth in Humans (Wagenen & M.E, 1965). The PGC ultrastructure is simple, consisting of one or two nucleoli surrounded by a small amount of cytoplasm. The germ cell includes a few mitochondria, undeveloped Golgi and sparse endoplasmic reticulum. A diagram of primordial cell migration can be seen in (Figure 2)

1.3.1.2. The Oogonial Period

The oogonial period begins when germ cells cease to separate following division and begin to form clusters. In the developing ovary the more mature oogonia are deeply embedded in ovarian tissue. Peripherally located stem cells form the new oogonia (Picton, 2001). Within the oogonial clusters, somatic cells that accompany the clusters are limited in number as they rarely divide.

In ruminants two germ cells with different functions arise from the last divisions of the PGC. One undergoes mitosis and the other remains in interphase, periodically dividing and giving rise to new generations of oocytes. As a result not all germ cells are at the same stage

of development. Structurally these cells have an increased number of organelles compared to their predecessors (cow (Russe, 1983)).

1.3.1.3. Meiotic Prophase and Isolation of the Oocyte from the Germ Cell Cord

PGCs in the innermost layers of the germ cell cord begin meiosis differentiating in to primary oocytes. This process occurs at week 11-12 in human, (McGee *et al.*, 1998), day 13.5-16.5 in mouse, (Borum, 1961), day 82 in cow, (Russe, 1983), day 40-75 in sheep, (Lundy *et al.*, 1999, McNatty *et al.*, 2000) of gestation. Their numbers reach a maximum of 6-7 million in humans (Gosden R. G., 1987) 6 - 26,000 in mouse, (Pepling & Spradling, 1998, Rowlands *et al.*, 1970) around the twentieth week of gestation.

Meiosis in the primary oocytes persists until near term (McGee *et al.*, 1998) before arresting in diplotene of the first meiotic division. The oocytes remain in this arrested state until puberty; the first meiotic division is then completed at ovulation and the second upon fertilisation. During meiotic prophase the germ cell grows by increases in nuclear and cytoplasmic volumes. Cytoplasmic degeneration and pyknosis result in the loss of many oocytes at this time. A complex extracellular matrix consisting of stroma cells, at various stages of differentiation, surround what is now termed the primordial follicle, located in the outer ovarian cortex where there is little vascular support. As they grow and develop primordial follicles migrate to the vascularised cortico-medullary region of the ovary. Growth initiation is characterised by change in the granulosa cells from a flattened to cuboidal appearance and their proliferation, a pre-requisite for continued oocyte growth, and rapid growth of the oocyte (human; (Gougeon A. & Chainy, 1987)). Oocyte growth is delayed in comparison to granulosa cell proliferation and does not occur until the granulosa cell number reaches 40 – (cow; (Braw-Tal & Yossefi, 1997)), (15 - human, sheep; (Cahill & Mauleon, 1981, Gougeon M. L. & Theze, 1987)), (10 – mouse; (Lintern-Moore & Moore, 1979)).

Those oocytes not enclosed by pre-granulosa cells are lost by apoptosis. It is generally believed that apoptosis is responsible for the loss of germ cells. Both death signals and survival signals exist in the embryonic gonad and it is thought that the apoptopic cascades involving bclz, bax and caspases are responsible for the alteration of the germ cell store via apoptosis for a review see (Driancourt & Thuel, 1998).

By or shortly after birth the mammalian ovary contains its complete supply of oocytes 3-400,000 in humans (Forabosco *et al.*, 1991, Johnson Martin H. & Everitt, 2000) and 150,000 in cows (Bao & Garverick, 1998).

1.3.1.4. Follicle Activation

Oocytes remain in an arrested state until the onset of cyclic recruitment at puberty. It has been reported that the primary follicle is under constant inhibition from systemic and local

factors, and these factors ensure that the follicle remains in the dormant phase (Wandji *et al.*, 1996). However, new data suggests that ovaries possess mitotically active germ cells which, based on rates of oocyte atresia, are needed to continuously replenish the follicle pool (Johnson J. *et al.*, 2004). When the primordial follicle store is established follicular recruitment begins. Recruitment and follicular growth are continuous and end in either an ovulation or degeneration of the follicle and oocyte by atresia (Picton, 2001). Initial recruitment begins after follicle formation when primordial follicles are activated. This occurs during the foetal period in man, cattle and sheep. Recruitment results from an increase in circulatory follicle stimulating hormone (FSH), which rescues a cohort of follicles from the default pathway of atresia (McGee & Hsueh, 2000).

Each day a small number of these follicles become activated and enter the initial growth phase, providing a constant stream of developing follicles (Hirshfield, 1997). The initiation or activation of follicle growth is defined as the transition of the primordial follicle from the quiescent to the growth phase (Braw-Tal, 2002).

Follicles that become activated prior to the resting stage degenerate through lack of somatic cell support. The period between activation and formation of a multicellular layer is slow and varies between species (Picton, 2001). The time taken for primordial to multilayer follicle status to occur in a number of species can be seen in Table 1.

During this period the follicle undergoes many ultra-structural changes supported by somatic cells, some of which will differentiate in to thecal cells and provide steroidogenic support to the follicle (Picton, 2001).

The initiation of follicular growth has been achieved in vitro in several species and this has enabled the study of the regulators of follicle activation. In bovine, primate and rodent follicle initiation appears to be independent of gonadotrophins or other blood-borne factors (Fortune *et al.*, 1999). Oocyte-granulosa cell interactions are important in the early stages of follicle development and the key players in this interaction have been identified as growth differentiation factor 9 (GDF 9) and kit ligand (Hayashi *et al.*, 1999). GDF 9 is a homo-dimeric protein of the transforming growth factor (TGF)/activin family, known to signal via the serine threonine kinase receptor pathway in primordial follicles in the bovine system (Bodensteiner *et al.*, 2000).

The only specific factor that has been linked to activation of primordial follicles is kit ligand or stem cell factor, which is produced by the granulosa cells. Primordial germ cells, oocytes and theca cells express the receptor for kit ligand known as c-kit (Manova *et al.*, 1993, Motro & Bernstein, 1993, Yoshida H. *et al.*, 1997).

Table 1 Characteristics of primordial follicles from different species

Species	Number of Pre-GCs	Follicular diameter (μm)	Oocyte diameter (μm)	*Growth time (days)
Cow	24	≤45	30	> 30
Sheep	15 - 16	41	35	> 25
Human	12 ± 6	35	32	>150
Mouse	10	12	17	10

*Growth time refers to the time taken for growth to occur from a primordial to a multilayer follicle. Data adapted from (a) Braw-Tal and Yosefi (Braw-Tal & Yossefi, 1997), Fair et al (Fair *et al.*, 1997), Telfer et al (Telfer *et al.*, 1988), (van Wezel & Rodgers, 1996), (b) McNatty et al (McNatty *et al.*, 1999), (c) Gougeon (Gougeon A., 1996), (d) Lintern-Moore and Moore (Lintern-Moore & Moore, 1979), Pederson (Pedersen, 1970), Wassarman and Albertini (Wassarman & Alberton, 1994).

1.3.2. Folliculogenesis

In mammals, which follicles will mature to ovulation is determined by a series of processes beginning with recruitment and followed by selection and support of a dominant follicle, the latter stage known as dominance. During folliculogenesis the stroma of the ovary provides external support tissue for the follicles and condenses to accommodate follicular growth. Folliculogenesis varies in duration and the number of follicles that mature and ovulate (1 - >100) is strictly regulated and species specific. Early antral follicles do not require gonadotrophic support and are destined for atresia unless rescued (Johnson Martin H. & Everitt, 2000, Scaramuzzi *et al.*, 1993).

The physical changes seen in the follicle during folliculogenesis are described below.

The first signs of activation of a dormant follicle are rapid growth of the primordial follicular diameter from 20μm to 200-400μm in cows (Driancourt *et al.*, 1985, Fair *et al.*, 1995) with concomitant oocyte growth and maturation and formation of the membrana granulosa, the whole surrounded by the basal lamina. Later, a fluid filled cavity or antrum develops. These two stages of development are termed pre-antral and antral respectively. The basic antral follicular structure is depicted in (Figure 3)

Figure 2 Diagram of Primordial Germ Cell Migration. Diagram adapted from http://sprojects.mmi.mcgill.ca/menstrualcycle/follicular development page.html.

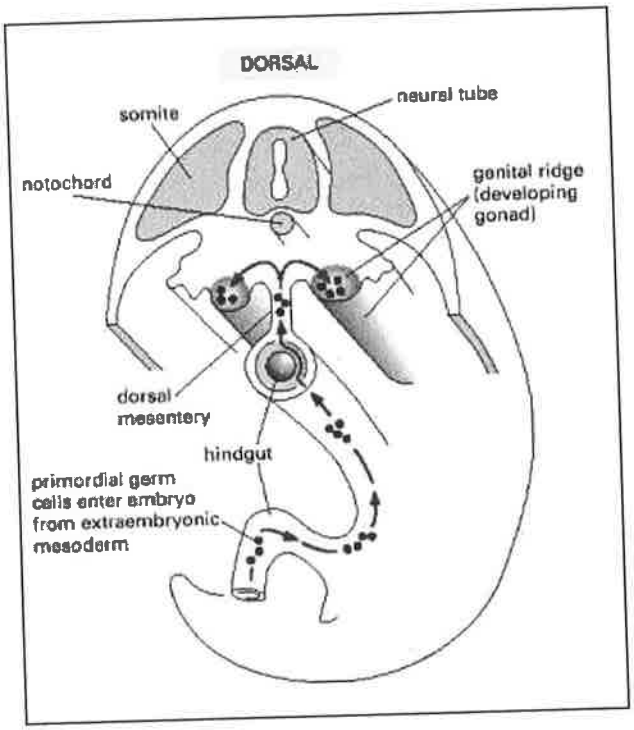

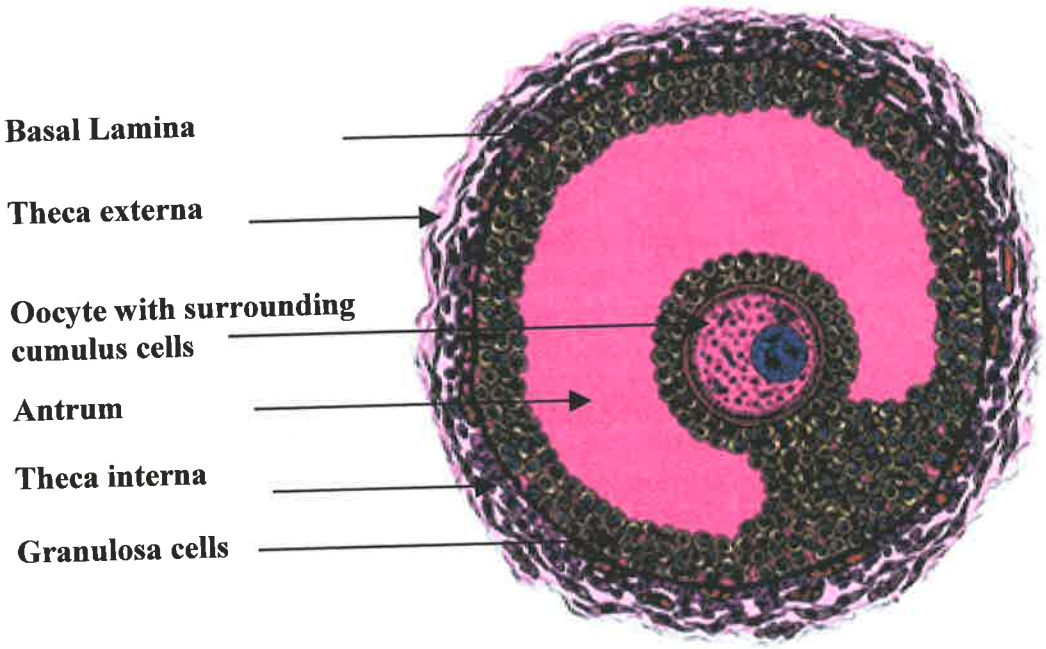

Figure 3 Diagram of an antral ovarian follicle.

Following activation, the follicle passes through the next main stages of development forming 1) primary, 2) pre-antral and 3) antral follicles.

Stages 1-2 are gonadotrophin independent and development is controlled by locally produced growth factors, while stage 3 is gonadotrophin dependent whereby FSH controls growth and development under modulating influences of growth factors. Follicular recruitment, selection and dominance are reviewed in 1.3.4. A diagram of follicular development can be seen in (Figure 4)

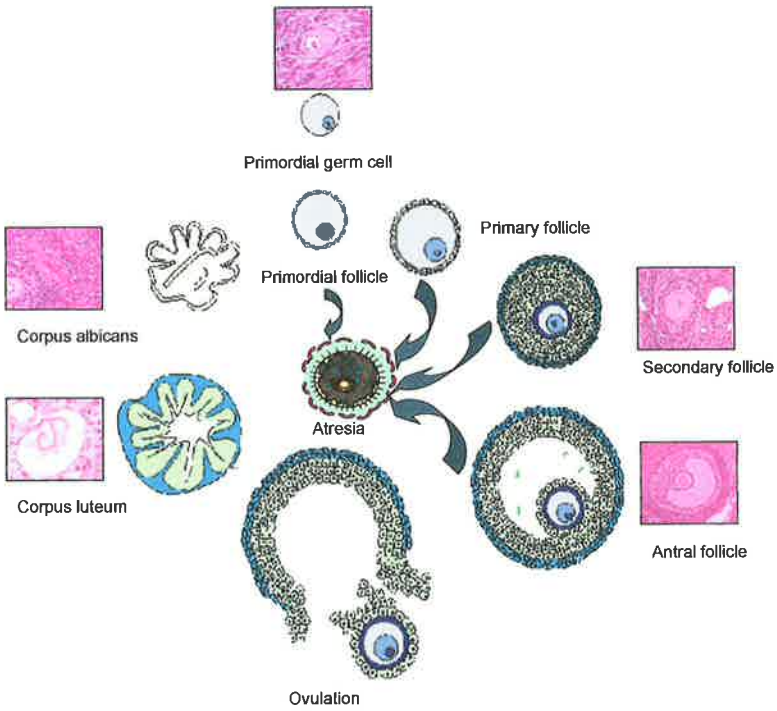

Figure 4 Diagram of Follicle Development derived from http://sprojects.mmi.mcgill/menstrual cycle/follicular development.html

1.3.3. Oocyte Growth and Development

Still in its arrested state until ovulation when the first meiotic division is completed (Johnson Martin H. & Everitt, 2000), the oocyte begins to grow. During the follicle maturation process the oocyte and the follicle undergo certain morphological changes. As soon as granulosa cells become cuboidal they start to express follistatin, RNA and proteins (Braw-Tal, 1994) and evidence suggests this triggers oocyte growth, with rapidly progressing oocytes at the cortico-medullary junction growing earlier than those further away (Hirshfield, 1991).

Ultra-structural analysis of the oocyte showed major morphological changes occurred at this time. The nuclear membrane surrounding the dictyate chromosomes breaks down, the location of the mitochondria changes, the number of organelles increases, and the cytoplasmic and nuclear volumes swell (cow; (Fair *et al.*, 1997), mouse; (Lintern-Moore & Moore, 1979)). The oocyte continues to grow rapidly during early follicular growth and reaches its full size early in the maturation process. In the tertiary follicle the nucleus is activated and the nucleolus changes from a sponge-like to a shell-like form. Rough endoplasmic reticulum also appears and piles up to form annulate lamellae. In the pre-ovulatory follicle the nucleus is vesicular. In cattle and sheep the extrusion of the first polar body occurs after ovulation with only fertilised eggs completing meiosis (Russe, 1983).

As the antrum forms, the follicle expands and the oocyte complex and granulosa cells become increasingly connected via specialised cell junctions, known as gap junctions (Larsen *et al.*, 1996). Gap junctions are transmembrane channels between cells that allow free movement of ions and small molecules. The gap junction network is essential for oocyte growth and maturation, provision of substrates for energy and metabolism, and maintenance of meiotic arrest.

During maturation the oocyte begins to secrete glycoproteins, which condense around it to form the zona pellucida (ZP) (see section 1.3.3.2). In addition 5 growth factors are produced by the oocyte, including GDF-9 (McGrath *et al.*, 1995), bone morphogenetic protein 15 (BMP-15) (Dube *et al.*, 1998, Laitinen *et al.*, 1998), BMP-6 (Lyons *et al.*, 1989), transforming growth factor $\beta 2$ (TGF $\beta 2$) (Schmid *et al.*, 1994) and fibroblast growth factor 8 (FGF-8) (Valve *et al.*, 1997). GDF-9 and BMP-15 are only expressed by the oocyte, which suggests they are obligatory for normal folliculogenesis (Dong J. *et al.*, 1996). In the absence of GDF-9, follicles are also unable to emit a signal to recruit theca cell precursors to surround the follicle (Elvin *et al.*, 1999a). GDF-9 has been shown to stimulate granulosa cell proliferation and BMP-15 to stimulate granulosa cell mitosis (Otsuka *et al.*, 2000). Thus the oocyte has a fundamental role in the physiological mechanisms that control dominant follicles and ovulation. Both GDF-9 and BMP-15 are FSH independent however; they are able to

modify FSH-stimulated granulosa cell differentiation by blocking FSH action and/or FSH receptor expression (Otsuka *et al.*, 2001) suggesting they may actively regulate FSH action during folliculogenesis (Erickson & Shimasaki, 2001).

Oocyte growth is not apparent in antral follicles. However, synthesis of RNA and turnover of proteins continue. In some species it can take over six months before the oocyte is capable of being fertilised (human; (Gougeon A., 1993, Lefevre *et al.*, 1990)).

1.3.3.1. Granulosa cell Proliferation and Formation of the Membrana Granulosa

After initial recruitment, granulosa cells in the primary follicle acquire characteristics of the epithelial cells of secondary follicles. Granulosa cells proliferate from a single cuboidal layer (primary follicle) (Irving-Rodgers & Rodgers, 2000) to form several layers (secondary follicle) around the oocyte. In cattle the number of granulosa cells doubles 21 times (van Wezel & Rodgers, 1996) with 19 doublings of follicle surface area from the primordial to the 18mm antral follicle. As they divide the granulosa cells form layers within the follicle, containing up to 2000-2500 cells in the mature pre-ovulatory follicle (rat; (Hirshfield, 1997)) (50,000 –mouse; (Spears *et al.*, 1998)). These layers form the membrana granulosa of which two distinct subpopulations can be determined:

1. Cells in close proximity to the oocyte, which directly surround the zona pellucida and form the cumulus oophorous
2. Cells closely aligned with the basal lamina that forms the membrana granulosa.

The former attach to the egg via cell processes. In cattle, gap junctions and desmosomes develop at the point of contact (Anderson & Albertini, 1976). In vitro studies have shown that the granulosa cell-oocyte communication pathways are essential to continuing survival of the oocyte with oocyte growth halted if separated from the granulosa cells (Tsafriri *et al.*, 1998). The gap junction protein connexin 37 may be responsible in part for the maintenance of the gap junction and hence the communication pathway. The importance of oocyte-granulosa cell communication (Eppig *et al.*, 1997) is further supported by evidence of oocyte secretions that regulate granulosa cell functions such as granulosa cell division (Vanderhyden *et al.*, 1992), LH receptor formation (Eppig *et al.*, 1998), cumulus oocyte complex expansion (Elvin *et al.*, 1999b) and steroidogenesis (Nekola & Nalbandov, 1971, Vanderhyden & Macdonald, 1998) with only fully-grown oocytes able to undergo meiosis.

Studies of the mitotic indices of granulosa cells indicate that the mitotic activity of the cells closest to where the oocyte attaches to the wall are highest, indicating that not all granulosa cells have the same potential for division. In humans during the first phase of basal follicular growth (mitotic cycles 1-7), the follicle grows slowly and the rate is tightly related

to proliferation of granulosa cells and mainly under the control of paracrine growth factors. In these follicles, FSH may exert an indirect mitogenic effect on granulosa cells by enhancing expression of growth factors or growth factor receptors.

In the second phase (terminal follicular growth – cycle 7 onwards), growth of the follicle is rapid and occurs by fluid accumulation and enlargement of the antrum to form the antral follicle and the granulosa cells begin to express FSH receptor. Studies have demonstrated that FSH signalling is a fundamental part of growth and differentiation of the dominant follicle through its ability to promote follicular fluid accumulation, cell proliferation oestrogen production and LH receptor expression (Fortune, Rivera et al 2001). During the last few cell divisions, granulosa cells become steroidogenic and convert androgens to estrogens by aromatisation they also begin synthesis of hormones and acquire receptors for LH. FSH stimulation of these LH receptors is required to induce ovulation and luteinisation. Luteinising hormone receptor expression is not induced in granulosa cells until the dominant follicle reaches the pre-ovulatory stage. It has been suggested that LH may enter the follicle in the latter stages of development in the follicular fluid and may replace FSH as the principle regulator of cyto-differentiation. Shortly after the ovulatory stimulus the gap junctions of the membrana granulosa are destroyed, the network breaks down and the oocyte becomes activated and resumes meiosis. At the same time the cumulus oocyte complex detaches from the membrana granulosa, a necessary prerequisite before its expulsion from the follicle (Larsen *et al.*, 1996). Following the pre-ovulatory gonadotropin surge, follicular cells begin morphological, endocrinological, and biochemical changes associated with luteinisation. Luteinisation involves the transition of a pre-ovulatory follicle in to a highly vascular corpus luteum capable of secreting large quantities of progesterone but is not in itself dependent on follicular rupture (Smith M. F. *et al.*, 1994).

1.3.3.2. Formation of the Zona Pellucida

The developing oocyte is surrounded by a structure termed the zona pellucida (ZP), which is laid down shortly after the primordial follicle resumes growth. The oocyte produces ZP proteins in the pig (Takagi *et al.*, 1989) however; there is increasing evidence that ZP proteins are expressed by the granulosa cells and oocyte and that all of these may play a role in granulosa cell differentiation and ZP formation (Dunbar *et al.*, 2001). Four different ZP proteins have been described in the pig and bovine systems, all structurally conserved and expressed in a stage-specific fashion (Aviles *et al.*, 2000, Bercegeay *et al.*, 1993, Dunbar *et al.*, 2001, Hedrick & Wardrip, 1987, Kolle *et al.*, 1998, Takagi *et al.*, 1989, Topper *et al.*, 1997) and three in the mouse (Bleil & Wassarman, 1980). Marked differences exist in size and structure of the different ZP proteins and the degree of conservation varies between

proteins. Each ZP has a different glycosylation pattern and it is understood such differences in protein structure and glycosylation status may explain the variation seen in its biochemical, physiological and immunochemical properties.

1.3.3.3. Basal Lamina Synthesis

Basal lamina synthesis occurs in order to accommodate the increasing follicle expansion. The basal lamina of the follicle is similar to basal laminae of other tissues with its major components being type IV collagen, laminin, fibronectin and heparan sulphate proteoglycans (HS proteoglycans) (Luck & Zhao, 1993, Luck *et al.*, 1995). Many of the membrane components are synthesised from within the theca with some contribution from the granulosa cells in rat (Bagavandoss *et al.*, 1983) and cow: (Rodgers H. F. *et al.*, 1995a). During the course of follicular growth, the basement membrane increases over 400 fold in area in the cow and this occurs in a manner that maintains its integrity throughout the expansion process (Dr Raymond Rodgers, personal communication). The basal lamina of primordial and growing follicles completely envelops the follicle and undergoes considerable modification during ovulation and atresia. In pre-ovulatory follicles the basal lamina is thinner and discontinuous, in contrast to its thickened and ruptured appearance in atretic follicles. Fibronectin has been localised in the inner granulosa cells of small and medium-sized growing follicles, and as a broad, irregular layer around the cavity of degenerated follicles. Each stage of follicular growth and involution is associated with precise patterns of distribution of laminin, type IV collagen and fibronectin. It is likely that these proteins may play a role in the local control of ovarian follicular dynamics (Bortolussi *et al.*, 1989).

1.3.3.4. Development of the Theca

The theca interna and theca externa form the outer layers of the follicle. In the mouse the theca is first recognisable when there are 2 - 3 layers of granulosa cells (Peters, 1969). The theca differentiates from the stroma of the ovary and surrounds the follicular basal lamina, which separates it from the granulosa cells. The theca cells proliferate as the follicle grows. The theca interna is vascularised and forms a reticular network of fibroblasts containing steroidogenic cells with which produce androstenedione, which is converted to oestradiol by granulosa cells. Examination of the theca interna by electron microscopy shows the steroidogenic thecal cells are rich in smooth endoplasmic reticulum, mitochondria with tubular cristae. IThe proportions and distribution of steroidogenic cells changes during maturation (Clark *et al.*, 2004).

Examination of the theca externa reveals it consists of myofibroblasts, differentiated from the stroma, interspersed with cells with cytoplasmic filaments and dense staining bodies

characteristic of smooth muscle cells (O'Shea, 1981). It consists of connective tissue and stromal cells with vessels forming a plexus of flattened cells. LH stimulates steroidogenesis in theca cells and in a mature follicle these are major sources of androgens and angiogenic factors, which stimulate proliferation and migration of endothelial cells (Makris *et al.*, 1984).

The interaction of granulosa and theca cells may have a role in early follicle development since androgen treatment of cultured mouse pre-antral follicular cells leads to follicle growth. Secreted proteins from rat pre-antral follicles increase growth and differentiation of theca cells before expression of their LH receptors (Gelety & Magoffin, 1997) while co-culture of granulosa and theca cells resulted in an increase in steroidogenesis in both cell types (Kotsuji *et al.*, 1994).

1.3.3.5. Development of the Follicular Capillary Network

Small follicles have no capillary network and rely on vessels in the surrounding stroma while intermediate-sized follicles (rat: 80-100um diameter) have one or two arterioles that terminate in an anastomotic network in the theca outside of the basement membrane (Bassett, 1943).

As an antrum develops in the follicle, the thecal layer acquires a vascular sheath consisting of two capillary networks located in the theca interna and externa, respectively. Because all capillaries remain outside the follicular basement membrane, the granulosa layer with its fluid-filled antrum and the cumulus cell-oocyte complex remain avascular until after ovulation. There is limited evidence suggesting that antral follicles vary in their degree of vascularity (Stouffer *et al.*, 2001). These data led to the hypothesis that acquisition of an adequate vascular supply is a rate-limiting step in the selection and maturation of the dominant follicle(s) destined to ovulate. Establishment of such vasculature would provide access to nutrients and hormones, e.g., gonadotropins, which are essential for final development. In contrast, insufficient vascular supply could limit further growth and lead to follicular degeneration or atresia.

In bovine follicles, detectable blood flow increases gradually over time and is first detected at the base of the follicle. Over time these increasing blood flow is accompanied by increasing plasma oestradiol (E2) concentrations until ovulation. However, oestradiol does not seem to exert any effect on follicular angiogenesis (Acosta *et al.*, 2003). Bovine dominant follicles during the follicular phase show well-developed capillaries with active and spatial dependent angiogenesis in the inner capillary layer (Jiang *et al.*, 2003). After the expulsion of the oocyte the capillary network of the theca rapidly invades the membrana granulosa provoking transformation of these cells in to the large luteal cells of the corpora lutea in a process termed luteinisation

1.3.3.6. Formation of an Antrum and Fluid Accumulation

Follicles do not possess an antrum until the granulosa cells have passed through 11 - 12 mitotic cycles when the follicle contains approximately 2 - 3000 cells in humans (Gosden R. G. *et al.*, 1988). Around this time pools of fluid accumulate between the granulosa cells and coalesce to form a single cavity or antrum bound by granulosa cells. The antrum characterises the mature follicle of most but not all mammals (Mossman & Duke, 1973). Two reasons exist as to why an antrum and the fluid within might be advantageous:

1. A means of extrusion for the cumulus oocyte complex out of the follicle at ovulation. Wide variations in fluid volume to follicular size occur between species and so it is unlikely that this is its sole function.
2. A nutrient supply and means of contact between the oocyte and granulosa cells.

During follicular expansion a reduction in the number of layers of granulosa cells occurs due to the increased surface area of the follicle and the distance between the granulosa cells and oocyte is increased. A fluid filled antrum allows the blood supply and granulosa cells to be in comparatively close contact, enabling nutritional and hormonal support of the egg.

In the follicle there is no structural barrier comparable to that of the "blood-testis barrier" in the male. This results in an increased ability of large molecules to enter the follicular antrum compared to the equivalent situation in the seminiferous tubules. Follicular fluid arises from the filtration products of thecal blood. Follicular fluid contains low molecular weight serum proteins (50% to >100% of the amount of protein in serum) (Keikhoffer *et al.*, 1962, Manarang-Pangan & Menge, 1971, Perloff *et al.*, 1955, Shalgi *et al.*, 1973) and growth factors crucial to follicle, granulosa cell and oocyte growth and development, and it is widely accepted that some of these components are synthesised by the granulosa cells (Anderson & Albertini, 1976). The properties of follicular fluid will be discussed later.

1.3.4. Follicular Recruitment, Selection and Dominance

1.3.4.1. The Follicular Wave

The main events that occur during a follicular wave are as follows. At recruitment, a cohort of follicles begins its final growth phase as it enters gonadotropin-dependent folliculogenesis. At selection, the number of growing follicles becomes equal to the number

of ovulations. As a consequence, the ovulatory follicle becomes dominant and the other follicles of the cohort regress by atresia (Driancourt, 2001).

In cattle recruitment of a cohort of follicles results from transient rises in FSH every 8 - 10 days. The interplay of FSH and LH results in continual release of emerging follicles from which a dominant follicle (DF) matures to ovulation. If not recruited, follicles continue along the default pathway to atresia (Driancourt, 2001).

Although most follicles become atretic the recruited cohort continues to grow beyond the stage when atresia normally occurs. In some species (e.g. rats, primates and pigs), dominant follicles develop only during the follicular phase and are thus destined for ovulation. In others (e.g. cattle, sheep and horses), recruitment, selection, and dominance occur at regular intervals, only the dominant follicle present during the follicular phase ovulates the rest of the recruited follicles being saved from atresia and for only a short time.

Recruitment of the cohort containing the future pre-ovulatory follicle occurs during a "recruitment window" which lasts 1, 2, or 3 days in sheep, cattle or horses, respectively.

Only gonadotrophin-dependent follicles are recruited. While recruitment and follicle gonadotrophin independence can be temporally linked in most species, the number of recruited follicles growing in the cohort appears to be highly variable between species, ranging from over 50 in pigs, to 5 to 10 in cattle and 1 to 4 in horses.

All follicles of the cohort are potentially capable of ovulating, however some follicles may have a competitive advantage as they mature toward ovulation (Driancourt, 2001).

At selection, the dominant follicle is chosen and the remaining follicles of the cohort become subordinate follicles and enter atresia. This is usually demonstrated by a block in their growth rate followed by a steady decrease in size. It is generally assumed that the largest follicle of the cohort is likely to be the one selected for ovulation (Ginther *et al.*, 1996).

In all species, the selected follicle appears to be the first one developing LH receptors on its granulosa cells. Follicles develop LH receptors when they reach 4 mm, 5 mm to 6 mm, 8 mm or 25mm diameter in sheep, pigs, cattle and horses, respectively (Driancourt, 2001).

During follicular dominance, preovulatory follicular growth and maturation occur. The other follicles of the cohort complete regression by atresia, while no recruitment occurs. There is a direct relationship between the presence of the dominant follicle and the absence of recruitment (Ko *et al.*, 1991).

In cattle, there are three key maturational steps associated with selection and appearance of a dominant follicle. The appearance of LH receptors on granulosa cells (Ireland J. J. & Roche, 1983a) is a pre-requisite for the establishment of follicular dominance and ovulation following an LH surge. The follicle, which is able to tolerate the lowest FSH level, by either increased sensitivity to or increased numbers of receptors for FSH becomes the dominant

follicle and demonstrates enhanced growth and steroidogenesis. The dominant follicle then maintains low FSH levels thereby preventing the emergence of further cohorts (Ginther, 2000, Ginther *et al.*, 1999, 2000, Ireland J. J. *et al.*, 1984). Secondly, the reduction in the amounts of IGF binding proteins such as IGPBP1 and IGFBP4 (Dalin, 1987, Mihm *et al.*, 1997, Monget *et al.*, 1996). This appears to be mediated by reduced production in the case of IGFBPI or increased proteolysis in the case of IGFBP4. Both events occur when the follicle is around 8 mm in diameter. Third, there is a selective decrease in the amounts of the 34kD inhibin dimer present in follicular fluid, while no major change is detectable amongst the other inhibin forms (Mihm *et al.*, 1997).

If luteolysis occurs during the period of the dominant follicle then the dominant follicle will ovulate. If however the corpora lutea (CL) suppresses the LH pulse yet again then a third wave of follicles will emerge and the second dominant follicle will regress by the same processes mentioned above. Only when the CL regresses can the LH pulse allow the dominant follicle to undergo the final stages of maturation, ovulation and luteinisation. This wave of emergence is continuous and occurs during all reproductive states in cattle (Adams *et al.*, 1992, Cooke *et al.*, 1997, Evans *et al.*, 1994, Ginther *et al.*, 1989, Stagg *et al.*, 1998).

A diagram proposing the functional coupling of FSH concentrations and follicular diameter can be seen in (Figure 5).

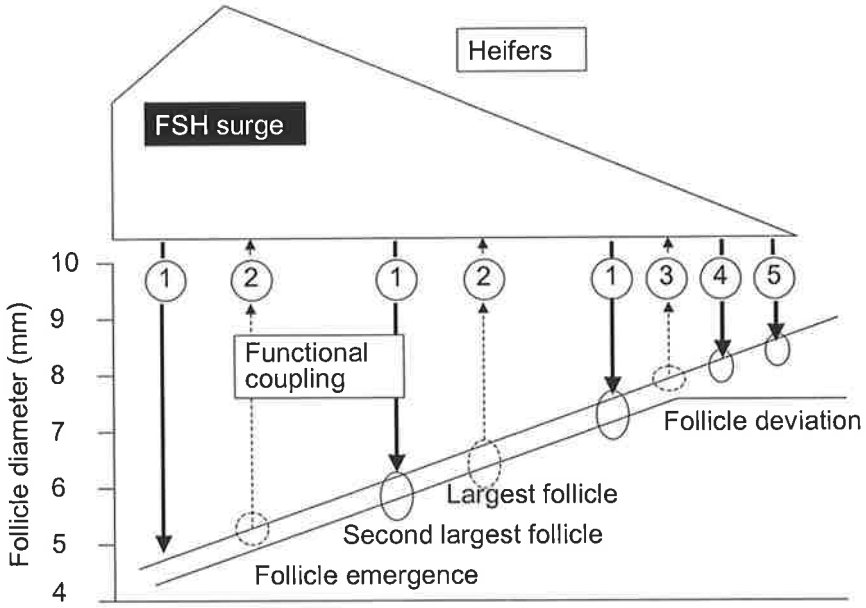

Figure 5 Diagram of the proposed functional coupling between FSH concentrations and diameters of the two largest follicles during development of the follicular wave. 1) Emergence of the follicular wave stimulated by an FSH surge that has peaked when the largest follicle reaches 4 mm 2) 5 mm follicle develops FSH suppression capability, all follicles ≥5 mm contribute to the decline in FSH for approximately 2 days 3) At 8.5 mm a follicle plays a major role in SH decline. Follicle suppression begins when FSH levels fall below that required by smaller follicles. These smaller follicles become subordinate. 4) Reduced FSH levels support the dominant follicle after the commencement of deviation. 5) LH begins its role in growth of the dominant follicle. From (Ginther 2000).

Steroidogenic profiling during follicular waves has shown that estradiol levels are high in healthy follicles and low in atretic ones (Austin *et al.*, 2001). This high expression of oestrogen is accompanied by enhanced expression of 3β hydroxyl steroid dehydrogenase (3βHSD), FSH receptors and the acquisition of LH receptors in the granulosa cells (Bao *et al.*, 1997, Evans & Fortune, 1997, Ireland J. J. & Roche, 1983b). Following the FSH decline the emerging cohort separates in to two groups, those that maintain rapid growth and estradiol synthesis and those that do not. The former may be one of the factors behind the success of the dominant follicle. Concomitant with these changes are changes in the amounts of inhibin and insulin-like growth factor (IGF) family intra-follicular proteins.

Inhibins suppress the action of FSH in the pituitary and may also influence the FSH response of the follicle. Activin is a dimer that links two inhibin β subunits, and its receptor interactions are regulated by the levels of follistatin, which neutralises the functions of activin in the pituitary and ovary (Findlay, 1993, Robertson *et al.*, 1987).

Inhibin binding sites are located in the pituitary, granulosa and theca cells and is thus thought to be important in the regulation of follicular development via paracrine, autocrine and endocrine mechanisms and the acquisition of FSH receptors (Chapman & Woodruff, 2003, Chong *et al.*, 2000, Draper *et al.*, 1998, Hertan *et al.*, 1999, Knight *et al.*, 1998). Inhibin was first purified from bovine and porcine follicular fluid where it was found in high amounts and identified first as a gonadal hormone that potently inhibits pituitary synthesis and secretion of FSH. The hormone also influences the development of granulosa cells and inhibits the FSH-stimulated synthesis of oestrogens. The FSH-stimulated release of inhibin can be potentiated by IGF-1 and is blocked by EGF and TGFα (Piferrer *et al* 1997).

Inhibins are related to TGFβ with approximately 35 percent sequence homology in the carboxyterminal region and based on a pattern of conserved cysteine residues in the alpha and beta subunits. At least one form of inhibin is identical with Sertoli cell factor (SCF) but little is known of its true function in follicular development (Jimenez-Krassel *et al.*, 2003). The inhibin/activin βA subunit mRNA is only expressed by the granulosa cells of the antral follicles greater than 0.8 mm diameter (Torney *et al.*, 1989).

During the FSH decline, low molecular weight IGFBPs appear to be at low levels in the fastest growing follicles. Once the dominant follicle is selected IGFBPs remain low resulting in an increase in IGF bioavailability. Levels of bioactive IGF appear to be essential for dominant follicle selection and its ability to tolerate declining FSH levels (de la Sota *et al.*, 1996, Mihm *et al.*, 1997, Stewart *et al.*, 1996).

In atretic follicles oestrogen activity is reduced and the levels of low molecular weight IGFBPs increase with a lowering of high molecular weight inhibins, and reduced levels of FSH. The decline in FSH appears to be critical to dominant follicle selection and it is thought

that high FSH may inhibit intra-follicular function. Although the dominant follicle is relatively FSH-independent it is known to require basal levels for maintenance (Bergfelt *et al.*, 2000, Ginther *et al.*, 2000, Turzillo & Fortune, 1993).

The role of LH in this scenario is interesting since follicle growth and dominance can occur at any stage in the reproductive cycle and thus under different LH conditions (Rahe *et al.*, 1980). This implies that levels of LH do not affect cohort growth prior to the selection of the dominant follicle. The rise in LH prior to dominant follicle differentiation (Kulick *et al.*, 1999) shows that oestrogen activity and period of dominance are LH pulse-dependent (Mihm *et al.*, 2002). This is supported by data from Savio (Savio *et al.*, 1993), who showed that reduction in the amplitude of the LH pulse results in atresia of the dominant follicle.

1.3.5. Ovulation

Selection and maturation result in the development of the pre-ovulatory follicle. This structure consists of a thin layer of granulosa cells, basement membrane and thecal cells containing an attached oocyte and associated cumulus cells, the cumulus oocyte complex and follicular fluid. The cumulus oocyte complex expands 20-30-fold in volume prior to ovulation (Bost *et al.*, 1998) achieved in part by accumulation of hyaluronic acid a follicular glycosaminoglycan, which forms a spongy matrix with the cumulus cells. During ovulation one area of the follicle the stigma, becomes thin and avascular and the surrounding connective tissue breaks down causing the follicle to rupture (Espey, 1994, Tsafriri, 1995, Tsafriri & Reich, 1999). The follicular fluid containing the oocyte and its surrounding cumulus cells move out on to the ovarian surface (human; (Rodbard, 1968)) or bursa (sheep, horse; (Fortune *et al.*, 1991)) where they are captured by cilia and moved in to the oviduct. The cumulus matrix adheres to the oviduct and from here is transported through the ostium (Lam *et al.*, 2000).

1.3.6. Corpus Luteum

Collapse of the follicle after ovulation results in its transformation in to a corpus luteum (luteolysis). Corpora lutea result from the continuation of follicular maturation. The structure is formed from the granulosa and theca interna cells, which form large and small luteal cells respectively. Following the pre-ovulatory surge in gonadotrophins the follicular cells undergo morphological endocrinological and biochemical changes. Following ovulation the follicle becomes highly vascular and begins to secrete progesterone. In some species there is production of a carotenoid pigment known as lutein from which the cells derive their name, which imparts an orange colour to the corpus luteum (CL). During formation of the CL, the fibrin core undergoes fibrosis and the membrana propria breaks down allowing invasion of

blood vessels in to the antrum (Amselgruber *et al.*, 1999). Luteolysis (non-primate) may take up to 14 days, is species specific and may be controlled by endometrial prostaglandin $F_{2\alpha}$ ($PGF_{2\alpha}$), see (Sheep; (Driancourt *et al.*, 2000, Juengel & Niswender, 1999, Rodgers R. J. *et al.*, 1985) Cow; (Juengel & Niswender, 1999, Rodgers R. J. *et al.*, 1988)). $PGF_{2\alpha}$ production is stimulated by oxytocin secreted by the corpus luteum (Rodgers R. J. *et al.*, 1985, Terranova & Rice, 1997). Small and large luteal cells differ in their ability to secrete progesterone. Small luteal cells may stimulate angiogenesis while large luteal cells respond to the luteolytic signal of $PGF_{2\alpha}$ (Fitz *et al.*, 1982, Wiltbank *et al.*, 1990). Biochemical communication between the two cell types appears essential to normal development of the CL, although the mechanisms underlying it are not clear. Regression terminates in the collapse of the lutein cells, ischaemia and progressive cell death leaving a corpus albicans, which becomes absorbed in to the stromal tissue. At this time there is an appreciable fall in progesterone production (Rodgers R. J. *et al.*, 1988).

1.4. Atresia

Most activated follicles will not ovulate and will undergo atresia and regression, this being the default pathway of follicular maturation. Atresia is characterised by death of the oocyte, pyknosis and fragmentation of the granulosa cells (Byskov, 1974), disintegration of the basal lamina and regression of both the theca interna and externa (O'Shea *et al.*, 1978). During atresia expression of mRNA declines rapidly and becomes low or undetectable (Bao & Garverick, 1998). In early atresia, inhibin/activin βA mRNA is located in the cumulus cells, whereas inhibin alpha and follistatin mRNAs are present in the granulosa cells. As atresia progresses mRNA for inhibin alpha and follistatin, disappear (Braw-Tal, 1994).

Follicular atresia occurs at different times during folliculogenesis and is more common in the larger antral follicles than small pre-antral follicles. In cattle two forms of atresia have been defined (Irving-Rodgers *et al.*, 2001).

1. Basal atresia occurs where the granulosa cell layers begin to die, from the basal lamina upward, while those antrally positioned remain alive.
2. Antral atresia occurs where the pattern of death is reversed.

Follicular development is strictly dependent upon the gonadotrophins FSH and LH, but paracrine factors (growth factors, cytokines, steroids, constituents of extracellular matrix) also play important roles in amplifying gonadotrophin action in follicular cells. Some pathological situations such as premature ovarian failure result from accelerated follicular atresia, triggered by interactions between follicular cells and cells of the immune system.

1.5. Follicular Fluid

Follicular fluid provides a buffer for the internal environment of the follicle against the external environment and has been termed the "culture medium" of the granulosa cells and oocyte (Brambell, 1928, Gosden R. G. *et al.*, 1988, Longley, 1911, McNatty *et al.*, 1981). Follicular fluid contains many of the plasma proteins and some large molecules (e.g. proteoglycans see section 1.8) produced by granulosa cells (Ax & Ryan, 1979). Filtration of the blood through the theca and basal lamina results in exclusion of 50% of molecules MW of 250,000 and over and 100% of proteins MW< 850,00 (Shalgi *et al.*, 1973).

The proteins of follicular fluid and serum are very similar but there are differences in their relative concentrations (see Edwards 1974, for review). A study by Andersen (Andersen *et al.*, 1976) revealed that the concentration of protein in individual bovine follicles varied with follicular development and ranged from 75% to 114% of serum from the same animal. In addition he noted that the proportions differed between healthy and atretic follicles. Retention of certain proteins in follicular fluid, at greater levels or larger size, provides a means whereby an osmotic potential can exist.

Non-protein components of fluid include lipids and electrolytes, a comprehensive list of known follicular fluid electrolytes from large antral follicles can be seen in Table 2. Since the majority of these are small enough to cross the follicular wall they are not able to generate an osmotic potential.

Several glycosaminoglycans (glycosaminoglycans see section 1.8) have been identified in follicular fluid. They are hyaluronic acid (HA), dermatan sulphate (DS) and chondroitin sulphate (CS) (Ax & Ryan, 1979, Grimek & Ax, 1982, Grimek *et al.*, 1984, Lenz *et al.*, 1982, Mueller *et al.*, 1978, Yanagishita & Hascall, 1979, Yanagishita *et al.*, 1979). Several glycosaminoglycans found in the follicle have been shown to play an important role in fertilisation, specifically hyaluronan in the cumulus oocyte complex (Bellin & Ax, 1987a, Bellin *et al.*, 1986, Camaioni *et al.*, 1996, Eriksen *et al.*, 1997, Grimek & Ax, 1982, Kobayashi *et al.*, 1999, Parillo *et al.*, 1998, Salustri *et al.*, 1989, 1990a, Salustri *et al.*, 1990b, Tsuiki *et al.*, 1988). Follicular fluid composition and a potential role of follicular fluid in egg maturation (Grondahl *et al.*, 1995) have been related to the size of a follicle and its developmental stage (Anderson *et al.*, 1976, Bellin & Ax, 1984, Grimek *et al.*, 1984, Henderson *et al.*, 1982, Shalgi *et al.*, 1973, Short, 1962, Yanagishita, 1994). In relation to ovulation some researchers have suggested that fluid accumulation may aid in rupture of the follicle at ovulation, and yet others have suggested that ovulation results from contraction of involuntary muscle fibres and others from the digestion of the follicle wall by matrix metalloproteinases. However, it should be noted that some species never acquire antral

cavities and thus it is unlikely that follicular fluid is solely responsible for follicular rupture and that a combination of the above occurs (Duke, 1966, Mossman & Duke, 1973).

Table 2 Electrolyte concentrations (mmol/l) of follicular fluid*

Species	Na^+		K+		Cl-		Ca2+		Mg2+		References
	FF	S	FF	S	FF	S	FF	S	FF	S	
Human	124	145	4.4	4.6	109	104					Shalgi et al (1972)
	143	154	5.4	5.4	140	146	0.94	1.04	0.76	0.68	Chong et al (1997)
Rabbit	133	125	7.0	4.3	136	127	3.56				David et al (1973)
	140	136	6.2	5.7	144	139	2.29	3.85	1.4	1.67	Burgoyne et al (1979)
Sheep	149	149	4.7	4.9	107	106		2.28	0.89	0.87	Gosden and Hunter (1988)
Pig	128	143	15.9	5.2							Schuetz and Anisowicz (1974)
	142	147	7.6	7.1			10.3	10.8			Chang et al (1976)
	145	140	4.9	4.8							Knudsen et al (1979)
	141	138	3.8	3.8	97.3	95.7	2.3	2.27	0.75	0.77	Gosden and Hunter (1988)
Cow	132		9.2		149.5						Olds and Van Denmark (1957)

*Follicular fluid (FF) from large follicles compared with plasma or serum (S) from medium follicles. After (Gosden R. G. *et al.*, 1988)

1.6. Osmosis and Osmotic Potential

Osmosis is the one colligative property responsible for fluid movement across semi-permeable membranes i.e. the follicular basal lamina (Comper *et al.*, 1990, Gu *et al.*, 1993, Hammel, 1999, Haussinger, 1996). In the follicle variations in permeability of the basal lamina are believed to occur during follicular development, this in turn would allow fluid movement and partial regulation of fluid loss and accumulation. Small fluctuations in volume and concentration of molecules present in the antrum may lead to changes in cell gene expression and regulation and therefore may be critical to oocyte maturation (Haussinger, 1996, Rodgers R. J. *et al.*, 1999a). High water permeability of membranes and an inability to withstand great hydrostatic potential means that net movement of water molecules is almost exclusively driven by osmosis. In many tissues in the body osmotic gradients result from the build up of large molecules i.e. proteoglycans on one side of a semi-permeable membrane. These molecules are generally unable to pass across membranes and so concentrate on either

side of the lamina causing a differential in osmotic potential between those that can diffuse in to the follicle and/or are synthesised from within it and those that cannot pass from the capillary blood supply.

Controversy surrounds the results of osmotic potential measurements for human follicular fluid (Edwards, 1974, Shalgi *et al.*, 1972a, Zachariae, 1958). Early studies estimated that the follicular fluid of unstimulated follicles was much lower than that of plasma and of pre-ovulatory follicles (Smith J.T & Ketteringham, 1937). This difference was possibly linked to the permeability of the basal lamina during antrum formation (Hess *et al.*, 1998). The properties and osmotic effects of proteoglycans and glycosaminoglycans and their potential role in fluid accumulation are described below 1.8.

1.7. Follicular Fluid Formation

The morphology of the membrana granulosa suggests it is permeable to water and dissolved substances from outside of the follicle. Channels, allowing molecules up to 100-850kDa to pass, separate granulosa cells. Evidence suggests that the majority of these molecules will cross the follicular wall in to the antrum via a concentration gradient (Jinga *et al.*, 1986).

In order to enter the follicular antrum, serum proteins must first passage through the following structures, the capillary wall, the theca interna and basement membrane and the membrane granulosa. It is possible that the selective permeability of any of these will affect the flow of fluid in to the antrum.

FSH stimulates the formation of an antrum and accumulation of follicular fluid (Johnson Martin H. & Everitt, 2000). Polypeptides or steroids may regulate accumulation (Gosden R. G. *et al.*, 1988). In the cow the growth rate of follicles from 1-12mm appears to be continuous and constant (Marion *et al.*, 1968a). The capillary network, surrounding the antral follicle, is supplied by arterial blood from the theca and and drained by veins that are in close contact with lymph vessels, allowing direct fluid transfer (Bassett, 1943, Robinson, 1918). At the onset of oestrous in cattle the dominant follicle is approximately 10 mm in diameter, progression to a 16-18mm pre-ovulatory follicle occurs within 24 hours translating to a six-fold increase in fluid volume at a rate of 0.33mm/hour. Accumulation in these latter stages may result from the greater permeability of the follicular wall via pre-ovulatory increases in blood flow and permeability, which boost filtration of the blood (Macchiarelli *et al.*, 1992). An alternative mechanism maybe via active transport such as in the gall bladder where salt concentration is modified by water flux up and down an osmotic gradient (Ericson & Spring, 1982). Such a similar mechanism may apply in the follicle, perhaps under hormonal control. In an expansion of this concept hydrolysis of macromolecules in the fluid

might result in a rise the osmotic potential of the fluid causing a serum: fluid potential differential but this hypothesis has not been investigated (Zachariae, 1958, 1960, Zachariae & Jensen, 1958).

In the follicle water movemet will be affected by the magnitude and size of the molecules present in the follicular fluid and plasma, which in turn affects their relative osmotic potentials. The differences between plasma and follicular fluid molecules are the probable cause of fluid accumulation in the follicular antrum. While the osmotic pressures of the two fluids may be similar, the osmotic potential that determines net water movement may be considerable. To date evidence for fluid transport in the follicle via an osmotic gradient is inconclusive but transudation of water and solutes from the thecal arteries is no doubt only part of the story.

In considering the hypothesis of Zacharaie and Jensen, research has suggested that proteoglycans and their glycosaminoglycan side chains may be partially responsible for the osmotic forces active during fluid accumulation within the body by causing water sequestration during hydration of the proteoglycans and glycosaminoglycans present (Buschmann & Grodzinsky, 1995, Comper & Laurent, 1978, Comper & Zamparo, 1989, Gu *et al.*, 1993, Ishihara *et al.*, 1997, Khalsa & Eisenberg, 1997, Kovach, 1995, Laurent T. C., 1987, Zamparo & Comper, 1989). In addition, their osmotic effects are enhanced by the effect of their size and ability to bind other osmotic molecules. Since follicular fluid from several species contain some of these molecules it follows that they may be active in follicular fluid accumulation (Andrade-Gordon *et al.*, 1992, Bellin & Ax, 1987a, Bellin *et al.*, 1987, Bellin *et al.*, 1986, Boushehri *et al.*, 1996, Bushmeyer *et al.*, 1985, Edwards, 1974, Eppig & Ward-Bailey, 1984, Grimek *et al.*, 1984, McArthur *et al.*, 2000, Parillo *et al.*, 1998, Reyes *et al.*, 1984, Sato *et al.*, 1987a, Sato *et al.*, 1988, Shimada *et al.*, 2001, Tadano & Yamada, 1978, Tsuiki *et al.*, 1988, Vanderboom *et al.*, 1989, Varner *et al.*, 1991, Wise & Maurer, 1994). It is feasible that molecules secreted by the granulosa cells in to the fluid may be able to produce osmotic gradients down which molecules may move in to the antrum.

1.8. Proteoglycans and Glycosaminoglycans

Proteoglycans are the most complex and multifunctional molecules in the animal kingdom (Iozzo & Murdoch, 1996). They form a ubiquitous family of heterogeneous macromolecules localised within the cell, at the cells surface and in the extracellular matrix (Kjellen & Lindahl, 1991). The proteoglycan family consists of over 30 members with a wide variety of biological functions (Iozzo & Murdoch, 1996). Structurally, they consist of a protein core with one or more unbranched glycosaminoglycan side chains covalently attached as a post-translational modification. Proteoglycans vary in size from 80kDa to 3500 kDa and

have limitless heterogeneity due to the variability of their core proteins and the type and degree of sulphation of their attached glycosaminoglycan chains (Alberts *et al.*, 1989). They play an important role in extracellular matrix organisation, influence cell growth and tissue migration and are involved in the regulation of matrix turnover by the binding and inactivation of growth factors and protease inhibitors (Hardingham & Fosang, 1992, Hering, 1999, Hildebrand *et al.*, 1994, Kresse & Schonherr, 2001, Poltorak *et al.*, 2000, Salustri *et al.*, 1999). In addition they provide structural supports to tissues, function as growth supportive or suppressive molecules, possess adhesive and anti adhesive properties and are able to act as biological filters (Iozzo & Murdoch, 1996).

The dynamics of water transport associated with proteoglycan solutions has been studied in relation to their osmotic flow and hydraulic permeability (Price *et al.*, 1996, Scott D. *et al.*, 1997, 1998a). Central to the kinetics of water flow are the hydrodynamic frictional coefficients of both water and proteoglycan solutions (Scott D. *et al.*, 1997). These coefficients are concentration dependent. Structural features and organisation within solution dictate that the proteoglycan be diffusely mobile and that the concentration gradient be osmotically active (Fraser J. R. *et al.*, 1988, Rosengren *et al.*, 2001). The number and position of the glycosaminoglycan side chains is a key to this diffusibility, the influence of the poly-ion on the micron-ion distribution in its vicinity creating the Gibbs - Donnan effect which is the electrical potential set up either side of a semi permeable membrane by two solutes (Buschmann & Grodzinsky, 1995, Comper & Preston, 1974, Comper & Williams, 1987, Comper & Zamparo, 1989, Comper & Williams, 1990, Comper *et al.*, 1990, Urban & Maroudas, 1981, Zamparo & Comper, 1989).

1.8.1. Biosynthesis of Proteoglycans

The biosynthesis of the large cartilage proteoglycan aggrecan is taken as the model for all proteoglycan synthesis. Aggrecan is about 2500 kDa, and a typical large keratan sulphate/chondroitin sulphate proteoglycan in cartilaginous tissue. Its distribution pattern is restricted to brain, aorta and tendon and cartilage. The core protein of 210-250 kDa binds hyaluronic acid. Aggrecan provides a strongly hydrated space filling gel due to the large number of polyanionic glycosaminoglycan chains covalently attached to the protein core.

Studies of the biosynthetic routes of construction of proteoglycans have revolved around aggrecan; these mechanisms are generally considered the norm for all proteoglycans with the exception of some unique glycosaminoglycan structures found in deep-sea fish. Specific mRNA is transcribed from DNA and used as a template for core protein construction in the endoplasmic reticulum. Glycosaminoglycan chain synthesis is initiated by the addition of specific linkage region monosaccharides and is based on consensus sequences found in the

core protein. After translocation to the Golgi, glycosaminoglycan chain elongation is completed and the chain is rapidly sulphated. Proteoglycans destined for the extracellular matrix are then packaged in to secretory vesicles and their contents exported from the cell (Grebner *et al.*, 1966, Lindahl & Kjellen, 1991). The proteoglycan is then either secreted (aggrecan, decorin, biglycan), transported to the cell membrane, or to intracellular compartments. Extracellular processing may occur after secretion, for example aggrecan may only bind hyaluronan several hours post secretion (Knudson C. B. & Knudson, 2001).

1.8.2. Glycosaminoglycans

The members of the glycosaminoglycan family are essential components of proteoglycans. Glycosaminoglycans are composed of repeating sulphated disaccharide subunits of uronic acid (or neutral sugar) and a hexosamine (Table 3) to form unbranched carbohydrate polymers, which may be extensively modified by epimerisation, acetylation and/or sulphation, forming highly diverse polysaccharide chains. Glycosaminoglycans are highly negatively charged due to their attached carboxylate and sulphate groups, and as such are strongly hydrophilic. They attract and bind cations such as Na^+ and Ca^{2+} that have the potential to increase the overall salt concentration in a biological system and hence the osmotic potential of the fluid or tissue where the glycosaminoglycans reside. The extended conformation imparts high viscosity to a solution. Along with the high viscosity of glycosaminoglycans comes low compressibility, which makes these molecules ideal as lubricating fluids in joints. At the same time, their rigidity provides structural integrity to cells and provides passageways between cells, allowing for cell migration. There are five glycosaminoglycans of physiological significance, defined by their sugar residues, how these residues are linked, and the number and location of sulphate groups. They are hyaluronic acid (HA), dermatan sulphate (DS), chondroitin sulphate (CS), heparin, heparan sulphate (HS), and keratan sulphate (KS). Although each of these glycosaminoglycans has a predominant disaccharide component, heterogeneity does exist in the sugars present in the make-up of any given class of glycosaminoglycan. A table of glycosaminoglycan localisation and more significant properties can be seen in Table 4 and a diagram of the basic structure of GAGs can be seen in (Figure 6)

Table 3 The Structure of Glycosaminoglycans

Glycosaminoglycan	*Disaccharide unit*	*Modifications*
Heparan sulphate (HS)	[GlcA/IdoAβ or α1-4GlcNAc α1-4]	N deacetylation, N-sulphation
Heparin		C5 epimerisation of GlcA
		C2 sulphation of IdoA
		C3, C6 sulphation of GlcNAc
Chondroitin sulphate (CS)	[GlcA/ IdoAβ or α1-3GalNAcβ1-4	C5 epimerisation of GlcA
Dermatan sulphate (DS)		C2 sulphation of IdoA
		C4, C6 sulphation of GlcNAc
Keratan sulphate (KS)	[Galβ1-4GlcNAc β1-3]	C6 sulphation on Gal/GlcNAc
Hyaluronan (HA)	GlcAβ1-3GlcNAcβ1-4	Up to 25,000 repeating disaccharides
N-acetyl-D-glucosamine (GlcNAc), N-acetyl-D-galactosamine (GalNAc), Iduronic acid (Ido A) Galactosamine (Gal), Glucosamine (GlcA)		

Table 4 Glycosaminoglycan localisation and properties

Glycosaminoglycan	*Localisation*	*Comments*
Hyaluronan	Synovial fluid and vitreous humour	ECM of loose connective tissue large polymers, shock absorbing most abundant Glycosaminoglycan
Chondroitin sulphate	Cartilage, bone, heart valves	
Heparan sulphate	Basement membranes, components of cell surfaces	Contains higher acetylated glucosamine than heparin.
Heparin	Component of intracellular granules of mast cells lining the arteries of the lungs, liver and skin	More sulphated than heparan sulphates
Dermatan sulphate	Skin, blood vessels, heart valves	
Keratan sulphate	Cornea, bone	Cartilage, aggregated with chondroitin sulphates

1.8.3. Hyaluronic acid (HA) or Hyaluronan

Hyaluronan is synthesised by almost all animals and by some bacteria and viruses. Hyaluronan is the only glycosaminoglycan to be synthesised as a free chain. However in most tissue types it is found as either the free glycosaminoglycan or in complexes with proteins and proteoglycans. It binds to proteoglycans containing hyaluronan-binding domains (see later section 1.10.2.1) to form extra-cellular matrix macromolecules (Laurent T. C., 1987, Laurent T. C. & Fraser, 1986). The contour length of an hyaluronan chain of M_r 4 x 10^6 is 10 μm (Fessler & Fessler, 1966) and at concentrations of 1mg/l it will overlap and form a continuous polymer network with unique physio-chemical properties i.e. rheological properties, flow

resistance, osmotic potential, exclusion properties and filter effects (Laurent T. C. *et al.*, 1960). At concentrations of 1mg/ml it stimulates the expression of matrix metalloproteinases (MMPs) and the activation of latent MMPs (Isnard *et al.*, 2001) involved in a range of physiological processes including tissue remodelling and wound repair (Shapiro, 2000). This wide range of functional activities shown by hyaluronan is possibly related to the large number of hyaluronan-binding proteins (or hyaladherins) that exhibit significant differences in their tissue expression, cellular localisation, specificity, affinity and regulation.

1.8.4. Chondroitin Sulphate (CS)

Chondroitin sulphate is composed of glucuronate and N-acetylgalactosamine having one attached sulphate group per disaccharide unit, in the 4 and/or 6 positions on N-acetylgalactosamine (Kuettner & Kimura, 1985). The function related to the position of the sulphated group is unknown. CS is found in articular cartilage forming up to 80% of the glycosaminoglycan species present. The C-6 form is spatially more freely oriented and this appears to increase its ability to interact with collagen in the extracellular matrix (ECM) (Shibata *et al.*, 1992). Fluid from healthy follicles has been shown to contain reduced chondroitin sulphate levels compared to that of fluid from atretic follicles (Grimek *et al.*, 1984). In addition follicular fluid chondroitin sulphate has been shown to inhibit some cellular processes that result in increased HA-synthesising activity. The sulphated glycosaminoglycans also have the ability to suppress HA-synthesising activity during cumulus expansion. However, the sulphated glycosaminoglycans are not believed to be directly responsible for enzyme inhibition (Eppig & Ward-Bailey, 1984).

1.8.5. Dermatan Sulphate (DS)

Dermatan sulphate is formed by the intracellular epimerisation of glucuronate to iduronate of chondroitin sulphate (Rosenberg *et al.*, 1986). Fifty percent of porcine follicular fluid proteoglycans have been shown to contain 50% dermatan sulphate (Yanagishita *et al.*, 1979). In mouse follicular fluid dermatan sulphate is believed to be a crucial element of the hyaluronan matrix formed by the cumulus cells during the cumulus expansion process (Camaioni *et al.*, 1996)

1.8.6. Heparan Sulphate (HS) and Heparin

Heparin and heparan sulphate have the same basic structure. The size of an individual chain may reach 100 kDa but is generally below 50 kDa. Heparin is well known for its anticoagulant action. Structural and functional criteria make it difficult to separate these two

molecules. They both may have numerous variations in sulphation or epimerisation but as a general rule the sulphation status of heparan sulphate is below 50% where as it is above 70% in heparin. Heparan sulphate proteoglycans (HS proteoglycans) are essential in immune response systems and wound repair functioning as co-receptors and co-factors (David, 1991, Klagsbrun, 1991, Ruoslahti & Yamaguchi, 1991). Five heparan sulphate core proteins mRNA (perlecan; syndecan-1, -2, and -4; and glypican-1) are expressed by granulosa cells during the development of the ovarian follicle. Anti-coagulant HS proteoglycans direct their action to control fibrin deposition in the follicle (Hasan *et al.*, 2002, Princivalle *et al.*, 2001), providing attachment for anticoagulant heparan sulphate chains on the cell surface and in the extracellular matrix. These core proteins are constantly expressed during the oestrus cycle, indicating that modulations of HS proteoglycan levels observed in the ovary are likely controlled at the level of the biosynthesis of anticoagulant heparan sulphate glycosaminoglycan chains (Princivalle *et al.*, 2001).

1.8.7. Keratan Sulphate (KS)

Keratan sulphate is substituted with amine and sulphate groups in different positions, which results in differences in their detailed structure (Kuettner & Kimura, 1985) and in mammalian tissues two forms are found (KS I and KS II). In large proteoglycans associated with cartilage KS II is found while in fibromodulin and lumican two small leucine rich proteoglycans (SLRPs) it is the KS I form which is found (Hoffman *et al.*, 1967). Keratan sulphate is found in cartilage, intervertebral discs and cornea.

Figure 6 Diagrams Depicting the Basic Structure of GAGs.

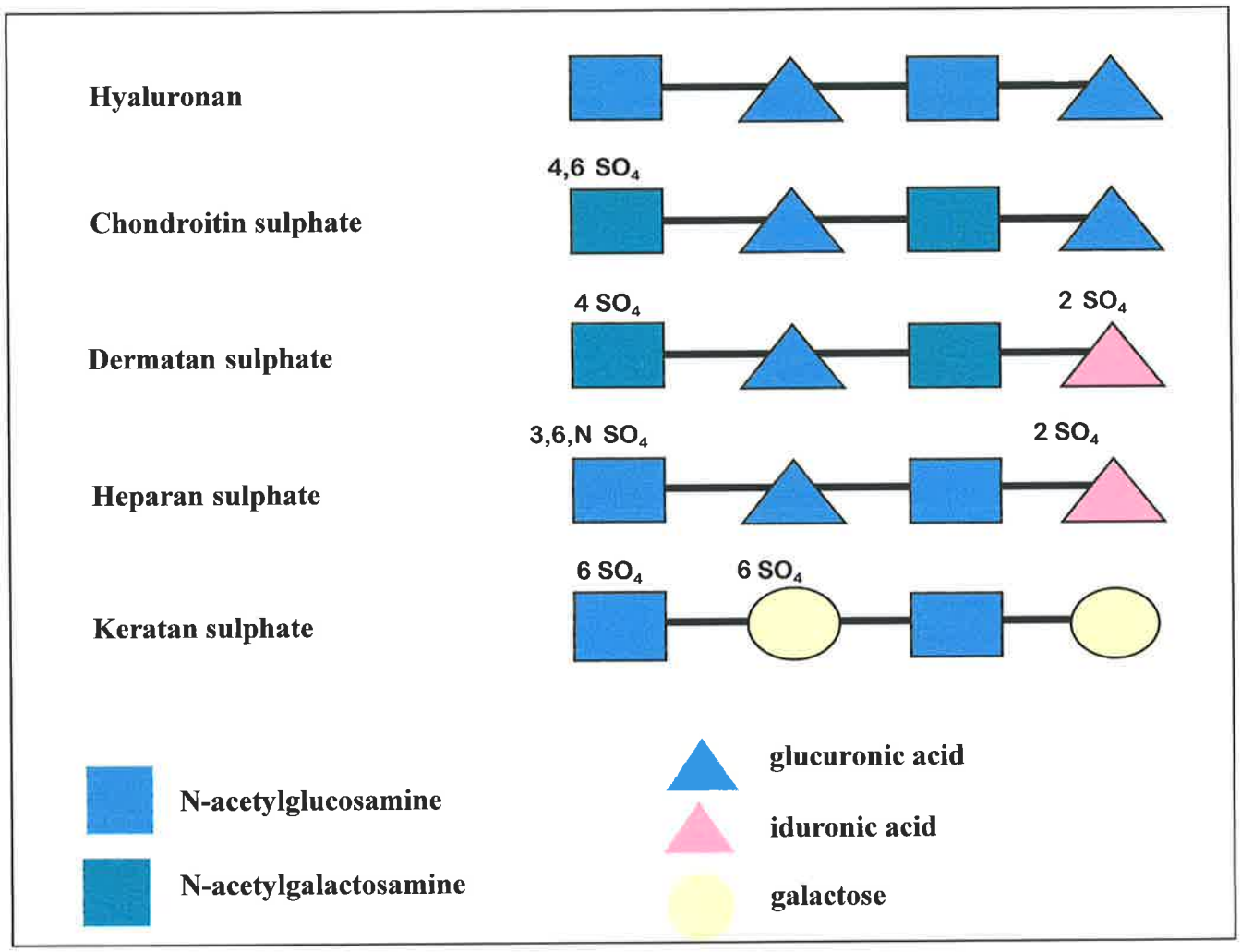

1.9. Cell Associated Proteoglycans

Cell associated proteoglycans form a variable group of molecules with many functions. The best-defined members of the group are listed below.

Serglycins: are found intracellularly in the secretory vesicles, and contain, either CS or HS chains covalently linked to the core protein (Humphries *et al.*, 1992).

Syndecans: consists of at least four different types: syndecan 1, syndecan 2 (fibroglycan), syndecan 3 (N-syndecan) and syndecan 4 (ryudocan, amphiglycan). Many cell types can express more than one type but the expression levels may change during development (Elenius *et al.*, 1991) and differentiation. Syndecans bind collagens with a high affinity and specificity.

Betaglycan: Type III TGF-β receptor, is now called betaglycan, and has been shown to contain both HS and CS chains (Cheifetz & Massague, 1989). TGF-β signals via a protein kinase receptor, and betaglycan presents the growth factor directly to the kinase subunit of the signalling receptor enhancing the cell response (Lopez-Casillas *et al.*, 1993).

CD44 is a "part-time" proteoglycan. It can bind can be either chondroitin sulphate or heparan sulphate. CD-44 is a cell surface receptor for hyaluronan (Miyake *et al.*, 1990). Alternative splicing of CD44 has been reported (Screaton *et al.*, 1992). Extracellular domain contains three disulphide-bonded loops, and it has a high homology with the hyaluronan-binding region of aggrecan, link protein, neurocan and versican (Goldstein *et al.*, 1989).

Thrombomodulin is an integral protein that contains one CS/DS chain. It binds to thrombin and act as a cofactor in the activation of protein C catalysed by thrombin (Wen *et al.*, 1987).

1.10. Extracellular Proteoglycans

Extracellular proteoglycans can be divided in to two groups based on their ability to bind hyaluronan and biological function. These are the small leucine rich proteoglycans and the modular proteoglycans (Iozzo & Murdoch, 1996).

1.10.1. Small Leucine Rich Proteoglycans (SLRPs)

SLRPs are classified in to three structurally related members involved in cellular communication and cytodifferentiation (Hildebrand *et al.*, 1994, Lindahl & Hook, 1978, Yamaguchi & Ruoslahti, 1988). SLRPs as the name suggests are composed primarily of leucine rich tandem repeats. They are secreted proteoglycans with a core protein structure containing three regions. These three regions comprise an amino acid region containing

CS/DS or tyrosine sulphate, a central domain containing the leucine rich repeats and a carboxyl region. Table 5 lists members of this group and a summary of their protein core sizes and tissue distribution. Decorin and biglycan are the two most investigated molecules of this group and have been grouped together based on amino acid (aa) sequence similarities. SLRPs bind to and interact with proteins involved in matrix assembly and control of cell proliferation and tissue morphogenesis. Decorin is known to inhibit fibrillogenesis and it is assumed that it may have a non-globular protein core, which allows increased surface area for interaction with smaller globular proteins (Kobe & Deisenhofer, 1994). SLRPs appear to have some common features one of which is the ability to bind type I collagen, albeit to different sites.

Expression studies have shown that that SLRP genes rarely overlap, suggesting a tissue dependent expression with concentration ratios changing between tissues (Iozzo & Murdoch, 1996). This appears to be true; for example, decorin is associated with connective tissues such as dermis, tendon and cornea while biglycan is associated with cell surface epithelia. In both cases their transcription appears differentially regulated by growth factors and cytokines; for example in most cases transforming growth factor β down regulates decorin while up regulating that of biglycan (Sonal, 2001).

*Table 5 Structure and properties of small leucine rich secreted pericellular proteoglycans**

General features	*Designation*	*Protein core*	*Type and number of GAG chain*	*Tissue distribution*
SLRP	Gene product	Size kDa	Type (No)	
Small ubiquitous proteoglycans enriched with leucine, with 24 aa tandem repeats flanked by cysteine clusters	Decorin	38	CS/DS (1)	Ubiquitous, bone, teeth, collagenous matrices
	Biglycan	36	CS/DS (1-2)	Interstitium, cell surfaces
	Fibromodulin	42	KS (4)	Collagenous matrices
	Lumican	38	KS (2-3)	Cornea, intestine, liver, muscle, cartilage
	Epiphycan	36	CS/DS (2)	Epiphysal cartilage

*After Iozzo 1996 (Iozzo & Murdoch, 1996)

1.10.2. Modular Proteoglycans

Modular proteoglycans can be subdivided in to two groups, the hyalectans and the non-hyaluronan-binding modular proteoglycans.

1.10.2.1. Hyaladherins (or hyalectins)

Hyaluronan is a unique glycosaminoglycan since it lacks covalent linkages to proteins, preventing it from forming proteoglycans. The one exception to this rule is seen with its interaction with pre-alpha-trypsin inhibitor and inter-alpha-trypsin inhibitor. In this situation an ester link is formed between the heavy chains of the inhibitor and the C6 of the glucosamine residue.

Hyaluronan associates with proteins and proteoglycans to form extracellular hyaluronan-rich matrices, which affect cellular behaviour. This characteristic is derived from the large number of associated hyaluronan-binding proteins or hyaladherins that exhibit significant differences in tissue expression, cellular localisation, specificity, affinity and regulation (Fraser J. R. *et al.*, 1997, Knudson C. B. & Knudson, 1993, Laurent T. C. *et al.*, 1996, Toole, 1990, 2000, Turley, 1984).

The hyaladherins include the link module family. The link module is comprised of an immunoglobulin domain and two contiguous link modules. This molecular arrangement is found in the G1-domains of the chondroitin sulphate proteoglycans aggrecan, versican,

neurocan and brevican. The immunoglobulin domains are probably responsible for the link protein-proteoglycan interaction, while the link modules mediate binding to hyaluronan (for a review see (Neame & Barry, 1994)). The common feature of the hyaladherins is the presence of a hyaluronan-binding motif in their core protein. Some well-defined hyaladherins are listed below.

- Link Protein, The link module is made up of approximately 100 amino acids and forms a 40-48 kDa glycoprotein, which stabilises the aggregates of hyaluronan (Camaioni *et al.*, 1996, Kobayashi *et al.*, 1999, Sun *et al.*, 1999).

- Hyalectins, Aggrecan/Versican Family of large chondroitin sulphate proteoglycans

- Tumour necrosis factor stimulated gene 6 (TSG-6), located in the extracellular matrix (Carrette *et al.*, 2001, Yoshioka *et al.*, 2000). TSG-6 has a three dimensional structure of two α helices and two, triple stranded, antiparallel β sheets arranged around a large hydrophobic core. TSG-6 is a flexible molecule being able to bind both chondroitin sulphate and hyaluronan. TSG-6 has been shown to have a structural role in cumulus oocyte complex matrix formation possibly mediating cross-linking of separate hyaluronan molecules through its binding to inter-alpha-trypsin inhibitor. Research has also shown that TSG-6 is part of a negative feedback loop in the control of the inflammatory response (Wisniewski *et al.*, 1996).

Hyaluronan and lectin binding proteoglycans consist of a core protein containing two hyaluronic acid or lectin binding domains, bisected by a glycosaminoglycan-chain binding region. These proteoglycans may act as bridges between cells and the extracellular matrix, and influence water ion content in these tissues. There are currently four members of this family: versican, aggrecan, neurocan and brevican (Iozzo & Murdoch, 1996). They share a common tri-domain structure consisting of and N-terminal region that binds hyaluronan, a central glycosaminoglycan-carrying region and the c-terminal, which binds to lectins (Iozzo, 1998).

Versican, so called because of its versatility, is one of the largest members of the hyalectin family with a core protein of 265-370 kDa and was originally isolated form fibroblasts (Krusius *et al.*, 1987). It has also been located in keratinocytes, smooth muscle cells, brain, kidney and follicle of the mammalian ovary (Iwata *et al.*, 1993, Karvinen *et al.*, 2003a, Lemire *et al.*, 2002, McArthur *et al.*, 2000, Paulus *et al.*, 1996, Reardon *et al.*, 1998, Shibata *et al.*, 1999, Sorrell *et al.*, 1999). It is capable of binding large hyaluronan fragments up to 4 nm (LeBaron *et al.*, 1992) as well as heparan sulphate and heparin (Ujita *et al.*, 1994).

Versican has been located within the theca of the ovarian follicle (McArthur *et al.*, 2000) and has been implicated in the regulation of cell adhesion, migration, pattern formation, and regeneration (Camaioni *et al.*, 1996, Lebaron, 1996, Shibata *et al.*, 2001). It has fewer chondroitin sulphate side chains than aggrecan and as such does not have the same water holding capacity.

Aggrecan consists of a core protein 220 kDa and is secreted by chondrocytes. Aggrecan is the major proteoglycan from cartilage forming a supramolecular (<100 molecules) aggregate with hyaluronan and link protein. Aggrecan attracts large amounts of fluid in to the cartilage, by virtue of its negatively charged sulphate groups allowing the cartilage to cope with high compressive forces (Watanabe *et al.*, 1997).

Neurocan and Brevican are both found in the brain, the former synthesised by neurons and the latter by glial cells. They exist in a soluble matrix, which localises to the plasma membrane. Neurocan is the most abundant chondroitin sulphate proteoglycan in the brain.

1.10.2.2. Non-hyaluronan Binding Proteoglycans

Non-hyaluronan binding proteoglycans carry heparan sulphate or chondroitin sulphate glycosaminoglycans (Noonan *et al.*, 1991). Perlecan is the most complex of this group, which, in addition to perlecan contains agrin and testican. Acting as an anchor for heparan sulphate in basement membranes perlecan allows the formation of structural barriers (Iozzo *et al.*, 1994) and has been shown to interact in extracellular matrix components (Battaglia *et al.*, 1993, Grant & Ayad, 1988, Iozzo *et al.*, 1994). Perlecan has been found as a component in basement membranes of kidney glomeruli and in blood vessels, skin and placenta. It is believed to be involved in cell attachment and is known to interact with laminin, collagen IV, and fibronectin and nidogen components of the basement membrane.

A table, listing members of the modular group can be seen below Table 6

*Table 6 Structure and properties of modular pericellular proteoglycans**

General features	*Designation*	*Protein core*	*Glycosaminoglycan*	*Tissue distribution*
Modular Proteoglycans	Gene product	Size kDa	Type (No)	
Modular multidomain proteoglycans with modules homologous to the Ig superfamily, Selectin, SGF, Laminin, LDL receptor and protease inhibitors	Versican	265-370	CS/DS (10-30)	Blood vessels, brain, skin
	Aggrecan	220	CS (≈100)	Cartilage, brain, blood vessels
	Neurocan	136	CS (3-7)	Brain, cartilage
	Brevican	100	CS (1-3)	Brain
	Perlecan	400-467	HS/CS (3-10)	Basement membrane (BM), cell surfaces, cartilage, sinusoidal spaces
	Agrin	200	HS (3-6)	Synaptic sites of neuromuscular junctions, renal BM
	Testican	44	HS/CS (1-2)	Seminal fluid

*After Iozzo 1996 (Iozzo & Murdoch, 1996)

1.10.3. Glycosaminoglycans in the Ovary

Glycosaminoglycans have been identified in the follicular fluid of pigs (Ax & Ryan, 1979, Sato *et al.*, 1990, Yanagishita & Hascall, 1979), cows (Bellin & Ax, 1987a, Bellin *et al.*, 1983, Grimek & Ax, 1982, Grimek *et al.*, 1984, Lenz *et al.*, 1982) humans (Bellin *et al.*, 1986, Eriksen *et al.*, 1994) and rats (Gebauer *et al.*, 1978, Mueller *et al.*, 1978) and play an important role in fertilisation (Tsuiki *et al.*, 1988). Chondroitin sulphate concentrations in follicular fluid appear to be good indicators of follicular development and oocyte potential (Bellin *et al.*, 1986) with higher concentrations recorded in small follicles compared to that of large (Grimek & Ax, 1982). Relative concentrations also appear to change with respect to health status, the concentrations being higher in atretic follicles than in healthy. However, evidence suggests that there may also be species variation in the level and type of glycosaminoglycans present at any one time (McArthur *et al.*, 2000).

1.10.4. Glycosaminoglycans in Fertilisation

One glycosaminoglycan, which plays a vital role in formation of the cumulus-oocyte complex, is hyaluronan. Prior to the gonadotrophin surge the cumulus cells are tightly packed and in close proximity to the oocyte forming the cumulus-oocyte complex. Hyaluronan

(0.5mg/ml) can be detected with other accessory proteins, namely the heavy chains of namely inter-alpha trypsin inhibitor (ITI), versican, a hyaladherin, known to be present in the ECM of the follicle believed to be important in the expansion of the cumulus oocyte complex (Camaioni *et al.*, 1993, Camaioni *et al.*, 1996, Chen L. *et al.*, 1992, Fulop *et al.*, 1997b). Accumulation of hyaluronan within the cumulus oocyte complex creates a spongy, reversibly deformable matrix, which aids in the protection and extrusion of the oocyte at ovulation (Chen L. *et al.*, 1993b). FSH activates a cAMP response element-binding protein facilitating this process (Canipari *et al.*, 1995). A defect in the ITI-hyaluronan complex has been associated with severe female infertility as a result of defective hyaluronan cumulus oocyte complex matrix formation and failure of cumulus expansion (Zhuo *et al.*, 2001).

1.10.5. Proteoglycans in the Ovary

Proteoglycans have been isolated from ovarian follicles and some have been sequenced and characterised. Heparan sulphate proteoglycans have been localised to the matrix associated with the granulosa cell walls, the concentrations increase during atresia suggesting a role in proliferation and modification of the extracellular matrix (Huet *et al.*, 1997).

Evidence of proteoglycans in the ovary and the follicle has been demonstrated by a number of authors (Drahorad *et al.*, 1991, McArthur *et al.*, 2000, Meng *et al.*, 1994, Rodgers R. J. *et al.*, 1995b). Chondroitin/Dermatan sulphate proteoglycans are synthesised by rat granulosa cells in response to FSH, LH and testosterone stimulation and by porcine granulosa cells in response to FSH stimulation in *invitro* culture systems (Ax & Ryan, 1979, Bellin *et al.*, 1983, Yanagishita *et al.*, 1981). This indicates there is a functional role for FSH in the signalling of production of proteoglycans within the follicle.

Proteoglycans may also be responsible for follicular fluid viscosity and maintenance of follicular shape (Smith J.T & Ketteringham, 1937). They have been implicated in ovarian cell growth, differentiation, proliferation, migration and water homeostasis as well as growth factor binding (Ax & Ryan, 1979, Bellin *et al.*, 1983, Hildebrand *et al.*, 1994, Kobayashi *et al.*, 1999, Yamaguchi & Ruoslahti, 1988).

In other systems in the body as explained above proteoglycans bind to extracellular matrix components such as fibronectin, collagens and laminins and as a result increase the stability of the extracellular matrix. It is likely that they perform the same role within the follicle. Follicular fluid proteoglycans isolated by fractionation and chromatography show that they range in size from 7.5×10^5 to 2×10^6 and contain large chondroitin sulphate proteoglycans and smaller HS proteoglycans (Grimek & Ax, 1982, Yanagishita *et al.*, 1979). Characterisation, of some proteoglycans produced by rat ovarian granulosa *in vitro* have shown that these proteoglycans include three hydrodynamic sizes of dermatan sulphate and

two different hydrodynamic sizes of heparan sulphate proteoglycans bound intercellularly, to the cell surface or cell membrane (Yanagishita & Hascall, 1979, 1983a, b, 1984a, b). Due to their large size proteoglycans are unable to diffuse across the basal lamina from membrana granulosa in to or out of the follicle (Shalgi *et al.*, 1973). As a result most are likely to be synthesised by granulosa cells and must also be degraded within the follicle. Yanagishita was one of the first people to suggest that a role for proteoglycans may lie in their ability to create an osmotic gradient down which fluid from the thecal layers moves in to the antrum however; he did not test the hypothesis (Yanagishita *et al.*, 1979).

1.11. Summary

The development of the follicle is tightly controlled by hormones and associated growth factors. During the maturation process the follicle grows at different rates and this requires the surrounding stroma and the follicle layers to undergo tissue remodelling via cell proliferation, differentiation and migration and angiogenesis. In addition, the mammalian follicle must form a fluid filled antrum. Proteoglycans are major components of the extracellular matrix and are involved in many of the processes named above. Additionally, proteoglycans and glycosaminoglycans have been identified within the follicular basal lamina and follicular fluid. The formation of the antrum is crucial to follicular expansion, supply of growth factors to the oocyte and buffering of external influences. Follicular fluid also appears essential to expulsion of the oocyte at ovulation. The commonest cause of anovulation, polycystic ovarian disease (PCO), is failure of the follicle to grow past 5mm diameter. IVF or ovulation-induction programs determine follicle growth by ultrasonography and follicular fluid accumulation. Evidence indicates that the granulosa cells produce proteoglycans. The accumulation of these proteoglycans within follicular fluid may provide the osmotic forces necessary to drive follicular fluid accumulation in ovarian follicles.

1.12. Hypothetical model of Follicular Fluid Accumulation Mechanism

A model of the proposed fluid accumulation mechanism can be seen in (Figure 7). The model assumes that there are sufficient proteoglycans present in the fluid to increase the osmotic potential of the fluid.

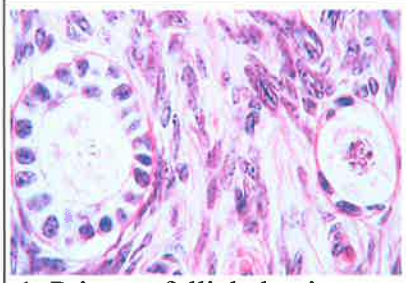

1. Primary follicle begins growth and GCs produce PGs

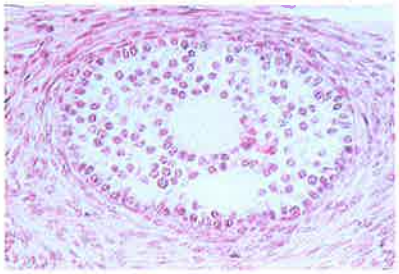

2. Slow antrum formation begins, with pockets of fluid accumulating within the follicle

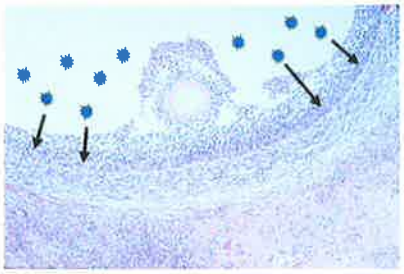

3. Rapid accumulation of FF begins with increased production of PGs

4. PGs and their GAGs too large to escape the basal lamina increase the specific negativity of the fluid via sulphate groups on the GAGs causing an osmotic differential either side of the basal lamina.

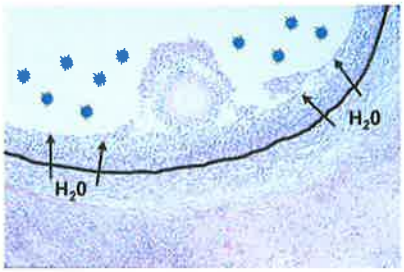

5. The osmotic differential draws water and small serum molecules into the follicle where they combine with some of the PGs present to form large aggregates thus increasing the colloid osmotic pressure further. Alternatively hydrolysis of the PGs may result in increased colloid osmotic pressure (Zachariae 1958; Zachariae and Jensen 1958).

6. The colloid osmotic pressure differential is maintained during the rapid fluid accumulation process. Local degradation of the PGs then occurs by core degradation and release of GAGs into the fluid where they are degraded further or cleared through normal vascular exchange routes.

Figure 7 Model of the proposed follicular fluid accumulation process.

1.13. Thesis Aims

The goal of this thesis is to:

- To determine whether proteoglycans and glycosaminoglycans contribute to the osmotic potential of follicular fluid from healthy and atretic follicles with the aim of determining the classes of the key contributors to this potential.

- Identify the proteoglycans and glycosaminoglycans involved by a variety of techniques including ion exchange and size exclusion chromatography, ELISA, Western blotting, and immunohistochemistry.

- Localise their production to key cell types within the follicle and:
- Identify the cell types expressing the molecule with the greatest effect on the colloid osmotic pressure of the follicle during antrum expansion.

- Characterise the expression of the key molecule contributing to the colloid osmotic pressure in follicles during antral development. Determine the expression pattern in healthy and atretic follicles to identify any differences between the follicle types.

- Propose a role for these proteoglycans and glycosaminoglycans in follicular fluid formation.

The data provided by this thesis aims to provide greater understanding of the mechanisms involved in fluid accumulation within the follicle and provide information on whether this process can be driven by osmosis. The information provided on follicular fluid accumulation will undoubtedly assist women in ovulation-induction programs and IVF programs. It may also be important in the understanding of polycystic ovary disease where no antrum is formed in the follicle resulting in infertility.

This project will add significantly to our knowledge of follicular fluid accumulation processes.

Chapter 2 Materials and Methods

2.1. Introduction

The first objective of the studies described in this thesis was to design a method of measuring the colloid osmotic pressures of bovine follicular fluid and serum. In doing so to identify any differences in colloid osmotic pressure between the follicular fluids from healthy and atretic follicles, follicles of different sizes and serum. The second objective of this study involved the identification of the classes of molecules, which contributed the greatest proportion of the measured potential. The third objective was to identify some of these molecules and assess the expression profile within the bovine ovarian follicle of the key molecules contributing to the fluid accumulation process within the follicle.

The methods described in this chapter were set out to reflect the logical progression of experiments aimed at identification of a dialysis system, which would allow the removal of different sizes of molecule. This analysis would allow identification of which molecules were able to enter the follicle across the "blood-follicle" barrier. Also described are methods for isolation of follicles from whole bovine ovaries and collection of follicular fluids for colloid osmotic pressure determination. Once collected, the class and identity of some of the molecules responsible for the colloid osmotic pressure, was characterised. Finally having assessed the colloid osmotic pressure from fluid and identified key molecules involved, the expression profile of one the molecules from this group was investigated. Also described are methods for the polymerase chain reaction (PCR) amplification of the bovine specific enzymes responsible for the synthesis of the identified molecule and the construction of plasmids and probes for use in Northern blots and in situ hybridisation experiments. A detailed compilation of materials commonly used and reagents and their suppliers can be found in appendices A and B.

2.2. Materials

2.2.1. Colloid Osmotic Pressure Determination and Proteoglycan Identification

Animal tissues were collected from the local abattoir (Cooma Abattoir, Polo Flat Rd, Cooma, NSW and Lobethal Abattoir Pty Ltd, Ridge Rd, Lobethal, SA). Earle's balanced-salts (EBSS) (#E6132), decorin sulphate, 2,2'–azino-di- (3-ethylbenzthioazoline-6-sulphonic acid) DEAE sephacel and CL-2B sepharose were obtained from Sigma Chemical Company, St Louis, MO. Enzyme suppliers were: Sigma Chemical Company (St Louis, MO) for DNase 1 and Heparanase 1; Seikagaku Corporation, Tokyo, Japan for *Streptomyces* hyaluronidase, chondroitinase ABC and keratanase. Proteinase K was obtained from Boehringer Mannheim, Mannheim, Germany, and collagenase 1 from ICN Biomedicals Seven Hills, NSW, Australia.

Dr. Tracey Brown, Department of Biochemistry, Monash University, Victoria, Australia kindly donated hyaluronic acid standards. Membranes for dialysis were from Pierce, Rockford, USA. A 10 kDa was used to replace the standard 10 – 30 kDa membrane supplied by the manufacturer in the osmometer. The 10, 100, 300, 500 kDa membranes used in dialysis were purchased from Millipore Corporation, Bedford, USA. The colloid osmometer was a Gonotec 050 from Gonotec GmbH, Berlin, Germany. Albumex ® 4 was from CSL Ltd., Parkville Vic. Australia, SDS gels were from Gradipore, French's Forest, NSW, Australia, Novex Tris Acetate gels, and SSP1 DNA marker (DMW-S1) were from Geneworks Adelaide Australia, Gel Code Blue, super signal chemiluminescence western blotting kit and Bradford assay kit were from Pierce, Rockford, USA, Stains-all from Bio-rad laboratories, Hercules, CA, and uronic acid standards were from Sigma Chemical Company. Scintillation fluid used was Wallac optiphase Hisafe3 from Perkin – Elmer Life Sciences Wallac OY Turku Finland. Safsolvent was obtained from Ajax chemicals Australia (#3260-25G), and Gurr® DePeX mounting medium (BDG#361254DX).

Hybond C+ and Hybond P (PVDF) membranes were from Amersham Pharmacia Biotech, Piscataway, New Jersey, USA. All other chemicals were reagent grade from Sigma Chemical Company.

2.2.2. In Situ Assays and Hyaluronan synthase (HAS) PCRs and Northern Blots

Primers were made and supplied by Sigma Genosys Castle Hill Australia Pty Ltd, PCR kits used were from Invitrogen (#10342-053), pGem-T-Easy vector system (#A1380) was from Promega, Annandale, NSW, Australia, L-broth and L agar from Difco laboratories, Detroit, Michigan, USA. The plasmid purification kit (#12145) and protocol were from Qiagen, Clifton Hill, Victoria, Australia. DIG riboprobe kit (#1175025), CDP-star®, NBT and BCIP and IPTG and X-Gal and Sheep anti-dig alkaline phosphatase secondary antibody were from Roche Diagnostics, Mannheim, Germany. RNase inhibitor (RNasin), SP6 (#1487671) and T7 (#0881775) RNA polymerase were from Promega, Annandale, NSW, Australia. APES (#3648), DEPC and Ampicillin (#A9393) from Sigma Chemical company, St Louis, MO USA. Hybond C extra, Hybond N+ were from Amersham Piscataway, NJ, USA. tRNA (*Escherichia coli* tRNA RNase free) from Boehringer Mannheim, Germany, normal goat serum, RNA later (#AM 7020) and RNABee (#BL-104) were from Geneworks, Adelaide, Australia, DNase I (AM-1906) and Random hexamers and millennium RNA markers were from Geneworks, DIG easyhyb mix (#1796895) from Boehringer Mannheim.

2.2.3. Proteoglycan Identification

2.2.3.1. Antibodies

The primary monoclonal antibodies used in proteoglycan (PG) identification by ELISA and Western blots are described below. Primary antibody directed toward 4-sulphated chondroitin sulphate/dermatan sulphate (CS/DS) (2B6) (Caterson *et al.*, 1985) 6-sulfated CS/DS (3B3) (Caterson *et al.*, 1985) were purchased from ICN and aggrecan (1C6) (Caterson *et al.*, 1985) was purchased from Developmental Studies Hybridoma Bank (DSHB) Department of Biological Sciences, The University of Iowa, Iowa City, IA, USA. Antibodies recognising bovine decorin (LF94) and bovine versican (GAGβ), recognising the GAGβ, domain present in splice variants V_0 and V_1 (Schmalfeldt *et al.*), were obtained from Drs Larry Fisher, Bone Research Branch, National Institutes of Health, Bethesda, MD and Dieter Zimmermann, Molecular Biology Laboratory, Department of Pathology, University of Zurich, Switzerland respectively. The antibody recognising heparan sulphate (HS) containing the PG perlecan (A76) was kindly donated by Dr. Anne Underwood, CSIRO Molecular Science, North Ryde, NSW, Australia. The antibody recognising human inter-alpha-trypsin inhibitor (ITI) (A0301) (Salier *et al.*, 1987) was from Dako, Glostrup, Denmark. The antibody recognising hyaluronic acid binding protein (HABP) (Cat. # 400763) was from Siekagaku America, MA USA. Secondary antibodies used sheep anti-mouse IgG conjugated to horseradish peroxidase, and sheep anti mouse conjugated to streptavidin IgG were supplied by Silenus laboratories, Victoria, Australia. Secondary antibody Goat anti-rabbit was from Chemicon Australia, Victoria, Australia.

2.3. Methods

2.3.1. Introduction

This research was conducted using the cow since it represents an ideal model for the study of the ovary in view of the fact that the ovary and follicles are of a similar size to human, with comparable fluid volumes. The ovary of the cow could be easily obtained from the slaughterhouse and the medium to large follicles, were amenable to the collection of large amounts of fluid required for the analyses conducted in this thesis. In addition there was a good supply of literature on the appropriate collection and handling of fluid. There was also some data available on certain constituents of fluid and limited sequence data available in Genbank for key candidates.

2.3.2. Tissue Collection Protocols

Ovaries were collected from cycling heifers of mixed breeds of *Bos taurus*, visually assessed as being non pregnant, from the local abattoir within 20 min of slaughter and placed

in to HEPES-buffered EBSS, pH 7.5, containing 10 mM N-ethylmalemide, and protease inhibitors 5 mM benzamidine, 0.5 mM phenylmethlsulphonylfluoride, 1 μg/ml pepstatin A, 1 μg/ml leupeptin, 0.01 M EDTA and 0.1% sodium azide. The ovaries selected had no apparent abnormalities and were transported on ice to the laboratory where they were rinsed in EBSS.

Whole follicles were used in size exclusion experiments see section 2.7.

Fluid from follicles of 2 – 16 mm diameter was used in the initial experiments of the determination of colloid osmotic pressure.

2.3.3. Tissues for Follicular Health Determination

Tissues for the histology experiments were dissected in to 4% formaldehyde in 0.2 M phosphate buffer and allowed to fix overnight 4°C. Following fixation the tissues were embedded in paraffin and 5 μm-thick sections cut on to (3-Aminopropyl) triethoxysilane (APES) treated slides.

2.3.4. Tissue Collection for Fluid Analysis

On arrival in the laboratory selected ovaries were rinsed in cold EBSS at room temperature and then individual follicles were dissected from the ovary using a #22 sterile scalpel blade. Each follicle was stored in cold EBSS until punctured for fluid collection.

In initial experiments follicles were categorised on size alone. These categories were as follows: size 1 = 2-4 mm, size 2 = 4-6 mm, size 3 = 7-9 mm. size 4 = 10-12 mm, size 5 = 13-16 mm, size 6 = 16+ mm.

2.3.5. Tissue Collection for In Situ Hybridisation Assays

Tissues for histology and in situ hybridisation experiments, were dissected in to 4% formaldehyde in DEPC treated 0.2 M phosphate buffer and allowed to fix overnight 4°C.

2.3.6. Tissue for RNA, cDNA synthesis and PCR

100, 120 and 160-day bovine foetuses were collected on ice from the local abattoir. The amnion was kept intact until the foetus was removed to prevent contamination of the tissues prior to collection. Tissues to be used for RNA and subsequent cDNA synthesis (see 2.22 and 2.23) were dissected using sterile RNase free instruments in to RNA later or RNABee on ice.

2.4. Follicular Fluid Collection

All procedures were carried out on ice or at 4°C. Antral follicles (n = 171) 11 – 16 mm in diameter were isolated from whole ovaries (1 follicle/ovary) for the determination of the

colloid osmotic pressure of the fluid. Follicular fluid was aspirated with a 23G hypodermic needle and a 1 or 2 ml syringe within 2 h of slaughter. The fluid samples were centrifuged at 2000 r.p.m for 30 min in order to remove cellular debris and protease inhibitors (5 mM benzamidine, 0.5 mM phenylmethlsulphonylfluoride, 1 μg/ml pepstatin A, 1 μg/ml leupeptin, 0.01 M EDTA and 0.1% sodium azide) were added before storage at –20°C. The remaining follicle walls were then fixed in Bouin's solution and embedded in paraffin and processed for histological examination (see section 2.5). Histological assessment of follicular health was undertaken by light microscopy analysis of hematoxylin and eosin-stained 5 μm-thick sections using an Olympus BX50 microscope (see section 2.5.1). On completion of assessment of follicular health, fluid samples were pooled based on their health status. Each pool of fluid from healthy follicles comprised 10 follicles and each pool of fluid from atretic follicles comprised 8 follicles with 4 pools used for each health status.

Individual follicles in the range of 2 - 20 mm, not characterised for health status were harvested and fluid extracted from them as described above for initial determinations of colloid osmotic pressure evaluation. Follicles in a range of sizes from 2 - 15 mm were isolated for the determination of ITI levels and their fluid harvested as above. In addition a large pool of fluid from unclassified antral follicles of all sizes was collected as above for chromatographic isolation. In all experiments bovine serum was used as a control. Bovine serum was obtained by centrifugation of whole blood collected from an 18-month non-pregnant cycling heifer.

2.5. Histology

Tissue sections were deparaffinised in xylene or safsolvent (2x 10min) and re-hydrated through descending grades of alcohol 2x 100%, 1x 95%, 90%, 70%, 50%, H_2O (2 min). Following this the sections were stained with haematoxylin and eosin. Briefly, paraffin sections that had been de-waxed as above were stained with haematoxylin for 4 min and then rinsed in running tap water before being placed in ammonia water (0.5%) 5 - 10 sec. Following this the slides were then washed again with running tap water and placed in to 1% HCl for 5 - 10 sec and the tap water step repeated followed by a second ammonia wash and a further tap wash. Next the slides were placed in eosin stain for 1 min followed by a wash with tap water and dehydration to safsolvent through an alcohol series and finally cover-slipped using Gurr® DePeX mounting medium.

2.5.1. Histological Assessment of Follicular Health

Isolated follicles were classified according to their health status as defined by (Irving-Rodgers *et al.*, 2001). Briefly, follicles were designated as antral atretic if they had numerous

pyknotic nuclei in the layers of the membrana granulosa closest to the antrum or in the antrum itself in close proximity to the membrana granulosa. Follicles where the granulosa cells in the cell layer adjacent to the basal lamina appeared to have lost contact with the basal lamina and the remaining granulosa cells had increased numbers of pyknotic nuclei (> 10%), were designated as being basally atretic. Follicles were designated as healthy if they had many well-rounded granulosa cells in close association with each other and none of the atretic changes noted above.

2.5.2. Histological Preparation of Tissues for In Situ Hybridisation

Following fixation the tissues were embedded in paraffin and 5 μm-thick sections cut on to RNase free APES treated slides. Tissue sections were then deparaffinised in xylene or safsolvent (2x 10min) and rehydrated through descending grades of alcohol made up in DEPC treated water in RNase free glassware 2x 100%, 1x 95%, 90%, 70%, 50%, H_2O (2 min).

2.6. ITI and Versican GAGβ in the Follicle

2.6.1. Extraction of Surface Proteins from Granulosa and Theca Cells

In order identify whether ITI and versican GAGβ were bound to the granulosa cells of the follicle two extraction methods were employed to a) remove weakly bound membrane proteins using 3-[(3-Cholamidopropyl) dimethylammonio]-1-propanesulfonate (CHAPS) and 2) tightly bound membrane proteins using sodium dodecyl sulphate (SDS).

2.6.1.1. Granulosa Cell Collection

Granulosa cells were obtained by horizontal slicing of a follicle to release the follicular fluid and then gentle agitation of the cell wall with the blunt side of the blade to release the granulosa cells. Granulosa cells were pooled from similar sized follicles and collected in to EBSS at 4°C. Once the collection was complete the granulosa cells were centrifuged at 1300 r.p.m and the EBSS removed, fresh EBSS was added and the cells re -centrifuged and the EBSS again removed.

2.6.1.2. CHAPS Extraction

Granulosa cells were placed in CHAPS extraction buffer 9.5 (1 ml) and allowed to sit on ice for 30 min, before centrifugation at 1300 r.p.m. The supernatant was removed and stored at –20 °C until used in subsequent assays

2.6.1.3. SDS Extraction

Granulosa cells were placed in SDS extraction buffer 9.6 (1 ml) and boiled at 95°C for 5 min, before centrifugation at 1300 r.p.m. The supernatant was removed and stored at – 20°C until used in subsequent assays.

The separation of extracted proteins was carried out by small format SDS polyacrylaminde gel electrophoresis (PAGE) (see section 2.15.2) and the proteins transferred to polyvinylidene fluoride (PVDF) membrane for subsequent immunoblotting (see section 2.16).

2.7. Dextran Experiments

Dextran of known sizes was obtained from Sigma Aldrich. Sizes of dextran obtained were 10.5 kDa, 67.3 kDa, 188 kDa, 2 x 10^6 Da. Solutions of 0.1 mM dextran were used in all experiments. Whole follicles (n = 5) were blotted dry of media and weighed on a fine balance then immersed in the dextran solutions of differing molecular weights for a period of time determined by earlier volume equilibrium experiments (not shown). These experiments had determined the time taken for the follicle to stabilise its weight for each size category of follicle and for each size of dextran molecule in solution. The follicle was then reweighed following immersion. % Gain or loss was recorded as % of total follicle weight.

2.8. Colloid Osmotic Pressure Determination of Follicular Fluid

2.8.1. Dialysis Membrane Selection

A number of membrane systems were selected for appraisal based on stability of pore size, protein binding capacity and holding volume. A series of experiments were designed to determine which membrane would perform best under conditions set for the dialysis protocol. The criteria set for good performance were low protein binding, consistency of pore size at 37°C and efficiency of clearance of molecules below the molecular weight cut off (MW cut off) given by the manufacturers. In addition the dialysis unit had to be able to hold a minimum volume of 540μl required for subsequent analyses.

The experiments involved a 1:10 dilution of follicular fluid sample with EBSS followed by dialysis against water containing 0.1% sodium azide for 24h at 4°C. The efficiency of the membrane dialysis was assessed by determination the concentration of the remaining proteins and SDS PAGE to check the size of the protein products removed.

2.8.2. Temperature and Salt Dependent Dialysis

The effect of salt and temperature on the efficiency of dialysis of follicular fluid products was tested. This was done following initial tests of colloid osmotic pressure

following enzyme dialysis with Streptomyces hyaluronidase and chondroitinase ABC where an increase in potential was recorded. This suggested that multiple degraded hyaluronan and CS/DS units were re-aggregating as proposed by (Turner *et al.*, 1988) and/or not escaping the membranes during dialysis as suggested by (Lord, 1999). Initially follicular fluid diluted in EBSS (1:10) was digested with S. hyaluronidase and either dialysed or not dialysed against ultrapure water containing sodium azide in a 100 kDa membrane at 4°C and 37°C. If they were not dialysed the samples were held at the same temperature as its dialysis counterpart. Significant differences were noted but there was still incomplete removal of the breakdown products therefore salt was added to the dialysis step (2M NaCl) as suggested by Turner. Following digestion the samples were dialysed against 2M NaCl and then through a series of 0.75, 0.5, 0.25 M NaCl to water at both 4°C and 37°C and then colloid osmotic pressure recorded. Bovine serum in EBSS (1:10) was used as a control. Following dialysis the samples were snap frozen and lyophilised and then resuspended in their original start volume in EBSS prior to colloid osmotic pressure tests.

Table 7 Treatment profile to test effect of temperature on dialysis

Sample	Enzyme treatment	MW cut off	Dialysis	Dialysis temperature (°C)
Follicular fluid	None	100 kDa	+	37
	S.hyaluronidase	100 kDa	+	37
	None	100 kDa	-	37
	S.hyaluronidase	100 kDa	-	37
	None	100 kDa	+	4
	S.hyaluronidase	100 kDa	+	4
	None	100 kDa	-	4
	S.hyaluronidase	100 kDa	-	4

2.8.3. Size Exclusion Dialysis

In order to determine the contribution of the macromolecular components in the aspirated fluids, the follicular fluid samples (54 μl) were diluted 1 in 10 with EBSS and placed in membranes of differing molecular weight cut off 10, 100, 300, 500 kDa and dialysed against distilled water containing sodium azide (0.1%) for 24 h at 4°C. These membrane sizes were chosen to allow removal of low molecular weight molecules and electrolytes (10 kDa), molecules known to be able to traverse the basal lamina freely (100 kDa), molecules of a size able to enter the follicle in reduced concentrations (300 kDa) and retain those liable to have been made locally within the follicle (500 kDa). Following dialysis samples were freeze-dried before reconstitution to their pre-dialysis volumes (540 μl) with EBSS and colloid osmotic pressure measurement. An aliquot of this material (4 μl) was

retained and assessed by 10% SDS- PAGE according to the method of (Laemmli, 1970) to confirm the removal of appropriately sized molecules.

2.8.4. Enzyme Digestion of Follicular Fluids

To quantify the contribution of classes of molecules to the colloid osmotic pressure of follicular fluid, samples (54 μl) were diluted 1 in 10 with EBSS, pH 7.5 to a total volume of 540μl, and treated with a range of enzymes (Table 8). Control pools of undigested fluid were held at 37°C or 25°C for 4 h whilst enzyme treatments were underway. Following digestion, dialysis (100 kDa or 300 kDa) was carried out against 2 M NaCl, 24 h at 37°C. Dialysis at high salt concentrations and temperature was necessary in this experiment to ensure removal of potentially aggregating digested molecules (Turner 1988). All samples were then dialysed against distilled water for 24 h at 4°C. The samples were stored freeze-dried and reconstituted to their original volumes in EBSS prior to colloid osmotic pressure measurement. Once again an aliquot of this material (4 μl) was assessed by 10% SDS -PAGE to confirm the removal of appropriate molecules. The colloid osmotic pressure of the fluid samples was measured as described below.

Table 8 Enzyme digestion conditions of follicular fluid

Enzyme	Conditions	Source	Substrate
DNase I	5mg/ml/37°/pH7.0	Sigma	DNA
Proteinase K	0.1mg/ml/37°/pH7.2	Boehringer	Proteins
Streptomyces hyaluronidase	0.14U/20μl/37°/pH7.2	Seikagaku	Hyaluronic acid
Chondroitinase ABC	0.02U/20μl/37°/pH8	Seikagaku	Chondroitin/Dermatan sulphate
Keratanase	0.02/20μl/37°/pH6	Seikagaku	Keratan sulphate
Collagenase I	100U/ml/37°/pH7.4	Sigma	Collagen
Heparanase I	1U/ml/25°/pH7.5	Sigma	Heparan sulphate
No enzyme control 1	25°/pH7.5		
No enzyme control 2	37°/pH7.2		

2.8.5. Gonotec 050 Osmomat Osmometer

The colloid osmotic pressure was measured using a Gonotec 050 osmomat osmometer with a reference membrane of 10 kDa molecular weight cut-off. All solutions were de-gassed via a vacuum pump for 20 min prior to colloid osmotic pressure measurement. The reference solution was EBSS. The experiments were performed with EBSS in order to maintain high ionic strength and thus minimise charge interactions of the molecules and decrease the Donnan effect to the colloid osmotic pressure. In this way steric exclusion is the main effect, this allows ascertainment of the degree to which macromolecules affect colloid osmotic pressure. All measurements of colloid osmotic pressure were recorded as cm of water and

repeated four times against a 10 kDa membrane at room temperature. Bovine serum (diluted 1:10 with EBSS) was used as a control in each batch of measurements.

The Gonotec 050 osmometer measures the colloid osmotic pressure of a solution by means of an osmotic cell. In this experiment the lower half of the osmotic cell, which is closed off to the outside, was filled with electrolyte-containing EBSS solution. The upper half of the cell, which is open to the outside, was filled with the sample solution. A semi-permeable membrane separates the two halves of the cell from one another; in this case a 10 kDa MW cut off was used. This membrane possesses defined pores through which only water and electrolyte molecules can permeate. When there is an colloid osmotic pressure differential between two solutions, solvent permeates from the lower in to the upper half of the measuring cell until equilibrium is reached between the underpotential in the lower half of the cell and the osmolal concentration of the colloids. An electronic potential measuring system, which is mounted in to the lower half of the cell, transduces the underpotential in to an electric signal, which is shown on a digital display. The cell volume is 10 μl with the sample quantity required being approximately 150 μl. The resultant colloid osmotic pressure is displayed as mm water (± 0.05 mm water). An image of the Gonotec Osmomat 050 osmometer can be found in (Figure 8)

2.8.5.1. Calibration of the Osmomat 050 Osmometer

Calibration of the osmometer was carried out according to the manufacturers instructions. A reference solution of commercially available albumin (Albumex® 4) of known colloid osmotic pressure was used in order to provide a consistent colloid reference in addition to the machine calibration. Albumex® 4 was chosen since albumin is the component which contributes most of the potential of serum and has been identified in the extracellular space of connective tissues. Calibration of the machine was done prior to colloid osmotic pressure measurement and then at eight sample intervals.

2.8.6. Colloid Osmotic Pressure Measurement

150 μl of sample reference solution was injected in to the sample port and two colloid osmotic pressure readings were obtained at equilibrium (approx 1 min). This represented the highest and the lowest reading obtained. If the two readings were identical or within 0.2 mm water the reading was accepted and recorded, outside of this range the osmometer would not give an "accept result" tone. The machine was then rinsed three times with EBSS and allowed to return to zero before the next sample was tested.

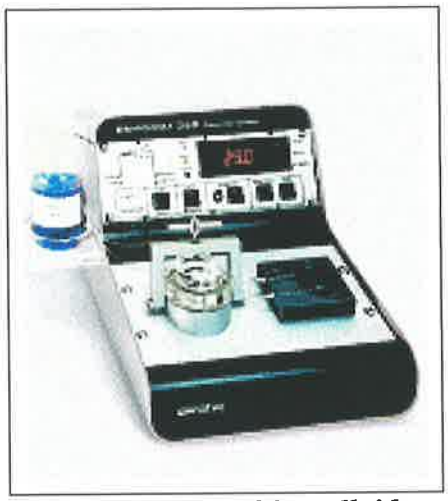

Figure 8 Image of Gonotec 050 Osmomat used in colloid osmotic pressure measurements of follicular fluid. Image obtained from (http://www.gonotec.com).

2.9. Confirmation of Dialysis for Size Exclusion and Enzyme Digestion

The removal of certain sized molecules was confirmed using SDS PAGE. For the methodology see 2.15.2.

2.9.1. GelCode® Blue Staining of Polyacrylamide Gels

Following gel electrophoresis the gel was removed in to a clean tray and rinsed 3 x 5 min with 100-200 ml of ultra pure water. GelCode® Blue was then gently resuspended according to the manufacturers instructions and 20 ml added per 8 X 10 cm gel for 1 h to stain the gel. Once stained the gel was placed again in to several changes of ultra pure water over a 2 h period to develop weaker protein bands. The gel was then photographed and dried see section 2.15.4.

2.10. Proteoglycan Extraction

The proteoglycans of interest in follicular fluid are the soluble proteoglycans. To this end a method was chosen which would allow for the specific extraction of soluble proteoglycans within the follicular fluid. The method chosen was derived from that of Savolainen (Savolainen, 1999). Soluble proteoglycans were extracted from 40 ml pools of follicular fluid from unclassified follicles using the standard method of 4 M urea and 0.05 M sodium acetate at pH 7.5. Pools of frozen follicular fluid, which had previously been centrifuged to remove particulate matter, were defrosted on ice and mixed 1 to 5 with the urea/sodium acetate mix. The use of urea ensures denaturing conditions are maintained; the urea also prevents protein macromolecule interactions and protein precipitation events that may result in a decrease in yields. Extraction at 4°C also reduces denaturing of the sample. The maintenance of high pH aids in the separation of proteoglycans from macromolecules and thus improves separation.

2.11. Ion Exchange Chromatography

Isolated follicular fluid proteoglycans in 4 M urea; 0.05 M sodium acetate buffer, pH 7.5, were applied to 5 ml of DEAE-Sephacel ion exchange column at 4°C. Anion exchange beads bind the negative charges of the sulphate groups from the attached glycosaminoglycans while allowing passage of positively charged molecules. Ion exchange chromatography allows separation of proteoglycans from a large proportion of soluble proteins within follicular fluid. The column was washed with 10 volumes of 4 M urea in 0.05 M sodium acetate buffer, pH 6.0. Proteoglycans were eluted from the column in the same buffer containing 2 M NaCl. The fractions containing proteoglycans, as determined by uronic acid measurement (see section 2.13.2), were pooled due to the low amounts of glycosaminoglycan

present within the extracts, dialysed at 4°C in a 3500 Da snake dialysis membrane from Pierce against water and lyophilised.

2.12. Size Exclusion Chromatography

Further characterisation of the extracted PGs was carried out by size exclusion chromatography. The sample obtained from the ion exchange column above was resuspended in 500 μl of 2 M guanidine-HCl, 0.1 M sodium acetate, 0.05 M Tris, pH 7.5, and applied to a Sepharose CL-2B (6.5 mm x 1000 mm) size exclusion column at a flow rate of 5 ml/h. Forty-five ml of column buffer was run through the column and ninety 500 μl fractions were collected, dialysed against ultrapure water and lyophilised for analysis of protein using the Bradford assay method and glycosaminoglycans (GAGs) using the carbazole method published by (Blumenkrantz & Asboe-Hansen, 1973). 300 μl of each collected fraction was retained for enzyme-linked immunosorbent assay (ELISA) see section 2.14.

2.12.1. V_0/V_t Determination

V_0 is the void volume of the column and V_t the total volume of the column. These fractions in the column need to be identified in order to know where the sample fractions have been eluted. In order to determine the position of the column front (V_0) and final fraction (V_t) a sample was mixed with 500 μl of column buffer containing 20 μl of radioactive carbon (14C) and loaded on to the size exclusion column. Ninety 500 μl fractions were collected at a flow rate of 5ml/h. Each fraction was then added to 400 μl of scintillation fluid and counts per minute recorded on a Wallac 1409 scintillation counter. The peak in counts shows the end of the column.

2.13. Protein and Glycosaminoglycan Determination

2.13.1. Quantitative Protein Determination

Protein concentrations were assayed by a method derived from the Bradford assay (Bradford, 1976) using a kit from Pierce chemicals. Kit constituents were reagent MA containing sodium carbonate, sodium bicarbonate and sodium tartrate in 0.2M sodium hydroxide, reagent MB containing 4% Bicinchonic acid (BCA) and reagent MC containing 4% cupric sulphate, pentahydrate in water. The working reagent was prepared by mixing 2 parts MC with 48 parts MB and then adding 50 parts MA. The assay was carried out in a micro titre plate where a set of protein standards was set up using decreasing dilutions of bovine serum albumin that covered the expected range of the sample protein concentrations. To a micro titre plate 100μl of each standard or sample was placed in a well, to this was added

100μl of working reagent. Samples were mixed for 30 sec on a plate shaker. The plate was then covered and incubated for 2 hours at 37°C, the absorbance was then read at 595 nm on a Bio-rad micro plate reader # 170-6935 and a standard curve plotted using micro plate manager software version 2.1 and the sample concentrations determined by extrapolation from the standard curve.

2.13.2. Glycosaminoglycan Determination

2.13.2.1. Estimation of Glycosaminoglycan (GAG) from Whole Follicular Fluid

Estimation of GAG from whole follicular fluid and bovine serum required pre-treatment of the samples with fresh 0.5 M NaOH at room temperature overnight with stirring to remove the protein components from the samples. The samples were pre-treated with S.hyaluronidase and chondroitinase ABC in order to determine the relative amounts of chondroitin sulphate and hyaluronan present.

2.13.2.2. Estimation of Glycosaminoglycan from Isolated Column Fractions

GAG concentrations were determined by assaying the uronic acid concentration according to the method of Blumenkrantz and Asboe-Hanson (1973). This method was used since it was anticipated, from previous assays of whole follicles (McArthur *et al.*, 2000) that only small quantities of GAG would be present and this method is sensitive to ng quantities of GAG. Briefly, a sample fraction from the column isolations containing an estimated 05 to 20 μg of uronic acid was added 1.2 ml of sulphuric: acid containing 0.0125M sodium tetra borate, tubes were chilled on ice and then vortexed for 2 min and the tubes heated for 10 min at 100°C. Samples were cooled again and 20μl of metahydroxyphenyl reagent (0.15%) in 0.5% sodium hydroxide added and the tubes vortexed for 30 sec. The absorbance was read within 5 min at 520 nm in a spectrophotometer. The carbohydrate forms a pink brown chromogen with the sulphuric acid: sodium tetraborate at 100 °C. A blank tube containing no sample and standard curve using D-glucuronic acid lactone at concentrations of 0, 1, 2, 5, 10 and 20 μg were also set up for each assay. Uronic acid concentrations of the samples were determined by extrapolation from the standard curve.

2.14. Enzyme-Linked Immunosorbent Assay (ELISA)

2.14.1. ELISA Method

ELISA using a panel of antibodies directed against epitopes of interest was used to identify the GAGs present in column fractions. These antibodies were specific to versican, decorin, aggrecan, perlecan and ITI and general antibodies to 4 sulphated

chondroitin/dermatan sulphate (CS/DS) and 6 sulphated CS/DS. Samples (10 μl) to be tested were diluted in 140 μl of phosphate buffered saline (PBS) and incubated for 1 h at 37°C in 96-well plates. The wells were then rinsed in PBS/Tween 20 (0.05%) and incubated with 0.1 ml PBS containing 1% skimmed dehydrated cows' milk and the appropriate dilution of primary antibody [1:1000- for ITI (A0301), versican (GAGβ), 4-sulfated CS/DS (2B6), 6-sulfated CS/DS (3B3) and aggrecan (1C6)] and incubated for 1 h at 37°C. The secondary antibodies were sheep anti-mouse IgG conjugated to horse-radish peroxidase for the mouse monoclonal antibodies, and goat anti-rabbit conjugated to horse-radish peroxidase for the rabbit polyclonal antibodies, diluted at 1/2000-1/5000 in PBS 1% milk and incubated for 1 h at 37°C. Horseradish peroxidase was measured as a colour reaction using 100 μl of 2,2'–azino-di- [3-ethylbenzthioazoline-6-sulfonic acid] (ABTS) as substrate with 0.01% hydrogen peroxide. The optical density was recorded at 415 nm.

2.14.2. Pre-treatment of Samples

2.14.2.1. Chondroitinase ABC Digestion

Samples analysed for 4-sulphated CS/DS or 6-sulphated CS/DS required pre-digestion with chondroitinase ABC. Briefly an aliquot of proteoglycan extracted from follicular fluid was treated with chondroitinase ABC (0.5 units per 10ml in 0.1M Tris acetate buffer containing 0.1% BSA pH 8.0) lyase to expose the antigen. Samples were treated in the same 96 well to which they had been previously attached and incubated for 1 hour at 37°C.

2.14.2.2. Dithiothrietol Reduction

Samples analysed for the presence of aggrecan using the 1C6 antibody required a reduction treatment with DL-dithiothrietol (DTT) prior to analysis. Following attachment to the wells the samples were treated with 10mM DTT (100°C 10 min) and then alkylated with 20mM iodoacetic acid in the dark (2 h).

2.15. Gel electrophoresis

2.15.1. Agarose Gel Electrophoresis

Agarose (0.8%) gels were used for the separation of high molecular weight proteoglycans and hyaluronan. These gels were separated at 50 - 80v over a period of 2 hours prior to washing with buffer and transfer or staining with Stains-All®.

2.15.2. Polyacrylamide Gel Electrophoresis

Small format analytical polyacrylamide gels were routinely used for separation of proteins obtained in a number of experiments described in this thesis. The separation by one-dimensional SDS PAGE was according to the methods of Laemmli (Laemmli 1970). Small format (0.75 x 8 x 10 cm) resolving gels were used at 8, 10, or 12% or 4-20% gradient. The gels supplied by Gradipore (igels #NG21-010) had no stacking gel attached. Gels were placed in to an electrophoresis apparatus (Biorad protean III) and electrophoresed in tris/glycine buffer (appendix 1 53). The samples were solubilised in loading buffer (appendix 1.34), heated at 95 °C for 5 min and loaded in to the wells of the gel. To facilitate calibration pre-stained SDS PAGE standards (Biorad #161-0318) were loaded as a reference. Electrophoretic separation was conducted at constant voltage 150 V with cooling and terminated when the tracking dye had migrated to the bottom of the gel. Gels were subsequently removed and either stained with GelCode® blue (section 2.9.1) or prepared for Western transfer (2.15.3.1). Wet gels were illuminated on a light box and photographed using the Alpha Innotech Fluorchem® 8800 gel documentation system using the number 3 daylight filter. The gel was then dried using the gel drying system from Promega (#V131), for methodology see 2.15.4.

2.15.3. Gel Transfer

2.15.3.1. Western Transfer of Polyacrylamide Gels

Polyacrylamide gels were transferred to polyvinylidene difluoride membrane by the standard Western method (Towbin *et al.*, 1979). Briefly, gels were equilibrated in Western transfer buffer (25mM Tris-HCl, 195mM glycine, 20% methanol) for 5 min. Hybond P PVDF membrane was pre-wet in methanol and equilibrated in western blotting buffer. Four pieces of 3MM blotting paper cut to the same size as the gel and the transfer cassette sponge inserts were pre-soaked in blotting buffer. The blotting apparatus (BIORAD Protean III transfer system) was assembled according to manufacturers instructions and the positions of the gel lanes marked on the membrane when the gel was in place. The proteins were transferred to the PVDF for 1 hour at constant current (250mA) with cooling to 4°C. Following transfer, the membranes were blocked overnight at 4°C in 5% skim milk in PBS for immunohistochemistry or immunoblotting see section 2.16.

2.15.3.2. Agarose Gel

Agarose gels were transferred to Hybond P PVDF membrane by the capillary blot method using the same transfer buffers as above. In brief, a piece of Whatman 3MM paper was pre-soaked in Western transfer buffer and placed on top of a "bridge" resting in a shallow

reservoir of the same buffer thus creating a wick. Two more pieces of pre-wetted paper cut to the same size as the gel were then placed on top of this wick with the gel then placed face up on top of these. Next a piece of pre-wetted PVDF membrane was placed on top of the gel and a sterile pipette rolled over the membrane to remove air bubbles. Next two further pieces of 3MM were added, again removing the air bubbles. Finally the blot arrangement was topped with a large wad of paper and a glass plate weighed down by 200 – 400g. The system was placed in the fridge overnight to transfer.

2.15.4. Gel Drying

Both agarose and polyacrylamide gels were dried by the same method. Following separation of the fluid proteins before or after transfer to PVDF membrane, the gels were washed twice in ultrapure water (15 min) and transferred in to gel drying solution (9.6.6.1) (2 X 15 min). Following equilibration in gel drying solution the gels were placed between two sheets of gel drying film (Promega # V7131) and placed in a drying frame (Promega # 7120) overnight.

2.16. Immuno and Ligand Blotting

The proteins of follicular fluid, granulosa and theca cells were characterised by electrophoresis on 0.8% agarose gels, 10% 12% or 4-20% gradient SDS-PAGE. The proteins were transferred to Hybond C+ by capillary transfer (agarose gels) or to PVDF by electro transfer (polyacrylamide gels) see sections 2.15.3.1 and 2.15.3.2 (Towbin *et al.*, 1979).

Membranes containing electro blotted proteins were blocked in PBS 5% skim milk (1 h at 37°C), and rinsed with 3 X PBS/Tween 20 (PBST) for 5 min at room temperature. After rinsing the membranes were incubated with an appropriate dilution of primary antibody directed against specific proteoglycan species or with biotinylated hyaluronan binding protein (HABP) (0.5μg/ml), in PBS/1% skim milk and incubated for 1 h at 37°C. The membrane was then washed 3 X PBST for 5 min at room temperature before incubation with an appropriate dilution of secondary antibody in 1% skim milk (1 h at 37°C). The membrane was then rinsed 3 X PBST for 5 min at room temperature and the result visualised using either DAB or Super Signal western blotting detection system according to the manufacturers protocol. In the case of chromogenic development, protein was visualised after immersion in PBS containing 0.05% (w/v) 3'3' diaminobenzidine (DAB) and 0.003% (v/v) hydrogen peroxide. In the case of chemiluminescent development an ECL detection kit was used. Membranes were developed for 1 min in chemiluminescence reagents 1 and 2 (1:1) (Hyperfilm ECL, Amersham) for 30 sec to 10 min in the dark. Exposed film was developed using standard procedures.

2.17. Hyaluronic Acid Size Determination

Hyaluronic acid, characterised for size, was used as a size indicator for agarose gels. The sizes of the hyaluronan used were 220 kDa, 860 kDa and 1.6 x 10^6 Da.

2.18. DNA Measurement

The concentration of a DNA sample was carried out using spectrophotometric methods with an Eppendorf biophotometer (Eppendorf #952000004). Optical density was obtained at A_{260} and the concentration calculated on the basis 1 unit ds DNA = 50μg/ml H_2O. The purity of DNA was calculated by obtaining the optical density at A_{260} A_{280}. Pure DNA = $A_{260}/A_{280} \geq 1.8$.

2.19. DNA in Follicular Fluid

DNA components of follicular fluid were resolved on a 1% agarose gel in 0.5M TAE buffer and stained with either Stains-all® or ethidium bromide. Prior digestion with proteinase K or RNase free DNase (1 mg/ml for 1 h 37°C) was carried out to identify DNA and protein previously observed in these gels (Jones, 2001; Mandel-Gutfreund, 1995). Differential staining with Stains-all® of follicular fluid components, following separation on agarose, allowed identification of the nucleic acid and protein components present.

2.20. Protein Sequencing

The collagen component within fluid was analysed by digestion with collagenase I and subsequent PAGE. At the termination of the transfer the PAGE, gels were stained briefly with GelCode® Blue and the bands of interest carefully excised with a clean scalpel blade. Excised bands were washed in 50% methanol in water (v/v) and then dried in vacuuo. They were subsequently rehydrated in a minimal volume of 2% SDS, 0.2 M Tris/HCl, pH 8.5. Ten volumes of water were added to the rehydrated gel pieces and PVDF membrane soaked with methanol added to adsorb the diffusing proteins from the gel. Following complete transfer of the proteins to the PVDF, the membrane was washed five times in 0.5 ml 10% methanol in water (v/v), dried and loaded in to a reaction cartridge of an ABI PROCISE CLC protein sequencer (Applied Biosystems Inc., Foster City, CA) followed by the identification of amino acids via HPLC. The N- terminal amino acid sequence of the proteins was assessed by automatic Edman degradation directly from the membrane. The Biomedical Resource Facility at the John Curtin School of Medical Research, The Australian National University, Australia performed the sequencing. Where the gel pieces included protein mixtures, sequence calls were made on the basis of relative abundance and were compared with mammalian databases

using PROWL (http://prowl.rockefeller.edu). A 90% identity was required before identification was recorded.

2.21. Immunohistochemistry

2.21.1. Tissue Processing

Samples to be analysed by immunohistochemistry were collected from the abattoir as described above, dissected from the parent tissue and placed in Bouin's fixative overnight. The following day the samples were taken through repeated changes of alcohol until the yellow colouration from the Bouin's had gone. The tissues were then completely dehydrated in a graded series of ethanol, cleared in xylene and embedded in molten Paraplast. Serial sections of 5 μm were cut on a Spencer microtome and mounted on poly-L-lysine coated slides. The sections were dried on an electrothermal drying platform (54°C). Prior to use, paraffin was removed from the sections by successive changes in xylene and rehydration through reducing concentrations of ethanol to water and then PBS.

Where peroxide conjugated secondary antibodies were used endogenous peroxidase activity was blocked by pre-treatment of the slides with 0.03% hydrogen peroxide for 10 min. Non-specific antibody binding was prevented by pre-incubation of the tissue sections in 3% (w/v) pre-immune goat serum albumin in PBS (1 h 37°C). Sections were then incubated in a humidified chamber with primary antibody or ligand for 1 h at 37°C and washed 3 times in PBS/Tween. Incubation with the secondary antibody was conducted in the presence of either fluorescein (FITC) or horseradish peroxidase (HRP) conjugated IgG for 1 h at 37°C. The sections were then washed 2 times in PBS/Tween and once in PBS alone. FITC labelled slides were mounted with an antifade reagent to minimise signal quenching, and viewed with a confocal microscope (Bio-Rad MRC-1000 Laser Scanning Confocal Imaging System).

HRP labelled sections were developed in a solution of PBS containing 0.05% (w/v) 3'3' diaminobenzidine (DAB) and 0.03% hydrogen peroxide for 5 - 15 min. sections were then washed in ultra pure water for 5 min and counterstained with Gills heamatoxylin for 1 min and placed in Scott's tap water substitute for 1 min. Slides were dehydrated though an increasing ethanol series and cleared in two washes of xylene before being mounted under cover slips in Medite Pertex mountant for examination by light field microscopy (BHT Microscope system Olympus Optical Co. Ltd., Tokyo, Japan). Sections where the primary antibody was substituted with non-specific antibody were included routinely as negative controls.

2.21.2. Antibodies

The antibodies used in immunohistochemical localisations and Western blot are listed at the beginning of this chapter.

2.22. RNA Extraction

Follicles were dissected from bovine ovaries on ice and 100 mg of follicular or tissue material was placed directly in to RNA Bee (Biogenesis). The tissues were then homogenised using an Ultra-Turrax homogeniser. Following homogenisation 0.2 ml of chloroform was added and the samples placed on ice for 5 min before centrifugation at 14000 rpm for 15min. Following centrifugation the top aqueous layer was removed in to a new tube and 0.5 ml of isopropanol added to precipitate the RNA, the samples were then placed overnight at 4°C. The precipitate formed was centrifuged at 14000g for 15min 4°C and the pellet washed with 1 ml 75% DEPC treated ethanol and re-centrifuged at 14000g 10min 4°C. The pellet was then air dried and resuspended in DEPC treated water.

Dilutions of 1:100 were made of each sample and the amount of RNA calculated by reading the optical density at A_{260} on an Eppendorf biophotometer (Eppendorf #952000004) and the concentration calculated on the basis 1 unit ss RNA = 40μg/ml H_2O. The purity of DNA was calculated by obtaining the optical density at A_{260} A_{280}. Pure RNA = A_{260}/A_{280} $\geq$2.0.

2.23. cDNA Synthesis

The cDNA used was made from RNA extracted from several tissues reported as having hyaluronan synthase activity, namely, eye, skin, lung, brain, cartilage heart and colon. The following primer sets were selected based on published data as indicated.

RNA (10μg) above was treated with DNase I (2 units, 37°C for 30 min) according to the manufacturers instructions. Following DNase I treatment cDNA synthesis was carried out using random prime hexamers. Briefly 1-5μg of total RNA was dissolved in a total volume of 10μl of DEPC treated ultrapure water. To this 1μl (1μg) of random primer and 18 μl of DEPC treated ultrapure water was added. This cocktail was heated for 2 min at 72°C and then cooled on ice for 2 min to allow annealing to take place. Following this, the reverse transcription reaction was set up using the Invitrogen Superscript II® RNase H reverse transcription kit (#18064-014). To the above was added 5 X first strand buffer (10 μl), dithiothrietol (DTT) (5 μl) RNase inhibitor (40U/ul) (1 μl) and 10mM dNTPs (2.5 μl). The total reaction mix volume was equal to 48 μl. This mix was then split in to two portions. To 36ul to be used for reverse transcription was added 1 μl of Moloney Murine Leukaemia virus reverse transcriptase MMLV-RT and 1.5 μl of DEPC treated ultrapure water and labelled the RT tube. To the

remaining 12 μl of the mix was added 1 μl of water and this was labelled the – RT tube. This and the RT mix were incubated at 42°C for 75 min and then at 90°C for 5 min to destroy the enzyme activity. Samples were stored at -20°C until required.

2.24. Polymerase Chain Reaction

2.24.1. HAS 1, HAS 2, HAS 3, 18S, Inhibin/Activin βA, and P450 SCC Primer Design

In order to localise the site of hyaluronan synthesis and its degree of expression within the follicles of different size and health status, PCR primers were designed to three hyaluronan synthases. Sequence alignments of hyaluronan synthases (Bos taurus) gi: 4586933 (HAS1), gi: 4586935 (HAS2), gi: 12049661 (HAS3) respectively, were performed using Clustal W 1.4. Primers were designed for HAS 2 and 3 by the author using primer Express software to be specific to each bovine hyaluronan synthase. The primers for HAS 1 were the ones reported by (Schoenfelder, 2003).

Primers were designed to exon 4 and 5 of the HAS 1 sequence. The forward primer was targeted to base 85 of exon 4 and the reverse primer to base 268 of exon 5. The expected amplicon size was 182 bp.

HAS 2 primers were designed to exon 4. The forward primer was targeted to base 53 and the reverse primer to base 325. The expected amplicon was 310 bp

Primers were designed to exon 3 and 4 of the HAS 3 sequence. The forward primer was targeted to base 749 of exon 3 and 894 of exon 4. The expected amplicon was 243 bp.

The housekeeper genes used were bovine 18S AF176811 and Oryctolagus cuniculus GAPDH L23961.

Control probes of inhibin/activin βA and P450 side chain cleavage were used in in situ and Northern blot assays. Inhibin/activin βA was used as a reliable marker of granulosa cell integrity. The inhibin/activin βA subunit mRNA is only expressed by the granulosa cells of the antral follicles greater than 0.8 mm diameter (Torney *et al.*, 1989).

P450scc was used as a control for theca cell integrity. Inhibin/activin βA primer was designed to the βA subunit of the inhibin/activin molecule. Primers were designed to exon 1 and 2 of the inhibin/activin βA gene. The forward primer was targeted to base 1652 to 1672 (5'-TGGAGATAGAGGACGACATCG-3') of exon 1 (accession: U16238, base 1743 = base 1 of intron) and the reverse primer (5'-TCTCCTGACACTGCTCACAG-3') was targeted to bases 738 to 758 of exon 2 (accession; U16239, base 339 is the first base of exon 2) The expected product size being 449bp.

The P450 side chain cleavage (SCC) product was obtained by amplification of the P450 side chain insert obtained from the plasmid pBSCC-4. This plasmid was donated by Dr Raymond Rodgers of the Dept. Obstetrics and Gynaecology, The University of Adelaide SA, Australia, and contained M13 Universal sequence forward primer (USP) (GTAAAACGACGGCCAGT) and M13 Reverse sequence primer (RSP) (CATGGTCATAGCTGTTTCCTGTGTG). All primer sequences and amplicons can be found in Chapter 5.

In the ovary P450scc is involved in the cleavage from cholesterol of its side chain component to yield pregnenolone (Stone & Hechter, 1954). P450scc expression at the protein level occurs in granulosa cells of healthy and atretic 10 mm follicles in cattle (Irving-Rodgers *et al.*, 2003). While in sheep thecal cells express P450scc just before antrum formation (Logan *et al.*, 2002), thus P450scc was used as a control for theca cell integrity in the in situ assays.

2.24.2. PCR Protocols

The PCR protocol used was that provided by Invitrogen (#10342-053). PCR amplification was performed using 2 µl of template DNA. The taq mix used for HAS 2 and HAS 3 was: 10X PCR buffer minus Mg (2.5 µl); 10 mM dNTP mixture (0.75 µl); 50 mM $MgCl_2$ (0.75 µl); 1.5 mM, Primer mix 20 µM (1 µl); 0.5 µM, *Taq* DNA Polymerase (5 U/l) (0.125 µl); and the reaction mix made up to 25 µl with autoclaved distilled water.

Taq mix used for HAS 1 was: 10X PCR buffer minus Mg (2.5 µl); 10 mM dNTP mixture (0.75 µl); 25 mM $MgCl_2$ (1.5 µl); 1.5 mM, Primer mix 20 µM (1 µl); 0.5 µM Template DNA (2 µl); *Taq* DNA Polymerase (5 U/l) (0.125 µl) 2.5 units; autoclaved distilled water to (25 µl).

The PCR cycle program was 94°C for 10 minutes for the HAS 1 PCR using amplitaq gold or 94°C for 5 min for the HAS 2 and 3, inhibin A and GAPDH PCRs. This was followed by 94°C for 30 s, an annealing stage at 60°C for 30 s for bovine HAS 2, HAS 3, inhibin A, GAPDH and 18S or an annealing stage of 62°C for 30 s for bovine HAS 1. Next an extension stage was added for 1min at 72°C. The amplification was performed for 35 cycles and then incubated for an additional 5 min at 72°C. The reaction was then held at 11°C. The sample was stored at –20°C until use. The amplification products were observed by electrophoretic separation on a 2% agarose gel and visualised by ethidium bromide staining. A pUC 19/HpaII digested ds DNA molecular weight marker was used to identify band sizes.

2.24.3. PCR Product Purification

PCR product (20 µl) was added to sterile distilled water (180 µl). 1 volume = 200µl. Phenol: chloroform (1 volume) was added to the above and mixed well, followed by centrifugation (14000 rpm 5 min 4°C). The upper layer was removed in to a clean sterile eppendorf tube and 1/10 volume of 3M sodium acetate and 2 $^{1/2}$ volumes of cold ethanol added and allowed to stand to precipitate the DNA (4°C for 2 hours). Centrifugation at 14000 rpm, 15min 4°C, removal of supernatant and washing of the remaining DNA pellet with 1ml 70 % clean ethanol was followed by a second centrifugation (1400 rpm 10 min 4°C). The subsequent DNA pellet was air dried before re-dissolving in sterile distilled water (5µl). 1 µl of cleaned product was separated on a 2 % agarose gel and visualised by ethidium bromide staining. A pUC 19/HpaII digested ds DNA molecular weight marker was used to identify band sizes.

2.25. Cloning

2.25.1. Ligation

This was done using the Promega pGem-T-Easy vector system (#A1380). All components were defrosted on ice. The ligation mix used was: 2X Rapid Ligation Buffer, T4 DNA Ligase (1µl), pGEM ® T Easy Vector (50ng)(1µl), PCR product X µl* or Control Insert DNA (2µl), T4 DNA Ligase (3 Weiss units/µl) (1µl), *Deionised water was added to a final volume of 10µl. The reaction mix was incubated overnight at 4°C.

2.25.2. Cloning

Cleaned ligated PCR product (2 µl) was added to 50µl JM109 or XL-1 blue competent cells, which had previously been thawed on ice under sterile conditions. C. pGEM ® -T Easy Vector Sequence #A1360 Promega*

The pGEM ® -T Easy Vector had been linearised with EcoR V at base 60 of this sequence and a T added to both 3′-ends. The sequence is complementary to RNA synthesized by the SP6 RNA Polymerase. The vector sequences can be located at: www.promega.com/vectors

The mix was kept on ice (20 min) to allow the DNA to stick to the cells. The mix then underwent heat shock (50 sec/42°C). The cells were returned to ice (2 min) and 1 ml L-broth added before recovery by incubation in a shaking incubator (37°C for 1.5 h). Cells were then centrifuged (2000 rpm 5 min). Some of the L-broth was removed (850µl) and IPTG (20µl) and X gal (20µl) added before gentle re-suspension of the cells and spreading on to an agarose

plate containing ampicillin (10mg/ml). The plate was placed upside down in a 37°C incubator overnight and examined for positive white colonies.

2.26. Plasmid Purification

Several white colonies were picked from freshly streaked selective agar plates in to L-broth (70 ml) containing 1µl/ml ampicillin and incubated in a shaking incubator (200rpm 37°C overnight). Plasmid purification of the cloned products was achieved using the plasmid purification kit from Qiagen (#12145) according to the manufacturers instructions. The purified plasmid DNA was washed in clean 70% ethanol (2ml) before air-drying the pellet. Each plasmid was resuspended in sterile distilled water (50 µl). 1 µl of each cleaned product was separated on a 2% agarose gel and visualised using ethidium bromide staining. Spp1/EcoRI digested ds DNA molecular weight marker was used to identify band sizes. The quality of the DNA was assessed by spectrophotometry Abs_{260}/ Abs_{280}. Sequence analysis of the HAS 1, HAS 2 and HAS 3 plasmids (100ng) was carried out by the University of Newcastle Biomolecular research facility, Newcastle, Australia. The John Curtin School of Medical Research, The Australian National University, Australia sequenced the Inhibin alpha and P450scc products.

Sequence data from plasmid sequencing confirmed that all products had been successfully cloned in to the pGem T Easy vector.

2.26.1. Production of P450scc plasmid

The original P450scc insert used was sub-cloned by enzyme digestion with Pst I and Pvu II from the bluescript II SK + pBscc-2 (John *et al.*, 1984) in to the plasmid pBscc-4. This plasmid was received from Dr Raymond Rodgers and this insert was amplified with universal primers T3 and T7. This plasmid along with the others mentioned above was then used in the production of in situ probes.

2.27. Production of In Situ RNA probes

2.27.1. PCR

Bulk preparations (10 X 50 µl) of the HAS DNA's by PCR of the HAS 1, 2, or 3 insert from the plasmid DNA was performed under the conditions mentioned above using the plasmid as the template DNA and the primer sets USP and RSP, both forward and reverse for each, which are located in the SP6 and T7 regions of the plasmid.

PCR reactions were set up as follows:

10X PCR buffer minus Mg (25 µl)

10 mM dNTP mixture (5 µl)

50 mM $MgCl_2$ (7.5 µl)

1.5 mM Primer mix at 20 µM (10 µl)

0.5 µM template plasmid DNA (4µl)

Taq DNA Polymerase (5 U/l) (1.25 µl) 2.5 units

Autoclaved distilled water to 50 µl

The PCR cycle program was 94°C for 10 minutes (HAS1-amplitaq gold) or 94°C/ 5 min (HAS 2 and 3), 94°C for 30 s, Anneal 60°C for 30 s (bovine HAS 2, HAS 3 and 18S). Anneal 62°C for 30 s (bovine HAS 1), Extend 72°C for 1min, perform 35 cycles of PCR amplification then incubate for an additional 5 min at 72°C. The reaction was then held at 4°C until sample storage at –20°C until use. The amplification products were analysed by separation on a 2% agarose gel and visualised with ethidium bromide staining. pUC 19/HpaII digested ds DNA molecular weight marker was used to identify band sizes. PCR products then purified as per section 2.24.3.

2.27.2. DIG Labelling of RNA probes

All reactions were carried out in nuclease free plastic or glassware.

Using the DIG riboprobe kit (Roche #1175025) and using the manufacturers recommended amount of 100-200 ng of linearised plasmid DNA the following reaction was set up on ice:

Water (DEPC treated) (12µl)

10 X Transcription buffer (2µl)

Linearised plasmid (1µg/µl)(1 µl)

10 X dNTPs (2 µl)

RNase inhibitor (RNAsin) (1 µl)

SP6 (#1487671) or T7 (#0881775) RNA polymerase (2 µl).

The reaction was incubated (2 h 37°C) and then DNase 1 (1 µl) added and incubated 15min 37C. 0.2M EDTA (2 µl) was added to stop the reaction followed by 3M sodium acetate (2 µl) and 100% ice-cold ethanol (60 µl) to precipitate the RNA (–70°C for 30 min). Centrifugation (12,000g 15 min 4°C) gave a pellet of RNA which was washed with DEPC

treated 75% ethanol and air-dried. The pellet was dissolved in autoclaved DEPC water (21 μl).

The resultant probe was diluted 1:10 with DEPC water and 2 μl separated on a 1.5% agarose gel. Probe brightness was compared to that of corresponding SSP1/EcoR1 standard band to estimate probe concentration.

2.27.3. Quantitation of DIG Probes

A sample of the probe was diluted to 10ng/μl using in freshly prepared RNA dilution buffer (DEPC water: 20X SSC: formaldehyde 5:3:2). Serial dilutions of the probe and a control DIG labelled RNA from the manufacturer were made to give 10ng/μl, 1ng/μl, 100pg/μl, 10pg/μl, and 3pg/μl. 1 μl of each dilution was spotted on to Hybond C extra membrane. The membrane was air-dried for 10 min UV cross-link to the membrane for 30 min and blocked with 5% skim milk/ tris buffered saline (TBS) 30 min at room temperature. Anti-DIG alkaline phosphatase 1:5000 in 1% skim milk/ TBS/Tween 30 min was added and the membrane then washed with alkaline phosphatase buffer 9.9.1.9 for 2 min. The colour development was carried out using Nitro-blue tetrazolium /5-bromo-4-chloro-3-indolyl phosphate p-toluidine salt (NBT/ BCIP) in alkaline phosphatase buffer (9.9.1.9) for 10-30 min at room temperature.

2.27.4. Hydrolysis of DIG In Situ Probes

Prior to in situ the probes were hydrolysed. The following reaction was set up on ice in a 0.6ml nuclease free tube:

1 μg RNA probe (500ng/μl) (2μl)
DEPC water (2μl)
Carbonate buffer (4μl) (appendix 1.9)

The above mix was incubated (60°C 10 min). Hydrolysis neutralisation buffer (8μl) was added, followed by 100% cold ethanol (50μl) to precipitate the probe (–70°C 30 min). The probe was centrifuged (12000g 15 min 4°C) and the resultant pellet washed with DEPC treated 75% ethanol and re-centrifuged (12000g 15 min 4°C). The pellet was air-dried and resuspend in 30 μl DEPC water. Three microlitres were separated on a 1.5% agarose gel to observe the effectiveness of the hydrolysis. The remainder of the probe was used for in situ hybridisation.

2.28. In Situ Hybridisation

All glass ware and consumables used in these experiments were RNase free. All glassware was washed in 3%HCl/Ethanol or cleaned using RNA ZAP. Most reactions were carried out on a slide in a 50 ml tube with wet paper or in a humidified chamber.

2.28.1. Preparation of Slides

Slides were cleaned before use in in situ experiments. Prior to having sections placed on them they were treated with aminotriethoxypropylsilane (APS). Slides were first washed with DEPC treated water and then wrapped in two layers of foil and baked at 80°C for 3 hours. The slides were then removed from the oven and cooled before being placed in to a solution of 0.2% APS in acetone for 30 sec. Slides were then washed twice in acetone and once in DEPC water and put in to fresh foil and dried at 42°C overnight. Slides were stored in this manner until used for sections.

2.28.2. Preparation of Solutions

A. 0.2M HCl: 5ml of HCl in to 300ml DEPC ultrapure water

B. Proteinase K treatment 500ul EDTA + 500ul Tris-HCl in 4 ml DEPC water pre warmed solutions and container with wet paper tissue (DEPC) 37°C

C. 0.2% Glycine: 0.6g glycine powder in to 275 ml DEPC water + 15 ml 20 X PBS pre cooled to 4°C

D. 0.1M triethanolamine (TEA) 15ul /ml and + 2.5ul acetonitrile in 1 ml DEPC water

E. Pre/hybridisation solution: 25 ml deionised formamide (DIF)+ 7.5ml 20 X SSC + 1ml 50 X Denhardts = 16.5 ml 200mM phosphate buffer, pre-warmed to 42-55°C (*250ulDIF, 75ul 20xssc, 10ul 50 x D, 165 ul 0.2M Ph Buffer =500ul = 2-3 slides)*

Hybridisation buffer: take 10 ml of above mix and add 1g dextran sulphate (10%) 200ul herring sperm and 200ul tRNA pre-warmed to 42-55°C

2 X SSC: 30 ml 20 X SSC + 270 ml DEPC water

1 X SSC: 15ml 20 X SSC + 270 ml DEPC water

0.1 X SSC 1.5ml 20 X SSC + 270 ml DEPC water

Anti DIG antibody dilute in blocking solution 1:1000

2.28.3. Procedure

The method used for in situ hybridisation was adapted from that supplied by Roche Applied sciences. Slides were cleaned and prepared and sections cut. The sections were then

de-waxed in 2 X 10 min changes of safsolvent or equivalent. Following this the sections were rehydrated to DEPC water through 100%, 95%, 70% DEPC/ethanol water dilution series. The sections were then washed in 0.2M HCl for 20 min with shaking. This done they were rinsed in 2 X DEPC water 5min and incubated with proteinase K 30 min 37°C. Washing the sections for 10 min 2 X 5 min DEPC water at room temperature stopped the reaction. The sections were rinsed in 0.1M triethanolamine/ 0.25% acetic anhydride 5 min with shaking and given two further washes in DEPC water. The pre-hybridisation buffer (150ul) was then added to the slide to cover the section and covered with cover slip and incubated in a damp chamber 1h at 42 – 55°C depending on the probe. Incubation temperature for probes HAS 1 and HAS 3 were 50°C and 47°C for HAS 2. Following this incubation appropriate probe concentrations were prepared and the probe activated by placing it at 80°C 5 min. The probe was then applied to the section and allowed to hybridise under cover slips in damp chamber overnight (HAS 1 and HAS 3, 55 °C HAS 2 47°C).

The following day the sections were washed in 2 X SSC 15 min before treatment with a 20ug/ml RNase A in 20 X SSC for 30 min. The sections were then washed in 2 X SSC>1 X SSC>0.1 X SSC for 15 mins each 37°C. Visualisation of the hybridised probe was achieved using a sheep anti-DIG alkaline phosphatase antibody (Roche# 1093274) according to the manufacturers instructions. Briefly, the sections were washed with buffer 1 (9.8.1.2) (2x 10min), blocked with DIG blocking solution 1 (1hr/37°C) (# 1096176 Boehringer), and then incubated with 1/5000 dilution of sheep anti-dig alkaline phosphatase in buffer 1 (1hr/37°C). Following the DIG antibody treatment the sections were washed 2 X 15 min in Buffer 1 and then buffer 2 (9.8.1.3)(2 X 15min). Alkaline phosphatase was measured as a colour reaction with NBT/BCIP/levamisole for 30 min - overnight in a light tight humidified chamber, the degree of the reaction being checked every hour for the first 3 hours (6.5ul MBT/3.5ul BCIP/1mM levamisole/ml). The reaction was stopped by rinsing the slides with water 2 X 5 min. Sections were not counterstained but mounted in glycerol amyl alcohol aqueous mounting solution Zymed (#00-8000).

2.29. Northern Analysis

Samples of RNA prepared above were cleaned using the RNEasy mini protocol for RNA clean up from Qiagen according to the manufacturers instructions. Briefly, 20 ug of RNA sample, which had previously been treated with DNase I, was adjusted to a volume of 100 µl with RNase-free water. 350 µl Buffer RLT containing β-mercaptoethanol (10 ul/ml) was added and mixed thoroughly. 250 µl of 100% ethanol was added to the diluted RNA, and mixed thoroughly by pipetting. 700 µl of this sample was then applied to the RNeasy Mini

Elute Spin Column in a 2 ml collection tube and centrifuged for 15 s at 10,000 rpm. The flow-through was discarded.

The spin column was then transferred in to a new 2 ml collection and 500 µl of Buffer RPE pippetted onto the spin column before centrifugation for 15 s at 10,000 rpm. Again the flow-through was discarded. 500 µl of 80% ethanol was then added to the column and the column was centrifuged for 2 min at 10,000 rpm to dry the silica-gel membrane. The flow-through was again discarded. The spin column was then transferred to in to a new 2 ml collection tube and centrifuged in a microcentrifuge at full speed for 5 min. The flow through was discarded along with the collection tube. The column was then places in a new 1.5 ml collection tube and 14 µl RNase-free water pippetted directly onto the centre of the silica-gel membrane. The column was then centrifuged for 1 min at maximum speed to elute the RNA.

The RNA sample (10µg) was then separated on a 1% agarose denaturing gel containing 1X MOPS and 1.8 % formaldehyde in 10µl was incubated with RNA cocktail [500ul = 1X MOPS; formaldehyde (87.5µl); deionised formamide (250µl); ethidium bromide (0.01mg/ml) in DEPC water] 65 °C/10 min and snap cooled on ice for 10 min. Sample running dye (2µl) was added to the samples before loading on to the gel. The running buffer used was 1X MOPS in DEPC water. The gel was run at 80-100V. 1µl of marker was run per gel, which generates 9-11 bands (501/489 bp, 404 bp, 331 bp, 242 bp, 190 bp, 147 bp, 111/110 bp, 67 bp and 34 bp) on an agarose gel with ethidium bromide staining and UV fluorescence.

2.29.1. RNA Transfer

RNA from the gel was transferred to Hybond N+ membrane via capillary transfer in 20X SSC 9.9.1.11 overnight. The RNA was bound to the membrane by baking at 80 °C/2h.

2.29.2. Northern Blot Protocol

The membranes were then pre-hybridised with DIG easyhyb (#1-796-895 Roche GmbH, Mannheim, Germany)(10ml, 68°C for 30 min), this was removed and 5ug of DIG labelled probe added to fresh Easyhyb (Roche) and hybridised (68°C overnight). Following hybridisation the membrane was washed twice in 2X SSC at room temperature for 5 min then stringency washed (2 washes [2X SSC/ 0.1%SDS 68°C for 15 min] 2 washes [0.1X SSC/ 0.1% SDS 68°C for 15 min]) and then washed with maleic acid wash buffer (9.9.1.12) and blocked with blocking reagent made up in maleic acid buffer (Roche # 1096-176) and the probe binding visualised using the DIG wash and block buffer set from Roche according to the manufacturers instructions. Briefly, the membrane was washed in maleic acid washing buffer (5 min) and blocked in blocking solution (25°C/30 min) before adding antiDIG-

alkaline phosphatase antibody in blocking solution (1:5,000, 25°C/30 min). The membrane was then washed twice in washing buffer (25°C/15 min) before washing in 5ml of detection buffer followed by detection of the alkaline phosphatase using detection buffer (0.1M Tris – HCl, 0.1M NaCl, pH9.5) plus 1:100 CDP-star® a chemiluminescent substrate for the alkaline phosphatase reaction (25°C/3 min). The membrane was sealed in an acetate bag and exposed to chemiluminescent film or analysed on the Alpha Innotech Fluorchem® 8800 gel documentation system using the chemiluminescence filter. Following exposure to film the membranes were then stripped to remove bound probe and re-used for the next probe. The membrane stripping protocol used was that provided by Roche 2X SSC room temperature 15 min followed by (2 x [50% formamide/ 5% SDS/ 50mM Tris-HCl pH 7.5 80°C for 1 h]) followed by a second wash in 2X SSC room temperature 15 min.

2.29.3. One-Tube RT-PCR

Since the Northern blots were variable one tube RT-PCR was used to assess levels of HAS isoforms and inhibin alpha in granulosa and theca cell samples. The Titan One Tube RT-PCR System from Roche (# 11-855-476-001) is designed for sensitive, and reproducible analysis of RNA by high fidelity RT-PCR in a one-step reaction. It uses AMV reverse transcriptase for first strand cDNA synthesis and the Expand High Fidelity enzyme of Taq DNA polymerase and Tgo DNA polymerase for amplification of cDNA by PCR. Tgo DNA polymerase possesses proof reading activity leading to an increased PCR fidelity. RT-PCR is a highly sensitive method of determining gene expression at the RNA level and for quantifying the strength of that expression. The same primers described for PCR earlier were employed here. The fact that identical amounts of RNA are in the starting mix allows relative quantification of resulting products.

The method was carried out according to the manufacturers instructions. The method involves setting up two master mixes.

Master mix 1:

1.	Nuclease free sterile water	up to 25 µl
2.	dNTP mix at 0.2mM each	4 µl
3.	DTT solution at 5mM	2.5 µl
4.	Forward primer at 0.4 µM	1 µl
5.	Reverse primer at 0.4 µM	1 µl
6.	RNA template 0.5 µg	1 µl

Master mix 2:

1.	Nuclease free sterile water	up to 25 µl

2. 5 X RT-PCR buffer/$MgCl_2$ at 1.5mM10 μl

3. Titan enzyme mix 1 μl

Add 25 μl of each master mix to a 0.2 ml nuclease free PCR tube, mix and centrifuge briefly and place in thermocycler.

RT-PCR program was:

1. 50°C for 30 min
2. 94°C for 2 min
3. 60°C for 30 °C sec for HAS 2 and 3 and inhibin alpha 62 °C for 30 sec for HAS 1
4. 68°C for 1 min
5. Repeat stages 2 - 4 10 times
6. 94°C for 2 min
7. 60°C for 30 °C sec for HAS 2 and 3 and inhibin alpha 62°C for 30 sec for HAS 1
8. 68°C for 75 sec
9. Repeat stages 6 - 8 25 times
10. 68 °C for 7 min
11. 4°C hold

The resulting products were separated on a 2% agarose gel and stained with ethidium bromide before photographing.

2.30. Statistical Analysis

2.30.1. Follicular Fluid Colloid osmotic pressure Data

Statistical analyses were performed by one-way ANOVA using Statistics Package for the Social Sciences (SPSS) software.

2.30.2. In Situ Hybridisation Data

Statistical analyses were performed by chi squared analysis and or general linear modelling using Genstat software (6.2)

Chapter 3 Determination of the Colloid Osmotic Pressure of Follicular Fluid

3.1. Introduction

In order to obtain a detailed understanding of the mechanisms behind fluid accumulation within the follicle and subsequent follicular expansion the assumption will be made that the drivers of fluid accumulation within the follicle are similar to those elsewhere within the body. Fluid accumulates in the body as cysts or blisters, or in response to wounds or irritation caused by allergens. In the case of cysts, as in the follicle, growth occurs by epithelial proliferation and basement membrane growth and these are believed to be absolute requirements. Whether the forces for fluid accumulation precede or follow the stimuli for cell growth has not been determined (Welling & Welling, 1988). During ovarian follicular development in mammals a fluid-filled antrum develops in the avascular centre of the follicle. Follicular granulosa cells of the membrana granulosa do not have a network of tight junctions as present in some other epithelia. This suggests that it may be permeable to water and other solutes. Because of this small molecules, such as sodium, are unlikely to establish an osmotic gradient across the membrana granulosa such as occurs in the renal tubules. However, for larger molecules the establishment of a differential gradient is possible. If the composition of follicular fluid is similar to that of serum with respect to low molecular weight components, with most electrolytes being at similar concentrations in fluid and serum (Shalgi *et al.*, 1972b, Shalgi *et al.*, 1973), it is unlikely that a osmotic potential could exist without the presence of larger molecules in one or other fluid. In follicular fluid it has been determined that for increasing sizes above 100 kDa, plasma proteins are found at progressively lower concentrations than in plasma. Andersen et al found that mean protein concentration for small proteins was 86% that of serum with the larger proteins greater than 500 kDa at concentrations <15% (Andersen *et al.*, 1976). This suggests that there is a diffuse "blood-follicle barrier" at this level. The fluid accumulation process has been reported to occur at different rates throughout the development of the follicle (Marion *et al.*, 1968b) and it is possible that different colloid osmotic pressures exist in follicles at different stages of development, which may control the fluid accumulation process.

This chapter focuses on the investigation of the hypothesis that follicular fluid can create a sufficient osmotic differential using large molecular weight molecules, to move fluid from the surrounding vascularised stroma in to the antrum.

We use the term 'potential' rather than 'pressure'. Pressure is the net result of the production of osmotic molecules and their concentration. Thus if their production is counter balanced by net movement of fluid into the follicle no net gain in pressure can be measured, even if the production of such molecules was responsible for the recruitment of the fluid. In

the current experiments we are not monitoring pressure but rather identifying molecules whose production could be expected to generate osmotic forces during follicular growth. It is not the potential produced by the solution itself.

The osmometer used in the following experiments measured the colloid osmotic differential between a solvent and a solution held in 2 chambers separated by a semi-permeable membrane, permeable to the water and electrolytes of the solvent. When equilibrium was achieved between the two chambers of the osmometer containing the sample and solvent the electronic potential measuring system it transduced the potential reading into an electric signal, which was displayed on the instrument panel as an osmotic potential reading (http://www.gonotec.com).

In biological systems water flows from a position of high potential to one of low potential. This potential can be defined in terms of concentration, pressure, height or charge. Osmotic pressure equates to osmotic potential since osmotic pressure is equal to osmotic potential when the forces driving the water in to a system are in equilibrium with those driving it out. When discussed, the two terms are used interchangeably but in real terms one carries a negative score (potential) and the other a positive score (pressure) (Comper, 1994, 1996, Comper *et al.*, 1990). All results here are discussed in terms of potential i.e. it is the ability of the follicular fluid to drive water/fluid in to the follicular antrum that is being evaluated.

The objectives of the experiments conducted in this chapter were to

1. Identify whether large molecules are excluded from the follicular antrum and therefore establish that molecules larger than this in the fluid must have been made locally.

2. Design a reliable method for the removal of electrolytes and low molecular weight components from follicular fluid and serum such that the effect of any large molecules on the colloid osmotic pressure can be measured.

3. Determine a reliable method for measuring differences in colloid osmotic pressure between follicular fluids from different sized follicles and serum.

4. Isolate and collect fluids from individual follicles and record the differences in colloid osmotic pressure between follicular fluids from healthy and atretic pools and serum.

5. Determine the classes of molecules responsible for the colloid osmotic pressure of follicular fluids from healthy and atretic follicles.

3.2. Experimental Design

Successful isolation and collection of follicular fluid from individual follicles was crucial to the success of the experiments. Isolation of whole individual follicles from the whole ovary before aspiration had previously been determined as the most efficient way of obtaining follicular fluid free of contaminating blood and stroma tissue. Dissected follicles were given several washes in isotonic Earle's balanced salt solution (EBSS) prior to experimentation and it was these clean follicles that were used in molecular exclusion experiments.

In order to determine whether large molecules could enter the follicle across the follicular wall follicles were immersed in dextran solutions of different molecular weight. Dextran is a freely available molecule that can be synthesised in a large range of sizes and has been used by several investigators for similar exclusion/permeability assays (Dembczynski & Jankowski, 2001, Dong Z. *et al.*, 1998, Johnson A. *et al.*, 2003, Koster *et al.*, 2003) therefore, it was used here to determine whether there were differences in the permeability of the follicular wall of different sizes of follicle to different sizes of molecule. Time courses were determined for each size category of follicle and for each size of dextran molecule by measuring weight gain or loss of the follicle following immersion. At equilibrium % gain or loss was recorded as a % of total follicle weight.

Early studies by Edwards, Shalgi and Zachariae to determine the colloid osmotic pressure of follicular fluid (Edwards, 1974, Shalgi *et al.*, 1972a, Zachariae, 1958) were unable to clarify whether the follicular fluid of unstimulated follicles was lower than that of plasma or pre-ovulatory follicles (Smith J.T & Ketteringham, 1937) or higher. Any differences between these fluids may result from changes that occur in the permeability of the follicle wall during antrum formation and the ability of larger molecules (proteoglycans) to cross a membrane that might previously have been impervious (Hess *et al.*, 1998). The differences in reported colloid osmotic pressures in the literature may also lie in the method of assessment and the developmental stage of the follicle at the time of assessment. This thesis aimed to resolve some of these differences by providing fluid osmotic pressure data increasing sizes of follicle from a single species.

To determine the colloid osmotic pressure of follicular fluid, fluid was collected by methods outlined below, found previously to cause the least contamination of the sample. Follicular fluid was collected by needle punch and centrifuged to remove particulate matter and then used for determination of colloid osmotic pressure. Bovine serum was treated in the same manner and was used as a reference. Initial experiments were carried out to determine whether there were any differences in the colloid osmotic pressures of untreated follicular

fluid from different sizes of follicle and bovine serum. These experiments were conducted on follicular fluid collected from follicles of 2 – 16 mm diameter.

The determination of a reliable method for excluding electrolytes and low molecular weight molecules from follicular fluid was required in order to remove molecules of sizes known to be able to cross the follicular basal lamina. In order to achieve this a series of experiments were designed to find efficient exclusion/dialysis membranes for dialysis. Undigested fluids were diluted 1:10 with EBSS and placed in each of the dialysis test systems and dialysed against ultrapure water (containing sodium azide (0.1%)) for 24h at 4°C. Protein concentrations of samples before and after dialysis were measured and samples run on 10% SDS PAGE to confirm the removal of dialysed molecules.

Once an efficient membrane had been identified, experiments, which would dictate the dialysis protocol for subsequent colloid osmotic pressure measurements were designed. These included tests of the effect of temperature and salt on the effective removal of large and small molecules following digestion with specific enzymes. Follicular fluid samples were dialysed against ultrapure water and/or 2M NaCl at 4 °C and 37 °C before and after digestion with Streptomyces hyaluronidase. This was done to test the stability of the pore size of the membranes at both temperatures and to test the efficiency of dialysis of hyaluronan degradation products. Following earlier findings and data from Turner (1988) it appeared that low NaCl concentrations cause self-association of hyaluronan fragments which impede their escape from membranes at dialysis (Turner *et al.*, 1988).

Once a reliable dialysis membrane had been chosen and a method for efficient removal of molecules established an experiment was designed to measure the colloid osmotic pressure of follicular fluid from healthy and atretic follicles. Follicular fluid from healthy and atretic follicles, as determined by histology, was dialysed against membranes of different molecular weight cut off (MW cut off). These membranes allowed removal of low molecular weight molecules and electrolytes (10 kDa), molecules known to be able to traverse the basal lamina freely (100 kDa), molecules of a size unlikely to be able to enter the follicle from the vasculature and are therefore likely to be made locally or present in greatly reduced concentrations (500 kDa) and molecules between the last two groups which might have restricted movement (300 kDa). Colloid osmotic pressure was measured at room temperature with an osmometer.

The results obtained in the size exclusion dialysis experiment suggested that there were some differences between the colloid osmotic pressures of follicular fluid obtained from healthy and atretic follicles. An experiment was therefore designed to identify the classes of molecules present in these two fluid types and clarify this difference. Follicular fluid is known to contain many molecules common to serum and some produced by the granulosa cells (Ax

& Ryan, 1979, Shalgi *et al.*, 1973). Thus it is likely that proteins; DNA, collagens and molecules such as heparin, albumin, thrombin, small proteoglycans such as inter alpha trypsin inhibitor (ITI) and hormones are present. To determine which if any of these contribute to follicular fluid colloid osmotic pressure, follicular fluid was treated with enzymes known to digest some of the above molecules, and these included DNase, collagenase, proteinase K, and enzymes known to digest proteoglycan side chain components such as chondroitinase ABC, heparanase, Streptomyces hyaluronidase and keratanase. Untreated follicular fluid held at the same temperatures for the same period of time as those undergoing digestion was used as a controls.

3.2.1. Statistical Analyses

Statistical analyses were performed by one-way ANOVA using Statistics Package for the Social Sciences (SPSS) software, followed by Bonferroni's post-hoc test to determine significance between specific treatment For all figures, error bars indicate the SEM from at least four independent experiments

3.3. Results

3.3.1. Isolation of Follicles

Isolation of follicles from whole ovaries was performed successfully using a scalpel blade.

Follicles identified with arrows were isolated by crude dissection using a scalpel blade in to clean EBSS (Figure 9 and Figure 10) and these follicles were then cleared of visibly attached excess stroma using innox forceps and used in the permeability assays investigating the ability of molecules of known molecular weight to cross the basal lamina. Previous studies have shown that follicles isolated in the manner above contain an intact theca cell layer (Maravei *et al.*, 1997, Matikainen *et al.*, 2001). Follicular fluid from follicles isolated in this manner was aspirated with a needle and used in all experiments of the determination of colloid osmotic pressure of that fluid and for subsequent experiments in this and other chapters.

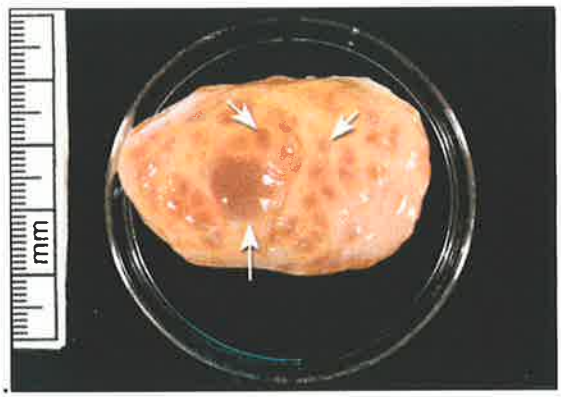

Figure 9 Bovine ovary with small and large antral follicles marked by arrows. Image taken from M.McArthur BSc (Hons) thesis, Flinders University 1998.

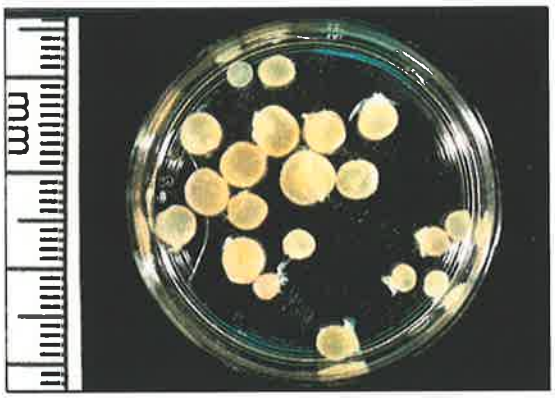

Figure 10 Isolated follicles 5 - 8 mm cleaned using innox forceps. Image taken from M. McArthur BSc (Hons) thesis, Flinders University 1998.

3.3.2. Determination of the Size of Molecule Able to Cross the Follicular Wall

This experiment was carried out in order to test a system for determining the size of molecules able to pass across the follicle wall of the follicle. Here the follicles were placed in 0.1 mM dextran solutions of differing molecular weight until no net flux was recorded i.e. there was no net weight gain or loss. The percentage weight gain or loss of the follicle was plotted against the width of follicle for each molecular weight of dextran. The results can be seen in (Figure 11).

Unfortunately this method did not prove to be reliable and the variation in readings was very large. General trends were observed across the treatments whereby follicles of size 2 – 4 mm and 13 - 15 mm showed a net loss in weight and follicles 5 – 6 mm had a large gain in weight and those 7 - 12 mm and $\leq$6 mm had small weight gains. However it was decided not to pursue this avenue of investigation further since reliable data could not be obtained.

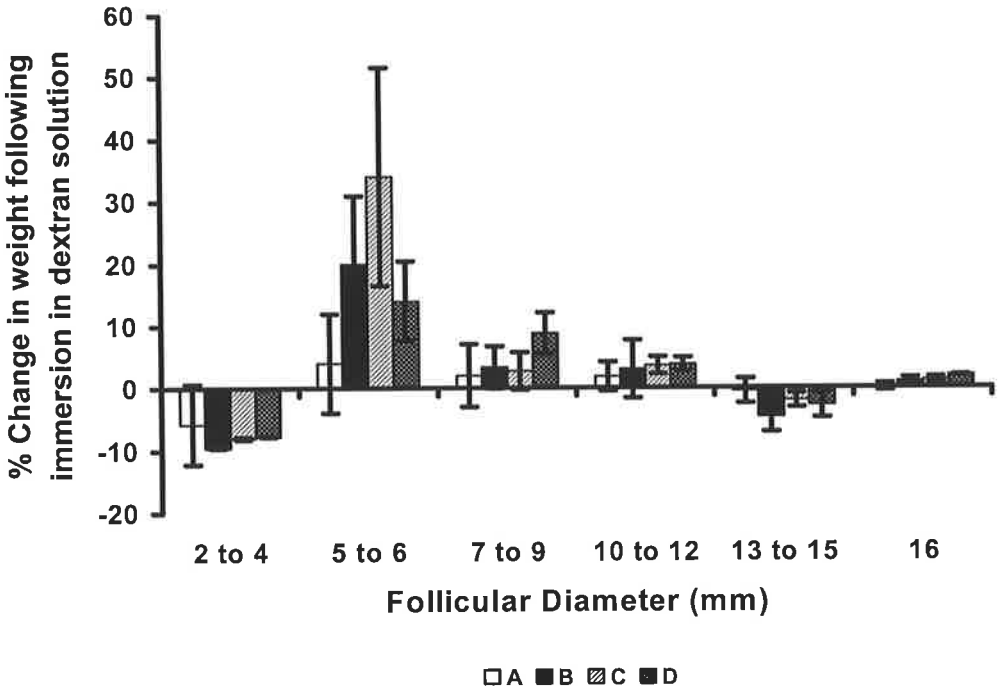

Figure 11 Graph showing cumulative data from 5 experiments of follicle weight gain or loss following immersion in 0.1 mM dextran solutions of different molecular weight. A, B, C and D refer to 10.5 kDa, 67.3 kDa, 188 kDa and 2 million Da dextrans respectively (n=5).

3.3.3. Follicular Fluid Volume

Prior to fluid collection the isolated follicles were observed to be turgid and clear on transillumination. Follicular fluid was aspirated from follicles as previously described in the methods. The volumes collected were recorded to assess whether there was any biased sampling occurring and whether sampling was more or less efficient from any particular size of follicle. On aspiration little or no fluid was lost through bleeding at the aspiration site. No obvious difference in viscosity or colour was noted between fluids of healthy and atretic follicles, excepting where the follicle was in advanced stages of atresia or close to ovulation. In these cases the fluid appeared to contain more blood. The diameter of the follicle and volume of the fluid collected was recorded. A graph of recovered volume of follicular fluid (μl) was plotted against follicular diameter (mm) and the expected total follicular volume (Figure 12). The total follicular volume does not take account of the volume taken up by the internal structures such as the granulosa cells, theca cells and oocyte. The volume these structures occupy as a proportion of the whole changes with follicular growth becoming smaller with respect to the total volume.

Follicular fluid volume recovered ranged from 285 μl and 241 μl (± SEM 84 and 37) in healthy and atretic follicles of 9 mm diameter to 5468 μl and 7699 μl from follicles of 30 mm diameter respectively. The graph (Figure 13) shows that the volume recovered from each of these follicle types was similar and reflected an unbiased sampling of fluid across the size range and health status of follicles used. The graph shows that the recovered follicular volume increases steadily until 12.5 mm to 13 5 mm in diameter when the rate of fluid accumulation appears to increase in order to fill the increase in follicular volume assuming a proportion of follicular space is filled by the granulosa cells and oocyte.

The graph in (Figure 12) shows pooled data from both healthy and atretic follicles.

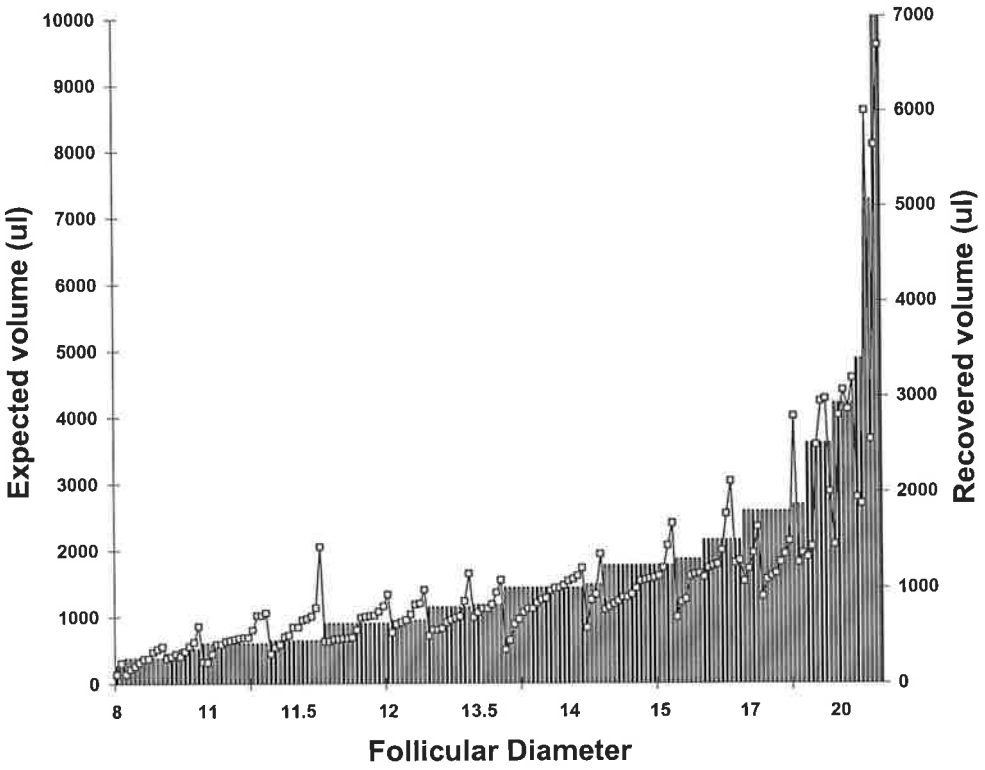

Figure 12 Graph of follicular volume recovered (µl) plotted against follicular diameter (mm) and total volume of the follicle (ul). (n = 171) A pooled data set from healthy and atretic follicles is shown.

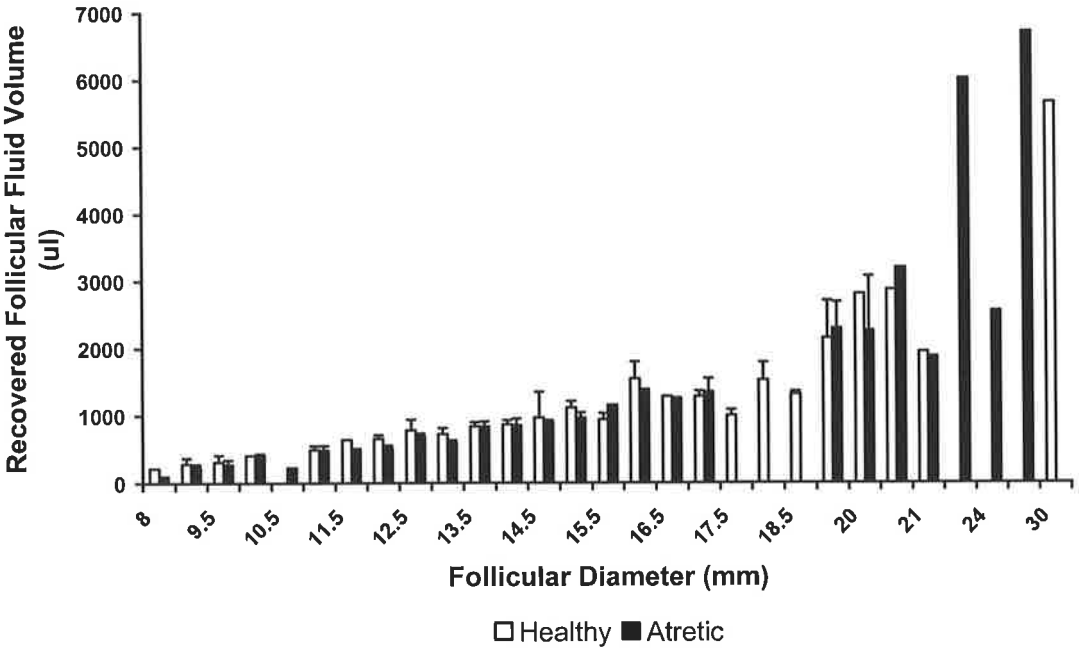

Figure 13 Graph of recovered follicular volume (ul) plotted against follicular diameter for healthy and atretic follicles respectively to show consistency between volumes of fluid collected from both follicle types (n = 171).

3.3.4. Colloid Osmotic Pressure of Follicular Fluid Components in Relation to Follicle Size

As mentioned above, there has been much controversy over the mean colloid osmotic pressure of follicular fluid. To date, few people have measured the mean potentials of follicular fluid and all of these measurements have been obtained from fluid collected from super-ovulated follicles. Prior to this work the mean colloid osmotic pressure of follicular fluid had not been tested from classified unstimulated follicles of cows.

In this investigation fluid was aspirated from unclassified follicles of sizes from 2 – 16 mm. The fluid was diluted 1:10 with EBSS because it was impossible to collect sufficient sample volume to fill the osmometer and conduct subsequent digestion experiments. EBSS was used because it maintains the correct physiological balance of ions. A sample of bovine serum diluted similarly and the colloid osmotic pressures of the serum and fluid samples measured using an osmometer fitted with a 10 kDa MW cut off reference membrane. EBSS closely mimics ionic conditions in vivo as well as maintaining high ionic strength to minimise molecular charge interactions. The colloid osmotic pressure of the follicular fluid samples was plotted as a percentage of the serum potential against the diameter of the source follicle. It should be noted at this point that measured pressure changes with temperature and that this change has been calculated to be 0.33% per ^{o}C (Tombs & Peacocke, 1974). Measurements here were carried out at room temperature and so the real fluid pressure at 39 ^{o}C, the temperature within the bovine ovary, would be 5.58% greater than recorded here. Since all measurements are reported as a % of serum potential or of untreated sample the relative results remain unchanged. The results from this experiment are presented in (Figure 14).

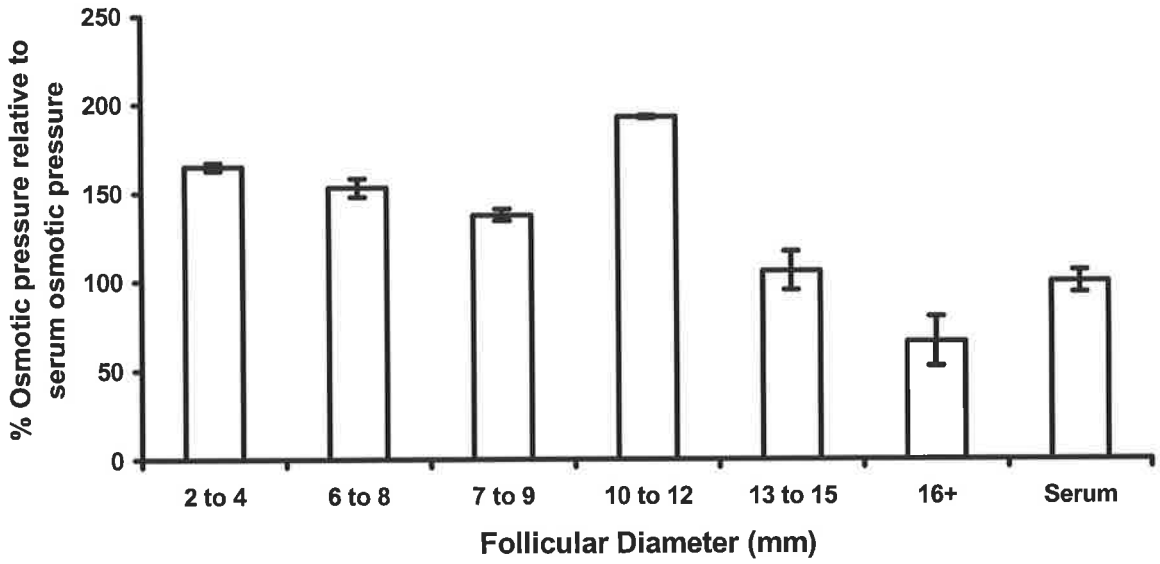

Figure 14 Colloid osmotic pressure of unclassified follicles of increasing size (colloid osmotic pressure calculated as a % of Bovine serum potential). (n=4).

The measurement of fluid colloid osmotic pressure indicated that the fluid from follicles 2 - 12 mm was greater (135.7 ± SEM 3.27 % – 193 % ± 0.8 % $p < 0.001$) than that of serum and that of pre-ovulatory follicles was less than (66% ± SEM 14 % $p<0.001$) that of serum. Fluid from follicles of 13 - 15 mm (106% ± SEM 10.9% $p = 0.15$) was similar to that of serum.

3.3.5. Membrane Tests

A search was conducted of dialysis and membrane products that provided a range of molecular weight cut offs (MW cut offs) of between 10 and 500 kDa for the reasons described earlier. The membranes tested for efficiency at dialysis were:

1. Dispo-dialysers Range 10 – 300 kDa from Spectrum Inc. Rancho Dominguez, California USA (Cat: 135550, 135552, 135554). This product is a dialysis tubing device with sealable top, further information can be obtained from http://www.spectrapor.com
2. Micron spin columns range 10 – 300 kDa from Millipore (Cat: 68010) further information can be obtained from http://www.millipore.com/
3. Flat membranes from Millipore folded and glued with Superglue® in to small pockets range, 10 – 500 kDa (Cat: PBGC, PBHK, PBMK, PBVK) (Figure 15).

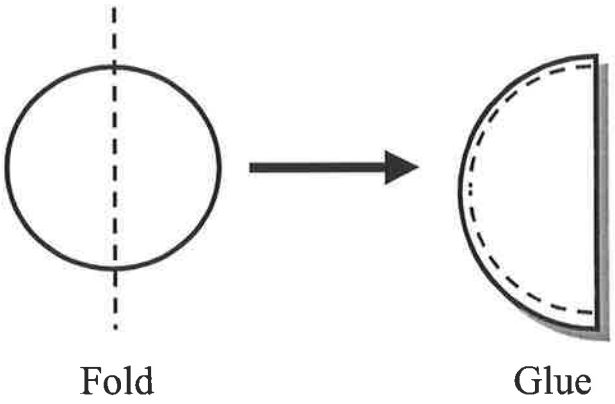

Figure 15 Diagram to show construction of Millipore "sealed pouch" membranes.

Samples of bovine follicular fluid diluted 1:10 with EBSS were placed in the test product and either dialysed against water, or in the case of the Micron spin columns fluid was diluted 1:10 with EBSS and centrifuged through the column according to the manufacturers instructions. Samples of the residual fluid were then subjected to electrophoresis on 10 % SDS PAGE in non reducing buffer and protein concentrations measured using the Bradford assay (Bradford, 1976) to determine the efficiency of removal of molecules below the nominal MW cut off stated by the manufacturer.

Protein concentrations following dialysis with the dispo-dialysers at 10, 100, 300 kDa showed that the dialysers had removed 1.2 %, 4.9 % and 11% of the original protein concentration respectively. SDS gels confirmed that no proteins below the nominal MW cut off had been completely removed and so this product was dismissed as an option for dialysis. Similar data were achieved for the micron spin columns and this product was not used further (data not shown).

Dialysis using the Millipore membrane pockets gave good removal of the products below the nominal MW cut off of all the membranes following dialysis (Figure 16) which shows clearance of products from follicular fluid below 100 kDa and below 500 kDa. Protein concentrations were reduced by 80% following dialysis at 300 kDa.

The Millipore membrane pockets were chosen for the dialysis experiments.

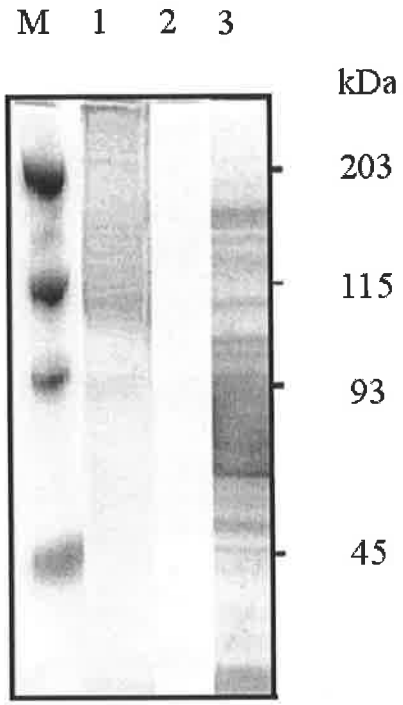

Figure 16 10%SDS PAGE of non-reduced follicular fluid sample following dialysis against 100 kDa (A) and 500 kDa (B), un-dialysed fluid (C). Bio-rad broad range molecular weight marker (M). 0.5 µl fluid loaded in each lane.

3.3.6. Temperature- and Salt-Dependent Dialysis

Pilot experiments measuring the colloid osmotic pressure of follicular fluid following enzyme digestion and subsequent dialysis against water showed that the colloid osmotic pressure recorded was greater than the original potential measured. Specifically, these results were recorded in the hyaluronidase treated samples. Since in theory some of the large molecules had been digested in to components that should have been free to escape the membrane on dialysis, the results appeared incorrect at first glance. Thus it appeared likely that multiple degraded hyaluronan units were re-aggregating as proposed by Turner et al (1998) and/or not escaping the membranes during dialysis because of low temperature as suggested by Lord (1999). Therefore it was decided that a test to determine the effect of salt and temperature on the clearance of follicular fluid products should be performed. To test whether the results obtained were being compromised by the dialysis conditions, follicular fluid was digested with Streptomyces hyaluronidase and either dialysed or not dialysed at 4°C and 37°C. If they were not dialysed the samples were held at the same temperature as its dialysis counterpart. Following dialysis the samples were snap frozen and lyophilised and then resuspended in their original start volume in EBSS prior to colloid osmotic pressure measurement. The results can be seen in (Figure 17).

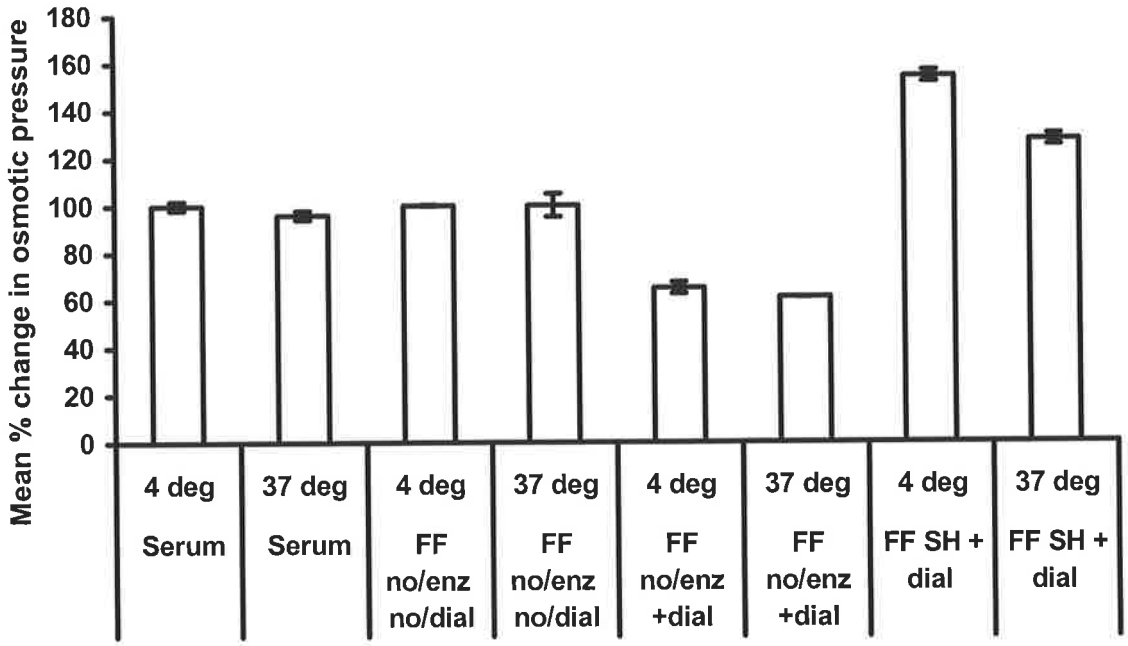

Figure 17 Results of temperature-dependent dialysis. (mean+/-SEM)% change in colloid osmotic pressure relative to no enzyme and no dialysis treatments plotted against treatment (FF = follicular fluid, Serum = bovine serum, no/enz = no Streptomyces hyaluronidase digestion, no/dial = no dialysis treatment, SH = Streptomyces hyaluronidase digestion, +dial = dialysis treatment performed post digestion with Streptomyces hyaluronidase) (n=4).

Results showed that fluid and serum colloid osmotic pressures were not compromised when untreated or held at 4°C or 37°C for comparable time periods, suggesting that there was no degradation of the sample as a result of the treatment regimen. The decrease in colloid osmotic pressure recorded for the undigested but dialysed fluid at 37°C was greater than that for the 4°C treatment being 39 % and 31 % respectively (Figure 17). This indicated that the dialysis was more efficient at the higher temperature. The results of the colloid osmotic pressure readings following these changes indicated that the dialysis was much improved but still did not show a complete removal of the total increase in potential recorded. The increase in colloid osmotic pressure following digestion with Streptomyces hyaluronidase and dialysis were in agreement with Turner's comments on the occurrence of re-aggregation under conditions of no or low salt conditions (Turner *et al.*, 1988). The percentage change between the colloid osmotic pressures pre and post digestion and dialysis were 61 % and 29 % for the 4°C and 37°C treatments respectively and this shows that the 37°C treatment appears to have dialysed more efficiently but that there was still aggregation occurring. This prompted us to re-visit the comments made by Turner et al and to change the dialysis condition to one where dialysis occurred firstly against 2M NaCl and then against decreasing salt concentrations to water containing 0.01% sodium azide. It was decided to conduct the dialysis at 37°C since this was seen to be the more successful protocol indicated in the results above. The results from this experiment (Figure 18) showed that salt dialysis did indeed remove the degradation products of hyaluronan as suggested by Turner et al (1988). This protocol was adopted for subsequent enzyme digestion and dialyses.

Finally conditions were established that allowed complete removal of digested products with no apparent degradation of the fluid samples and these were determined as being: dialysis overnight against 2M NaCl at 37°C followed by dialysis at 4°C through decreasing NaCl concentrations to water.

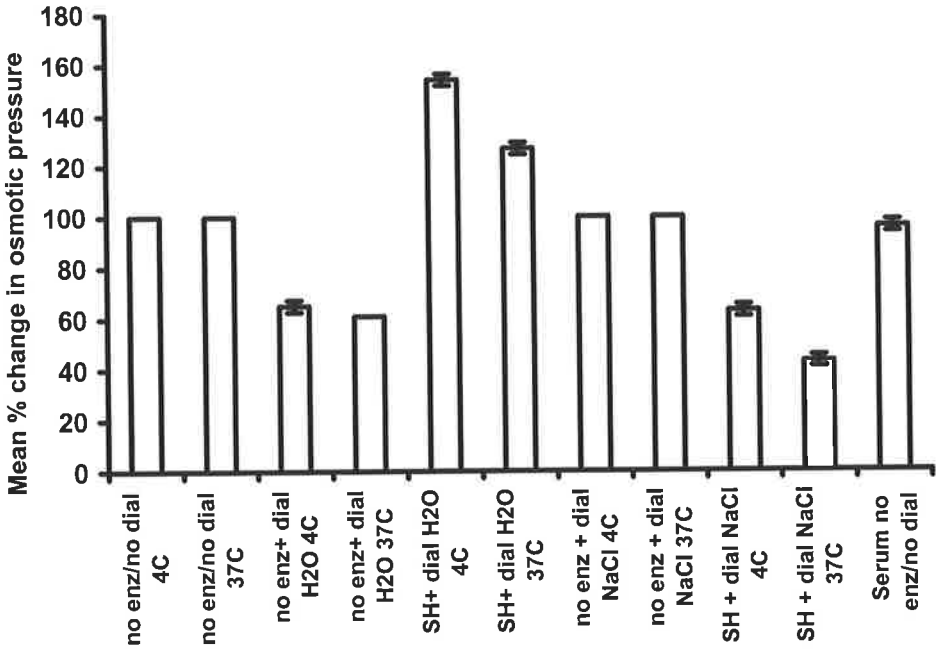

Figure 18 Results of temperature- and salt-dependent dialysis (mean+/-SEM) % change in colloid osmotic pressure relative to no enzyme and no dialysis treatments plotted against treatment (FF = follicular fluid, Serum = bovine serum, no/enz = no Streptomyces hyaluronidase digestion, no/dial = no dialysis treatment, SH = Streptomyces hyaluronidase digestion, +dial NaCl = dialysis against NaCl treatment performed post digestion with Streptomyces hyaluronidase, +dial H2O = dialysis against H2O treatment performed post digestion with Streptomyces hyaluronidase)(n=4).

3.3.7. Colloid Osmotic Pressure of Follicular Fluid

To determine the contribution of different sized molecular components to the colloid osmotic pressure of follicular fluid, pools of fluid were collected from healthy and atretic follicles and dialysed using "sealed pouches" constructed from a range of MW cut off membranes (10, 100, 300 or 500 kDa). Following dialysis, the colloid osmotic pressure of the dialysed samples was measured using the 10 kDa dialysate as the standard (Figure 19 and Figure 20). All dialysis was conducted under conditions previously established in this thesis; dialysis overnight against 2M NaCl at 37°C followed by dialysis at 4°C through decreasing NaCl concentrations to water. The colloid osmotic pressures, measured as units of cm of water, of the healthy (1:10 dilution, 2.45 ± SEM 0.45 cm water, n = 4) and atretic 2.35 ± 0.40, n = 4) were similar. A reduction in colloid osmotic pressures of approximately 8% and 1% were observed in fluid from healthy and atretic follicles respectively following dialysis with 100 kDa membrane. A 35% and 29% reduction in pressure was observed following dialysis of healthy and atretic fluids against 300 kDa membrane respectively. Dialysis against a 500 kDa MW cut-off membrane resulted in a 60% reduction in colloid osmotic pressure in fluid from healthy follicles and 80% reduction in fluid from atretic follicles. This data clearly indicated that large molecular weight molecules or aggregates of molecules contributed to the overall colloid osmotic pressure of follicular fluid of both healthy and atretic follicles.

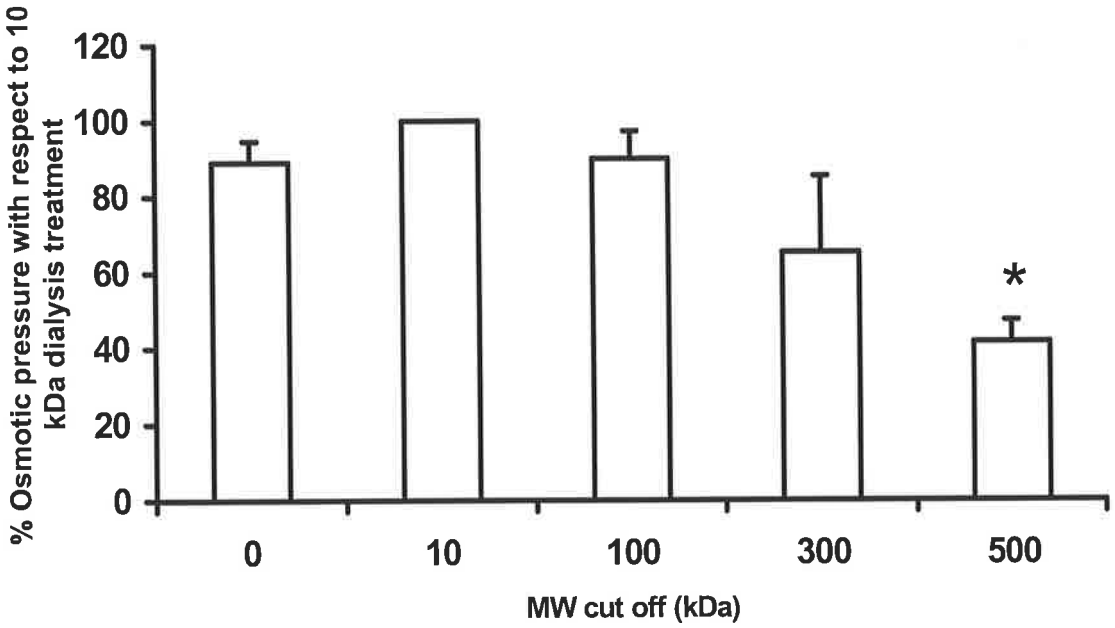

Figure 19 Effect of progressive removal of large molecules on the colloid osmotic pressure of follicular fluid from healthy follicles. Percentage change (mean+/-SEM, n = 4) in colloid osmotic pressure with respect to the 10kDa treatment plotted against the molecular weight cut off of the dialysis membrane. (*) Denotes significant differences (P < 0.05) between treatment and control at 10 kDa.

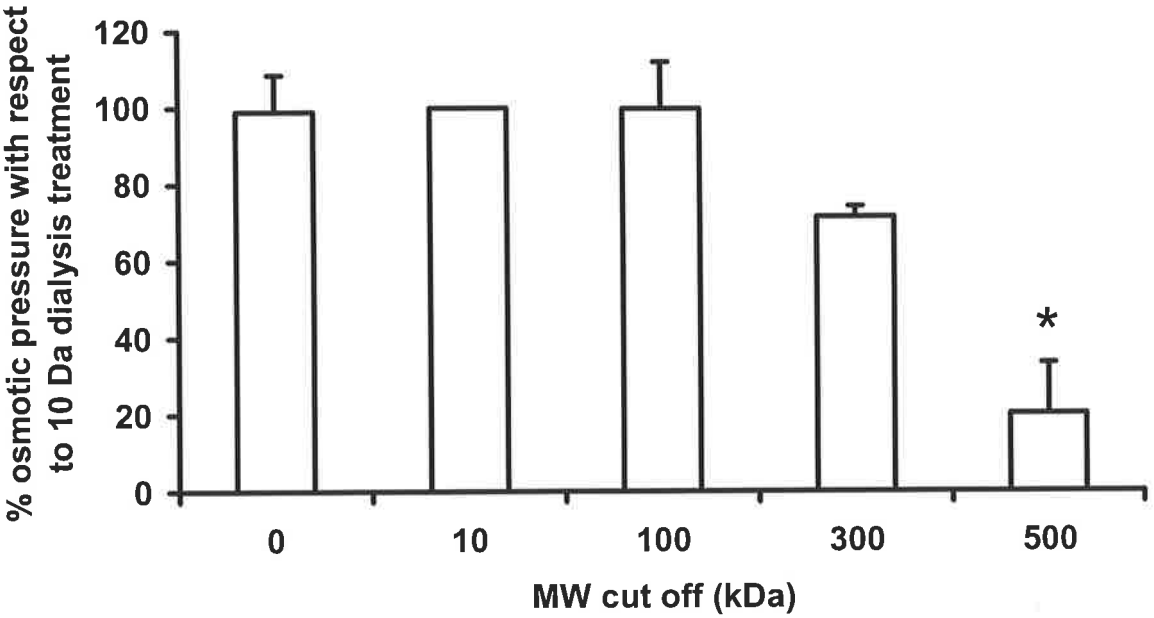

Figure 20 Effect of progressive removal of large molecules by dialysis on the colloid osmotic pressure of follicular fluid from atretic follicles. Percentage change (mean+/-SEM, n = 4) in colloid osmotic pressure with respect to the 10kDa treatment plotted against the molecular weight cut off of the dialysis membrane. (*) Denotes significant differences (P < 0.05) between treatment and control at 10 kDa.

3.3.7.1. Specific Enzyme Digests

Specific components of follicular fluid were digested with the enzymes listed in Table 8, and the digested fluids dialysed against 100 kDa or 300 kDa MW cut-offs and the resultant colloid osmotic pressure measured (Figure 21, and Figure 22). All digestion conditions resulted in some reduction of colloid osmotic pressure of follicular fluid compared to the undigested controls. Following dialysis against 100 kDa, results indicated that in fluid from healthy follicles, 43% ± SEM 6% of the potential was attributed to DNA sensitive molecules, and 43% ± SEM 2% and 53% ± 14% to hyaluronan and chondroitin sulphate/dermatan sulphate (CS/DS). In fluid from atretic follicles DNA sensitive molecules contributed 34% ± 1.9% of the fluid potential while collagen sensitive molecules contributed 38% ± 4.8%. Removal of heparan sulphate (HS) and keratan sulphate (KS) had no significant effect on colloid osmotic pressure of either healthy or atretic fluid. The major difference between follicular fluid from healthy and atretic follicles was that hyaluronan and CS/DS did not contribute significantly to the colloid osmotic pressure in atretic follicles.

Enzyme digestion and removal of a number of fluid components less than 300 kDa reduced the colloid osmotic pressure in fluids from both healthy and atretic follicles (Figure 23 and Figure 24). In fluids from healthy follicles, 58% ± SEM 9% of the potential was attributed to hyaluronan. In fluid from atretic follicles, DNA sensitive molecules contributed 51% ± SEM 2% of the potential and hyaluronan contributed 57% with protein contributing 32%. Removal of HS by heparanase followed by dialysis resulted in some reduction in colloid osmotic pressure while KS removal had no significant effect on the colloid osmotic pressure of either healthy or atretic fluids. Removal of hyaluronan resulted in the greatest reduction in colloid osmotic pressure of fluid from healthy follicles and atretic follicles.

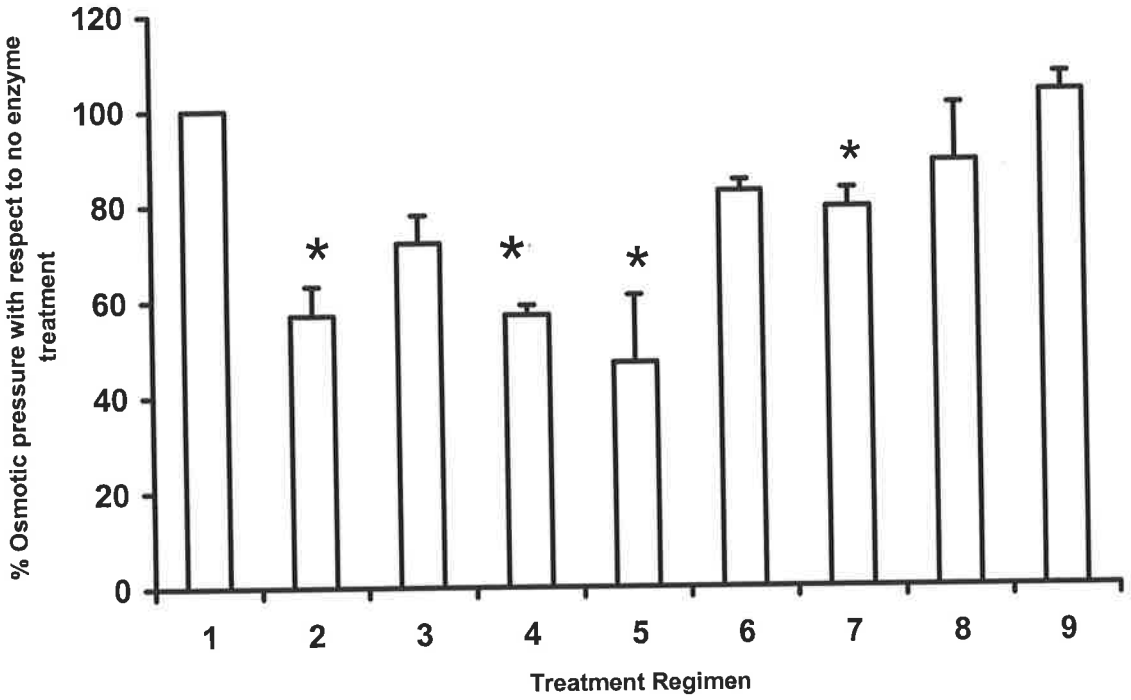

Figure 21 Effect of removal of specific components >100kDa on colloid osmotic pressure from healthy follicular fluid pools. The colloid osmotic pressure of the controls (1) were designated 100 % and the other treatments (2) DNase, (3) proteinase K, (4) Streptomyces hyaluronidase, (5) chondroitinase ABC, (6) keratanase, (7) collagenase, (8) heparanase, (9) bovine serum, were plotted as a % of these values. (*) Significantly different (P < 0.05) from control.

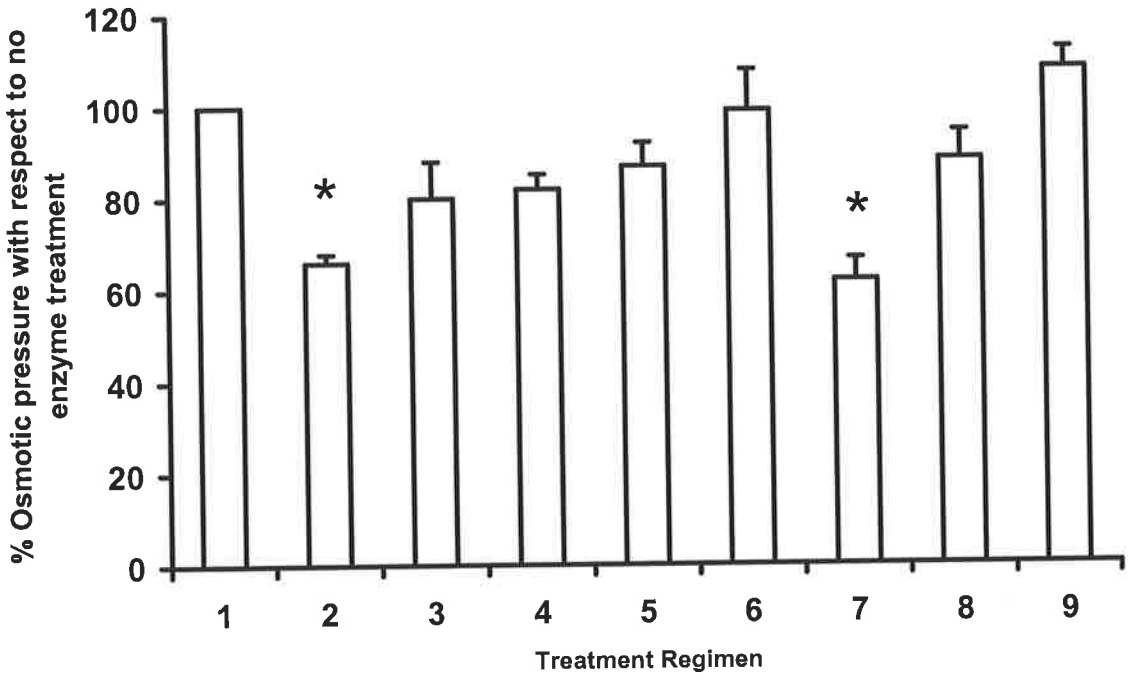

Figure 22 Effect of removal of specific components >100kDa on colloid osmotic pressure from atretic follicular fluid pools. The colloid osmotic pressure of the controls (1) were designated 100 % and the other treatments (2) DNase, (3) proteinase K, (4) Streptomyces hyaluronidase, (5) chondroitinase ABC, (6) keratanase, (7) collagenase, (8) heparanase, (9) bovine serum, were plotted as a % of these values. (*) Significantly different (P < 0.05) from control.

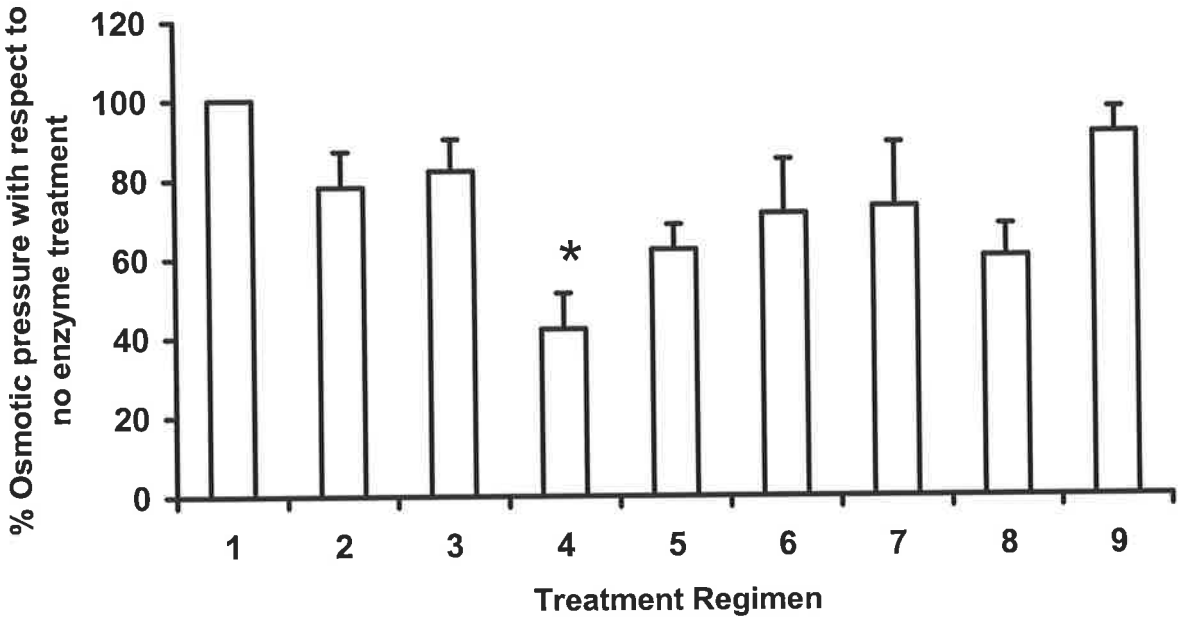

Figure 23 Effect of the removal of specific components >300kDa on colloid osmotic pressure from healthy follicular fluid pools. The colloid osmotic pressure of the controls (1) were designated 100 % and the other treatments (2) DNase, (3) proteinase K, (4) Streptomyces hyaluronidase, (5) chondroitinase ABC, (6) keratanase, (7) collagenase, (8) heparanase, (9) bovine serum, were plotted as a % of these values. (*) Significantly different ($P < 0.05$) from control.

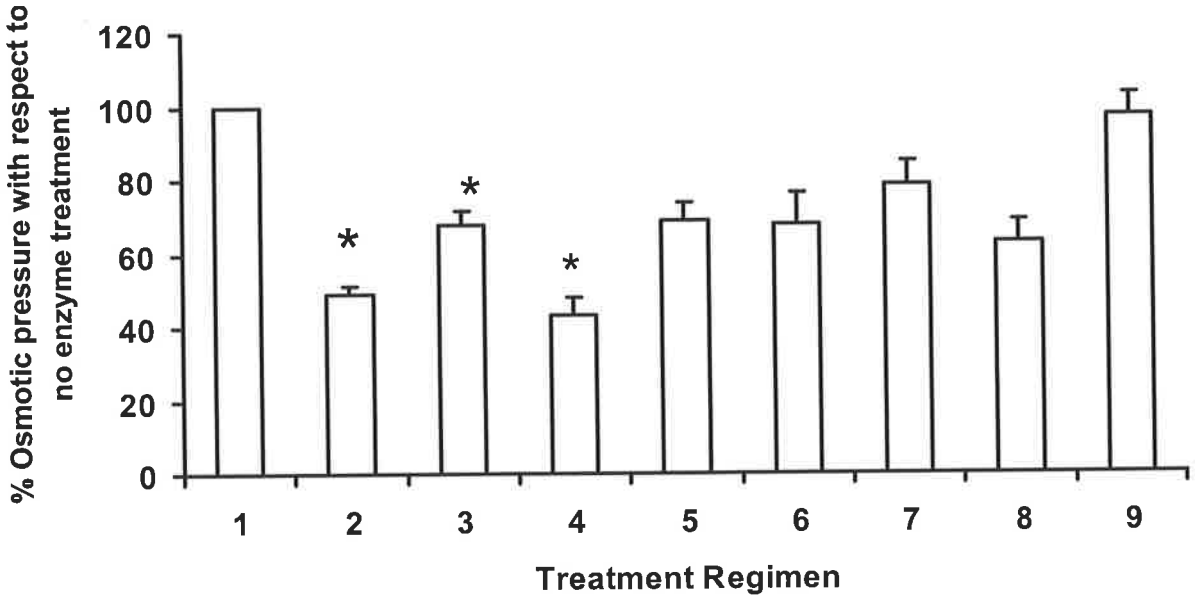

Figure 24 Effect of the removal of specific components >300kDa on colloid osmotic pressure from atretic follicular fluid pools. The colloid osmotic pressure of the controls (1) were designated 100 % and the other treatments (2) DNase, (3) proteinase K, (4) Streptomyces hyaluronidase, (5) chondroitinase ABC, (6) keratanase, (7) collagenase, (8) heparanase, (9) bovine serum, were plotted as a % of these values. (*) Significantly different ($P < 0.05$) from control.

3.3.8. Protein Concentration

Protein concentrations of the two follicular fluid pools were determined to be 52 ± 0.3 (SEM) mg/ml in healthy fluid pools and 21.5 ± 0.25 mg/ml in atretic pools.

3.3.9. Effect of Enzymatic Digestion and Subsequent Dialysis

SDS PAGE was carried out to confirm successful enzyme digestion of the fluid specific components. The gels were stained with GelCode® Blue and dried before photographing.

Observation of the gel after staining showed distinct changes in the fluid sample band patterns had occurred between enzyme treatments. Some of some proteins and glycosaminoglycans greater than 200 kDa had been removed by the S. hyaluronidase, chondroitinase ABC and keratanase treatments. The pattern of bands in the region of 80 - 200 kDa was significantly different following the collagenase digestion and this was investigated further. The results are shown in chapter 4. Proteinase K digested all protein components although it appeared that some residual protein of a size that indicated that it might be albumin that remained. Since the sensitivity of GelCode® Blue is in the nanogram range it was determined that greater than 99% of the protein component of fluid had been digested.

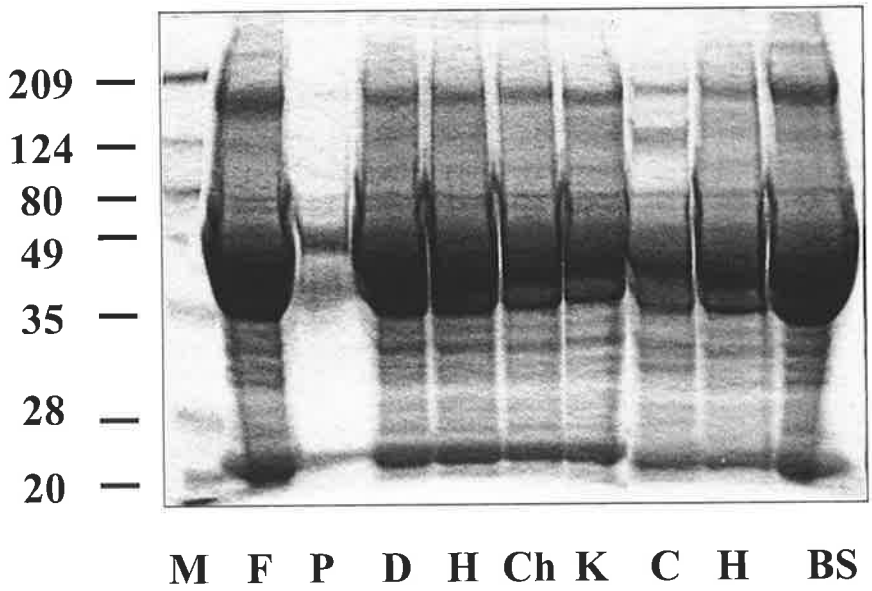

Figure 25 Non-reducing 10% SDS PAGE of follicular fluids following enzyme digestion. Labels as follows M = broad range molecular weight marker, F = undigested follicular fluid, lanes P – H represent digested fluids, P = proteinase K, D = DNase, H = Streptomyces hyaluronidase, Ch = chondroitinase ABC, K = keratanase, C = collagenase, H = heparanse, BS = undigested bovine serum. 0.5 µl of follicular fluid loaded in each lane.

3.4. Discussion

The development of the ovulatory follicle is primarily distinguished by the acquisition of a fluid-filled antrum. Increase in the diameter of the follicle during the antral stage is characterised by the increase in the size of the antral cavity (Hirshfield, 1991). The increase in antral volume noted following the gonadotrophin surge is rapid with pre-ovulatory follicular volume expansion occurring at a rate 50 – fold higher than earlier stages of antral growth (Gosden R. G. *et al.*, 1988). Follicular turgidity is maintained during the rapid growth phase of the follicle, and suggests a massive transport of fluid in to the antrum is required. Granulosa cells have previously been characterised as a leaky epithelia and therefore it is reasonable to assume that water can move from the blood supply in to the antrum via pericellular spaces between the granulosa cells (Gosden R. G. & Hunter, 1988). Shalgi et al did not find large proteins> 850 kDa in follicular fluid (Shalgi *et al.*, 1973). However, macromolecules including large proteoglycans, some of which are produced by the granulosa cells were found by Ax and Ryan within the antrum (Ax & Ryan, 1979).

The literature to date pertaining to follicular pressure has focussed on the role of follicular fluid in the rupture of the follicular wall at ovulation (Espey & Lipner, 1963, Matousek *et al.*, 2001, Rondell P, 1964, Schochet, 1916, Zachariae, 1958, Zachariae & Jensen, 1958). In this regard most research has concentrated on the intrafollicular hydrostatic pressure resulting from the accumulation of follicular fluid not the osmotic potential of the fluid.

This chapter was directed at determining whether an osmotic differential existed between circulating serum and follicular fluid and whether this difference was sufficient to cause an osmotically driven flow of fluid in to the antrum of the follicle.

Shalgi in 1972 (Shalgi *et al.*, 1972a) showed that follicular fluid proteins were 99% ± 2.2% identical to those of serum but relative proportions were vastly different to those measured in serum from the same individual. This data led to the hypothesis that a diffuse "blood follicle" barrier exists between the vasculature and the follicle, which acts as a molecular sieve, with the suggestion that this may be sensitive to molecular weight and not physical size (Shalgi *et al.*, 1973). Later Hess and Powers showed that this barrier was also sensitive to ions and that selectivity and permeability of the basal lamina was dependent on the charge carried by the molecule. (Hess *et al.*, 1998, Powers *et al.*, 1995). The properties of this so-called sieve are likely to be determined by the capillary wall, the theca interna and basement membrane and the membrane granulosa. It is possible that the selective permeability of any of these will affect the flow of fluid in to the antrum. The granulosa cells, a type of epithelial cell, separated by 20 nm wide channels which allow some molecules of up to M_r500000 to pass in to the antrum (Albertini & Anderson, 1974, Zachariae, 1958).

Early investigation of the chemical composition of follicular fluid reported that, while small molecules (<100 kDa) were able to move freely from the surrounding thecal blood supply in to the follicular antrum (and presumably *vice versa*), large macromolecules such as proteoglycans were not readily able to cross this "blood-follicle" barrier. Zachariae and Jensen (1958) commented on the presence of these macromolecules in fluid and made reference to their colloid osmotic potential in their studies of the mechanisms of ovulation, suggesting that these macromolecules were mucopolysaccharides and that in theory enzymatic degradation of the mucopolysaccharides might result in an elevation of the intrafollicular potential of the fluid however; they did not test their hypothesis (Albertini & Anderson, 1974, Zachariae, 1958, Zachariae & Jensen, 1958).

Together this information implied that the production of large osmotically active molecules produced within the follicle, presumably by granulosa cells, could generate an osmotic differential between the fluid and the circulating blood supply, either by virtue of their size and charge or by their degradation. There has been no investigation of this hypothesis until now.

The series of experiments in this chapter were designed to resolve issues of the relative osmotic potentials of follicular fluid to serum and to determine whether the follicle has the ability to create and utilise an osmotic gradient as a means of accumulating fluid. By determining a method of measuring the differences between fluid and serum while negating the effect of molecules common to both, it appears this goal has been achieved.

Initial experiments aimed at determining the permeability of the follicular wall by the immersion of isolated follicles in to solutions of increasing molecular weight of dextran were a type of test mimicking those of micro-dialysis assays used in the monitoring of the movement of large molecules in an extracellular matrix (Dong Z. *et al.*, 1998). The experiments were unsuccessful; possibly due to the difficulty in achieving complete removal of the stroma from the isolated follicle without causing some damage to the whole follicle. The data may have been more significant had it been possible to characterise the health status of the follicle prior to immersion in dextran and then relate health status to results obtained. Since this was not a possibility no further experiments were carried out.

During the collection of follicular fluid for use in subsequent experiments the aspirated fluid volumes were recorded to determine whether the fluid collection procedures were efficient. The average volume collected was then plotted against the total follicular volume. Calculations of the follicular volume of follicles of 8 – 20mm in diameter, showed that the volumes of fluid collected from 8 – 20 mm follicles were 60-100% of the total volume of the follicle. Allowing for internal structures within the follicle the data indicated that the majority of fluid was collected and was representative of the follicular fluid present in the follicle at

that time. It was interesting to note that follicular volume collected increased steadily with increasing diameter and matched the predicted volume increase within the follicle. In order to fill the predicted increase in follicular volume the rate of fluid accumulation in pre-ovulatory follicles must be very rapid. Given the short time period over which the pre-ovulatory stage of growth is known to occur (Marion *et al.*, 1968b) the rate of fluid accumulation at this time must be greatly increased over the previous 30-day accumulation period. The data here shows that the amount of recovered fluid increased dramatically with increased follicular diameter and hence stage of development and is therefore appears to support the claims of Marion et al (Marion *et al.*, 1968b). One further consideration that must be made is that of follicular surface area ratio to follicular volume, as this too will affect the fluid uptake. While the relationship shows an exponential the rate of area to volume ratio is greatly reduced from a 3:1 ratio to that of 0.15:1. Given this large difference it is likely a positive force such as osmosis is required to drive fluid accumulation in the follicle.

The next series of experiments focussed solely on the question of colloid osmotic pressure determination. In order to expand on data produced by Smith, Edwards, Zachariae and Jensen and Shalgi (Edwards, 1974, Shalgi *et al.*, 1972a, Smith J.T & Ketteringham, 1937, Zachariae & Jensen, 1958), all of who measured osmotic pressure of follicular fluid but none of whom assessed fluid from characterised follicles at different developmental stages, the colloid osmotic pressures of fluid from sized and characterised follicles was determined and related to their relative potential with respect to serum.

The initial experiments determining the colloid osmotic pressure of follicular fluid from uncharacterised follicles of different sizes showed that the colloid osmotic pressure from early stage follicles was significantly greater than that of serum while that of preovulatory follicles was similar to that of serum (Edwards, 1974, Shalgi *et al.*, 1972a, Zachariae, 1958). The data pertaining to the colloid osmotic pressure of preovulatory follicles was in agreement with that of Smith and Shalgi who determined the osmotic pressure to be less than or equivalent to that of serum. The colloid osmotic pressure of the smaller growing follicles has not previously been reported. It is interesting to note that it is far greater than that recorded from the fluid of pre-ovulatory follicle since it is during this latter stage that the growth of the follicle is at its greatest and therefore one might expect the potential to be at its highest. One explanation for this lies in some research carried out by McConnell in rats (McConnell *et al.*, 2002). Transcellular water transport occurs by a number of methods, firstly the slower methods of simple diffusion through the hydrophobic interior of the membrane, pericellular transport and lastly via a far more rapid method through proteinaceous water channels termed aquaporins, which support large volumes of water flow (Preston *et al.*, 1992). McConnell's data showed that 70 % of water transport in to the follicle occurred via the transcellular aquaporins and just

30% via pericellular diffusion. Given these data, it is reasonable to hypothesise that initial slow phases of growth occur via a different mechanism to that of the rapid growth phase. Slow growth may be driven by the established osmotic gradients within the follicle, which must exist according to the data shown here, while rapid growth may be initially driven by the same method but then is aided by a change in the permeability of the follicle caused by the aquaporins.

The next series of experiments were designed to identify the size and class of molecule responsible for the greatest proportion of the measured potential. In order to achieve this, membranes were chosen with nominal MW cut offs. These allowed for removal of low molecular weight molecules and electrolytes, molecules known to be able to traverse the basal lamina freely, molecules of a size able to enter the follicle in reduced concentrations and molecules whose movement would be severely restricted and likely to be synthesised locally. Since in similar work carried out by Tombs and Peacocke (Tombs & Peacocke, 1974) there was much criticism of nominal MW cut off membranes produced by manufacturers, it was decided that several membranes should be tested and a series of tests devised that would evaluate their accuracy and efficiency under dialysis conditions. Results revealed that despite claims made in the manufacturers literature, only the membranes supplied by Millipore were reliable and these products were used in subsequent experiments.

Once a membrane system had been approved, follicular fluid was collected from follicles of known health status and subjected to dialysis against membranes of increasing MW cut off. The results from size exclusion experiments showed that little or no change occurred in the measured colloid osmotic pressures of either fluid type on the removal of molecules less than 100 kDa. Molecules greater than 300 kDa in healthy and atretic follicles provided 65% and 71% of the fluid potential respectively. Molecules greater than 500 kDa contributed 40% of the colloid osmotic pressure in healthy follicles and 20% of that from atretic follicles. In addition, the data demonstrated that molecules in the range of 300-500 kDa contributed 15% of the potential in healthy follicle and 51% of the potential in atretic follicles. This implied that there were differences in molecular constitution of healthy and atretic follicles and these differences became apparent on determining the classes of molecules, contributing to the colloid osmotic pressure.

In order to determine which classes of molecules contribute to the colloid osmotic pressure enzymes known to degrade different classes of molecules were used. This was followed by dialysis to remove their digestion products from the follicular fluids. Dialysis was carried out at two MW cut offs 100 and 300 kDa, as this would remove the smaller molecules unlikely to be osmotically active and allow us to observe two groups of larger molecules.

Initial experimental data showed that the colloid osmotic pressure increased after digestion with Streptomyces hyaluronidase. A review of the literature indicated conditions of low or no salt caused these effects. This in turn results in concentration-dependent intermolecular association of short segments of hyaluronan, a capability for intramolecular association (hairpin formation) by larger hyaluronan segments. Such effects can occur with as few as 10-13 disaccharide units (Turner *et al.*, 1988). This issue was resolved by sequential dialyses first in salt then to water as suggested by Turner in order to break these associations by reducing the relative charges of the adjacent anti-parallel disaccharides.

In this chapter, follicular fluid protein levels between 52 ± 0.3 (SEM) and 21.5 ± 0.25 mg/ml were recorded for healthy and atretic follicles respectively. The protein content of bovine serum had previously been determined at 71.9 mg/ml. These data indicated that the protein concentration of healthy follicles was 72% that of serum while protein content of atretic follicles was just 30%. The data for healthy follicles is consistent with that recorded by Leroy et al (Leroy *et al.*, 2004).

Removal from follicular fluid of healthy follicles of the glycosaminoglycans, hyaluronic acid, chondroitin/dermatan sulphates, and DNA resulted in the greatest reduction in colloid osmotic pressure at both MW cut offs. Removal from follicular fluid of atretic follicles of the hyaluronan and DNA made the greatest reduction in colloid osmotic pressure at both MW cut offs with contributions from proteins and collagenase I sensitive molecules. The results indicated that there are differences in the osmotic potentials of fluid and suggest that the molecular reasons for this are associated with the hyaluronan, chondroitin and dermatan sulphates and DNA.

Hyaluronan has a variety of physiological functions in the extracellular matrix, as mentioned in chapter 1. Its osmotic effects provide a sensitive mechanism for volume buffering in the interstitium via the formation of highly entangled networks of flexible polysaccharide molecules in the extracellular matrices within the body. Hyaluronan is synthesised by one of three hyaluronan synthases. Unlike proteoglycans it does not have a core protein. However, there are a number of cell surface proteins (CD44, RRHAM and lyve-1) or other proteins (link protein, versican, ITI), which can bind to hyaluronan to make a more organised three-dimensional matrix (Jackson D. G., 2003). Here hyaluronan was observed to contribute substantially to the colloid osmotic pressure of follicular fluid, and at a sufficiently large size to exert osmotic potential in vivo. It is interesting to note that the overall reduction in colloid osmotic pressure caused by removing chondroitin/dermatan sulphates and DNA has resulted in what appears to be a total of 139% of the potential. This phenomenon can be explained by research conducted by Dick (Dick, 1966) and Laurent and Ogston (Laurent T. C. & Ogston, 1963).

The former showed that in ideal systems osmolarity is independent of the nature of the solute species but this is only true for simple solutions and of extreme dilutions. In real solutions, solution – solvent interactions occur and result in osmotic potentials greater or less than that predicted by the van't Hoff Equation (Van't-Hoff, 1887). In practice a pronounced deviation from ideal behaviour is observed when the osmotic coefficient, defined as a deviation in the behaviour of a solute from ideal behaviour, is at 2-3 instead of unity (Dick, 1966). The osmotic coefficient of proteins and related proteoglycans can change rapidly and nonlinearly with concentration. The result of this is that the contributions of hyaluronan, proteoglycans and collagen to the follicular fluid colloid osmotic pressure cannot be considered as mutually exclusive contributions, since each is known to interact with the other and as such removal of one may result in a reduction in the effective pressure of the other, thereby creating the illusion of a greater than 100% contribution effect overall.

Laurent et al (Laurent T. C. & Ogston, 1963) showed that hyaluronan can interact with proteoglycans and albumin resulting in an osmotic potential far in excess of that predicted by addition of their individual potential components. An exclusion volume created by the albumin around the macromolecules causes this. For albumin found within serum this exclusion volume has been calculated to be 25ml/ g hyaluronan. That glycosaminoglycans in follicular fluid exert osmotic activity is not surprising. Proteoglycans and their glycosaminoglycan side chains are thought to be partially responsible for the osmotic forces active during a number of fluid accumulation processes in the body (Buschmann & Grodzinsky, 1995, Comper & Laurent, 1978, Comper & Zamparo, 1989, Gu *et al.*, 1993, Ishihara *et al.*, 1997, Khalsa & Eisenberg, 1997, Kovach, 1995, Laurent T. C., 1987, Zamparo & Comper, 1989)

The colloid osmotic pressure of hyaluronan has been recorded on many occasions and is known to markedly affect the partition of diffusible molecules. This effect is caused by steric exclusion of macromolecular solutes containing randomly coiled hyaluronan. This phenomenon, in turn exerts a significant effect on the thermodynamics of the solution (Comper, 1994, Milas *et al.*, 2001). It may well be that the hyaluronan and proteoglycans in fluid are also responsible for maintenance of follicular cooling in the follicle reported by Luck et al (Luck *et al.*, 2001) since secretion of such molecules in to the follicle and their subsequent hydration would result in a constant uptake of heat from surrounding tissues.

In the ovary hyaluronan production by cumulus cells has been studied extensively (Chen H. L. *et al.*, 1993a, Chen L. *et al.*, 1993b, Chen L. *et al.*, 1996, Hess *et al.*, 1999, Hirashima *et al.*, 1997, Kobayashi *et al.*, 1999). However, the production of hyaluronan by cumulus cells is tailored to the release of the cumulus-oocyte complex at ovulation. For hyaluronan to be involved in follicular fluid formation it would need to be produced at a much

earlier stage than that produced prior to ovulation. Hyaluronan levels of human follicular fluid have been measured at 50.0 ± 2.6 ng/ml and it has been localised by immunohistochemistry adjacent to and including the spaces between antral granulosa cells (Saito *et al.*, 2000). Follicular hyaluronan has been reported as being at sufficiently large sizes for it to be retained in the follicular antrum, and recently low levels of hyaluronan synthase expression and hyaluronan production were observed in granulosa cells in culture following stimulation with FSH (Schoenfelder & Einspanier, 2003). Thus clearly hyaluronan has all the credentials to be a key player in the formation of follicular fluid.

Earlier research in a number of species has identified glycosaminoglycans DS and CS in follicular fluids, and has revealed that glycosaminoglycans and proteoglycans are synthesised by the granulosa cells in vitro if stimulated (Ax & Ryan, 1979, Bellin *et al.*, 1983, Eriksen *et al.*, 1997, Yanagishita *et al.*, 1981).

Hyaluronan and chondroitin/dermatan sulphates are strongly hydrophilic and highly negatively charged and this negative charge is responsible for the osmotic activity of the molecules with which they are associated (Schultz & G, 2005).

Essentially this means that water is drawn into proteoglycan molecules as a result of the charges on their glycosaminoglycan side chains, provided that the water can flow, an osmotic gradient can exist. Since this phenomenon is dependent on charge, it is molecular weight independent. Zamparo and Comper (Zamparo & Comper, 1989) have shown that the hydraulic conductivity of proteoglycans and their attached chondroitin sulphate side chains is high, leading to high osmotic pressures being created and indicate as above that it is the positioning and number of side chains along the protein core and not the chondroitin sulphate chains themselves that are responsible for this phenomenon. This implies that the osmotic pressure component delivered by the chondroitin sulphate proteoglycan in fluid is dependent on the proteoglycan present and not free chondroitin sulphate chains, which may be in the fluid.

In addition proteoglycans create hydration layers (excluded volumes) around themselves in solution this is because the electrical potential of proteoglycans create a strongly charged electrical field, this field potential extends beyond the physical boundary of the molecule itself and so it is therefore able to interact with other molecules without coming in to physical contact with them. These charges are also very important in relation to macromolecular recognition and adhesion (Gu *et al.*, 1993).

Glycosaminoglycans have previously been identified in follicular fluid and this study demonstrates that they contribute to the osmotic potential of follicular fluid and at sizes too large to leave the follicular antrum (Andrade-Gordon *et al.*, 1992, Bellin & Ax, 1987a, b, Bellin *et al.*, 1986, Boushehri *et al.*, 1996, Bushmeyer *et al.*, 1985, Edwards, 1974, Eppig &

Ward-Bailey, 1984, Grimek *et al.*, 1984, Parillo *et al.*, 1998, Sato *et al.*, 1987a, Sato *et al.*, 1988, Shimada *et al.*, 2001, Tadano & Yamada, 1978, Tsuiki *et al.*, 1988, Varner *et al.*, 1991, Wise & Maurer, 1994).

With respect to the DNA osmotic pressure measurements, the osmotic pressure of deoxyribonucleic acids, which are intensely hydrophilic biopolymers, has been measured by a number of authors and it has been shown that nucleic acids have osmotic coefficients as high as proteins of comparable molecular weights. The DNA found in follicular fluid is likely to be derived from granulosa cells that line the follicular antrum, which upon their death release DNA in to the fluid. These cells do not appear to die by apoptosis but rather a process more in common with terminal differentiation (Van Wezel *et al.*, 1999). This DNA may be entangled with larger molecules such as hyaluronan as suggested by several authors; this too would serve to increase the osmotic effect of the DNA by minimizing the loss of DNA or hyaluronan from the follicular fluid (Turner *et al.*, 1988). Experiments in chapter 4 investigate this phenomenon. However, the DNA content of follicular fluid is probably not regulated and potentially it could easily be degraded by release of cellular DNase. Thus DNA, whilst contributing to the osmotic pressure of follicular fluid as observed here and possibly in vivo, is probably not a regulated component.

The reduction in osmotic pressure by collagenase was interesting. Collagenase I (MMP-1), used in the digestion of the fluid samples cleaves all three strands of the intact native collagen, it is known to degrade fibrillar collagens. Studies on the osmotic potential of Wharton's jelly (Snashall, 1977), a gelatinous intercellular substance, which is the primitive mucoid connective tissue of the umbilical cord, showed that hyaluronan was stearically excluded from a proportion of interstitial water by fibrous matrices. This fibrous matrix was in most part made up of collagen and resulted in an effective increase in the concentration of hyaluronan in these areas. Collagen despite its insolubility exhibits pronounced volume exclusion effects and can increase the osmotic potential of fluids, which contain it, especially when macromolecules such as hyaluronan and chondroitin sulphate proteoglycans are present. Plasma proteins were also significantly excluded by collagen to similar effect. The end result was that the measured colloid osmotic pressure was above that predicted. Since chondroitin sulphate can associate with collagen in extracellular matrices a certain amount of chondroitin sulphate may have been removed on digestion and dialysis of the collagens by collagenase. Although a significant reduction in colloid osmotic pressure was observed in fluid from healthy follicles the greatest reduction was seen in fluid from atretic follicles. The apparent increase in free collagen present may result from the breakdown of the basal lamina and invasion of the thecal cells which can deposit collagen or from the production of collagen in

the membrana granulosa during atresia (Bagavandoss *et al.*, 1983, Huet *et al.*, 1997, Huet *et al.*, 1998).

Whilst most of the discussion presented here has focused on fluid from healthy follicles fluid from atretic follicles was also examined. Not all the processes leading to atresia are understood, but the final result is resorption of the follicular fluid and death of the granulosa and thecal cells. The follicular basal lamina, a possible site of the 'blood-follicle barrier', does not appear to be degraded in early atresia but can be breached by the theca and macrophages in the later stages (Irving-Rodgers *et al.*, 2002). For resorption to occur degradation of the osmotically active molecules must also occur, but in follicles examined during the process of atresia the measured colloid osmotic pressure was not significantly different to healthy follicles.

However, whereas molecules of 300-500 kDa contributed 25% of the potential in healthy follicles they contributed 51% in atretic follicles, implying that there were differences in the molecular constitution of healthy and atretic follicular fluids. The contribution of different classes of molecule to colloid osmotic pressure at the molecular weight cut offs observed here showed where these differences lay.

In atretic follicles fluid colloid osmotic pressure was reduced following the removal of DNA, protein and hyaluronan. The contribution made by DNA was not surprising given that considerable cell death occurs during atresia. However, the fact that chondroitin/dermatan sulphates were not major contributors to the colloid osmotic pressure in atretic follicles was interesting. Chondroitin sulphate concentrations in atretic fluids have been reported as higher than those of healthy fluids (Bellin & Ax, 1984). These molecules may still be present, however, more of them exist in an unbound form. The unbound sulphates may arise from the partial breakdown of large chondroitin sulphate containing proteoglycans, that may have previously contributed to the higher colloid osmotic pressure seen in the >500 kDa dialysate from healthy follicles. These degraded or partially degraded molecules may also be the cause of the higher fluid potential recorded by the 300 – 500 kDa dialysate of atretic fluid. Loss or degradation of these molecules could be an important step in follicular atresia.

3.5. Summary

In summary, the colloid osmotic pressure of bovine follicular fluid is different to that of bovine serum and therefore an osmotic gradient must exist between the follicle and the serum of the circulating vasculature. The osmotic pressure of fluid relative to serum changes from being greater than to less than during antrum growth and fluid accumulation (Figure 14). During the slow growth phase of the follicle, osmosis probably drives fluid movement via a positive osmotic differential between fluid and serum. In the latter stages it is possible that

other mechanisms assist fluid accumulation such as greater permeability of the follicular wall and increased blood flow as well as the expression of aquaporins by thegranulosa cells. The major contributors to the colloid osmotic pressures of follicular fluid from healthy follicles are hyaluronan CS and DNA. These molecules or their aggregates >500 kDa contribute 40 % of the overall potential recorded. The contributors to the colloid osmotic pressure from atretic follicles are DNA and collagen. Molecules of 300 – 500 kDa in size contribute the majority of the fluid potential. These data indicate that molecules of a size not easily able to escape the follicle can contribute to the osmotic pressure of follicular fluid.

Chapter 4 Proteoglycans and Glycosaminoglycans in Follicular Fluid

4.1. Introduction

In Chapter 3 it was determined that the colloid osmotic pressure of bovine follicular fluid was different to that of bovine serum and therefore that there was potential for an osmotic gradient to exist between the follicle and the serum of the circulating vasculature. The data showed that the major contributors to the colloid osmotic pressure of follicular fluid from healthy and atretic follicles were hyaluronan, chondroitin/dermatan sulphate, DNA and collagen.

The contribution of the chondroitin sulphate component identified in Chapter 3 was probably derived from chondroitin/dermatan sulphate proteoglycans (CS proteoglycans). Proteoglycans, hyaluronan and collagen are key constituents of the extracellular matrix (ECM). During ovarian growth and development the follicular ECM undergoes significant structural changes in response to external stimuli that signal changes in gene regulation, cell growth or differentiation. General properties associated with the ECM are the ability to bind growth factors, provide rigid or elastic mechanical support and to act in the fluid dynamics of tissues around the body providing osmotic forces and filtering capabilities (Culav *et al.*, 1999, Iwata & Carlson, 1993, Iwata *et al.*, 1993, Netti *et al.*, 2000, Rodgers R. J. *et al.*, 2003).

During follicular development a fluid filled cavity forms in the extracellular space surrounding the granulosa cells at the centre of the follicle. In the previous chapter it was determined that osmotically active molecules capable of retaining fluid such as chondroitin/dermatan sulphate glycosaminoglycans and hyaluronan were responsible for the increase in osmo-reactivity of the fluid over that of the circulating serum.

Chondroitin/dermatan sulphate proteoglycans, collagen and hyaluronan have been implicated in osmotic regulation in several regulated fluid systems (Aukland *et al.*, 1997, Comper & Zamparo, 1989, Culav *et al.*, 1999, Ehrlich *et al.*, 1998, Ghosh *et al.*, 1990, Iwata & Carlson, 1993, Iwata *et al.*, 1993, Khalsa & Eisenberg, 1997, Laurent T. C., 1987, Netti *et al.*, 2000, Ostgaard & Reed, 1994, Rodgers R. J. *et al.*, 2003, Wiederhielm & Black, 1976, Zamparo & Comper, 1989). Chondroitin/dermatan sulphates and hyaluronan are the osmotic drivers in wound repair and the maintenance and regulation of fluid movement through connective tissues such as the trabecular meshwork of the eye and the arachnoid of the brain. Both the eye and the brain "outflow" pathways contain chondroitin sulphate and hyaluronan in their biological filtration barriers. Glycosaminoglycans act to maintain the unidirectional character, low-flow fluid movement, and potential gradient between the trabecular lamellae and the drainage channels of the eye and the brain (Knepper & McLone, 1985), and it is

conceivable that similar processes are responsible during the slow phase of follicular growth and fluid accumulation.

The role of collagen in the maintenance of osmotic potential has been linked to its binding of proteoglycans and entanglement with hyaluronan. The roles and content of proteoglycans and hyaluronan in the follicle, specifically the cumulus oocyte complex and ECM, have been studied extensively in humans and mice (Carrette *et al.*, 2001, Eppig & Ward-Bailey, 1984, Eriksen *et al.*, 1997, Eriksen *et al.*, 1994, Eriksen *et al.*, 1999, Franchimont *et al.*, 1990, Gotting *et al.*, 2002, Sakata *et al.*, 2000, Sato *et al.*, 1987b, Shimada *et al.*, 2001). The composition of follicular fluid from humans and pigs has been analysed for glycosaminoglycans while other studies have been directed at the synthesis of glycosaminoglycans by stimulated granulosa cells (Andrade-Gordon *et al.*, 1992, Bellin & Ax, 1987a, b, Bellin *et al.*, 1986, Hamamah *et al.*, 1996, Sato *et al.*, 1990, Yanagishita *et al.*, 1979). Relative follicular fluid glycosaminoglycan concentrations have been shown to affect oocyte viability and fertilisation rates (Bellin *et al.*, 1986, Hamamah *et al.*, 1996).

Proteoglycans have been reported in bovine follicular fluid and linked to the enhancement of the acrosome reaction by positively affecting sperm velocity and retention during fertilisation (Eriksen *et al.*, 1994, Grimek *et al.*, 1984, Lenz *et al.*, 1982, McArthur *et al.*, 2000, Parillo *et al.*, 1998, Reyes *et al.*, 1984, Rodgers R. J. *et al.*, 1995b). In most cases the proteoglycans and glycosaminoglycans involved have not been characterised.

In order to determine the size and identity of the chondroitin/dermatan sulphate molecules in bovine, classic laboratory protocols were utilised. A review of the literature suggested that extraction of the soluble proteoglycans from the fluid was necessary (Boushehri *et al.*, 1996, Eriksen *et al.*, 1999, McArthur *et al.*, 2000, Schneyer *et al.*, 1996, Shimada *et al.*, 2001, Yanagishita *et al.*, 1979). Following extraction and identification localisation within the follicle was achieved using immunohistochemistry and molecular biology.

In Chapter 3 results indicated that atretic fluid contained more osmotically active molecules in the 300-500 kDa range than the healthy follicles however; the total colloid osmotic pressure of fluid from healthy and atretic follicles were not statistically different from one another. Therefore in order to obtain sufficient fluid for analysis the two fluid types were pooled.

This chapter focuses on the characterisation, identification and localisation of the chondroitin/dermatan sulphate proteoglycans present in follicular fluid. In addition, the sizes of hyaluronan present were identified and an attempt made to identify its interactions and its localisation within the follicle. In addition, the identification of the collagenase sensitive

molecules revealed in Chapter 3 was sought using protein sequencing and with further investigation of the DNA present in the follicular fluid.

4.2. Experimental Design

The study of proteoglycans from cartilage and synovial fluid has resulted in a plethora of proteoglycan extraction methods. The methods reported to date have been designed to provide the most effective extraction method for the particular tissue being studied. Proteoglycans within follicular fluid are derived from ECM debris or are in the form of soluble proteoglycans. In this thesis a method of extraction for soluble proteoglycans was derived from an original method described by (Savolainen, 1999) in order investigate the fluid proteoglycans. Fluids were collected from follicles as described in 2.3.4 of this thesis. Briefly, fluids were obtained by puncture of the follicle with a needle. The fluids from healthy and atretic follicles were pooled in order to provide sufficient sample for analyses. The method employed 4 M urea and sodium acetate followed by separation of proteoglycans by ion exchange chromatography. The use of urea ensured that denaturing conditions were maintained, while also preventing protein macromolecule interactions and protein precipitation events that might have resulted in a decrease in yield. Extraction at 4 ^{o}C also reduced the chance of degradation of the urea and of the sample. Ion exchange chromatography using DEAE sepharose was selected as a method of separation since it is a high capacity exchange product. Ion exchange chromatography can be used to separate chondroitin/dermatan sulphate and keratan sulphate and hyaluronan by gradual increase in salt concentrations. Sample fractions from this column type could also be subsequently analysed for protein and uronic acid content.

Proteoglycans are highly variable in their size and this makes estimation of their exact size difficult. Estimation of proteoglycan size can be carried out by a number of methods, which include centrifugation, column separation, light scattering and viscosity. Follicular fluid proteoglycans and hyaluronan have been identified in the previous chapter; the most common method used for the determination of the structural characteristics of the extracted proteoglycan samples is size exclusion chromatography. The proteoglycans were secondarily extracted using 4M-guanidine hydrochloride (GnHCl); this was done to ensure release of their non-covalent bonds (Sajdera & Hascall, 1969). Following this the sample was separated over a size exclusion column of CL – 2B sepharose which traps and releases globular proteins from 70,000 to 40,000,000 and dextrans from 100,000-20,000,000 in size. The collected fractions were then dialysed free of GnHCl prior to further analyses.

The protein content of the fluid fractions collected was measured by the Bradford method (Bradford, 1976).

Total uronic acid content was measured by the metadihydroxyphenyl-borate-sulphuric acid method of Blumenkrantz and Asboe – Hansen (1973). The total amount from pooled follicular fluid from follicles < 10 mm in size was measured and compared to that of bovine serum. Prior removal of protein from the sample, which interferes with the reaction, was achieved by pre-treatment with sodium hydroxide overnight. ELISA using antibodies to specific glycosaminoglycan epitopes or proteoglycans, with or without prior enzyme digestion, were then used to identify the proteoglycans and glycosaminoglycans present.

Since a spectrum of relevant antibodies were available for use it was decided that Western blot analyses of fluids separated by SDS PAGE and agarose gel electrophoresis would be an appropriate method to employ for identification of some proteoglycan and hyaluronan components, these methods allowed the fluid to be separated on charge and size or by size alone. In the case of hyaluronan, agarose gels were used in order to allow full penetration of the large hyaluronan molecule in to the gel. Following identification of the molecules involved, their localisation within the follicle was achieved using immunohistochemical techniques on Bouin's fixed tissues.

Digestion of follicular fluid with collagenase I in Chapter 3 identified a significantly different banding pattern to that seen following glycosaminoglycan, DNA or protein digestion. Identification of the collagenase sensitive molecules was necessary since there were no previous reports pertaining to this phenomenon in bovine follicular fluid. The method chosen to analyse these molecules was protein sequencing. Identification of the digestion products was done using the proteomics tool PROWL to search protein databases (http://prowl.rockefeller.edu/prowl). Analysis of the size and interactions of DNA within the fluid was analysed using EtBr and StainsAll® stained agarose gels.

4.3. Results

4.3.1. Protein Concentration

Measurement of protein concentration from pooled fractions collected after proteoglycan extraction and separation by chromatography can be seen in (Figure 26). The concentration within the fractions ranged from 20 – 80 mg/ml

4.3.2. Ion Exchange Chromatography

The proteoglycans were extracted from follicular fluid and isolated by anion-exchange chromatography. Twenty fractions (2.5 ml) were collected from the DEAE column and 200 μl of each fraction assayed for uronic acid content. The uronic acid concentration recorded from a sequential series of collected fractions ranged from 0.5 – 1.2 mg/ml

4.3.3. Size Exclusion Chromatography and ELISA

The proteoglycans isolated from follicular fluid, as determined by uronic acid assay of the collected fractions were then pooled and fractionated by size exclusion chromatography on Sepharose CL-2B. The results of assay by ELISA of 4-sulphated CS/DS and 6-sulphated CS/DS proteoglycans are shown in (Figure 27 A and B). ELISA to molecules known to interact with hyaluronan and/or known to be present in follicular fluid of other species are shown in (Figure 27 C – I). These are versican GAGβ, inter-alpha trypsin inhibitor, biglycan, decorin, TSG6 (not shown), perlecan and aggrecan. The glycosaminoglycan content for each fraction can be seen in (Figure 27 I). The chondroitin-containing material as determined by the C-4-S peak shows that the majority of the chondroitin sulphate proteoglycan eluted in the region of low protein content and as a symmetrical peak. A small peak of chondroitin containing material eluted in the void volume of the column indicating the presence of very high molecular weight proteoglycans or aggregates These data are similar to those reported by Grimek, Bellin an Ax (1984). The rest of the proteoglycans were eluted from further down the column indicating that they were of smaller size. The slow incline of the glycosaminoglycan peak indicated that there were low levels of large glycosaminoglycans or proteoglycans present in the follicular fluid sampled.

The glycosaminoglycan poly-disperse peak overlapped that of the protein and the 4-sulphated CS/DS. Versican was detected in a poly-disperse peak that overlapped the peak containing 4-sulphated CS/DS. No reactivity was detected against 6-sulphated CS/DS. Inter-alpha trypsin was recorded in fractions 23 – 65, these fractions also showed reactivity with protein.

No reactivity was seen with aggrecan or decorin, biglycan, perlecan. The TSG 6 antibody gave variable results in a number of samples and the data could not be verified and is therefore not shown here

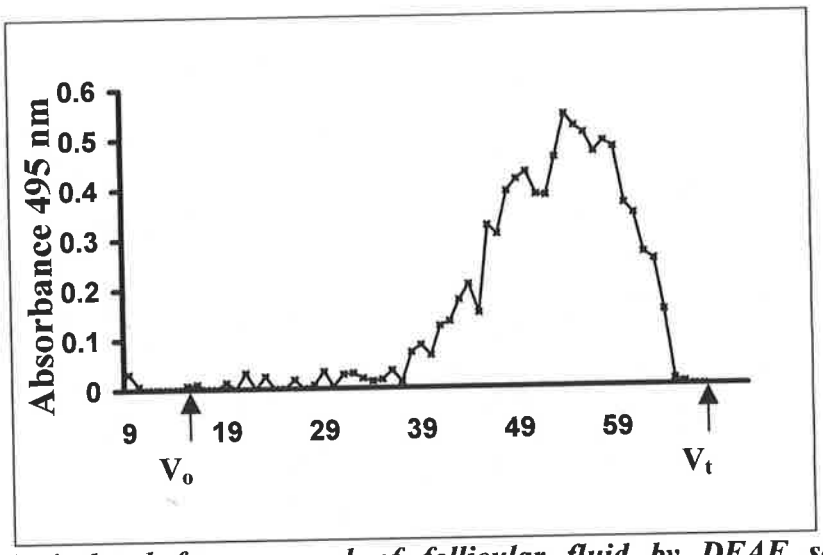

Figure 26 PGs isolated from a pool of follicular fluid by DEAE sepharose were chromatographed on CL-2B size exclusion column with 2 M guanidine-HCl buffer. The eluted fractions (9-65) were analysed for their concentrations of protein. The elution volume of the proteins occurs between the void volume (V_o) and the bed volume (V_t). The fraction number is displayed on the x-axis.

Figure 27 Size-exclusion chromatography of PGs isolated by anion-exchange chromatography. PGs isolated from a pool of follicular fluid by DEAE sepharose were chromatographed on CL-2B size exclusion column with 2 M guanidine-HCl buffer. The eluted fractions were analysed for their concentrations of A: 4-sulphated CS/DS, B: 6-sulphated CS/DS, C: versican, D: inter-alpha trypsin inhibitor, E: Aggrecan, F: perlecan, G: biglycan, H: decorin, I: GAG. The absorbance (415 nm) can be read on the y-axis with the fraction number indicated in the x-axis for panels A – H. The absorbance for the GAG assay was 520 nm. Vo shown in panel I indicate the void volume of the column while Vo - Vt represents the proteoglycan containing fraction. The antibody used for identification is denoted in brackets. The fraction number is displayed on the x-axis.

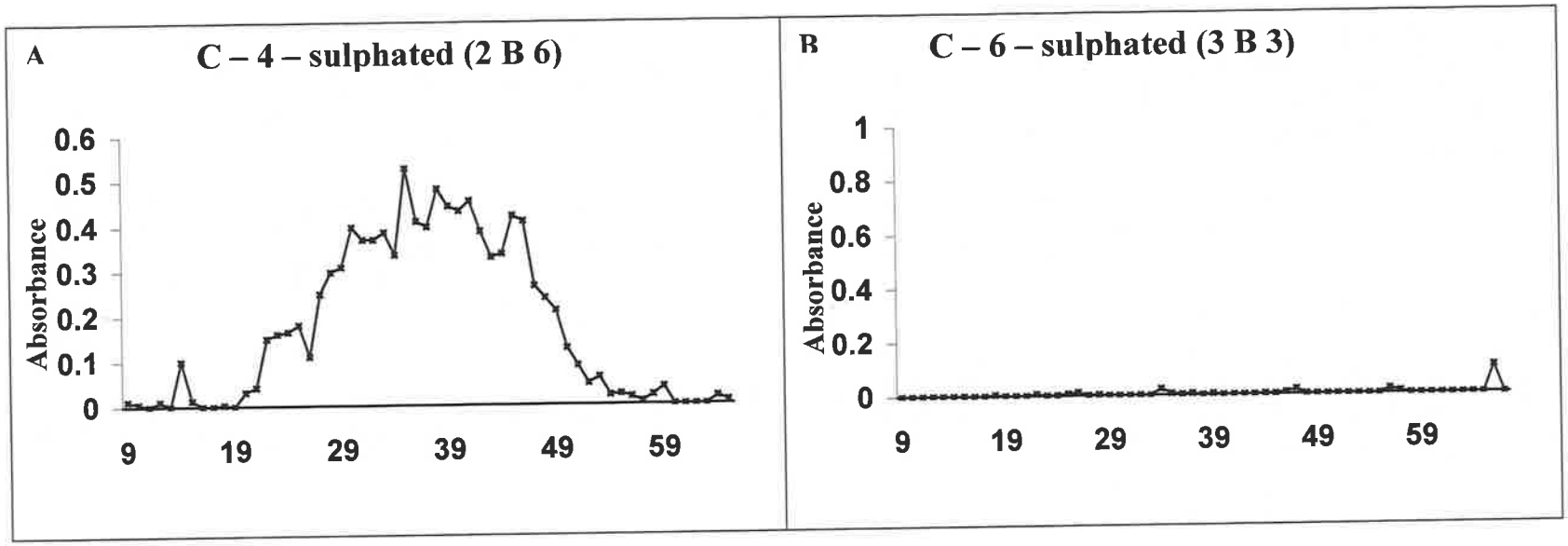

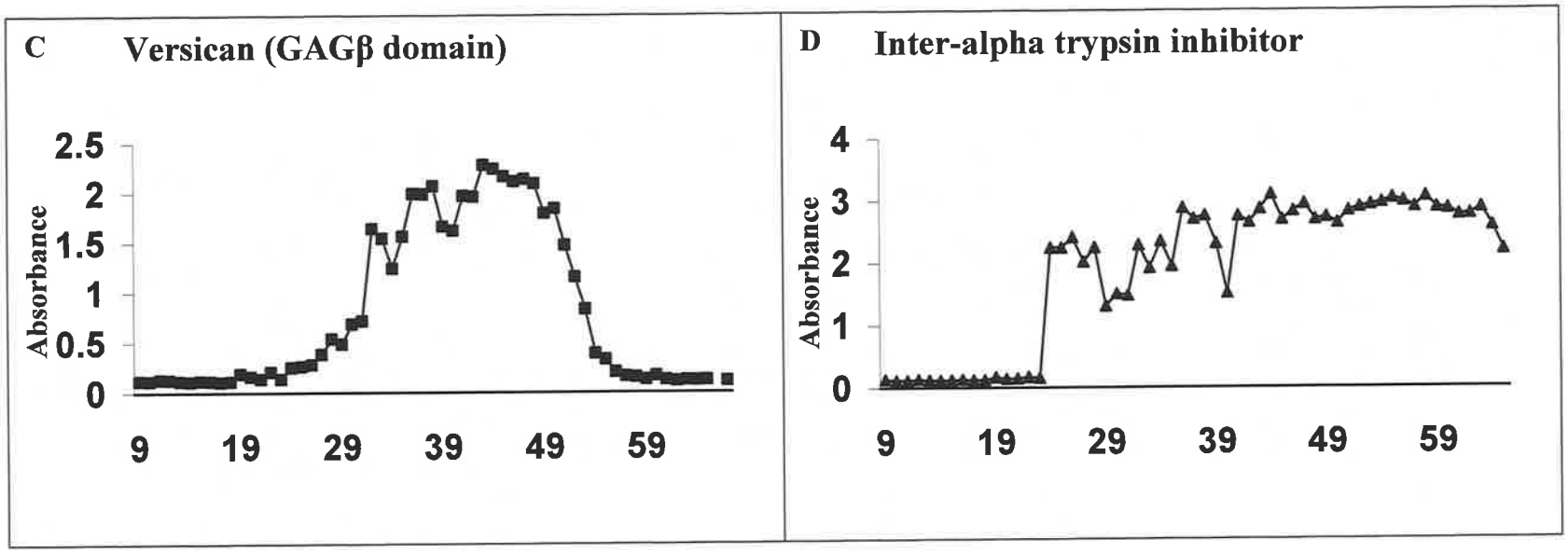
C
Versican (GAGβ domain)
Absorbance
2.5
2
1.5
1
0.5
0
9
19
29
39
49
59
D
Inter-alpha trypsin inhibitor
Absorbance
4
3
2
1
0
9
19
29
39
49
59

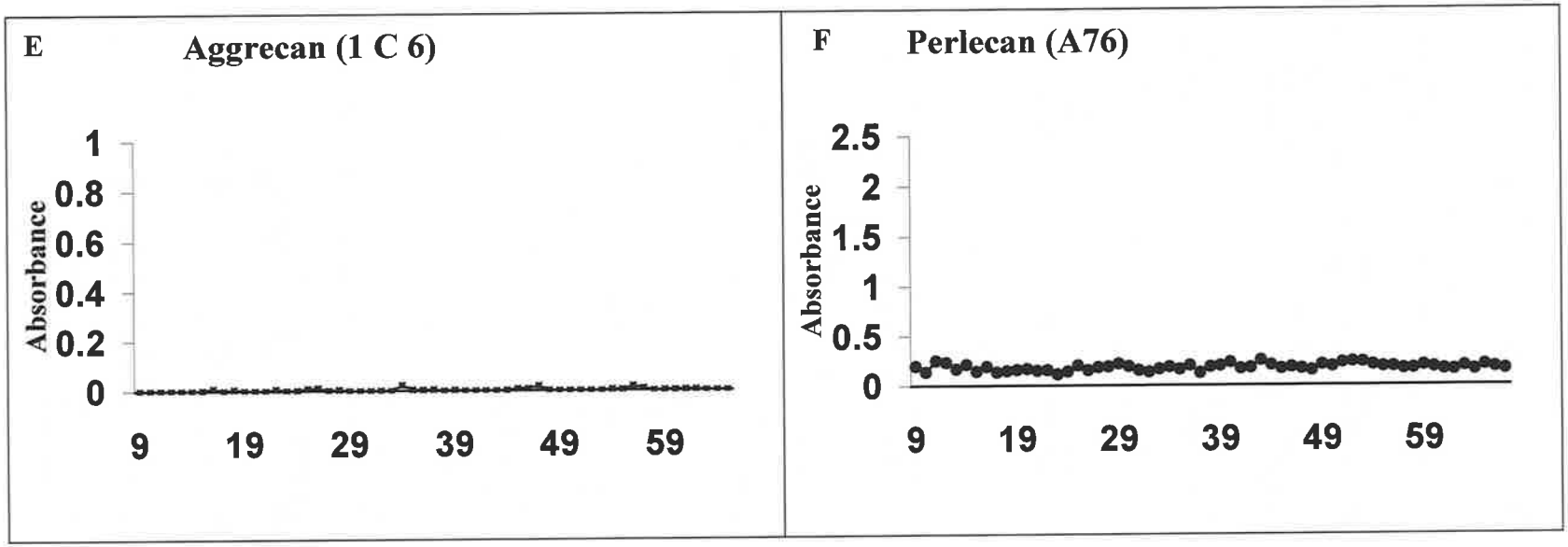
E
Aggrecan (1 C 6)
Absorbance
1
0.8
0.6
0.4
0.2
0
9
19
29
39
49
59
F
Perlecan (A76)
Absorbance
2.5
2
1.5
1
0.5
0
9
19
29
39
49
59

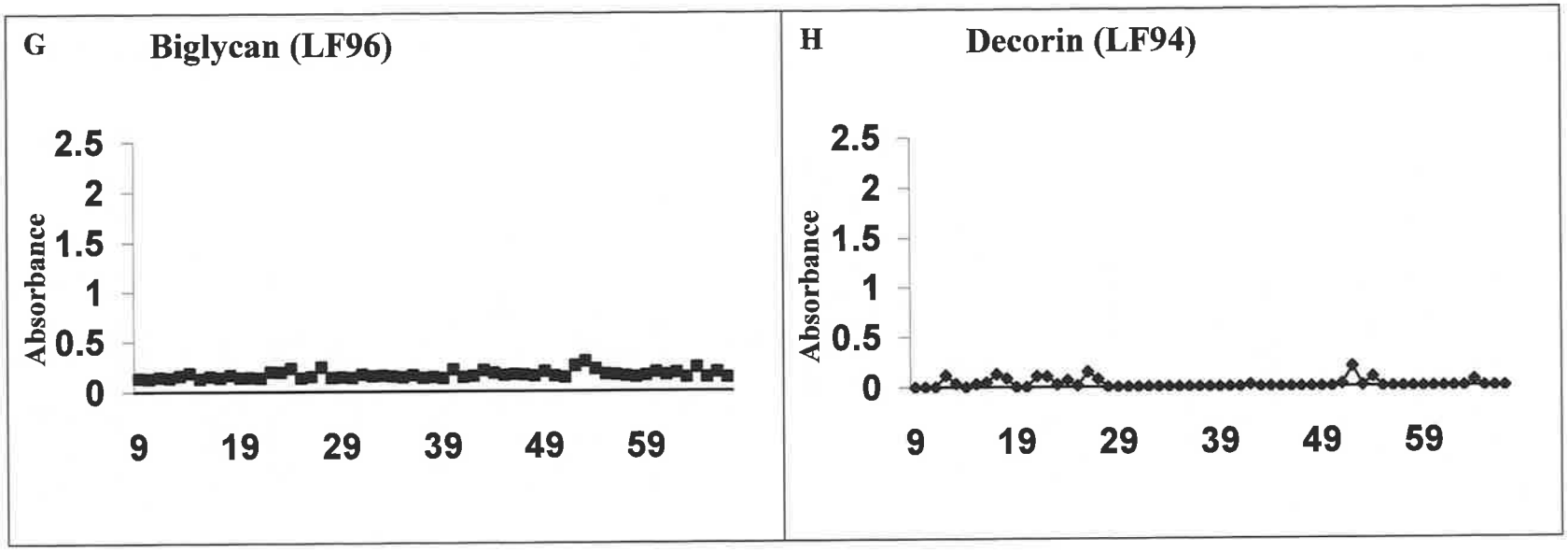
G
Biglycan (LF96)
Absorbance
2.5
2
1.5
1
0.5
0
9
19
29
39
49
59
H
Decorin (LF94)
Absorbance
2.5
2
1.5
1
0.5
0
9
19
29
39
49
59

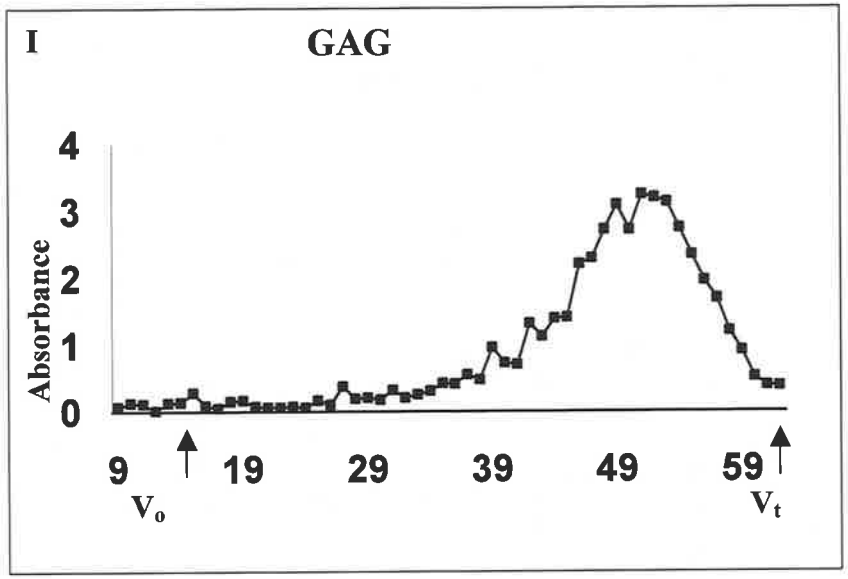
I
GAG
Absorbance
4
3
2
1
0
9
19
29
39
49
59
Vo
Vt

4.3.4. Uronic Acid Levels of Bovine Serum and Follicular Fluid

After the removal of proteins the uronic acid content, measured by absorbance at 520 nm of the chromogen product of meta-hydroxy diphenyl, of whole bovine serum was 0.45 mg/ml. The uronic acid content of follicular fluid following the same treatment was 1.04 mg/ml. hyaluronan and chondroitin sulphate contributions to the total uronic acid measured was achieved by digestion and removal of hyaluronan or chondroitin sulphate with chondroitinase ABC and hyaluronidase respectively, prior to assay. The results are represented in Figure 28 and 29.The hyaluronan and chondroitin sulphate contributions were 0.72 and 0.66 mg/ml respectively.

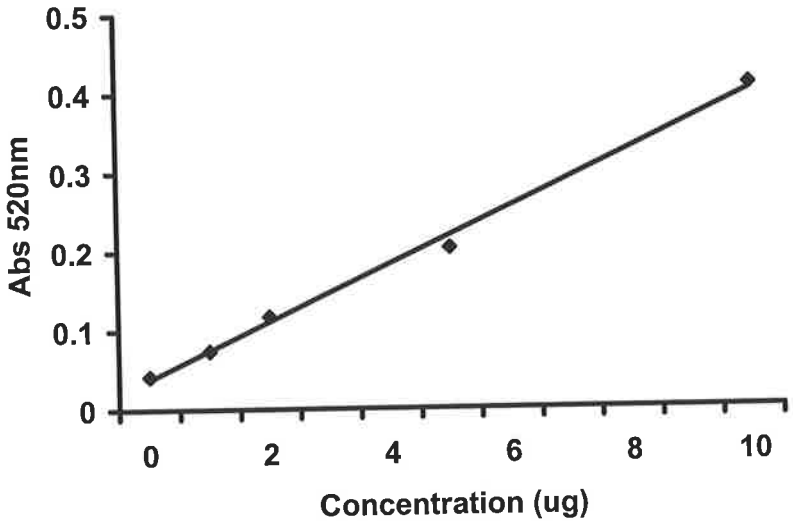

Figure 28 Uronic acid standard curve.

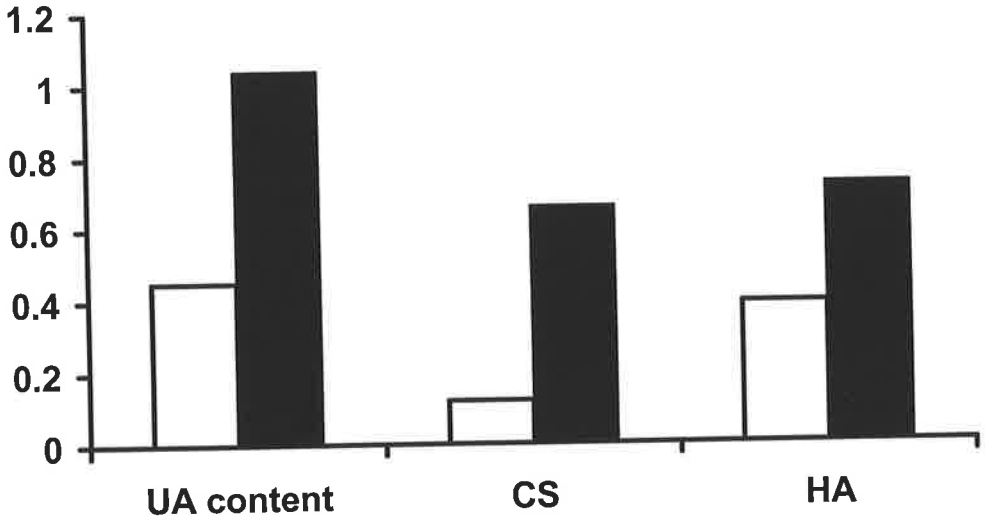

Figure 29 Graph showing uronic acid content (mg/ml) of bovine serum (clear box) and follicular fluid (filled box). HA and CS contributions to total uronic acid (UA) measured.

4.3.5. Proteoglycans and DNA in Follicular Fluid

The pools of follicular fluid from healthy and atretic follicles collected in Chapter 3 were separated on a 0.8 % agarose gel and stained with Stains-All® or ethidium bromide. The Stains-All® stained gel (Figure 30) showed proteoglycan smears of 157 bases or 5 kDa to > 400 kDa (purple) with a concentrated red spot indicating the presence of protein between 1000 and 3000 bp equivalent to 108 kDa. Digestion with proteinase K resulted in the removal of the majority of the protein spot and visualisation of very small digested protein fragments at the bottom of the Stains-All® gel. A greatly reduced residual proteoglycan/ glycosaminoglycan smear remained. Nucleotidase digestion using DNase free RNase showed little change in the original profile, while digestion with RNase free DNase revealed a smear at the top of the gel (dark blue).

The ethidium bromide stained gel (Figure 31) showed a smear of material from 500 bases to > 2 x 10^6 bases of DNA with a large brightly stained region at 1953 – 3000 bp. Since ethidium bromide is known to stain protein components, a digestion of the fluid with proteinase K was carried out (lane 2) this resulted in a clear visualisation of the DNA smear and removal of the region believed to be protein. DNase I digestion (lane 3) revealed that the DNA component was removed and the reduction in intensity of the protein "spot" suggested some of the DNA may have been entangled or that DNA of the same size as the protein existed in this region.

In summary digestion of the follicular fluid samples with proteinase K and DNase or RNase and subsequent separation demonstrated the presence of DNA and RNA components in the fluid as well as proteoglycans. The DNA component of healthy follicular fluid ranged in size from 2799 bases to > 9000 bases with some DNA remaining in the well suggesting it is of a very large size > 2 x 10^6 bases. The DNA component of atretic follicular fluid, ranged from 500 bases to 9000 bases.

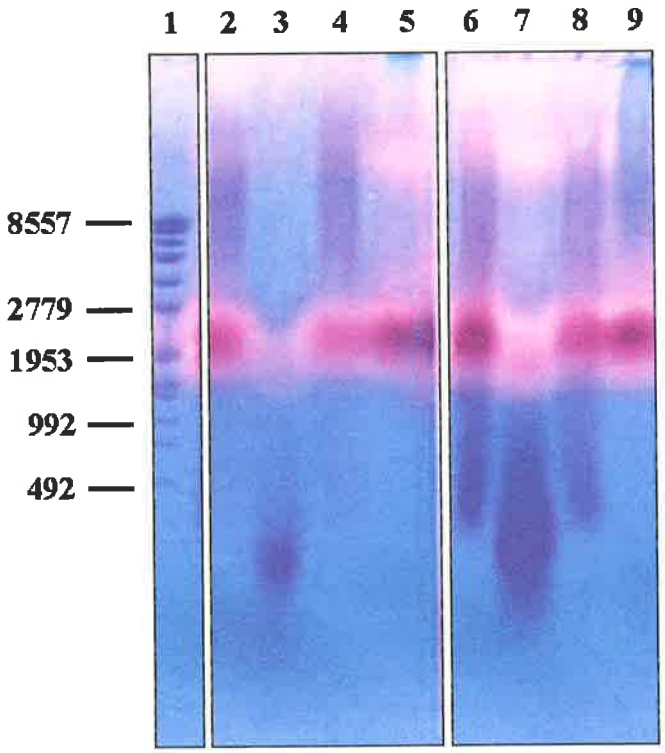

Figure 30 Follicular fluid from healthy and atretic follicles separated on 0.8 % agarose and stained with Stainsall® Lane 1, SSP1/EcoR1 mw DNA marker, lane 2, follicular fluid from healthy follicles, lane 3, follicular fluid digested with proteinase k, lane 4, DNA'se free RNase, lane 5, RNA'se free DNase lane, 6, follicular fluid from atretic follicles, lane 7, follicular fluid digested with proteinase k, lane 8, DNase free RNase, lane 9, RNase free DNase. Three micro litres were loaded in each lane.

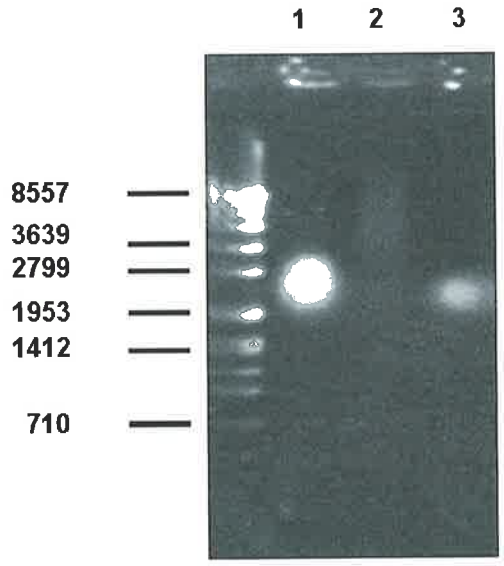

Figure 31 Pooled follicular fluid from uncharacterised follicles was separated by electrophoresis on non-denaturing agarose (1%) gel and stained with ethidium bromide. Size marker is EcoRI digested SPP-1 phage DNA marker. Follicular fluid treated with Lane 1, no enzyme; lane 2, proteinase K, lane 3, DNase 1. Three micro litres were loaded in each lane.

4.3.6. Western and Ligand Blots

Pooled, uncharacterised follicular fluid was separated on 0.8 % agarose gels and immuno-blotted against the antibodies, which had given a positive result in the fraction ELISA. The results obtained from these blots showed that the majority of the proteoglycan smear was derived from versican and ITI. Since both versican and ITI are known to interact with hyaluronan, an HABP ligand blot was also performed on the same membrane, following the identification of versican and ITI. The results revealed that hyaluronan or its associated molecules with the hyaluronan-binding motif were also present. The sizes of hyaluronan or molecules with the binding motif ranged from approximately 400kDa to 2 x 10^6 Da as determined by markers of hyaluronan of known size (Figure 32).

Confirmation of the presence of versican in follicular fluid samples was provided by Western immunoblot using the versican GAGβ antibody supplied by Dr Zimmermann, Department of Pathology, University of Zurich, Switzerland (Zimmermann *et al.*, 1994) (Figure 33) in which two immunoreactive bands were observed, probably corresponding to V_0 and V_1. Fractions from the size exclusion chromatography were treated with chondroitinase ABC and subjected to Western immunoblotting using an antibody to ITI (Figure 34). Heavy chains of ITI and bikunin were identified, though the intensity of the bikunin band was weak as observed previously by others in human serum samples (Rouet *et al.*, 1992). Since ITI was unexpectedly found in fluid collected from follicles of this size, based upon reports in rodents (Chen L. *et al.*, 1994), follicular fluid from follicles (2 mm to 15 mm) was examined. A repeat of the analysis using these samples showed that the follicular fluid of follicles 2 – 15 mm contained ITI (Figure 35). ITI and or its heavy chain components, pre-alpha inhibitor and inter-alpha like inhibitor were identified by Western blot analysis to be present in fluid from all follicle sizes examined. Perlecan, decorin and aggrecan were not detected by ELISA or with Western blotting of the chromatography fractions (data not shown).

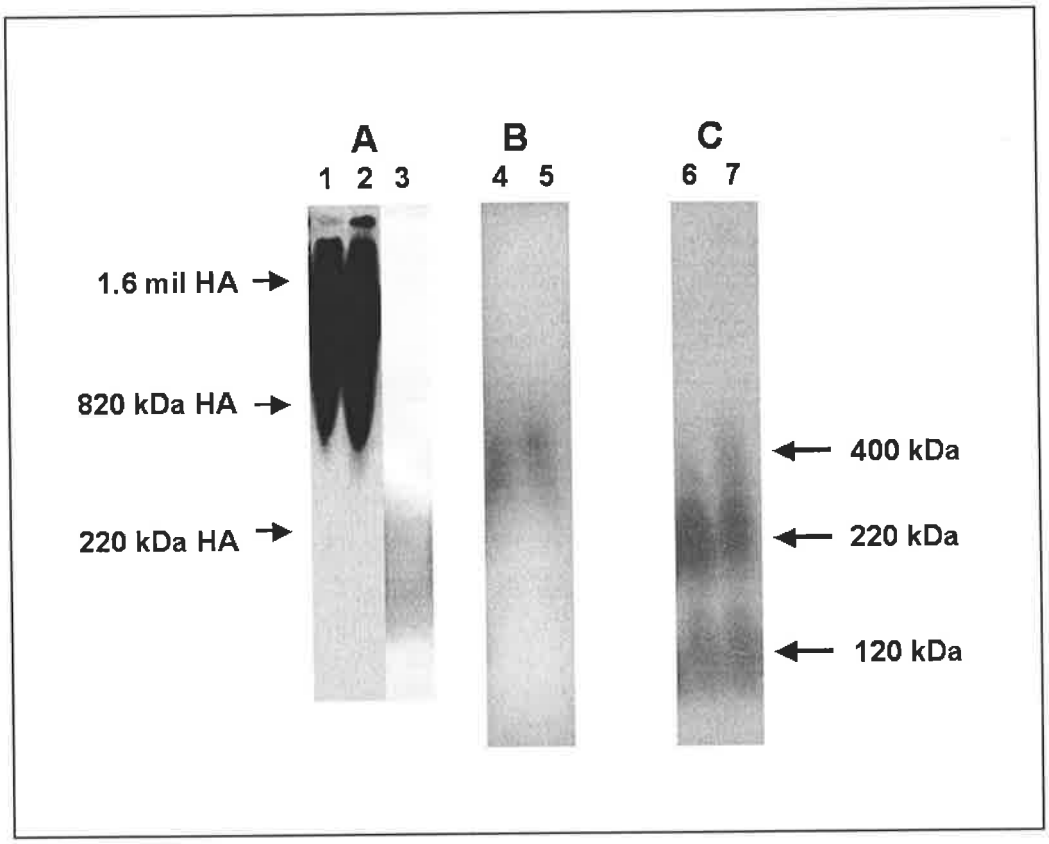

Figure 32 Follicular fluids separated by electrophoresis on non-denaturing agarose (0.8%) gels and immuno-blotted to identify HA, versican and ITI. (A) HA was visualised using biotinylated HABP. (B) Versican GAGβ (C) followed by re-probing for ITI. Lanes 1,4 and 6, follicular fluid from a pool of follicle 2 - 8 mm. Lanes 2,5,and 7, follicular fluid from a pool of follicles >10 mm. Lane 3 follicular fluid digested with Streptomyces hyaluronidase prior to blotting. Three micro litres of follicular fluid were loaded in each lane. MW indicators for all three gels are shown on the left and right hand sides of the figure.

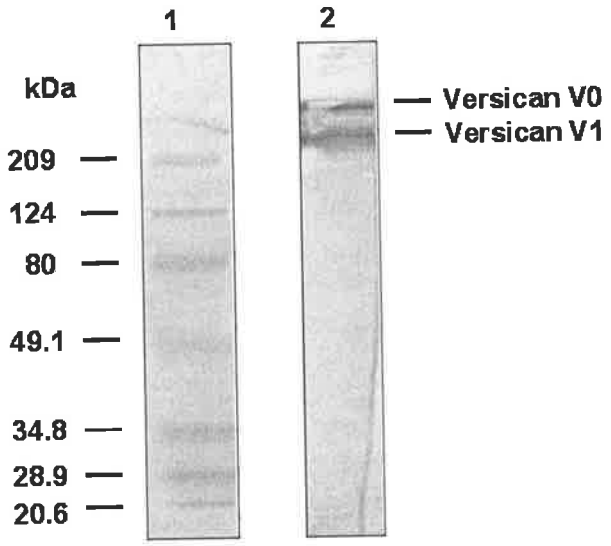

Figure 33 Western blot analysis of versican. Lane 1, Broad range molecular weight marker, lane 2, and follicular fluid treated with chondroitinase ABC with versican visualised using the GAGβ antibody. Three micro litres of pooled follicular fluid were loaded in each lane.

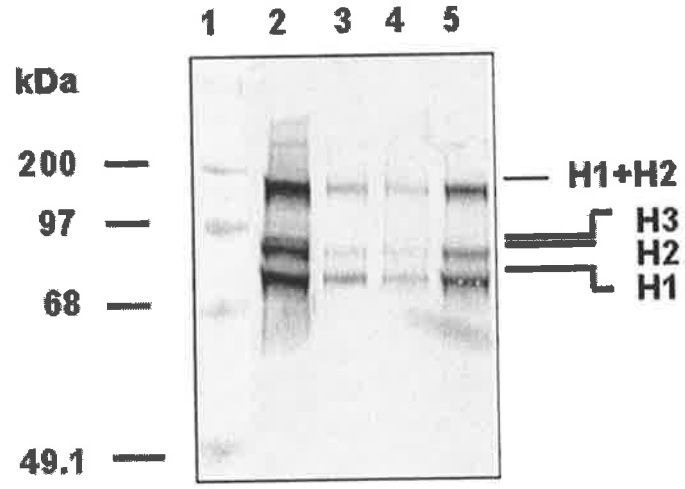

Figure 34 Western analysis of ITI. Follicular fluid was subjected to anion exchange and size exclusion chromatography, treated with chondroitinase ABC, separated by 10% SDS PAGE and visualised using the rabbit anti-human ITI antibody. Lane 1, Broad range molecular weight markers, lane 2, bovine serum, lane 3, fraction 28 from size exclusion column, lane 4, fraction 40, lane 5, fraction 52, five micro litres of fraction were loaded in each lane. Heavy chains H1, H2 or H3 and the H1 + H2 complex bound by the chondroitinase ABC resistant glycosaminoglycan bond are indicated based on a previous publication (Rouet, Daveau et al. 1992).

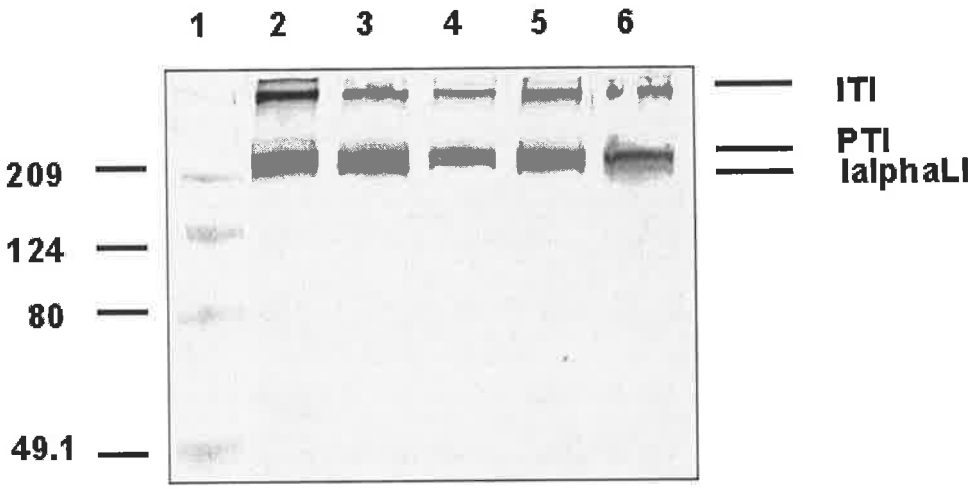

Figure 35 Follicular fluid from follicles (2-15 mm) separated on a 10% SDS PAGE, under reducing conditions without prior chondroitinase ABC treatment, immuno-blotted against ITI. Lane 1, Broad range marker, lane 2, 2-5 mm, lane 3, 6-8 mm, lane 4, 9-10 mm, lane 5, 11-12 mm, lane 6, 13-15 mm. The native molecules are indicated (Rouet, Daveau et al. 1992). Five microliters of sample was loaded in each lane. H1, H2 and H3 are heavy chains 1, 2 and 3 respectively, and pre-alpha TI and I-alpha like TI are pre-alpha trypsin inhibitor and inter-alpha like trypsin inhibitor, respectively.

4.3.7. Immunohistochemistry

Western and ligand blots identified ITI, versican and hyaluronan in follicular fluid samples collected from follicles < 10 mm. In order to localise these molecules within follicles (8 – 10 mm), from which the fluid samples had been obtained immunohistochemical techniques using fluorescene labelled secondary antibodies for ITI and versican were used to visualise their localisation. Healthy and atretic follicles of 8 – 10 mm were isolated and fixed with Bouins' fixative, before characterisation of health status and subsequent processing.

4.3.7.1. ITI

Figure 36 A to D show ITI localisation at x 100 and x 400 magnification in healthy follicles of 8 – 10 mm. ITI localised to the granulosa cell layer with some staining seen in the fluid of the follicle (Figure 36A). The staining appeared to be localised within the cytoplasm of the granulosa cells with intense staining seen in the intracellular spaces of the more antrally positioned cells (Figure 36 B). Staining was also noted within the cavities of the blood vessels (Figure 37 A).

Figure 37 A - D showed ITI localisation within atretic follicles of 8 – 10 mm was still primarily in the granulosa cells with no staining of the retained follicular fluid in the antra of atretic follicles as noted in the healthy follicles. However, there was clear staining of the fluid/serum within blood vessels. The intensity of staining observed in the atretic follicles was approximately one tenth of that seen in the healthy follicles (Figure 37 C), as determined by the confocal microscope. There was no staining seen in any of the primary antibody or secondary antibody only controls (Figure 37 D).

4.3.7.2. Versican GAGβ

The versican GAGβ antibody used in Western blot and ELISA analyses was used to detect versican within healthy and atretic follicles of 8 – 10 mm diameter. Versican localised to the granulosa cells and follicular fluid of healthy follicles (Figure 38 B) with the staining pattern being similar to that of inter-alpha trypsin inhibitor with the exception of the intracellular staining which appeared to be more variable in intensity than that of ITI. Additionally, there was some staining of the thecal cells in close contact with the basal lamina in some follicles. The intensity of intra-cellular staining of versican was quite intense (Figure 38 C).

Versican localisation within atretic follicles 8 – 10 mm was significantly reduced compared to that of healthy follicles with virtually no staining within the thecal layers noted (Figure 39 C). Low levels of staining could be seen in the granulosa cells with stronger

staining noted in the epithelial layer around the blood vessels (Figure 39 B). A weak signal was noted in the granulosa cells of the controls suggesting there may have been some trapped secondary antibody in this area.

There was no staining seen in the primordial or pre-antral follicles of any sections observed or any of the antibody only controls (Figure 39 D).

NB: The images obtained from the Bio rad MRC 1000 confocal microscope were taken in black and white as this was the only option available and using the highest resolution option (8 bits/pixel).

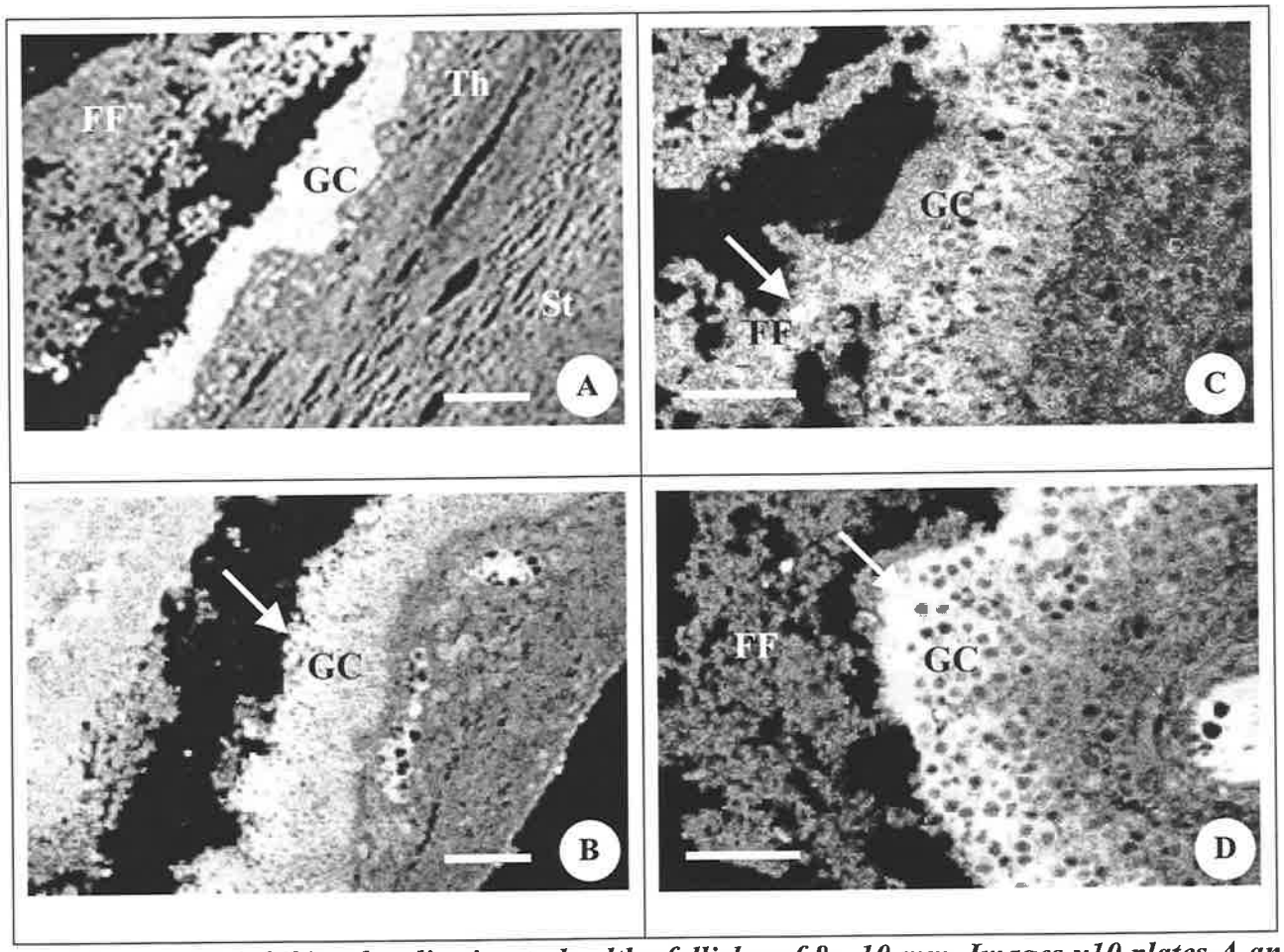

Figure 36 FITC labelled inter-alpha trypsin inhibitor localisation to healthy follicles of 8 - 10 mm. Images x10 plates A and B, x40 plate C, X 40 plate D.GC – Granulosa cells, FF –Follicular fluid, Th – Theca, St – Stroma. Positive staining can be seen in the granulosa cells, intracellular spaces and follicular fluid (arrows). Bar = 150 µm images A and B, = 50 µm images C and D. The images were taken in black and white on a C1000 Bio-rad confocal imager.

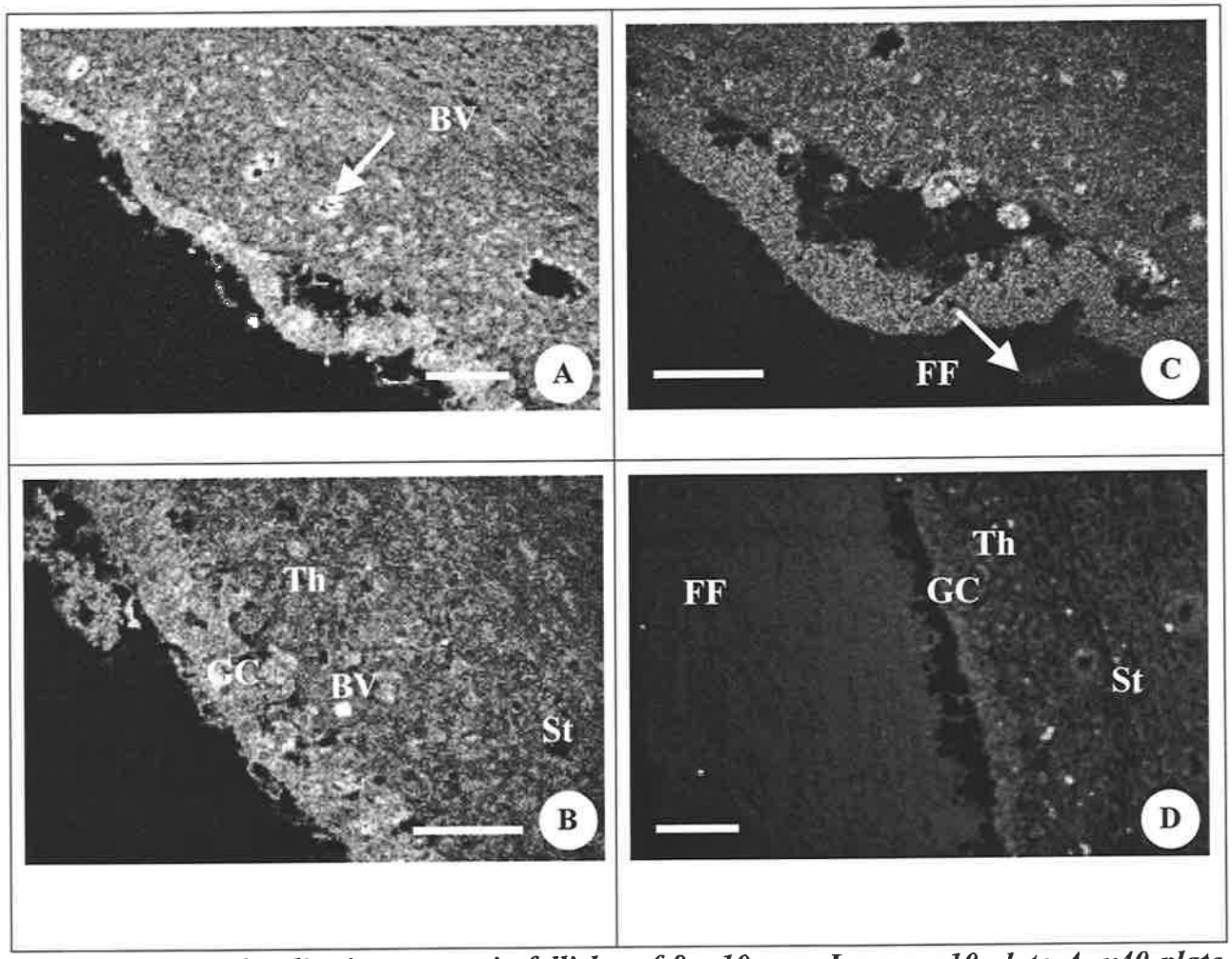

Figure 37 FITC labelled inter-alpha trypsin localisation to atretic follicles of 8 - 10 mm. Images x10 plate A, x40 plate B, x40 plate C from atretic follicles. Control x10 plate D. Granulosa cells, Th – Theca, St – Stroma. BV – Blood vessel, FF – Follicular fluid. Bar = 150 µm images A and D, = 50 µm image B and C. The images were taken in black and white on a C1000 Bio-rad confocal imager.

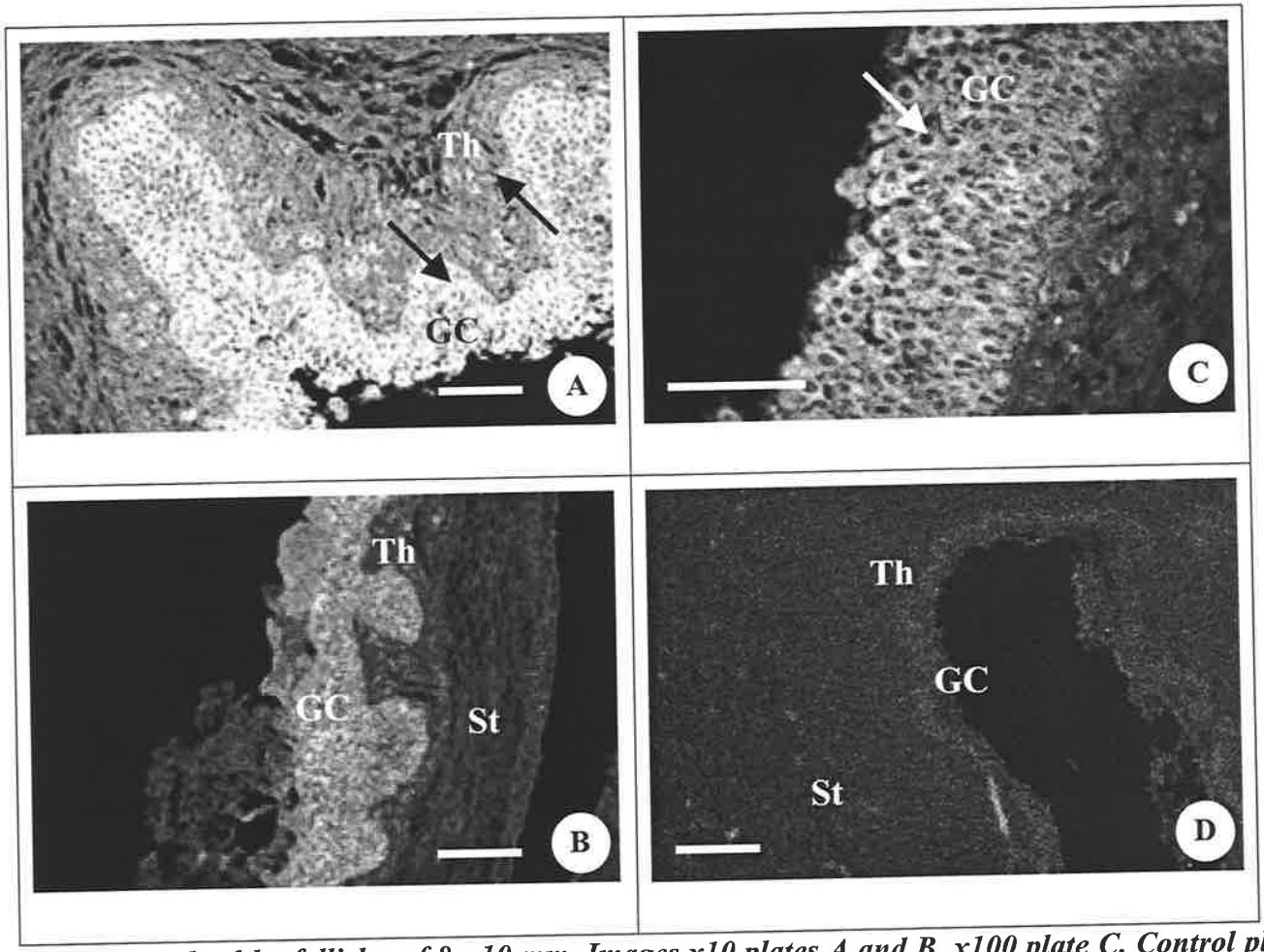

Figure 38 FITC versican localisation to healthy follicles of 8 - 10 mm. Images x10 plates A and B, x100 plate C, Control plate x10 D. GC – Granulosa cells, FF –Follicular fluid, Th – Theca, St - Stroma. Positive staining can be seen in the granulosa cells and follicular fluid with some staining of the theca. Bar = 150 µm images A, B and D, = 25 µm. The images were taken in black and white on a C1000 Bio-rad confocal imager.

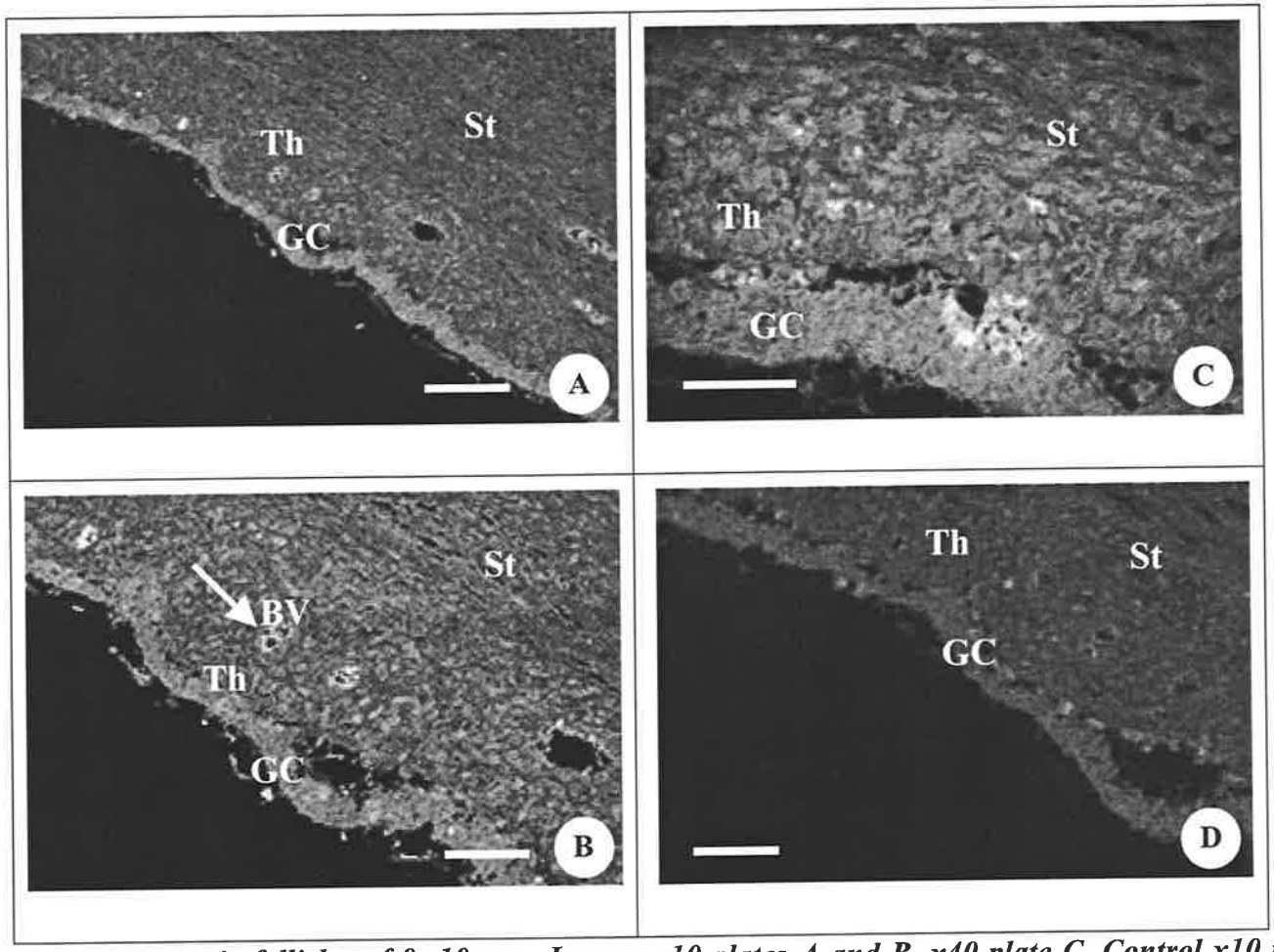

Figure 39 FITC versican localisation atretic follicles of 8- 10 mm. Images x10 plates A and B, x40 plate C. Control x10 plate D. BV – Blood vessel. Positive staining can be seen in the blood vessels with weak staining of the granulosa cell layer. Bar = 150 µm images A, B and D, = 50 µm image C. Granulosa cells, FF –Follicular fluid, Th – Theca, St – Stroma. The images were taken in black and white on a C1000 Bio-rad confocal imager.

4.3.7.3. HABP

Hyaluronan or its associated molecules with the hyaluronan-binding motif was localised within the follicle using the hyaluronan binding protein conjugated to biotin with visualisation of the binding achieved with streptavidin conjugated to horseradish peroxidase. Sections were then counterstained with heamatoxylin.

Immunohistochemical staining with HABP can be seen in Figure 40 A – F. Immunohistochemical staining with HABP of healthy follicles of 8 – 10 mm resulted in positive staining of the whole ovarian tissue section used. However, there was a proportional increase in the intensity of staining in the granulosa and theca cell layers (Figure 40 A). Both the nucleus and the cytoplasm of the granulosa cells were stained positively with the nuclei within the granulosa and theca interna cells more closely aligned with the basal lamina being more intensely stained (Figure 40 B). The nuclei of antrally situated granulosa cells were stained more positively than the stroma cells of the same section but less than those mentioned above. Atretic follicles had a similar staining pattern to that of healthy follicles but the number of granulosa and theca cells stained and the intensity of nuclear staining in both cell types was reduced.

Follicular fluid that had been trapped and fixed within the section had a strong positive signal for HABP. Sections stained with no secondary antibody or with secondary antibody only, had no staining (Figure 40 F). These results indicated that hyaluronan and or its associated molecules were present throughout the ovary but are more concentrated in the granulosa cells, theca interna and follicular fluid.

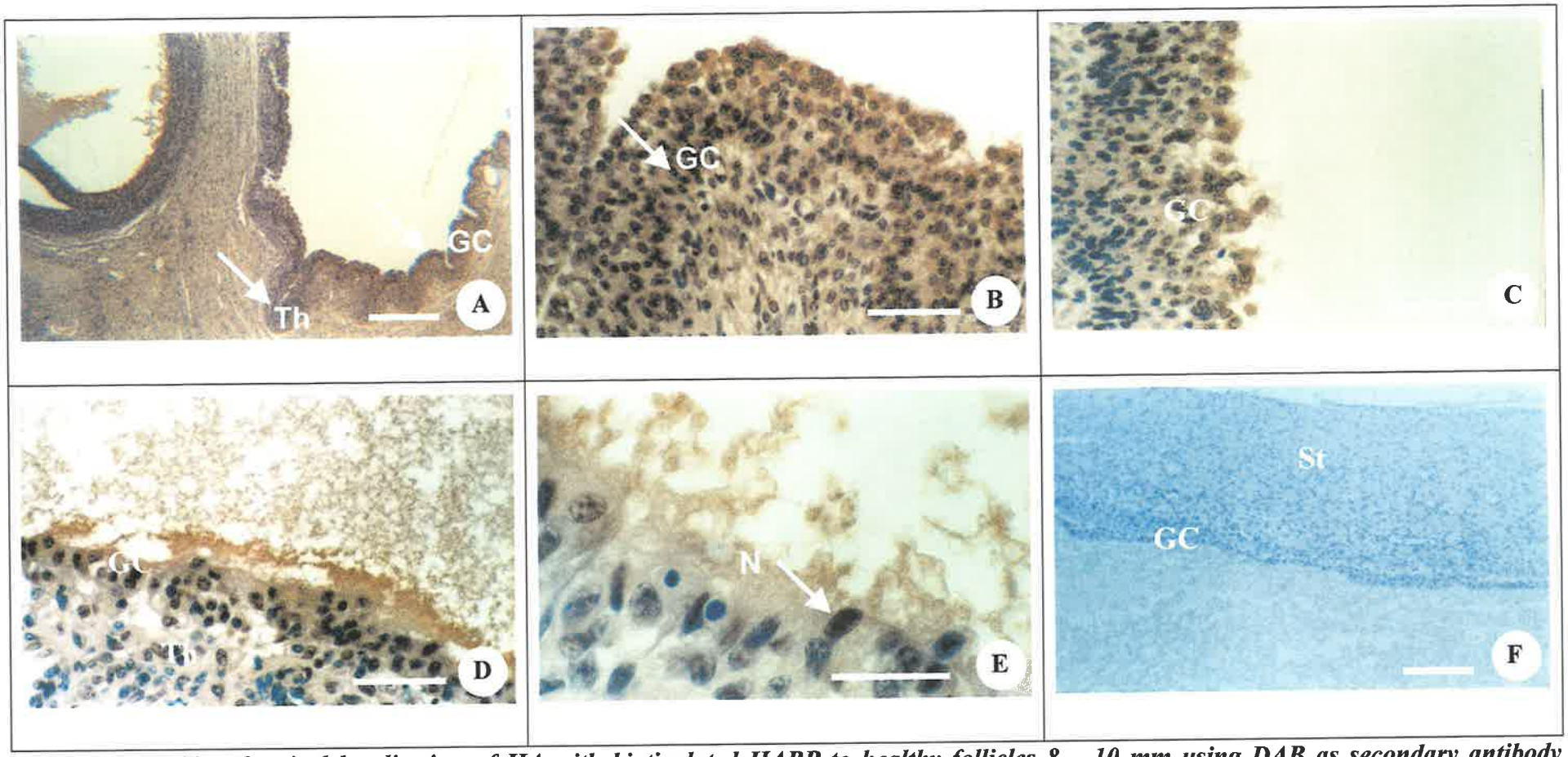

Figure 40 Immunohistochemical localisation of HA with biotinylated HABP to healthy follicles 8 – 10 mm using DAB as secondary antibody and sections counterstained with haematoxylin: A; .A; x5, B, C and D; x40, E; x100 F; negative control. GC – Granulosa cells, FF –Follicular fluid, Th – Theca, N = nucleus, St – Stroma. Bar = 300 µm image A, = 150 µm image F, = 50 images B, C and D, = 50 µm image E.

4.3.8. Collagenase Sensitive Molecules

On digestion of the follicular fluids with collagenase I some higher molecular weight proteins were degraded and new lower molecular weight molecules became apparent as observed by SDS PAGE (Figure 41). Three new major bands were identified following collagenase I digestion. To resolve what clearly was a mixture of bands the digested products were separated on a 7% tris-acetate gel after which 9 bands were identified and processed for N-terminal amino acid sequencing. Proteins identified in these bands and known to be collagenase sensitive are shown in Table 9. Several other sequences not listed in the table were identified as being present in the fluid samples, these were not known to be collagenase sensitive but are known constituents of serum and might therefore be expected in follicular fluid.

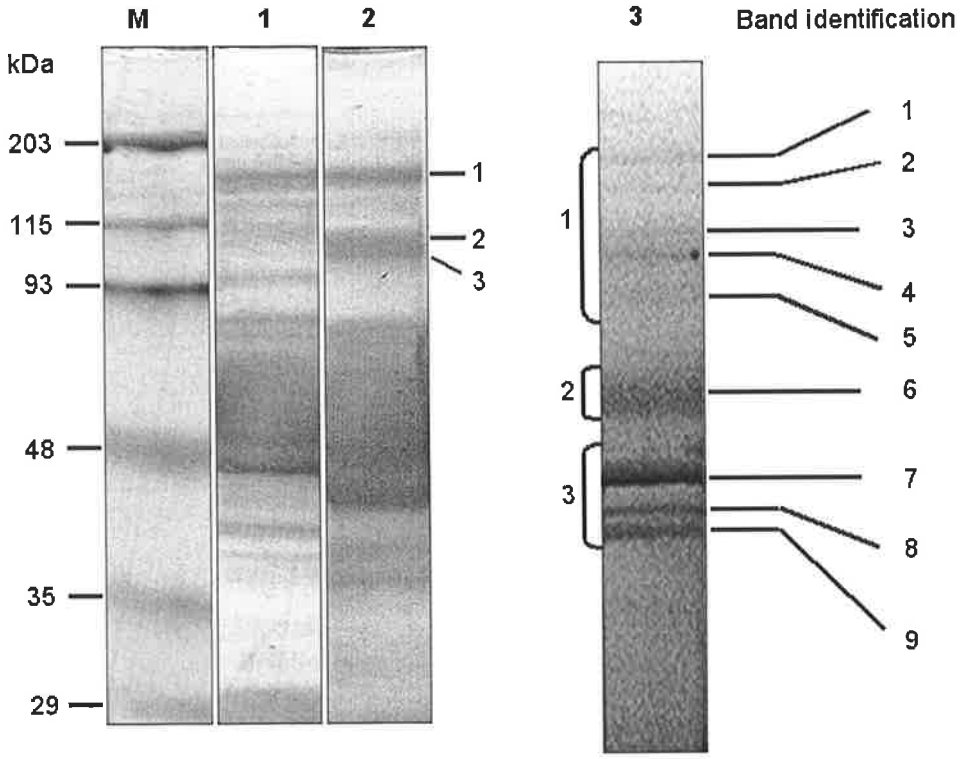

Figure 41 Five micro litres of pooled follicular fluid from uncharacterised follicles before (lane 1) and after (lane 2) collagenase I digestion were separated by 10% SDS PAGE. Three bands (1, 2, and 3) were identified in panel 2 as significantly different to the general profile obtained in lane 1. These bands were resolved further by Tris-acetate PAGE (7%) lane 3. Bands removed for sequence identification are indicated on the right hand side of the Tris-acetate gel (1-9). Lane M is the Bio-rad pre-stained broad-range molecular weight marker.

Band number	Peptide sequence	Homologous sequence	Sequence identity†		
3	LPEREGAR	LPSIREGAR	Secretin	Human	gi:107646
4	DQGVESPLF	EQGCESPLF	Hypothetical protein XP	Human	gi:75222627
5	PTLVETAGR	PTLVELAGR	Serum albumin	Bovine	gi:229552
	LKQEPKAQR	LKQEKAQR	Involucrin	Human	gi: 124723
	LTPSVKAGG	LTPSVKALG	Agglutinin-like protein precursor 3	Human	gi:5902760
6	DANTFLEAXR	RANTFLEEVR	Prothrombin precursor	Bovine	NP00497
	DANTFLEAXR	DANTFLEEXR	Coagulation factor X	Bovine	gi:119759
7	RANTFLEAYR	RANTFLEEVR	Prothrombin precursor	Bovine	gi:135806
	DPGPPGLPAY	DPGPPGLPAY	Collagen IV alpha 2	Human	gi:115349
	EPGPPPGALP	EPGPPPGLPAP	Collagen XIII alpha 1	Human	gi:178320
	HVPEGLRVGE	HVPEGLRVGF	Alpha-2-macroglobulin	Human	gi:825615

Table 9: Sequence identity of collagenase I sensitive proteins identified in follicular fluid.

Band numbers are identified in Figure 41. Sequence calls were made on the basis of relative abundance of the amino acid present in that position and identified using PROWL (90% similarity to mammalian sequence.

4.4. Discussion

Most of the literature relating to colloid osmotic pressure, glycosaminoglycans and proteoglycans in the body report on cartilage, vertebral discs and ocular tissue. In these cases it has been determined that the colloid osmotic pressure is created by the relative contributions of hyaluronan, proteoglycans and collagen and that the collagen provides tensile strength and compression resistance while hyaluronan, proteoglycans and their glycosaminoglycans provide large osmotically active, negatively-charged molecules that form hydrated gels or fluids which have the ability to attach to collagen (Auckland 1997). Aggregation and or interaction occur often in the extracellular space, the hydrated layers formed allow rapid diffusion of nutrients, metabolites and hormones. It is possible that a more fluid matrix of similar make-up exists in the follicle, which provides a capability for rapid growth and fluid accumulation on demand.

Histochemical studies have shown that follicular synthesis of glycosaminoglycans is regulated by gonadotrophins (Mueller *et al.*, 1978). The proteoglycans are secreted by the granulosa cells of a developing antrum and can be stimulated by FSH invitro (Yanagishita *et al.*, 1981). Similar effects have been achieved with cAMP. In a porcine model small follicles produced more proteoglycan than large (Schweitzer *et al.*, 1981) while in rat, FSH stimulated the production of small CS proteoglycans but did not alter the production of large proteoglycans in large follicles (Yanagishita *et al.*, 1981). LH in contrast appears to inhibit proteoglycan synthesis in large follicles (Gebauer *et al.*, 1978).

In Chapter 3 chondroitin/dermatan sulphate related molecules, hyaluronan, DNA and collagen were identified as significant contributors to the colloid osmotic pressure of follicular fluid. The maximum uronic acid concentration of fluid post extraction and separation was 1.2 mg/ml as determined by ion exchange. Reports of chondroitin and heparan sulphate concentrations exist however; there are no data relating to fluid uronic acid concentration and therefore it is hard to assess this data in light of previous measurements (Bellin & Ax, 1987a, Bellin *et al.*, 1986, Bushmeyer *et al.*, 1985, Eriksen *et al.*, 1997). Data available suggests that chondroitin and heparan sulphate concentrations in bovine fluid are between 0.9 – 1.4 mg/ml and 0.2 - 1.1 mg/ml respectively depending on the size of the follicle. The data presented here data came from a pool of fluid obtained from a range of sizes of follicle and so cannot be easily compared however; the results obtained were within the range given above.

Chondroitin 4-sulphated proteoglycans were identified as the main proteoglycan present in follicular fluid samples. Using a combination of techniques versican and ITI were identified in bovine follicular fluid. Perlecan, decorin, and aggrecan were not present. Perlecan has been identified previously in extracts of whole small antral bovine follicles of 1

– 3 mm and was localised by immunohistochemistry in the follicular basal lamina (McArthur *et al.*, 2000, Princivalle *et al.*, 2001). There was no evidence of it in bovine follicular fluid. The presence of a perlecan like proteoglycan in human follicular fluid of hCG treated ovulating follicles was reported by Eriksen et al (Eriksen *et al.*, 1999), Eriksen's work of 1997 (Eriksen *et al.*, 1997) measured proteoglycan synthesised by the granulosa cells at a concentration of 0.8 mg/ml. Seventy percent of this was contributed by large chondroitin sulphate proteoglycans whilst 30% was attributed to HS proteoglycans. A decrease in chondroitin sulphate proteoglycan was seen in larger follicles and was positively correlated with IVF outcome. Eriksen suggested that the heparan sulphate side chains of a perlecan like proteoglycan had an anticoagulation role in fluid during follicular expansion, since it is known to bind anti-thrombin III (Hosseini *et al.*, 1996). It has been shown in human follicular fluid, aspirated at ovulation, that heparan sulphate proteoglycans are proteolytically cleaved and heparan sulphate proteoglycan species are subsequently shed in to follicular fluid while the remainder of the heparan sulphate proteoglycans are internalised and degraded in the lysosomal compartment (Salustri *et al.*, 1999). It is thought that chondroitin sulphate proteoglycans are treated likewise. In the studies by Eriksen, fluid was aspirated at ovulation during embryo transplant procedures, the follicular basal lamina was probably degrading or had entered the fluid samples during sampling and the identification of perlecan in these samples may have been a result of follicular wall contamination of the fluid. The presence or absence of heparan sulphate proteoglycans such as perlecan in fluid from small antral follicles has not been explored to date and might provide a fuller explanation of the result seen here. It is unlikely that perlecan is a component of follicular fluid during follicle growth.

McArthur et al (McArthur *et al.*, 2000) had previously identified decorin from whole follicles; however it was not observed in follicular fluid. Decorin was found to localise outside of the follicular basal lamina only (H Irving-Rodgers personal communication). Hence it is not a component of follicular fluid.

Aggrecan was not detected in the follicular fluid fractions examined. Link protein, an extra-cellular matrix protein in cartilage, stabilises aggregates of hyaluronan and proteoglycans, including aggrecan and ITI. Cartilage link protein associated with aggrecan has been identified in the maturing rat and mouse ovary by immunohistochemistry. The expression of cartilage link protein was selectively detected in the cells within the granulosa compartment of the preovulatory dominant follicle (Sun *et al.*, 2002). Since the fluid sampled here was not pre-ovulatory, the negative results obtained confirmed expectations.

Using the versican GAGβ antibody of Schmalfeldt (Schmalfeldt *et al.*, 1998), which recognises the GAGβ, domain present in splice variants V_0 and V_1, versican was identified in follicular fluid. Versican is a CS proteoglycan hyalectan with a tri-domain structure. The first

domain consists of one IgG repeat followed by two hyaluronan binding regions known as the link modules or link protein mentioned above. The link module is very similar to that of the c-type lectin in the third domain except that the loop is smaller and it does not contain Ca^{2+} binding residues. The second domain comprises a central glycosaminoglycan-binding region. The hyaluronan-binding region is contained within an amino acid terminal globular domain with tandemly repeated loops. The glycosaminoglycan attachment domain has two alternatively spliced exons, which are termed GAGα and GAGβ (Dours-Zimmermann & Zimmermann, 1994, Naso *et al.*, 1994) and may hold up to 30 glycosaminoglycan chains as well as O and N linked oligosaccharides. Finally, in the third domain, the carboxyl terminal region of versican contains 2 EGF repeats, a c-type lectin-like domain and a CRP like motif. Versican binds hyaluronan with a Kd of 4 nM (LeBaron *et al.*, 1992) but can also bind heparan sulphate and heparin (Ujita *et al.*, 1994). Versican is up regulated by several growth factors including EGF (lung) (Potter-Perigo *et al.*, 2004) and IL-1 (lung) (Tufvesson & Westergren-Thorsson, 2000) and has been implicated in the regulation of neural crest migration (Landolt *et al.*, 1995). Messenger RNA analysis has determined that 4 variants of versican exist V_0, V_1, V_2 and V_3. V_0 and V_1 are the largest variants and have a broad tissue expression profile (Lemire *et al.*, 2002) being present in both mesenchymal and epithelial cells. The versican variant V_3 contains no glycosaminoglycan attachment sites and is therefore considered a "part time" proteoglycan (Turley 1984)

Versican has been shown to be present in extracts of whole bovine follicles (McArthur *et al.*, 2000), human follicular fluid of ovulating follicles (Eriksen *et al.*, 1999), and in the membrana granulosa (McArthur *et al.*, 2000) with V_0, V_1 and V_3 found in mouse ovary and V_0 and V_1 expressed by the granulosa cells (Russell *et al.*, 2003). V_2 is the major isoform found in the brain. The size of the versican core protein ranges from 80 kDa for V_3 to ~ 400 kDa for V_0, which contains both GAGα and GAGβ.

Versican is involved in expansion of the cumulus oocyte complex (Camaioni *et al.*, 1996, Carrette *et al.*, 2001), the heavy chains of ITI become covalently cross-linked to hyaluronan, and versican becomes linked to this complex stabilising the expanding cumulus matrix (Carrette *et al.*, 2001, Eriksen *et al.*, 1997, Eriksen *et al.*, 1994, Kimura *et al.*, 2002, Laurent T. C. *et al.*, 1995b, Saito *et al.*, 2000). Many functional properties of versican are determined by two glycosaminoglycan attachment domains, which are modified to allow attachment of long chondroitin sulphate side chains. These chains are responsible for its large molecular size and strong charge negativity as well as osmotic properties. Versican may contribute directly to the colloid osmotic pressure of follicular fluid via the high sulphation status of the chondroitin sulphate attached to its core protein. Versican may also contribute to the colloid osmotic pressure of follicular fluid by cross-linking other elements like hyaluronan

to form larger molecular weight components. By expressing particular splice forms of versican, cells may control the hydration properties of their pericellular hyaluronan environment (Dours-Zimmermann & Zimmermann, 1994) and thus could modulate interactions with the extracellular matrix of neighbouring cells. Versican binds to hyaluronan via the link protein this 45 kDa glycoprotein stabilises the structure. In vitreous gel Bishop et al (Bishop, 2000) showed that versican and link protein are in a 1:1 molar ratio however; the ratio of versican to hyaluronan was 1:150. Bishop determined therefore that versican link stabilised the complex but did not in itself link hyaluronan chains together. A similar scenario may occur in follicular fluid.

The immunohistochemical localisation of versican to follicles of 8 – 10 mm confirmed previous reports of versican localisation within the follicle (McArthur *et al.*, 2000, Rodgers R. J. *et al.*, 2003). The V_0 and V_1 isoforms recognised by the GAGβ antibody show that one or both of these isoforms exist in the bovine follicle. The staining profile in healthy follicles showed localisation to the granulosa with minimal amounts detected in the theca cells. It was noted that no staining was seen in the primordial or pre-antral follicles of sections used indicating that the presence of versican may be stage dependent. The presence of versican may be a sign for continuing health with the apparent reduction in levels observed in atretic follicles reflecting loss due to versican degradation or decreased integrity of the follicular wall. The strong versican signal to granulosa cells closely aligned with the basal lamina in healthy follicles was interesting since it is known that proteoglycans are sorted and transported to predetermined destinations by signalling molecules such as growth factors and γ interferon. Granulosa cells like other epithelial cells have two domains, an apical surface and a basolateral surface. To maintain the polarised organisation, efficient sorting mechanisms target newly synthesised and recycling molecules. Epithelial cells must ensure that proteoglycans of the ECM and those that attach to the basolateral surface are transported to the right side of a cell. Different sets of proteoglycans are secreted either apically or basolaterally. The apical secretion of versican, in to follicular fluid is not a controversial concept, since apical secretion of chondroitin sulphate proteoglycans has been reported in MDCK cells by Kolset et al (Kolset *et al.*, 1999). Kolset and colleagues suggested that chondroitin sulphate chains contain sorting information, which allows directional secretion to occur. In contrast, heparan sulphate chains are believed to have the opposite effect being secreted basolaterally. It is therefore not surprising they were not found in fluid but as located by others adjacent to the follicular basal lamina (McArthur *et al.*, 2000). Russell et al have analysed mRNA and identified isoforms V_0, V_1, and V_3 versican in mouse and rat ovaries throughout follicular development. In situ hybridisation localised versican mRNA most specifically to the granulosa cells (Russell *et al.*, 2003). Given the immunohistochemical

results, the question remains as to whether versican is actively secreted in to the follicular fluid.

ITI consists of two heavy chains linked by a chondroitin sulphate chain of bikunin. ITI is produced by the liver and is found abundantly in serum. In mice ITI is not seen in the follicular fluid until after the release of LH (Salustri *et al.*, 1990a). In mice, ITI appears to be sequestered from the blood stream as it appears within the follicular fluid within minutes of the LH surge (Chen L. *et al.*, 1992). On entering the fluid it associates with hyaluronan being synthesised by the cumulus cells, liberating free bikunin and producing a covalent bond between the heavy chains and hyaluronan. In bovine follicular fluid ITI (bikunin and its heavy chains) was observed in follicular fluids of earlier stages of growth. Its source is unknown at this stage but it may be derived from serum there being no apparent barrier to the transfer of ITI family molecules from the blood in cattle. The ITI identified here is unlikely to be a contaminant from serum, as there was no contaminating perlecan, decorin or aggrecan in the samples. ITI was detected in samples of fluid from follicles from 2 mm - 15 mm by Western analysis. These data are contrary to those previously published for the mouse system and the presence of ITI in follicles of a non-ovulatory size indicates that it may have additional roles in the bovine system or that its exclusion from the mouse and human follicle is critical to the normal development of those follicles. The recent discovery of ITI in follicular fluid from medium sized porcine follicles indicates that the follicular fluid of cows is not the only species in which ITI is found prior to the LH surge (Nagyova *et al.*, 2004).

The immunohistochemical localisation of ITI to healthy follicles 8 – 10 mm confirmed the data from the Western analysis and showed that ITI was present in follicles of earlier developmental stages than previously described in humans. ITI localised strongly to the granulosa cells and there was also positive staining of the follicular fluid. This pattern of staining was different to that of the atretic follicles where the granulosa cells remained positively stained, albeit to a lesser degree and the follicular fluid was not stained. These data implied that the level of ITI in the fluid from atretic follicles was significantly less than that from the healthy follicles. One of the reasons for this may be differential permeability of the follicular basal lamina between healthy and atretic follicles.

The apparently low level of ITI observed in the follicular fluid from atretic follicles was interesting considering that the versican levels were also extremely low in atretic follicles. It is interesting to speculate whether versican and/or ITI are the limiting factors in the formation of a hyaluronan matrix in fluid from these follicles and whether this was the cause of the reduced colloid osmotic pressure recorded in the fluid from atretic follicles in Chapter 3. If so, the level of versican and/or ITI in follicular fluid might be a useful indicator of atresia in bovine follicles. Further investigation of this relationship would be required to validate this.

In fluid from healthy follicles the chondroitin sulphate attached to ITI and ITI itself is unlikely to generate significant colloid osmotic pressure, especially since the basal lamina is freely permeable to it. If the role of ITI is to bind to hyaluronan and cross-link it to form larger aggregates, then by ensuring hyaluronan does not escape the follicular antrum, it will have an indirect effect on the osmotic potential.

The indication from the agarose gel probed for hyaluronan, versican and ITI suggests that the three components exist separately in the fluid from small 2 - 8 mm follicles since there appears to be no apparent overlap of the bands identified by the antibodies or ligand. Versican and ITI were identified as positively stained areas at 200 - 400 kDa and hyaluronan was detected in the application well and in the high molecular weight region of the gel (Figure 32 A1 and A2). Hyaluronan was not detected when follicular fluid was pre-treated with Streptomyces hyaluronidase (Figure 32 A3). The faint diffuse band starting at 200 kDa was probably degraded hyaluronan and not intact ITI, HABP does not bind to chondroitin sulphate and therefore ITI bound to hyaluronan would not be detected by it. Panels Figure 32 B4 and B5 show that free versican migrated in to the gel, and was subsequently transferred to the immunoblot membrane, its presence was confirmed with the GAGβ antibody. The same was true for ITI it being present as a single entity, its presence confirmed by the rabbit anti human ITI antibody. Although the samples were loaded in an 1mM EDTA based loading buffer it is unlikely that this would have disrupted the covalent bond that exists between hyaluronan and ITI when they are bound and this fact is supported by data from Odum et al (Odum L. & Jessen, 2002), who were unable to dissociate the bond in 10 mM EDTA.

It can therefore be said with some confidence that some of the hyaluronan and free ITI exist as free entities unlike the situation noted in the cumulus oocyte complex in humans and mice. The coupling of ITI occurred in humans only after initiation of ovulation by hCG (Odum L. & Jessen, 2002). It is possible that in the bovine system that ITI and hyaluronan are not covalently bonded since it is present in fluid from follicles of just 2 mm and therefore present in fluid earlier than that in humans and mice. This suggests that the hyaluronan is solely responsible for the fluid accumulation in the initial phases of antrum expansion and fluid accumulation since unbound ITI can move freely across blood-follicle barrier and would be unable to exert any osmotic force.

While versican and ITI were identified in fluid with a range of antibodies however, there undoubtedly exist chondroitin/dermatan sulphate proteoglycans in follicular fluid that are not identified without the possession of antibodies for their detection.

The DNA found in follicular fluid is likely to be derived from granulosa cells that do not appear to die by apoptosis (Van Wezel *et al.*, 1999). The comet assay in Van Wezels work indicated that degradation of the DNA occurred randomly (Van Wezel *et al.*, 1999). The

reason it was seen here and why it might affect the colloid osmotic pressure of follicular fluid is that DNA can become entangled with larger molecules such as hyaluronan; in theory this entanglement would increase the osmotic effect of the DNA by minimising the loss of DNA and/or hyaluronan from the follicular fluid (Turner *et al.*, 1988). The DNA content of follicular fluid is not regulated since it could too easily be degraded by release of cellular DNase. Thus DNA, whilst contributing to the colloid osmotic pressure of follicular fluid, is probably not a regulated component that contributes to the colloid osmotic pressure of follicular fluid.

The effects following follicular fluid collagen digestion and subsequent separation by SDS PAGE were interesting. Collagen is the most abundant protein in mammals making up 25% of the total protein mass. Human collagenase (MMP-I) similar to that used to digest the collagen in these experiments is secreted as a major 52 kDa and minor glycosylated 57 kDa proenzymes. Cleavage of the pro-peptide produces the active forms of 42 kDa and 47 kDa respectively. The nine residues RWTNNFREY (183-191) in the catalytic domain are essential for collegenolytic activity (Borkakoti, 1998, Yong *et al.*, 1998). Collagenase I (MMP-1), used to digest the fluid samples degrades type III collagen more efficiently than types I and II and degrades fibrillar collagens types I, II, III, VII, VIII, X aggrecan, serpins and α – macroglobulin (Hasty *et al.*, 1984, Mallya *et al.*, 1990). The following molecules were identified by N-terminal sequencing: secretin, serum albumin, involucrin, agglutinin like protein precursor, prothrombin precursor, coagulation factor X, prothrombin precursor, collagen IV α2, collagen XIII α1, and α2-macroglobulin. However, from this screen no molecules able to contribute to the colloid osmotic pressure were identified, as all were of a size able to traverse the follicular wall. It is likely therefore that the effect on colloid osmotic pressure noted on the removal of collagen is solely related to the intact collagen itself and not its digestion products.

The mobility and distribution of macromolecules in a number of tissues, including tendon, occurs in the interstitium, and their mobility is restricted by hyaluronan, proteoglycans and collagens (Aukland *et al.*, 1997). A similar scenario occurs in synovial fluid with the same molecules responsible. The exact contribution of each of these molecules to this mobility is unknown but it is believed that fluid circulates between the collagen fibrils within a matrix (Aukland *et al.*, 1997). Granulosa cells produce collagen in culture (Zhao M. *et al.*, 1995) and whether this collagen is used in the same way is yet to be established.

Collagens are known to bind glycosaminoglycans and proteoglycans, in addition to binding glycosaminoglycans they can also carry them, and are therefore referred to as part time or facultative proteoglycans themselves (Dong S. *et al.*, 2003, Halfter *et al.*, 1998). The negative charges associated with the attached proteoglycans and glycosaminoglycans increase

the extra-fibrillar space surrounding the collagen by creation of an excluded volume. This excluded volume increases with increased size of macromolecule (Aukland *et al.*, 1997). Thus in a case where proteoglycan, hyaluronan and collagen are present this excluded volume can be quite large. The exclusion matrix resulting from this structure prevents large molecules from entering this area but provides a large area for water-based solutions to reside (Aukland *et al.*, 1997). In the vitreous of the eye, which in many ways is comparable to follicular fluid in its matrix composition, collagen concentrations are not uniformly distributed. The highest concentrations reside at the vitreous base; hyaluronan distribution is similarly non-uniform and is polydisperse in molecular weight. These two phenomena and the local concentration of proteoglycan allow fine control of excluded volume and maintenance of osmotic potential within the ocular system (Bishop, 2000). The latter is interesting in light of the irregular versican-staining pattern noted within the healthy follicle granulosa cell layers. Versican can bind to hyaluronan and this irregular pattern may indicate that hyaluronan production is also non-uniform. This could not be confirmed by the HABP immunolocalisation experiments since hyaluronan is ubiquitous within the ovary and subtle deviances in local concentrations cannot be visualised with this ligand (Girard *et al.*, 1986, Lindqvist *et al.*, 1992).

The effect of hyaluronan on osmotic potential has been discussed to some degree in Chapter 3. The information gathered from data in this chapter suggested that hyaluronan in follicular fluid may interact with many of the common matrix molecules to form large hydrodynamic volumes. The molecular weight of hyaluronan was determined to be between 400 kDa and 2 x 10^6 Da. The larger sizes of hyaluronan found here supports earlier findings of fluid hyaluronan (Mueller *et al.*, 1978, Salustri *et al.*, 1999). Salustri et al proposed that proteoglycan synthesis was increased at the time of antrum formation and was the cause of increased fluid viscosity and maintenance of the distended follicular volume (Salustri *et al.*, 1999) however; the precise molecules involved were not identified.

The 400 kDa hyaluronan present may be derived from degraded hyaluronan, which has been degraded by the normal degradation pathway for hyaluronan, or synthesised at that size by one of the three hyaluronan synthases. In addition, it may be linked to molecules such as versican found in follicular fluid.

The immunohistochemical localisation of hyaluronan using HABP to follicle 8 – 10 mm (Figure 40), showed that hyaluronan was present throughout the follicular and stromal tissue. Since hyaluronan is a core component of the extracellular matrix of most tissues it was not surprising to see this result. It was interesting to note that there was increased localisation to the cytoplasm of granulosa and theca cells. The nuclear staining was confirmed in non-counterstained sections (data not shown) indicating that the result seen in the counterstained tissue was not caused by the counterstain or intensified by it. This showed that both cell types

produce hyaluronan, and that it existed in higher concentrations in granulosa and theca cells than the stroma. While the localisation of hyaluronan to the granulosa cells supported a hypothesis of hyaluronan extrusion in to the follicular antrum for provision of osmotic and structural support there, it is unclear what role hyaluronan plays within the theca. In situ, (see chapter 5) studies were aimed at clarifying this. Hyaluronan, although originally believed to be extracellular, has been located in the nuclei of rat brain and liver (Hascall *et al.*, 2004). Hascall et al found that hyaluronan was localised to the rough endoplasmic reticulum, plasma membrane and nucleus, showing a strong association with chromatin. Hascall et al were also able to co-localise TSG-6 with hyaluronan in the nucleus. The results appear to be real since pre-treatment with S. hyaluronidase removed all staining previously observed. It is thought that intracellular hyaluronan may facilitate nuclear separation at cell division; its function here is unknown.

Currently, most data available on follicular hyaluronan relates to its functions within the expanding cumulus oocyte complex prior to ovulation. In this work hyaluronan was present in bovine follicular fluid and located near the mural granulosa cells. Given its role in the fluid regulation processes in the body it has potential to act in a similar role within the follicle. In other systems hyaluronan swelling whether involving other molecules or not occurs at the site of hyaluronan synthesis on the cell surface. Situated on the membrane surface, hyaluronan is capable of displacing many cell surface components by exclusion. In vitreous gels hyaluronan acts as a hydrated polyion, space filler, sieve and osmotic buffer capable of excluding other large molecules and cells (Laurent U. B. & Granath, 1983). The space filling functions in relation to its ability to bind and interlink with proteoglycans and collagen have been discussed earlier. One other factor controlling hyaluronan volume, which is relevant to the situation in the follicle, is serum cation level. Cations are small enough to cross in to the follicle and so their effect on hyaluronan volume should be considered. Cations are known to affect hyaluronan chain union, if the cation is bivalent the volume is greater than if it is monovalent similarly hyaluronan volume is increased in acidic pH over alkali (Gomez-Alejandre *et al.*, 2000), and it is this change in volume, which can affect osmotic potential. As suggested previously, hyaluronan in dilute solutions creates an excluded volume. When this hyaluronan solution contains K^+ its osmotic potential increases by 7 % and when Ca^{2+} or Mg^{2+} are present it can increase by 10% and 11% respectively (Gomez-Alejandre *et al.*, 2000). This data generates an interesting question as to whether the circulating serum cations affect the exclusion volume of hyaluronan selectively throughout the oestrous cycle of cattle.

Exploring this question further, follicular fluid is known to derive from serum and that serum cations are in follicular fluids (Shalgi *et al.*, 1972b, Shalgi *et al.*, 1973). An active inward transport in to the follicle of cations occurs and differences in the cations present

occur between small and large follicles (Leroy *et al.*, 2004), and it has been demonstrated that metabolic changes in blood serum are replicated in follicular fluid composition (Gosden R. G. *et al.*, 1988). A question arises then as to whether variations in serum concentrations of cations occur in a controlled and regular pattern throughout oestrous? It appears that they do. Serum and fluid cations sampled daily throughout the bovine oestrous cycle (as determined by progesterone concentration) and measured by flame atomisation and atomic absorption spectroscopy (FAAAS) showed that while Mg^{2+} and Na^{+} were always higher and K^{+} always lower in serum with respect to oviductal fluid but Ca^{2+} varied throughout the cycle (Grippo *et al.*, 1992). This is replicated in follicular fluid (Eissa, 1996) and suggests that Ca^{2+} is under hormonal control and its regulation and transport are finely controlled (Grippo *et al.*, 1992). Cations are thought to be important in a number of fertilisation events that include glycosaminoglycans such as sperm capacitation and acrosome reaction (Herz *et al.*, 1985, Stock C. E. & Fraser, 1989, Yanagimachi, 1984, Yoshimatsu *et al.*, 1988). Their role in follicular fluid has not been determined since follicular fluid cation measurement have only been surveyed at static time points (Gosden R. G. *et al.*, 1988, Shalgi *et al.*, 1972b) and were not measured by us. Research conducted by Powers and Hess has shown that the follicular basal lamina is sensitive to ion transport (Hess *et al.*, 1998, Powers *et al.*, 1995) and hence may also have a role in the control of calcium levels in the follicle. It is therefore interesting to speculate whether variations in serum Ca^{2+} might be replicated in follicular fluid and if so whether in addition to its role in the coupling of ITI and hyaluronan through the action of TSG-6, Ca^{2+} might also affect the conformational properties of hyaluronan in fluid during the period of antrum formation in the oestrous cycle.

4.5. Summary

In 1999 Antoinetta Salustri suggested that the roles of proteoglycans in follicular fluid might be related to their hydrodynamic properties. The data provided here and in Chapter 3 provide some evidence to suggest that this may indeed be the case. The identification of versican, ITI, hyaluronan, collagen digestion products, and DNA has elucidated which members of the chondroitin/dermatan sulphate molecules in Chapter 3 were able to affect osmotic potential within the follicle. Further there has been discussion on how these molecules have the potential to interact to provide fine control of the osmotic potential in the follicle. The subtle changes in serum and fluid cations levels present throughout oestrous may also influence these associations.

Chapter 5 Hyaluronan Synthase Expression in the Bovine Follicle

5.1. Introduction

In Chapter 4 versican, inter-alpha trypsin inhibitor (ITI), hyaluronan, collagen, and DNA were identified as the major contributors to the colloid osmotic pressure of bovine follicular fluid. It was proposed that these molecules were not mutually exclusive with respect to their contribution to fluid potential, although it appears that hyaluronan, ITI and versican may exist to some extent as separate entities within the fluid and not in a complex as reported in the cumulus oocyte complex of mice and cows (Carrette *et al.*, 2001, Hess *et al.*, 1999, Odum L. *et al.*, 2002, Zhuo & Kimata, 2001). In addition it was suggested that the fluid matrix was no doubt affected by transient changes in gonadotrophins, growth factors and potentially serum cations during follicular growth, which control the production and conformation of matrix molecules.

The roles of hyaluronan, ITI and versican are well known in the process of cumulus oocyte expansion and have been much investigated in the follicle by other authors and excellent reviews are available (Rodgers R. J. *et al.*, 2003, Salustri *et al.*, 1996, Salustri *et al.*, 1999, Zhuo & Kimata, 2001). Their roles outside of the cumulus oocyte complex have not been so well studied. Since the role of this thesis is to investigate the fluid accumulation processes within the bovine ovarian follicle the focus of the thesis became the most osmotically active of these as determined by earlier experiments conducted in this thesis, hyaluronan. Hyaluronan is a highly osmotic and ubiquitous molecule of the ECM, with roles in many fluid accumulation mechanisms in the body.

Hyaluronan has been found in human follicular fluid by several authors (Hamamah *et al.*, 1996, Jessen & Odum, 2003, Jessen *et al.*, 1994, Saito *et al.*, 2000, Suchanek *et al.*, 1994), and has been recorded in bovine fluids (Odum L. & Jessen, 2002, Sato *et al.*, 1987a, Tempel *et al.*, 2000), but no-one has examined the cellular origins of hyaluronan or recorded the levels of expression of the enzymes responsible for its synthesis in bovine healthy and atretic antral follicles of increasing size.

Hyaluronan is an essential component of many extracellular matrices in mature tissues (Laurent TC, 1998) and in some cases is the major constituent; e.g. vitreous of the human eye (65 ± 400 mg/ml), adult bovine vitreous (570 mg/ml) (Grimshaw *et al.*, 1994, Reardon *et al.*, 1998), synovial joint fluid (3-4 mg/ml) (Scott D. *et al.*, 2000(a)), the cumulus cell matrix, (~0.5 mg/ml) (Salustri *et al.*, 1992). Hyaluronan can also be present in minute quantities in structural combination with proteoglycans e.g. cartilage (Hardingham and Fosang 1995). Hyaluronan is not structurally diverse and as such it is believed that many of its functions are related to chain length. Hyaluronan is a unique glycosaminoglycan in that it is unable to

covalently link to proteins to form proteoglycans. One exception is the formation of an ester link with the C-terminal aspartic acid of heavy chain 3 of pre-alpha trypsin inhibitor. Hyaluronan can also bind proteins via the structural binding motif, the link module (Day, 2001). The function of hyaluronan in a system may vary greatly depending on whether it interacts with proteins in tertiary or quaternary organisations or with water and ions in the formation of viscous solutions or gels. In joint tissue, such as the lining cells of the joint capsule of the knee, hyaluronan is synthesised and released in to the synovial fluid, where it is the major contributor to the viscoelastic properties of the fluid (Balazs, 1968, Seppala, 1969).

In dilute physiological solution, hyaluronan is believed to form stiff random coils, without specific chain interactions. This stiffness is caused by the chemical structure and results from the disaccharides and internal hydrogen bonds interacting with the solvent, to form a strong backbone. In addition to this, the axial hydrogen atoms form a non-polar hydrophobic face while equatorial side chains give rise to a polar hydrophilic face. This results in a twisted ribbon, which in physiological solution assumes an expanded random coil capable of occupying very large domains (Weissman & Meyer, 1954). The actual mass of the hyaluronan in this form is very low at approximately 0.1 % (wt/vol), but its expanded structure suggests that overlapping could occur between the domains of individual molecules at concentrations above 1mg/ml. At concentrations in which chains overlap, there is a change in the measured dynamic viscosity (Gribbon *et al.*, 2000). The dynamics of hyaluronan make it a perfect space-filling molecule since it can change shape within nanoseconds. This allows it to fill voids, adjust to surfaces and impose a counteracting force when moved significantly from its preferred extended state (Coleman *et al.*, 1999, Scott D. *et al.*, 2000(a)).

The domain structure of hyaluronan is important since the structure allows small molecules such as electrolytes, nutrients and water to diffuse freely through the solvent while large molecules, such as proteins, are partially excluded because of their hydrodynamic size in solution. The larger the hyaluronan molecule and hence its domain network, the less room there is for other molecules. This reduction in space results in slower diffusion of other macromolecules in a solution and hence reduces their concentration in the hyaluronan network compared to surrounding hyaluronan-free compartments. Hyaluronan molecules move constantly when in solution, therefore in a fluid matrix, the effective "pore" size available for large molecules to pass through is also constantly changing size. At any one time there will be a range of pore sizes present to pass through however; the ratios of large to small will be in constant flux resulting small fluctuations in the concentrations of molecules present (Choi-Miura *et al.*, 2001, Hardingham & Fosang, 1995).

Hyaluronan is synthesised by a group of monomeric enzymes known as hyaluronan synthases (HAS). The mode of synthesis is unique amongst macromolecules and it has been

proposed that synthesis occurs at the plasma membrane with hyaluronan being extruded directly in to the extracellular space (Prehm, 1984).

Spicer et al (1998), using degenerative PCR isolated the cDNAs encoding putative vertebrate hyaluronan synthases. Hyaluronan synthases 2 and 3 (HAS 2 and HAS 3) have been identified in a number of species including humans and mice and are highly conserved. Expression cloning led to the identification of an additional putative synthase hyaluronan synthase 1 or HAS 1, again in humans and mice. Later, identification of an invertebrate hyaluronan synthase indicated that biosynthesis of hyaluronan probably predated vertebrate evolution (Spicer & McDonald, 1998).

Vertebrate hyaluronan synthase enzymes synthesise large linear polymers of the repeating disaccharide structure of hyaluronan by alternate addition of glucuronic acid and N-acetyl glucosamine to the growing chain. The number of repeats of disaccharides, (n), in a complete hyaluronan molecule may reach 10,000, with an implied molecular mass of up to 4 million Daltons. The average length of a disaccharide is 1nm, which if a molecule of 10,000 repeats were produced would extend 10μm.

Sequence analysis indicates that eukaryotic hyaluronan synthases have a 25% identity with Streptococci hyaluronan synthases and that both encode a plasma membrane domain with multiple transmembrane domains. In humans, mice and cattle there are three hyaluronan synthases encoded by related genes. The encoded proteins share 57% - 71% identity; with the vertebrate HAS genes sharing the location of at least one intron. Recently, the first virally encoded hyaluronan synthase was found in *Paramecium bursaria chlorella* virus (DeAngelis *et al.*, 1997). This viral protein shares approximately 50% amino acid sequence identity with the vertebrate HAS proteins.

Although each form of HAS protein catalyses hyaluronan biosynthesis in eukaryotic cells, their enzymatic properties differ (Itano *et al.*, 2004). The physiological function of hyaluronan may be dependent on the associated enzymatic properties (Spicer & McDonald, 1998). HAS 3 is intrinsically more active than HAS 2, producing more product per enzyme unit at a greater rate, which is in turn more active than HAS 1. Analysis of hyaluronan product size as generated by each HAS protein *in vitro*, shows that hyaluronan chain length is controlled by the specific HAS protein synthesising hyaluronan. HAS 1 and HAS 2 proteins produce hyaluronan chains of similar lengths (up to 2 X 10^6 Da), whereas HAS 3 produces hyaluronan chains, < 3 X 10^5 Da. Hyaluronan chains of different lengths have different effects on cell behaviour, with short length hyaluronan involved in the stimulation of cell proliferation and initiation of signalling cascades (Deed *et al.*, 1997). Short hyaluronan chains can also be generated by degradation of extracellular hyaluronan, through the action of a hyaluronidase or oxidants. High molecular weight hyaluronan chains on the other hand, have

the opposite effect, causing the inhibition of cell proliferation. That HAS proteins synthesise hyaluronan chains of differing average lengths, may be a key factor in ECM regulation and fluid accumulation, although the functional significance of varying polymer length is not known.

This Chapter aimed to determine where in the follicle and at what stage of follicular development hyaluronan is being synthesised. In addition it aimed to identify which cells were responsible for its production, prior to cumulus oocyte complex involvement. In doing this support the data provided in Chapter 4 pertaining to hyaluronan protein production and localisation within the follicle and to propose a role for hyaluronan in a general model of fluid accumulation processes during the growth of the follicular antrum.

5.2. Experimental Design

In order to determine which cells within the follicle were producing hyaluronan and at what stage in their development, a combination of immunohistological, molecular and in situ hybridisation methods were employed. Since no commercial probes were available to the bovine HAS genes, primers were designed for PCR using known bovine sequences to HAS 1, 2 and 3 and to an identifier of follicular health, inhibin/activin βA, with the view to preparing digoxigenin (DIG) labelled probes for in situ hybridisation and Northern blot experiments. Probes for the housekeeper genes 18S ribosomal RNA (18S rRNA) and glyceraldehyde-3-phosphte dehydrogenase (GAPDH) were also made. In addition, a plasmid containing the cytochrome P450 side chain cleavage (P450scc) was sourced as a control for follicular thecal health. At the time of commencement of this work the available nucleotide sequences for the bovine HAS genes were AB017803, (HAS 1), AB017804, (HAS 2) and AB017805 (HAS 3). During the completion of this work a new set of sequence data was lodged in GenBank (NM_174079 – HAS 2 and AJ293889 – HAS 3). There was no new sequence for HAS 1 (AB017803) and so primers as described by Schoenfelder and Einspanier were made (Schoenfelder & Einspanier, 2003).

All primers were designed to provide probes that were bovine and HAS gene specific and would span introns where possible.

Sequence alignments of hyaluronan synthases were performed using Clustal W 1.4 with forward and reverse primers designed using Oligo program 4.0 or primer Express software. The primer sets shown in Table 10 were selected based on published data as indicated and were supplied by Sigma Genosys Castle Hill Australia Pty Ltd.

The housekeeper genes used were bovine 18S rRNA accession number: AF176811 and mouse GAPDH: XM284785

Inhibin/activin βA was designed to the βA subunit of the inhibin/activin molecule as the inhibin/activin βA subunit mRNA is only expressed by the granulosa cells of antral follicles greater than 0.8 mm diameter (Torney *et al.*, 1989). Forward and reverse primers were designed to exon 1 and 2 of the inhibin/activin βA gene respectively. The forward primer was targeted to base 1652 to 1672 of exon 1 (accession: U16238, base 1743 = base 1 of intron) and the reverse primer targeted to bases 738 to 758 of exon 2 (accession; U16239, base 339 is the first base of exon 2).

The P450scc product obtained by amplification of the P450 side chain insert was from plasmid pBSCC-4 (Figure 55). This plasmid was donated by Dr Raymond Rodgers of The University of Adelaide and contained the M13 Universal (USP) and M13 Reverse sequence primer (RSP). This plasmid was contained a 550 bp insert sub-cloned from pBSCC-2 (John *et al.*, 1984).

Batches of cDNA were made from RNA extracted as described in 2.22 and 2.23 from several foetal tissues reported as having hyaluronan synthase activity, namely, eye, skin, lung, brain, cartilage heart and colon. Following amplification of sequence and its confirmation by Clustal W alignment to the GenBank sequence, the amplicons were cloned in to pGEM T Easy™ vectors by standard methods. Following successful cloning of the amplicons tissues were collected from the local abattoir and processed for in situ hybridisation (see 2.3.5). DIG labelled RNA probes were made as described in 2.27.2 and a second series of follicles from mature ovaries were collected and processed for in situ assays. These follicles were collected and classified in to six groups based on follicular diameter, three containing healthy follicles and three of atretic follicles. The groups were 2 - 4 mm, 6 - 8 mm and 12 - 15 mm. In addition, whole ovaries were processed for in situ to allow assessment of hyaluronan expression in primordial through to early antral follicles. These groupings were chosen in order to provide data on hyaluronan production at different stages of follicular development and to investigate changes in the level of expression of hyaluronan with respect to health status. All follicles > 2 mm were classified for health by the same criteria applied in previous Chapters. Control probes of inhibin/activin βA and P450scc were used in in situ and Northern blot assays with the probe for GAPDH used solely for the Northern blots.

GAPDH is a common control gene expressed ubiquitously in the cell. GAPDH aids in the assessment of relative amounts of transcript present in a tissue sample. The GAPDH primers used in the PCR experiments were derived from the rabbit sequence, as these were freely available. Since the sequence homology of GAPDH across species is very high (Figure 56) there were no difficulties foreseen in using it.

As mentioned above, Inhibin/activin β A was used as a control as it is a reliable marker of granulosa cell integrity. P450scc was used as a control for theca cell integrity (John *et al.*,

1984). Further information on these controls can be found in the material and methods Chapter of this thesis and excellent reviews of their role in the follicle are available (Bao & Garverick, 1998, Campbell *et al.*, 2003, Mihm & Bleach, 2003, Risbridger *et al.*, 1990, Ying, 1987).

Following the in situ assays the percentage of positively stained follicles from different size categories and health status were calculated in order to provide insight in to the temporal expression of the three HAS enzymes. Tissue controls were also assessed for expression.

In order to confirm the findings from the in situ assays Northern blots were carried out using the RNA prepared from a pool of follicles of the same size categories used in the in situ assays. The same tissues were also tested and where available additional tissues were assayed. In addition to the above one-tube RTPCR using equal amounts of RNA starting material was carried out in order to assess relative levels of product from each tissue type.

5.3. Results

5.3.1. Sequence Data

In order to identify primers specific to the three HAS genes for use in PCR reactions sequence data for the HAS genes and for housekeeping genes 18S rRNA and glyceraldehyde-3-phosphate dehydrogenase (GAPDH) were sourced from the GenBank database. Sequence alignments were performed using Clustal W 1.4 (http://www.ebi.ac.uk/clustalw/). The nucleotide sequence alignment for bovine HAS 1, 2 and 3 is shown in Figure 42 and the protein alignment can be seen in Figure 43. The sequence homology of the bovine HAS genes at the nucleotide level was greater than 60%. The plasmid maps, sequences used and position of the HAS primers can be seen in Figure 51, Figure 52, and Figure 53. The amplicon sizes of each product can be seen in Table 10.

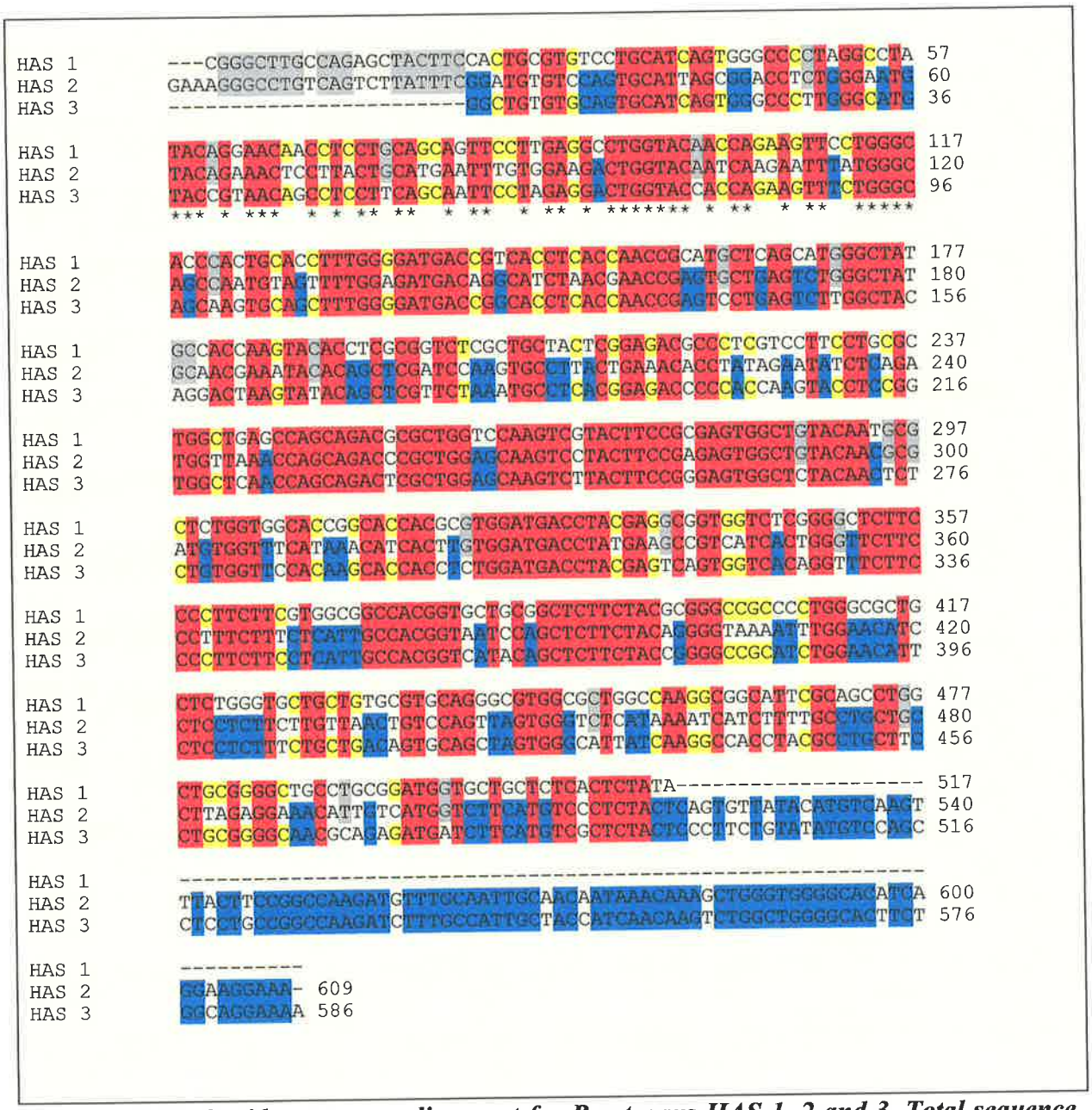

Figure 42 Nucleotide sequence alignment for Bos taurus HAS 1, 2 and 3. Total sequence homology (red box), HAS 1, 2 homology (grey box), HAS 2, 3 homology (blue box) HAS 1, 3 homology (yellow box). Sequence data obtained from http://www.ncbi.nlm.nih.gov. Accession numbers for HAS 1, 2 and 3 are AB017803 bases 1 - 517, AB017804 bases 1 - 609, and AB017805 bases 1 – 586 respectively. (Yamashita,H, Usui,T. and Suzuki,K.1999).

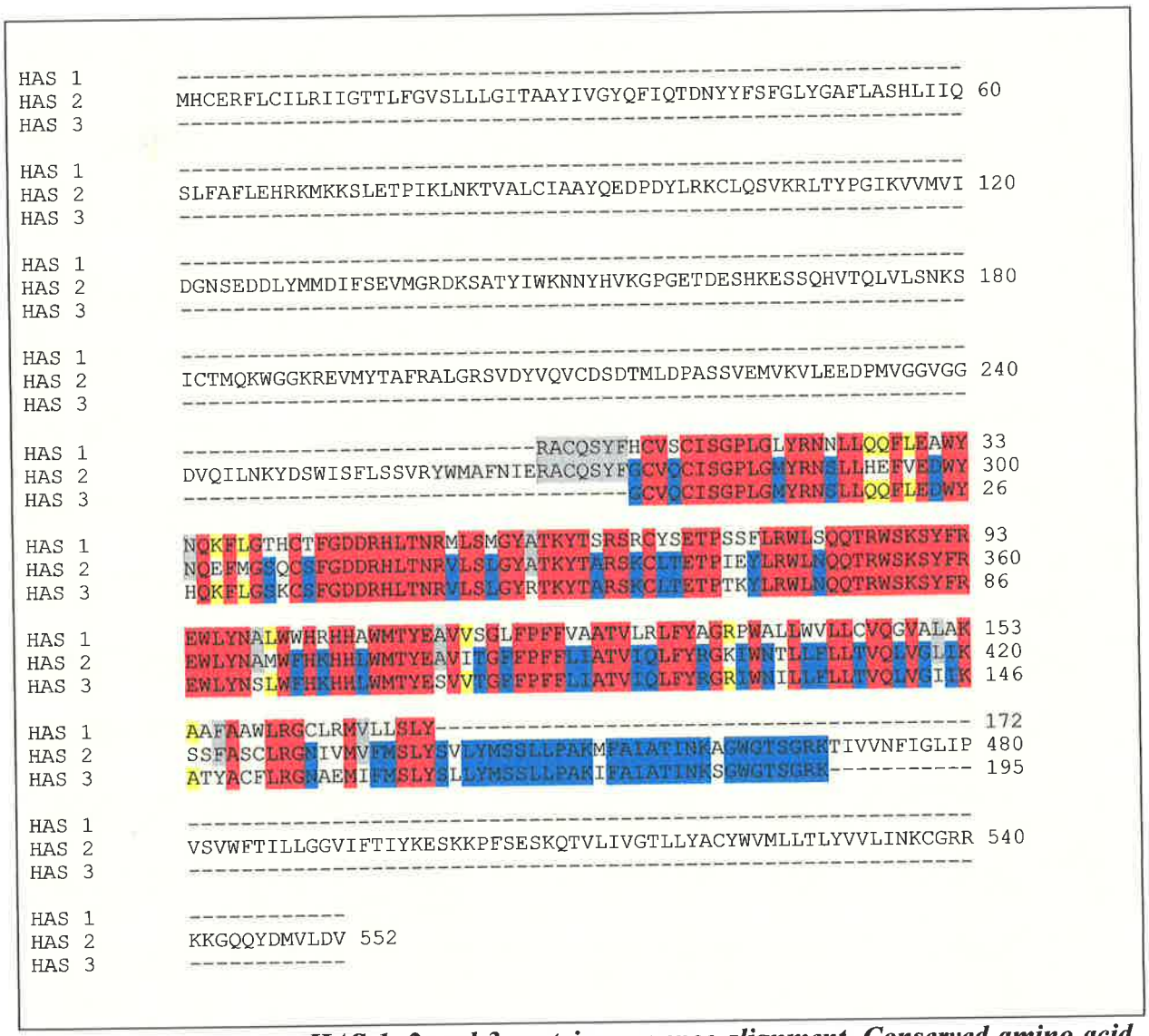

Figure 43 Bos taurus HAS 1, 2 and 3 protein sequence alignment. Conserved amino acid homology (red box), HAS 1,2 homology (grey box), HAS 2,3 homology (blue box) HAS 1,3 homology (yellow box). Sequence data obtained from http://www.ncbi.nlm.nih.gov. Accession numbers for HAS 1, 2 and 3 are BAA76546 amino acid 1 - 172, BA76547 amino acid 1 - 203, and BA76548 amino acid 1 - 195 respectively. (Yamashita,H., Usui,T. and Suzuki,K.1999).

Identification	Accession No.	Primer sequences 5' – 3'	Primer direction	Tm	Amplicon Size (bp)
Bos 18S rRNA	AF176811	AGAAACGGCTACCACATCCAA	Forward	60 C	90 bp
		CCTGTATTGTTATTTTTCGTCACTACCT	Reverse		
Bos HAS 1	AB017803	GGTACAACCAGAAGTTCCTGGG	Forward	65.5 C	182 bp
		CGGAAGTACGACTTGGACCAG	Reverse		
Bos HAS 2	gi:4586935	CTGGGAATGTACAGAAACTCCTTA	Forward	63.8 C	310 bp
		GGAAGAACCCAGTGATGACG	Reverse		
Bos HAS 3	gi:12049661	GTCCTGAGTCTTGGCTACAGG	Forward	70 C	243 bp
		GCCCCGGTAGAAGAGCTGTATG	Reverse		
Bos Inhibin/Activin βA	U16239	AGAGGACTGTGACGAGGTGTC	Forward	58 C	449 bp
	U16238	TGGAGATAGAGGACGACATCG	Reverse		
OL GAPDH	L23961	GGCGTGAACCACGAGAAGTATG	Forward	60 C	388 bp
		TCACCACCTTCTTGATGTCGTC	Reverse		
M13 U/USP-17		GTAAAACGACGGCCAGT	Forward	55 C	
M13 R/RSP-25		CATGGTCATAGCTGTTTCCTGTGTG	Reverse		

Table 10: Primer sequences used for the amplification of Bovine HAS 1, HAS 2, HAS 3, 18S rRNA, GAPDH and Inhibin/activin βA and sequences of the universal primers used for amplification of insert from the pGEM T Easy vector. The primer Tm and expected amplicon size are indicated

5.3.2. RT - PCR to Follicles and Tissues.

RNA was made from foetal tissues and from single follicles collected from the abattoir. Complementary DNA was then synthesised from RNA by standard methods and this cDNA was used for RT – PCR to amplify HAS genes and control genes alike. RT – PCR amplified a product from foetal tissue for each set of primers for bovine HAS 1, 2 and 3 and for bovine inhibin/activin βA, GAPDH and 18S rRNA. The sizes of the amplicon were 182 bp, 310 bp and 243 bp for HAS 1, 2 and 3 respectively and 449 bp, 388 bp and 90 bp for inhibin/activin βA, GAPDH and 18S rRNA.

5.3.2.1. Bovine HAS 1

Amplified DNA of the correct size was seen in all tissues tested. The size of the amplified product was 182 bp (Figure 44). NB: in the images below 2 – 4 mm GC denotes

granulosa cells obtained from a follicle of 2 – 4 mm diameter, 2 - 4 mm theca denotes theca cells obtained from a follicle of 2 - 4 mm

5.3.2.2. Bovine HAS 2

HAS 2 could be amplified in all tissues tested. The amplified product was 310 bp (Figure 45)

5.3.2.3. Bovine HAS 3

HAS 3 could be amplified from all tissues tested. The amplified product was 243 bp (Figure 46)

5.3.2.4. Bovine Inhibin/activin βA

Bovine inhibin/activin βA was only amplified from follicular tissue and skin. An amplicon was seen in all tissues tested, with the amplified product being 449 bp (Figure 47)

5.3.2.5. GAPDH

All tissues tested amplified a product of 388 bp. The intensity of the band staining in each case was equal in all tissues except the heart (Figure 48).

5.3.2.6. Bovine 18S rRNA

All tissues tested amplified a product of 90 bp. The intensity of the band staining in each case was again equal in all tissues as expected (Figure 49).

The PCR fragments isolated from the RT PCR were sequenced by standard methods at the John Curtin School Biomolecular Resource Facility, Australian National University, Australia and aligned to the known bovine sequences reported in Table 10. All amplified sequences had high homology > 98% with reported sequence.

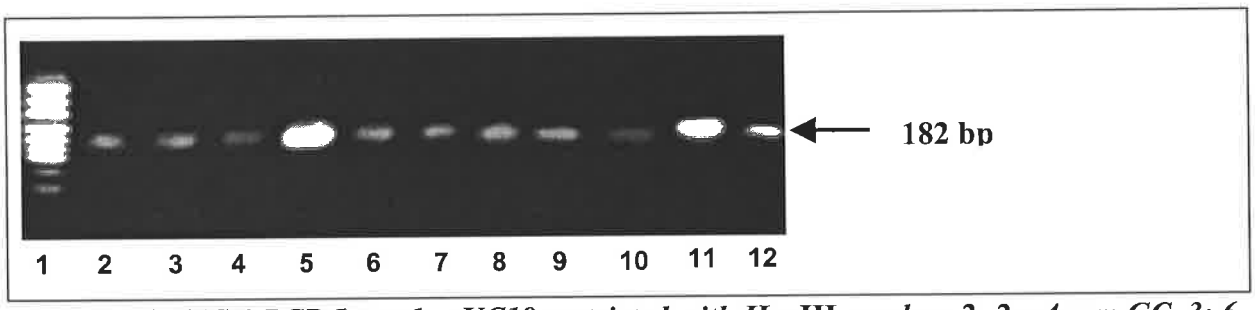

Figure 44 HAS 1 PCR Lane 1: pUC19 restricted with HpaIII marker, 2: 2 – 4 mm GC, 3: 6 – 8 mm GC, 4: 12 - 15 mm GC, 5: 2 - 4 mm theca, 6: 6 - 8 mm theca, 7: 12 - 15 mm theca, 8: eye, 9: skin, 10 hoof, 11 brain, 12 colon. PCR product size 182 bp, product separated on a 2 % agarose gel. NB 2 – 4 mm GC denotes granulosa cells obtained from a follicle of 2 – 4 mm diameter, 2 - 4 mm theca denotes theca cells obtained from a follicle of 2 - 4 mm.

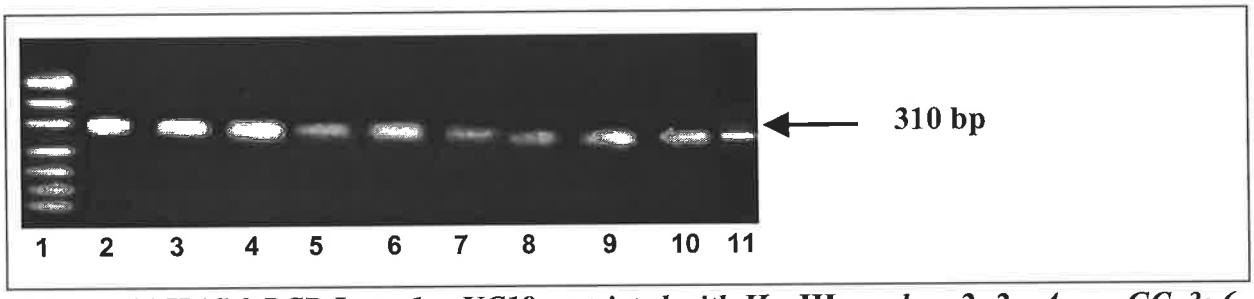

Figure 45 HAS 2 PCR Lane 1: pUC19 restricted with HpaIII marker, 2: 2 – 4 mm GC, 3: 6 – 8 mm GC, 4: 12 - 15 mm GC, 5: 2 - 4 mm theca, 6: 6 - 8 mm theca, 7: 12 - 15 mm theca, 8: eye, 9: skin, 10 hoof, 11 colon. PCR product size 310 bp, product separated on a 2 % agarose gel.

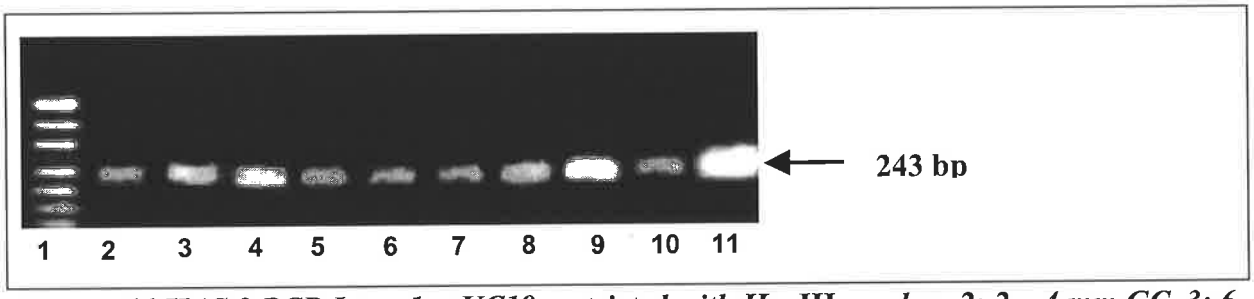

Figure 46 HAS 3 PCR Lane 1: pUC19 restricted with HpaIII marker, 2: 2 – 4 mm GC, 3: 6 – 8 mm GC, 4: 12 - 15 mm GC, 5: 2 - 4 mm theca, 6: 6 - 8 mm theca, 7: 12 - 15 mm theca, 8: eye, 9: skin, 10 hoof, 11 colon. PCR product size 243 bp, product separated on a 2 % agarose gel.

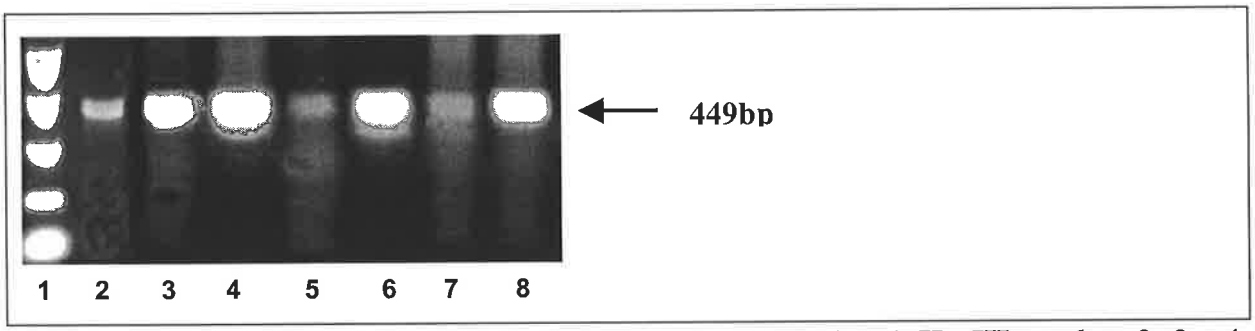

Figure 47 Bovine Inhibin βα PCR Lane 1: pUC19 restricted with HpaIII marker, 2: 2 – 4 mm GC, 3: 6 – 8 mm GC, 4: 12 - 15 mm GC, 5: 2 - 4 mm theca, 6: 6 - 8 mm theca, 7: 12 - 15 mm theca, 8: skin. PCR product size 449 bp, product separated on a 2 % agarose gel.

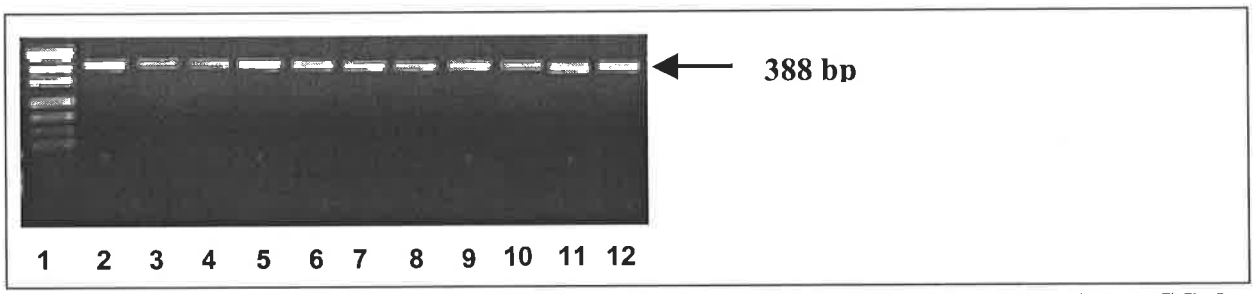

Figure 48 GAPDH PCR Lane 1: pUC19 restricted with HpaIII marker, 2: 2 – 4 mm GC, 3: 6 – 8 mm GC, 4: 12 - 15 mm GC, 5: 2 - 4 mm theca, 6: 6 - 8 mm theca, 7: 12 - 15 mm theca, 8: eye, 9: skin, 10 hoof, 11 colon 12: Brain. PCR product size 388 bp, product separated on a 2 % agarose gel.

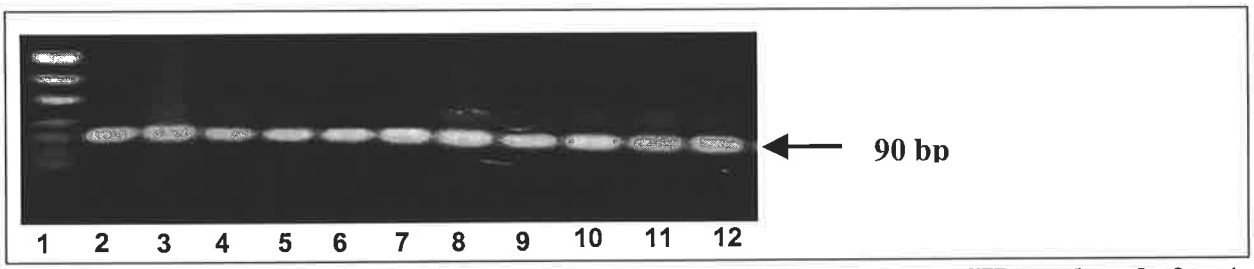

Figure 49 Bovine 18S rRNA PCR Lane 1: pUC19 restricted with HpaIII marker, 2: 2 – 4 mm GC, 3: 6 – 8 mm GC, 4: 12 - 15 mm GC, 5: 2 - 4 mm theca, 6: 6 - 8 mm theca, 7: 12 - 15 mm theca, 8: eye, 9: skin, 10 hoof, 11 colon, 12: Brain. PCR product size 110 bp, product separated on a 2 % agarose gel.

5.3.3. Sub-Cloning

Following successful amplification of the HAS 1, 2 and 3 and inhibin/activin βA genes the PCR product was purified by phenol chloroform extraction and the product ligated overnight and transformed in to pGEM T Easy™ vector using JM109 competent cells. Up to 20 positive colonies were picked and grown up in 70 ml cultures. Plasmid DNA (100ng) was then purified sent for sequencing to confirm the sequence of the insert. The vector maps and sequences can be seen below (Figure 50, Figure 51, Figure 52, Figure 53, Figure 54, Figure 55 and Figure 56). Positive clones were then used to make DIG labelled probes for in situ hybridisation and Northern blot assays by standard methods described in Chapter 2.

5.3.3.1. pGEM T Easy Vector System

The pGEM T Easy vector system multiple cloning site can be seen in Figure 50

5.3.3.2 pHAS 1

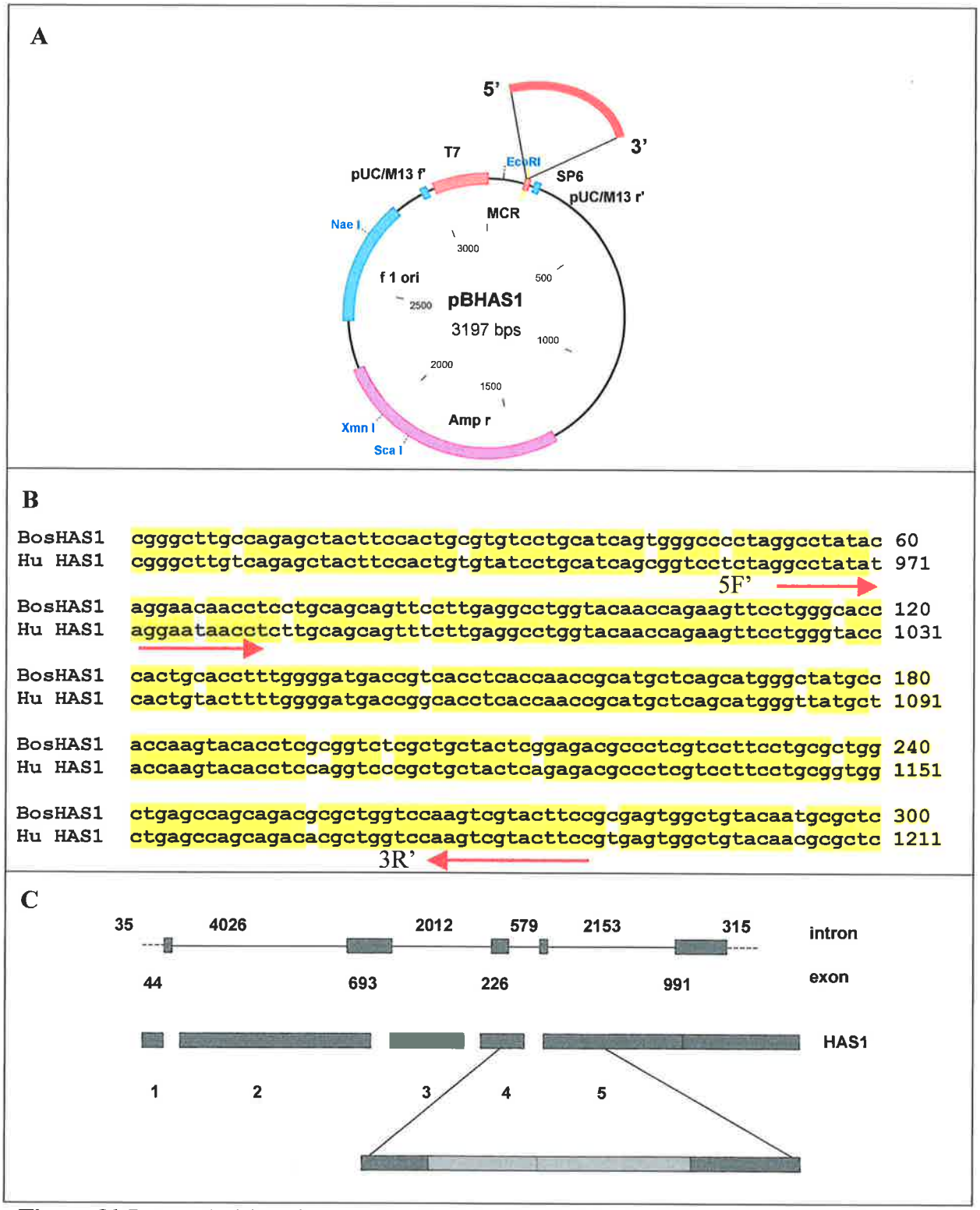

Figure 51 Image A: Plasmid map for HAS 1, B: Alignment of Bos taurus HAS 1 sequence with Human HAS 1 sequence, showing sequence homology (yellow box) and forward and reverse primer sequence positions, C: schematic showing position of amplified HAS 1 sequence spanning exons 4 and 5 of the known Human sequence. Expected amplicon size was 182 bp. Start position bp 85 exon 4, finish bp 268 exon 5 bovine sequence. Intron exon boundary marked by dotted line.

5.3.3.4 pHAS 3

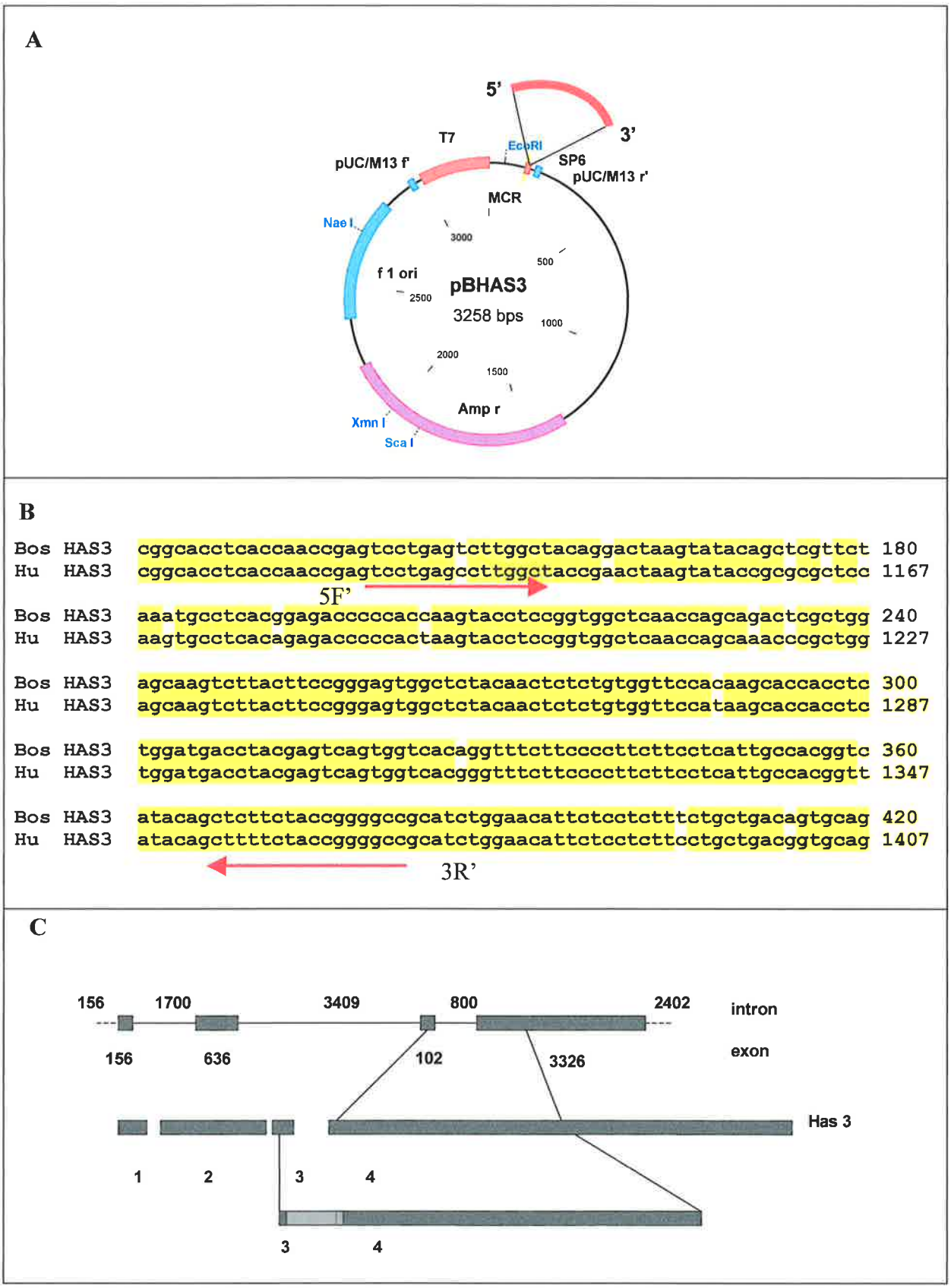

Figure 53 Image A: Plasmid map for HAS 3, B: Alignment of Bos taurus HAS 3 sequence with Human HAS 3 sequence, showing sequence homology (yellow box) and forward and reverse primer sequence positions, C: schematic showing position of amplified HAS 3 sequence spanning exons 3 and 4 of the known Human sequence. Expected amplicon size was 143 bp. Start position bp749 exon 3, finish bp894 exon 4. Probe position bp95 – 325 of bovine sequence. Intron exon boundary marked by dotted line.

5.3.3.3 pHAS 2

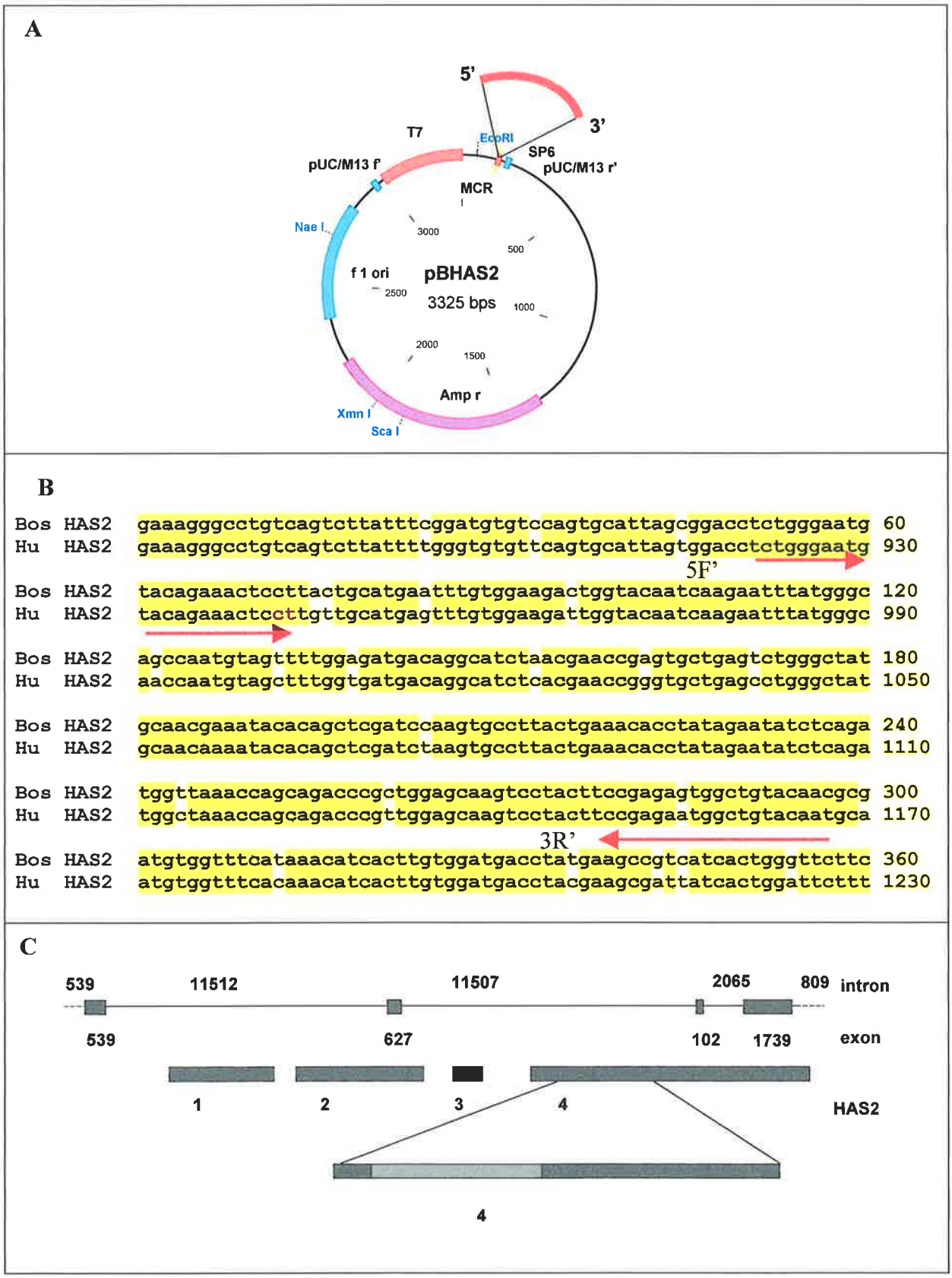

Figure 52 Image A: Plasmid map for HAS 2, Image B Alignment of Bos taurus HAS 2 sequence with Human HAS 2 sequence, showing sequence homology (yellow box) and forward and reverse primer sequence positions, C: schematic showing position of amplified HAS 2 sequence contained within exon 4 of the known Human sequence. Expected amplicon size was 310 bp. Start position bp53 exon 4, finish bp325 exon 4 of bovine sequence. Intron exon boundary marked by dotted line.

5.3.3.5 pInhibin/Activin βA

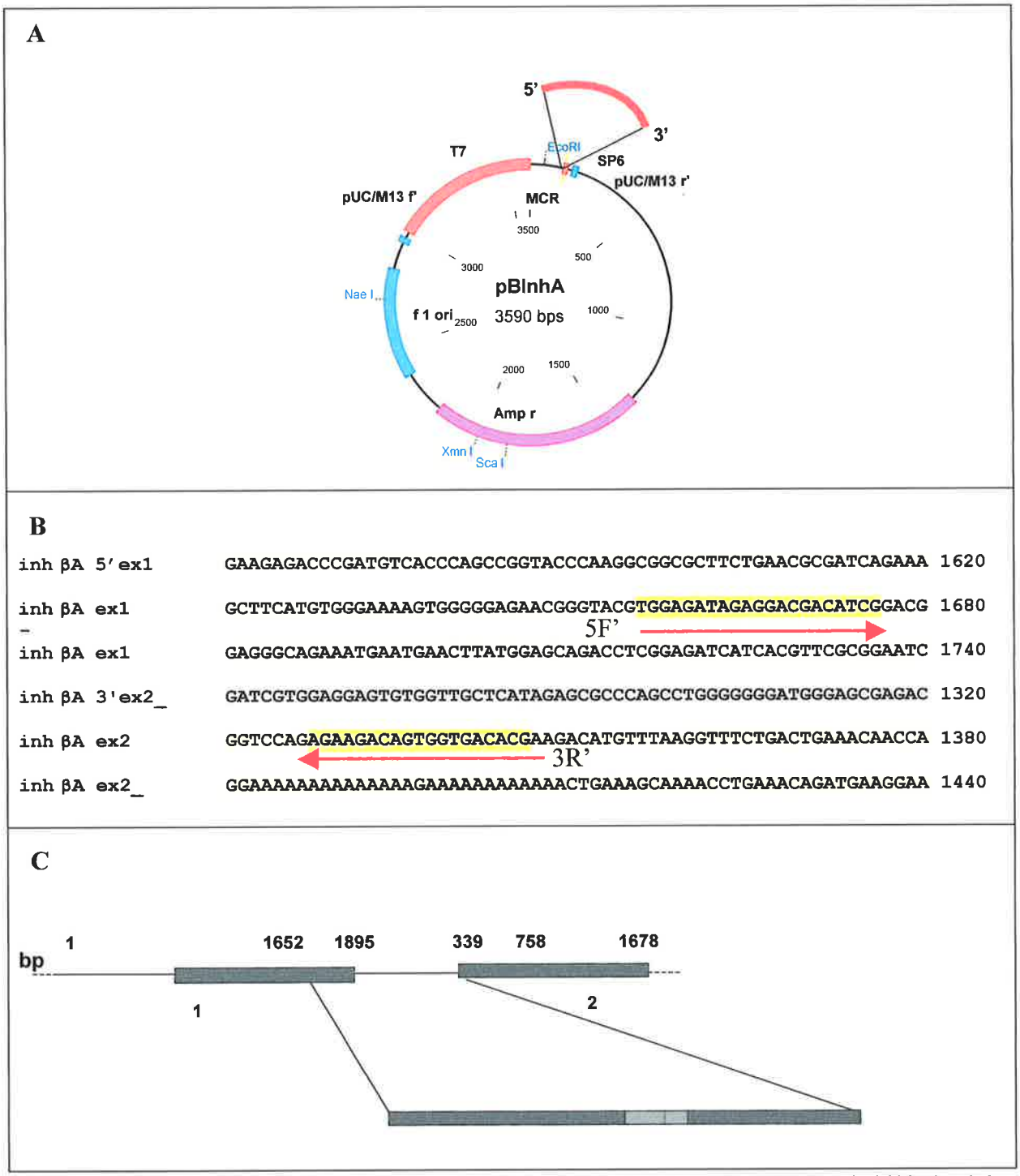

Figure 54 A: Plasmid map for Bos taurus inhibin/activin βA, B: Bos taurus inhibin/activin βA. Exon 1 sequence with 5'reverse primer indicated and Bos taurus inhibin/activin βA exon 2 sequence with 3'forward primer indicated. C: schematic showing position of amplified Bos taurus inhibin/activin βA sequence spanning exons 1 and 2 of the known Bos taurus sequence. Amplicon = bp 1652 to 1672 of exon 1 and bp 738 to 758 of exon 2. Intron exon boundary marked by dotted line.

5.3.3.6 P450 Map and Sequence

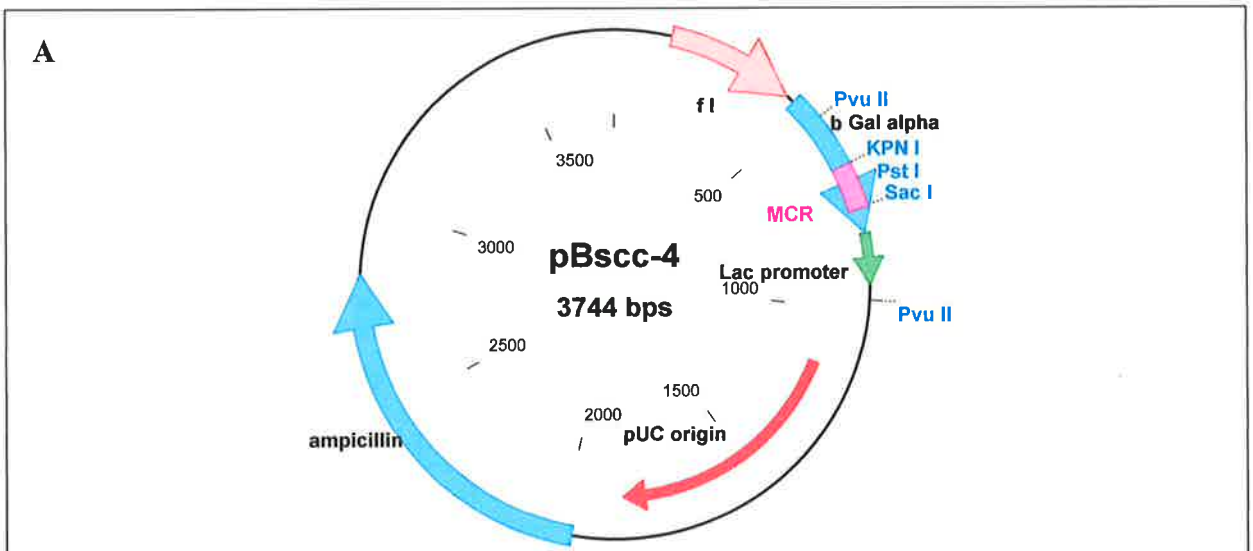

B

```
BosP450scc      ACTAAGTCCTGTCCGACTCTTTTGCGACTCCATAGACTGTAGCCCACC----AAGCTCCT 356
BosP450scc      CTGTCCATGGGATTTTTCTAGGCAAGAATACTGGAGTGGGTTGCCATTTCCTTCTCCCTG 416
BosP450scc      GG--ATCTTCCTA-ACCCAAG--GACTGAACCCTTGTCTCCTGCATTGCAGGTGGATTTT 471
                ---------->  5F'
BosP450scc      TTACCGACTGAGCCACCAGGGAAGTTATGTGTGCAAGAATCCGGGGTCATGGAAATTTTC 531
BosP450scc      CCTTAGATATACATCGTATCTAGGGACCAGTACAATGCAAATGCTTCC----TGTTTTTC 587
BosP450scc      TTCATCCTGAAGTCTCCTCAGGGTGCAT-TGAGGGAGGGAGTCCCCTC-AGGTGGGTGAC 645
BosP450scc      CACAGTGGCTGACGCTTGATGTTGTAGAACTGGAATGATGGGTTACATTCTTTCGTTTAC 705
BosP450scc      AGTACTGAGTCTGGGAGGAGCTGTGTGGGCTGGAGTCAGCCGGAGGAGGCTGACCGCCCT 765
BosP450scc      GTCAGCTTCTCACTTAGCCTTGAGCTGGTGATTATAAGCTGGGTCCCAGGGTCCCAGGGC 825
Bos             CAGA--GTCACCTGCTGCAGTACGAGCAGAGACAGCAGCAGCTGTGGGGGCAGCATGCTA 883
                <----------  3R'
```

Figure 55 A: original pBscc-4 plasmid containing 550 bp P450scc insert in the multiple cloning region (MCR). B: Inserted region of P450scc with start and finish positions marked by arrow. Amplicon size = 550bp.

5.3.3.7 pOLGAPDH Map and Sequence

A

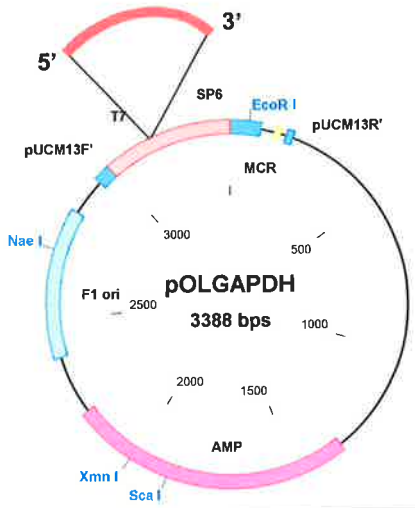

B

```
BTGAPDH    GGGTCATCATCTCTGCACCTTCTGCCGATGCCCCCATGTTTGTGATGGGCGTGAACCACG 376
OL GAPDH   GGGTCATCATCTCAGCCCCCTCCKCCGATGCCCCCATGTTTGTGATGGGCGTGAACCACG 480
                                                          5F'

BTGAPDH    AGAAGTATAACAACACCCTCAAGATTGTCAGCAATGCCTCCTGCACCACCAACTGCTTGG 436
OL GAPDH   AGAAGTATGACAACTCTCTCAAGATTGTCAGCAACGCATCCTGCACCACCAACTGCTTAG 540

BTGAPDH    CCCCCCTGGCCAAGGTCATCCATGACCACTTTGGCATCGTGGAGGGACTTATGACCACTG 496
OL GAPDH   CCCCCCTGGCCAAGGTCATCCACGACCACTTCGGCATTGTGGAGGGGCTCATGACCACGG 600

BTGAPDH    TCCACGCCATCACTGCCACCCAGAAGACTGTGGATGGCCCCTCCGGGAAGCTGTGGCGTG 556
OL GAPDH   TGCACGCCATCACTGCCACCCAGAAGACCGTGGACGGGCCCTCTGGGAAGCTGTGGCGTG 660

BTGAPDH    ACGGCCGAGGGGCTGCCCAGAATATCATCCCTGCTTCTACTGGCGCTGCCAAGGCCGTGG 616
OL GAPDH   ACGGCCGCGGGGCCGCCCAGAACATCATCCCTGCCTCCACTGGCGCTGCCAAGGCCGTGG 720

BTGAPDH    GCAAGGTCATCCCTGAGCTCAACGGGAAGCTCACTGGCATGGCCTTCCGCGTCCCCACTC 676
OL GAPDH   GCAAGGTCATCCCCGAGCTGAACGGGAAACTCACTGGCATGGCCTTCCGTGTGCCCACCC 780

BTGAPDH    CCAACGTGTCTGTTGTGGATCTGACCTGCCGCCTGGAGAAACCTGCCAAGTATGATGAGA 736
OL GAPDH   CCAACGTGTCGGTCGTGGACCTGACCTGCCGCCTGGAGAAAGCTGCTAAGTATGACGACA 840
                                                          <-

BTGAPDH    TCAAGAAGGTGGTGAAGCAGGCGTCAGAGGGCCCTCTCAAGGGCATTCTAGGCTACACTG 796
OL GAPDH   TCAAGAAGGTGGTGAAGCAGGCATCCGAGGGCCCCCTGAAGGGCATCCTGGGCTACACCG 900
           ------- 3R'
```

Figure 56 A: Plasmid map of pOLGAPDH used in the preparation of GAPDH probes. B: sequence alignment of Bos taurus GAPDH and Oryctolagus cuniculus GAPDH to show high homology of sequence (yellow box) used in probes for Bos taurus sequence amplification and position of primers used.

Quantification of the DIG probes was done using a dot blot assay using an anti – DIG-alkaline phosphatase antibody as described in the methods in Chapter 2. The quantitation of the probes showed that 10- 100 pg/μl of probe could be detected by this method.

5.3.4. In Situ hybridisation

5.3.4.1. Introduction

Tissues for in situ hybridisation assays were prepared as described in Chapter 2. The tissues chosen for assay were those reported to have some reactivity to each of the probes used (eye (Usui *et al.*, 1999), skin (Ramsden *et al.*, 2000), lung (Underhill *et al.*, 1993), colon (Wang *et al.*, 1996), bone growth plate (Waddington *et al.*, 1994). HAS signals are generally best observed in foetal tissues (Toole, 2001) and so tissues were sourced from a 100 - day old bovine foetus as controls. In order to determine the expression levels of HAS, follicles from primordial to 15 mm diameter were assessed for the message for HAS 1, 2 and 3 with both healthy and atretic follicles > 2 mm investigated. A full description of tissue and follicular localisation of message for the three hyaluronan synthases and controls for thecal health (P450scc) and granulosa cell health (inhibin/activin βA) can be seen below.

NB: Sense controls were not counterstained and were photographed with minimal phase contrast to show the real degree of negative staining. Staining these negative sections would have made distinction between positives and negatives more difficult when photographed/printed in black and white as was done here.

5.3.4.2. Cytochrome P450 Cholesterol Side Chain Cleavage

No staining was seen in either granulosa cell or theca cell layers of any of the primordial, primary, secondary and early antral follicles (Figure 58). The first evidence of staining was seen in the theca interna of the follicles of size 2 - 4 mm (Figure 57). In healthy follicles there was clear staining of approximately 40% of the theca interna cell population. This staining was localised to the cytoplasm and appeared to be more concentrated in those layers of the theca interna close to the basal lamina. In atretic follicles there was staining of the theca interna similar to that seen with the healthy follicles and this staining was slightly weaker also there appeared to be some staining of the theca externa in some more advanced atretic follicles. Once again the staining appeared to be localised within the cytoplasm although there was also some staining of nuclear material.

In healthy follicles of size 6 - 8 mm (Figure 57) the localisation of the p450scc signal was to the theca interna with additional localisation seen in some of the granulosa cells. The staining within the theca interna appeared strongest within the cells more closely aligned with

the basal lamina with approximately 60 - 70% of cells were positive at this level. Once again the staining was seen within the cytoplasm of the above cells.

In atretic follicles of size 6 - 8 mm (Figure 58) the staining was similar to that seen in healthy follicles, with the exception of what appeared to be leakage in to those theca externa layers closest to the theca interna. Again the staining was cytoplasmic with some apparent nuclear staining. It was considered that the nuclear staining seen may have been an artefact of the sectioning, in that the staining was in fact cytoplasmic but since it lay in section above, the staining appeared to be nuclear in origin.

In large healthy follicles of size 12 - 15 mm (Figure 58) the localisation of the P450scc appeared to be solely within the theca interna with approximately 40% of cells being positive. No staining was seen in the granulosa cells within the follicular antrum. In these theca interna cells the staining was clearly localised with the cytoplasm of the cells.

In atretic follicles of the 12 - 15 mm range the theca interna was stained most strongly however; some of the granulosa cell population were also stained. In both these sets of cells the localisation of the staining was mainly within the cytoplasm with some indication of nuclear staining.

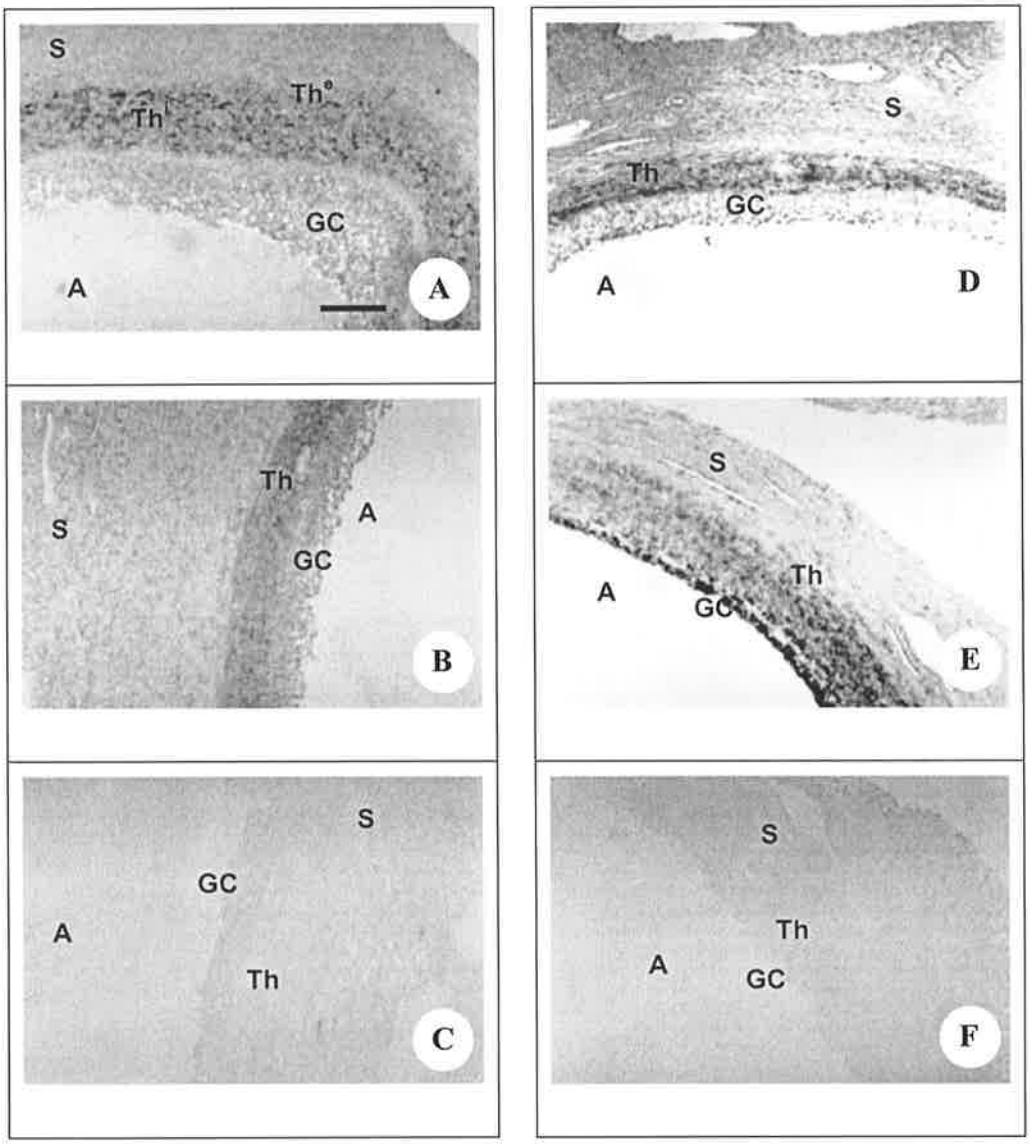

Figure 57 In situ hybridisation to follicles using the P450scc probe and localisation of the P450scc message. A and B show the results of in situ hybridisation in healthy 2 - 4 mm follicles. C: is the sense control. D and E show the localisation to 6 – 8 mm follicles. F: sense control. Bar = 150 µm for images A – F. A denotes the antrum, S denotes the stroma, GC denotes granulosa cell, Th denotes the thecal layers, Th^i denotes theca interna layer, Th^e denotes theca externa layer. NB: sense controls were not counterstained.

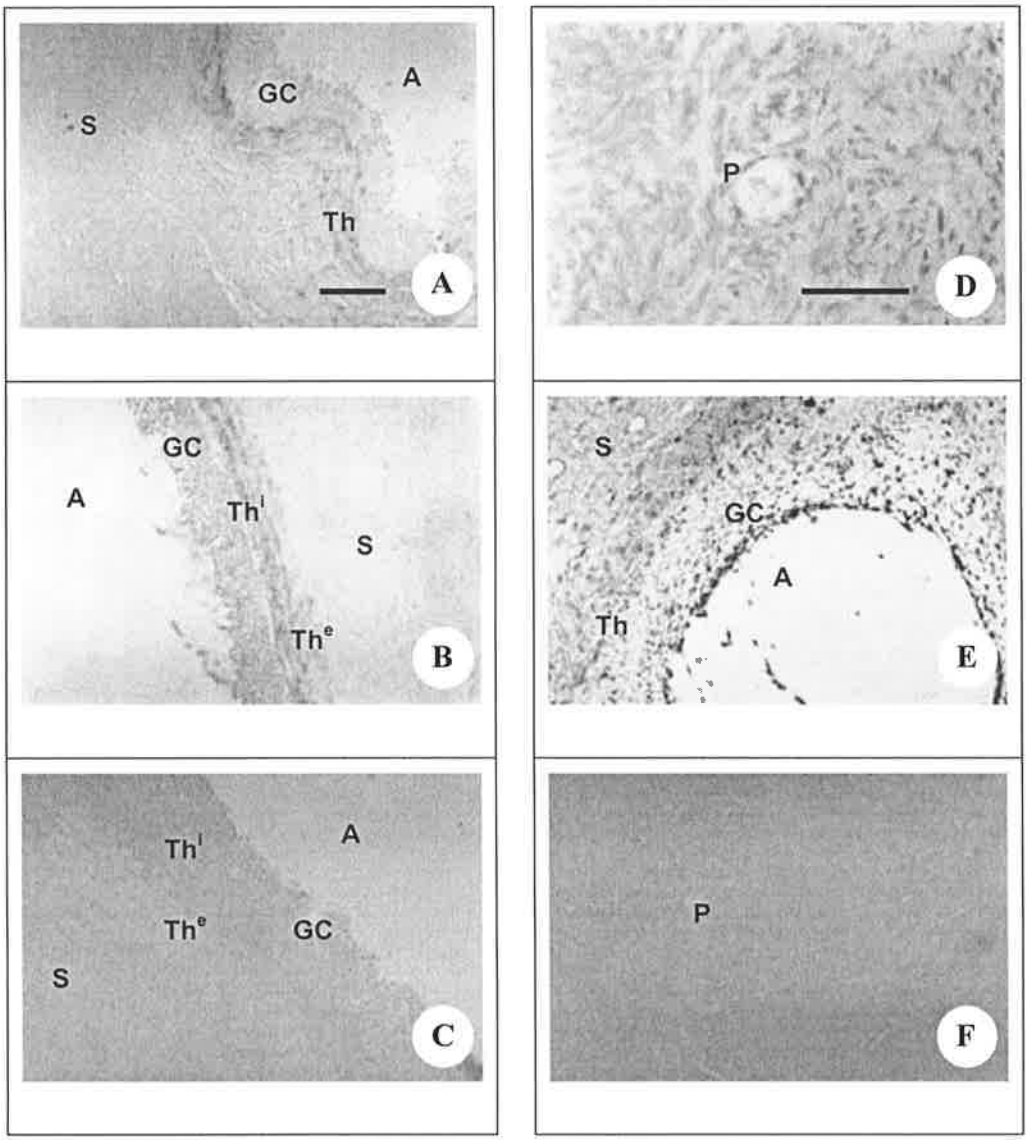

Figure 58 In situ hybridisation to follicles of the P450scc probe. A and B show the results of in situ hybridisation to healthy 12 – 15 mm follicles. C: sense control. D, E and F show the results obtained in primordial and primary follicles, atretic follicle, and corpora lutea respectively. Note no staining is seen in the early stage follicles. Bar = 300 µm images A and B, = 150 µm images C, E and F, = 25 µm image D. A denotes the antrum, S denotes the stroma, GC denotes granulosa cell, Th denotes the thecal layers, Th^{i} denotes theca interna layer, Th^{e} denotes theca externa layer, P denotes position of primordial follicle. NB: sense controls were not counterstained.

5.3.4.3. Inhibin/Activin βA

The messenger RNA for Inhibin/Activin βA could not be detected within primordial follicles (Figure 60). In primary follicles there was some weak staining noted within the granulosa cells (Figure 60). This staining was cytoplasmic but it was noted that not all cells were positive and as mentioned, the signal was weak. In secondary follicles the granulosa cells showed some degree of message for inhibin/activin βA but once again levels appeared low with localisation to the cytoplasm. In secondary follicles the staining pattern resembled that noted above with weak staining of the granulosa cells.

In early antral follicles staining was noted in the granulosa cells and thecal cells of the follicles. This staining appeared strong with the strongest reactivity seen in the granulosa cells. The staining in all cases was localised to the cytoplasm (Figure 60).

In healthy follicles of size 2 - 4 mm (Figure 59) the localisation of message for inhibin/activin βA was similar to that noted within the early antral follicles. The staining pattern appeared strongest within the cytoplasm of the granulosa cells and within this group the stronger stain was noted within the granulosa cells closest to the basal lamina. Some staining of red blood cells was also noted. Atretic follicles (Figure 60) of the same size (2 - 4 mm) also stained positive for inhibin/activin βA. In this case the antral granulosa cells were most strongly stained within the basally atretic follicles while the basal granulosa cells were the most strongly stained within the antrally atretic follicles. It is believed that this maybe an artefact, and result from accumulation of stain in small acellular areas of the follicle.

Healthy follicles of 6 - 8 mm (Figure 59) in size exhibited staining solely within the granulosa cells. This staining was distributed evenly between the granulosa cells although the apparent increase in density of the granulosa cells in proximity to the basal lamina gave an overall appearance of the stain being greater in these cells. In atretic follicles of the same size the staining was identical to that seen in the healthy follicles. In both cases the localisation of staining seen was within the cytoplasm with some weaker stain seen within the nucleus.

In healthy follicles of 12 - 15 mm staining was localised within the granulosa cells. Those granulosa cells associated with the oocyte were more weakly stained than antral granulosa cells and those attached to the basal lamina. In all cells the nuclear staining appeared stronger than noted previously. In comparison the cytoplasmic staining reduced. In atretic follicles of the same size the granulosa cells were stained positively but to a lesser degree than that seen within the healthy follicles. Additionally the staining within the nucleus was more pronounced than that seen in the healthy follicles.

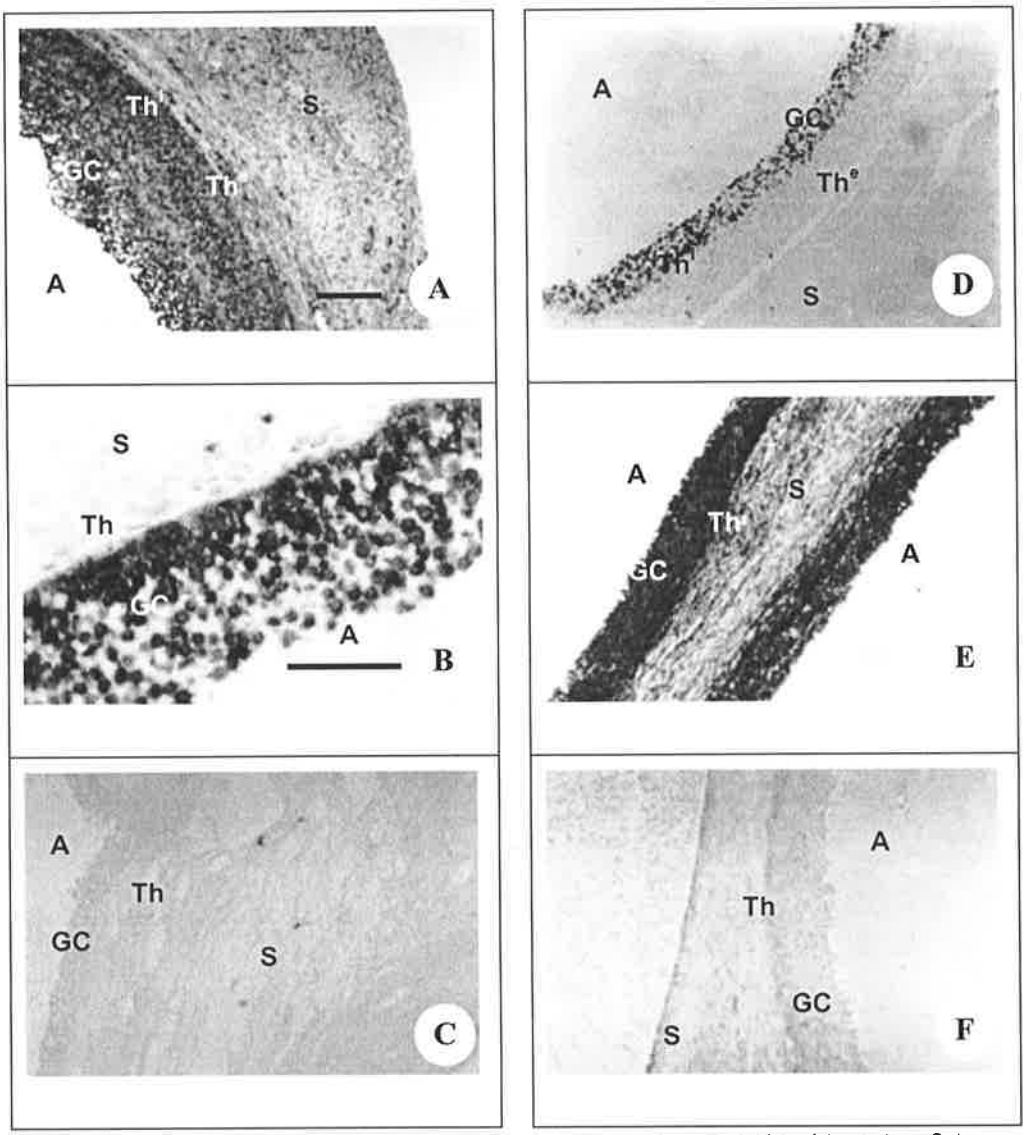

Figure 59 In situ hybridisation to follicles using the Inhibin/Activin βA probe and localisation of the Inhibin/Activin βA message. A and B show the localisation to healthy 2 - 4 mm follicles. C: sense control. D and E show the localisation to 6 – 8 mm. F: sense control. Bar = 150 µm images A, D, C and F, = 50 µm images B and E. GC denotes granulosa cell, Th^i denotes theca interna layer, Th^e denotes theca externa layer. A denotes the antrum, S denotes the stroma, Th denotes the thecal layers, NB: sense controls were not counterstained.

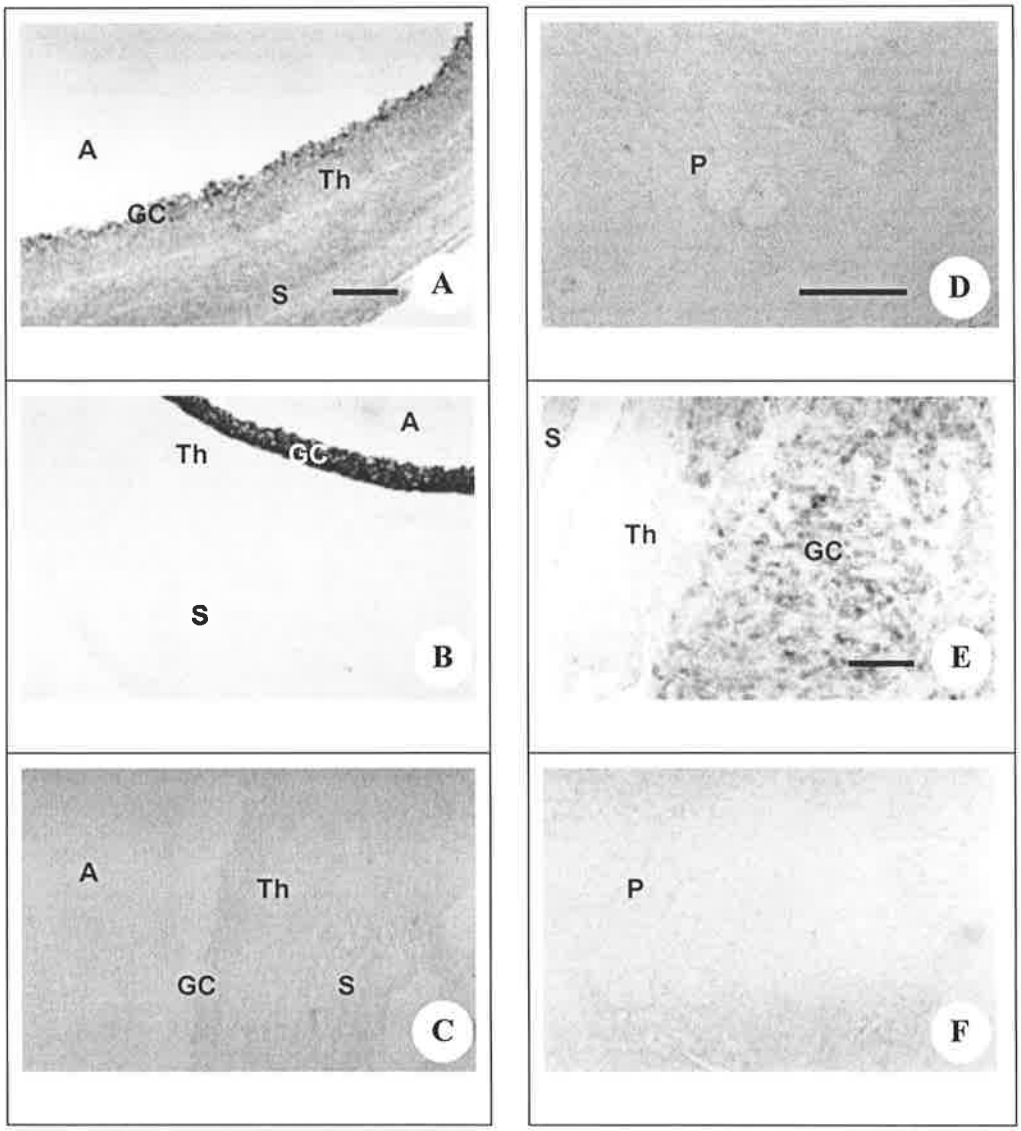

Figure 60 In situ hybridisation to follicles of the Inhibin βA probe. A and B show the localisation to 12 – 15 mm follicles. C: sense control. D, E and F show the result of in situ hybridisation in primordial and primary follicles, atretic follicle, and corpora lutea respectively. Bar = 300 µm images A, B and C, = 150 µm images E and F, = 25 µm image D. A denotes the antrum, S denotes the stroma, GC denotes granulosa cell, Th denotes the thecal layers, Th^i denotes theca interna layer, Th^e denotes theca externa layer, P denotes position of primordial follicle. NB: sense controls were not counterstained.

5.3.4.4. Tissue Localisation of HAS 1, HAS 2 and HAS 3

The tissues examined were taken from adult bovine eye (ciliary process and cornea) and the bovine foetal tissues of skin, hoof and colon. These tissues were used as controls for the HAS probes based upon previous reports in the literature (Nishida *et al.*, 2000, Sayo *et al.*, 2002, Sugiyama *et al.*, 1998, Usui *et al.*, 1999, Wang *et al.*, 1996). HAS 1 was not localised within the foetal eye but was positively located to the colonic epithelial cells, minimal areas of the growth plate region of the hoof and epidermal layers of the skin (Figure 61 and Figure 62). HAS 2 was localised to the anterior ciliary process within the bovine eye and to the epithelial cells of the foetal colon. The area of positive staining in the foetal hoof was again within the growth plate region of that tissue. The area stained incorporated more of the growth plate than was involved with the HAS 1 probe and the intensity of the staining approximately 3-fold greater. The localisation within the skin was to the epidermal layers and to the skin sweat gland (Figure 63 and Figure 64).

Observations of the HAS 3 localisation patterns within the tissues showed that it was similar to that seen with the HAS 2 probe in the ciliary area of the eye. In addition the corneal endothelial cells were positively stained. In the foetal hoof the staining pattern again resembled that of HAS 2 as it did with all other tissues examined (Figure 65 and Figure 66). In situ hybridisation to tissues of inhibin/activin βA and P450scc were also carried out and localisation of message was consistent with that indicated in the literature (data not shown).

Since all probes gave positive signals in the cell types of the tissues indicated in the literature the authors were therefore confident of their specificity.

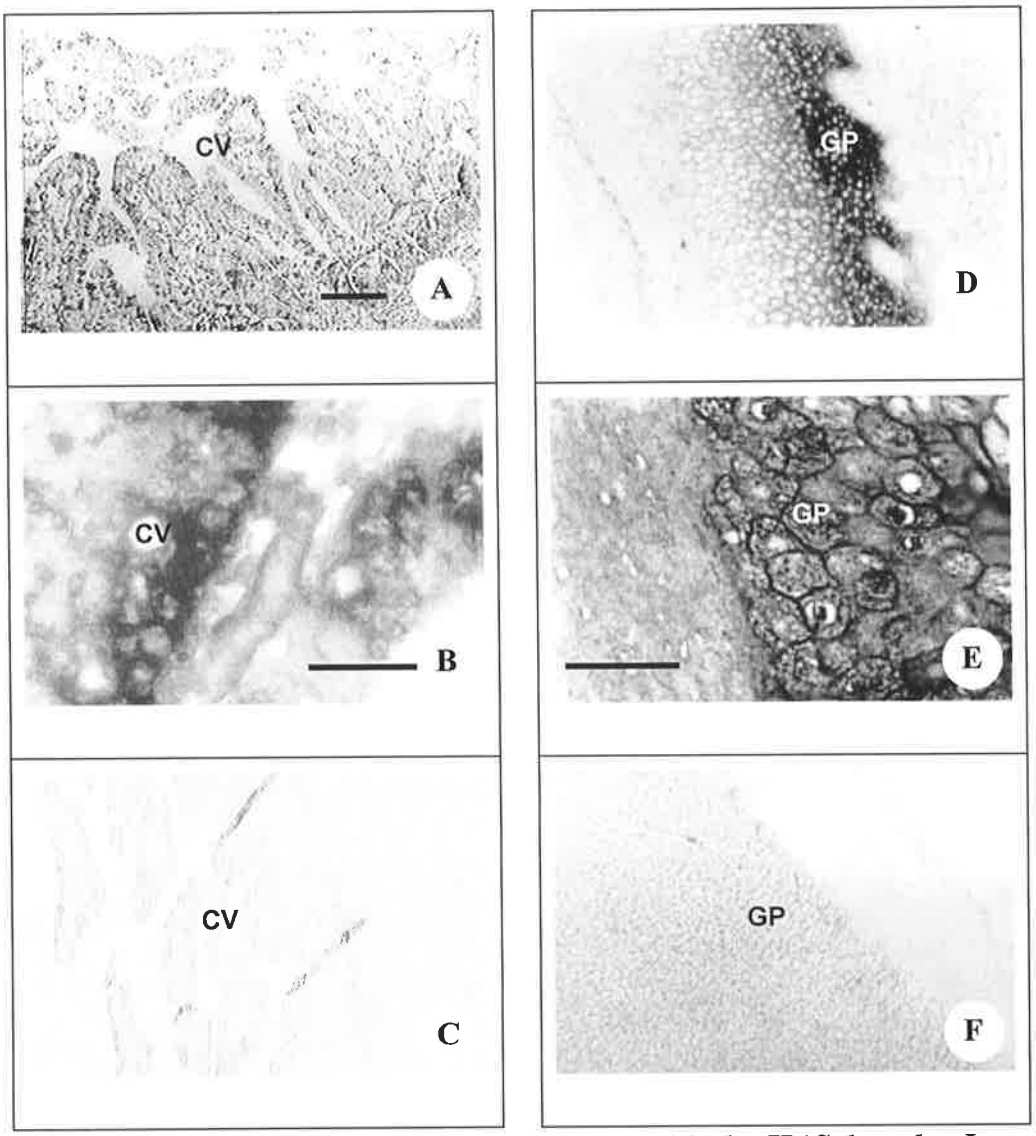

Figure 61 In situ hybridisation to bovine foetaltissue with the HAS 1 probe. Images A, B and C show the localisation within the foetalcolon (A, B) and the sense control (C). Images D, E and F show the localisation within the foetalhoof or growth plate (A, B) and the sense control (F). Bar = 150 µm images A, D, C and F, = 50 µm image E, = 25 µm image B. CV denotes colonic villus, GP denotes growth plate region.

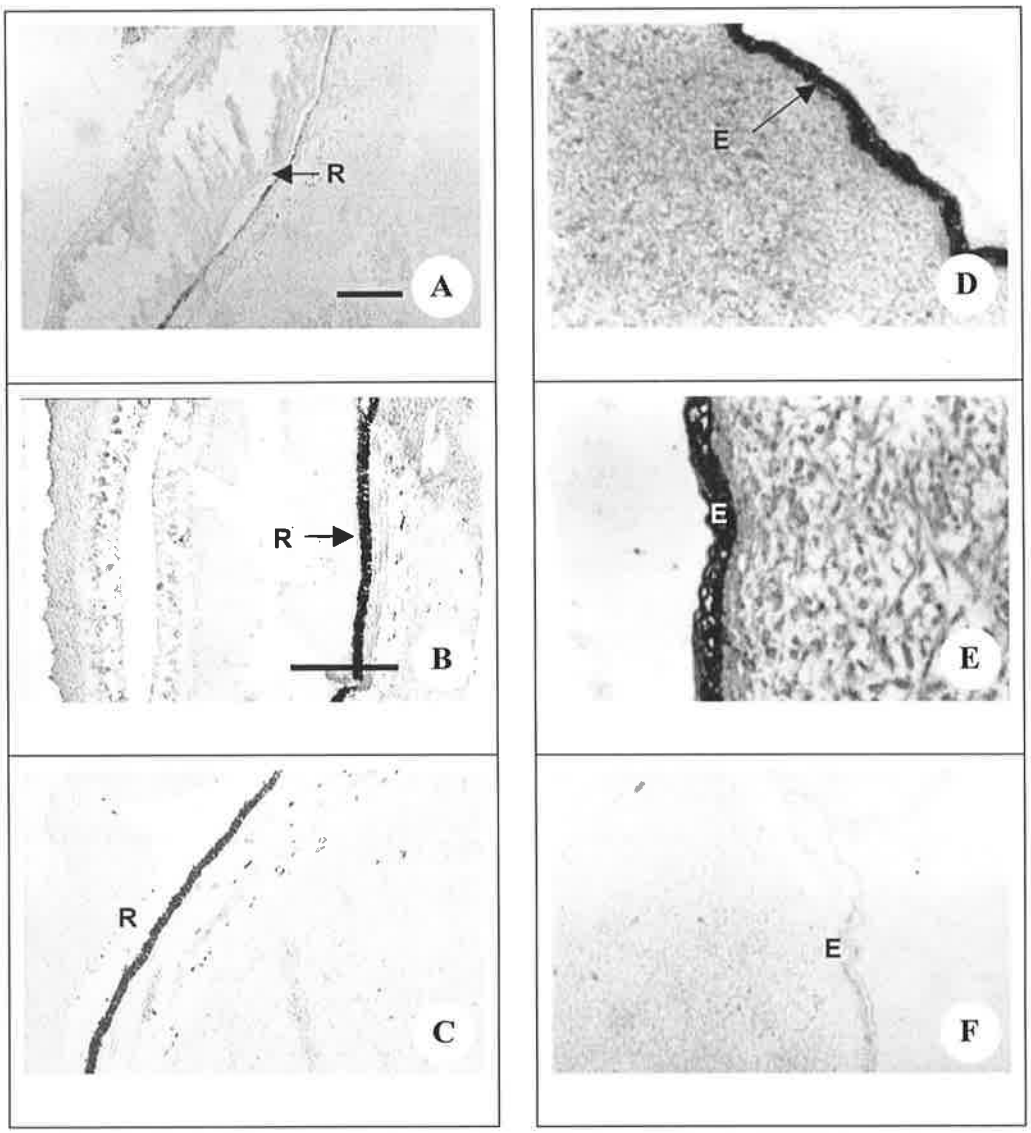

Figure 62 In situ hybridisation to bovine foetaltissue with the HAS 1 probe. Images A, B and C show localisation within the foetaleye (A, B) and the sense control (C). Images D, E and F show localisation within the foetalskin (A, B) and the sense control (F). Bar = 150 µm images A, D, C and F, = 25 µm image B and E. R denotes position of retina, showing cones and rods of the eye containing the retinoid pigment. E shows the position of the epidermal layer in the skin.

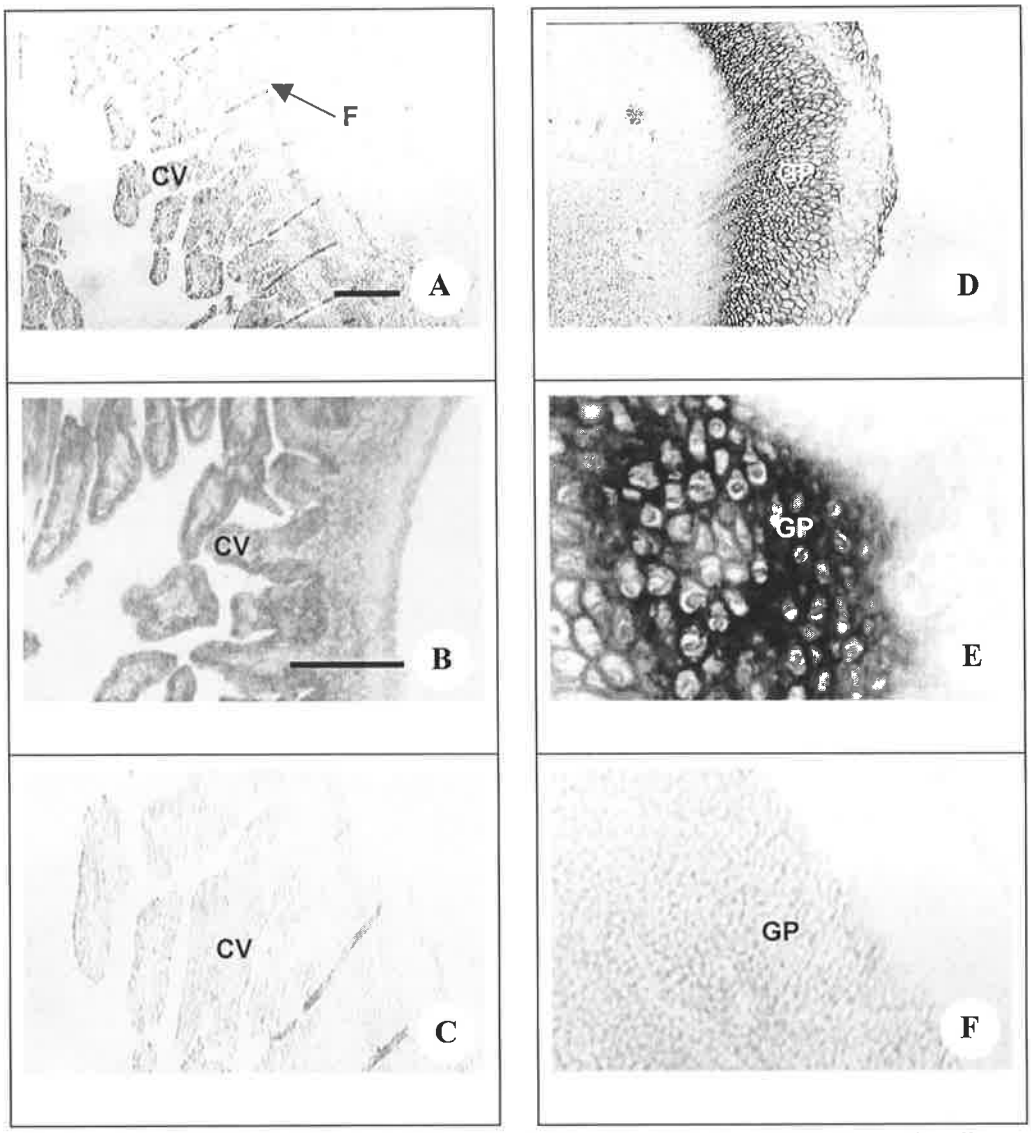

Figure 63 In situ hybridisation to bovine foetaltissue with the HAS 2 probe. Images A, B and C show localisation within the foetalcolon (A, B) and the sense control (C). Images D, E and F show localisation within the foetalhoof or growth plate region (A, B) and the sense control (F). Bar = 150 µm images A, D, C and F, = 50 µm images B and E. F shows the position of a fold in the tissue section. CV denotes colonic villus, GP denotes growth plate region.

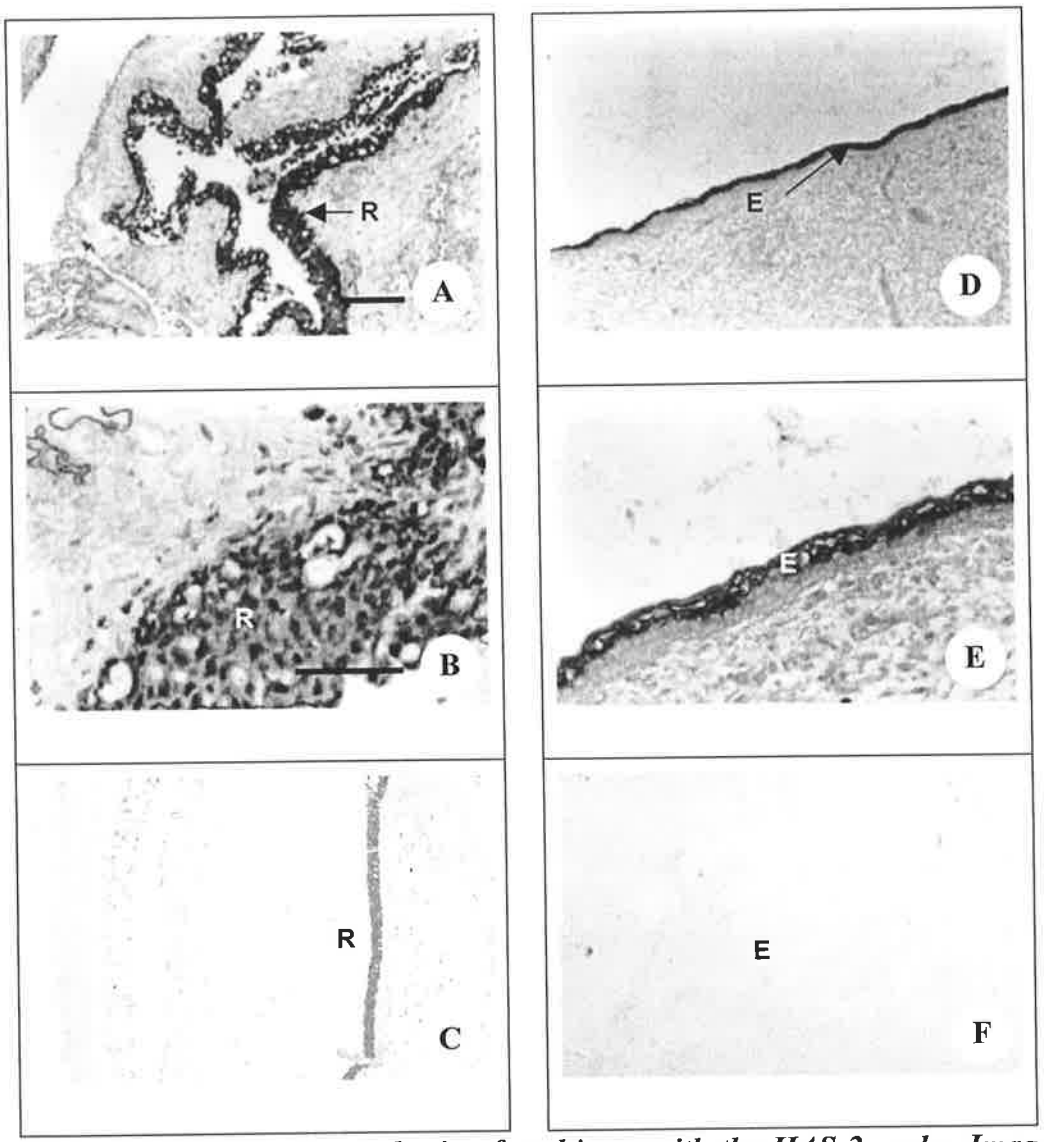

Figure 64 In situ hybridisation to bovine foetaltissue with the HAS 2 probe. Images A, B and C show localisation within the foetaleye (A, B) and the sense control (C). Images D, E and F show localisation within the foetalskin (A, B) and the sense control (F). Bar = 150 µm images A, D, C and F, = 25 µm images B and E. R denotes position of retina, showing cones and rods of the eye containing the retinoid pigment. E shows the position of the epidermal layer in the skin.

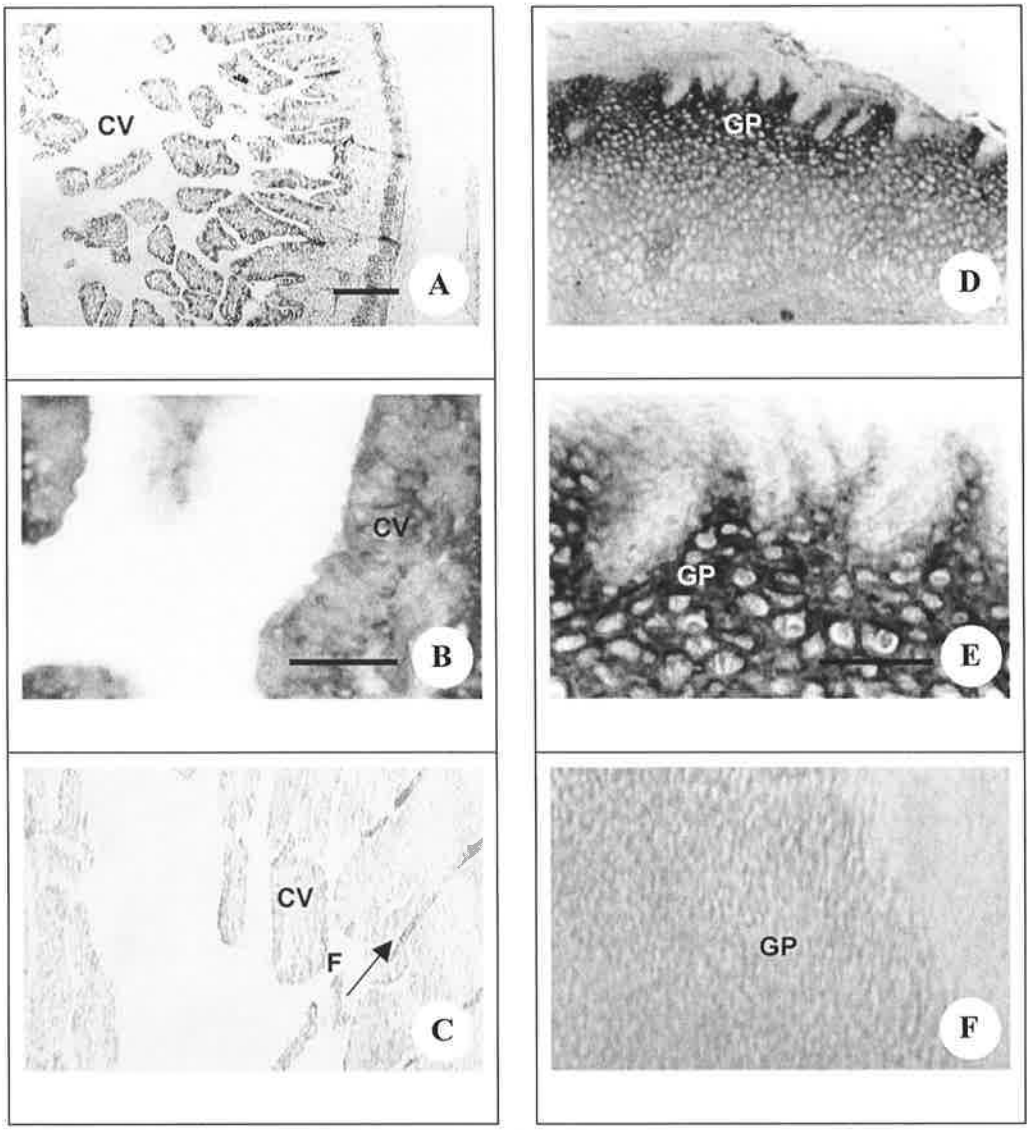

Figure 65 In situ hybridisation to bovine foetaltissue with the HAS 3 probe. Images A, B and C show localisation within the foetalcolon (A, B) and the sense control (C). Images D, E and F show localisation within the foetalhoof or growth plate region (A, B) and the sense control (F). Bar = 150 µm images A, D, C and F, = 50 µm image E, = 25 µm image B. CV denotes colonic villus, GP denotes growth plate region. F shows the position of a fold in the tissue section.

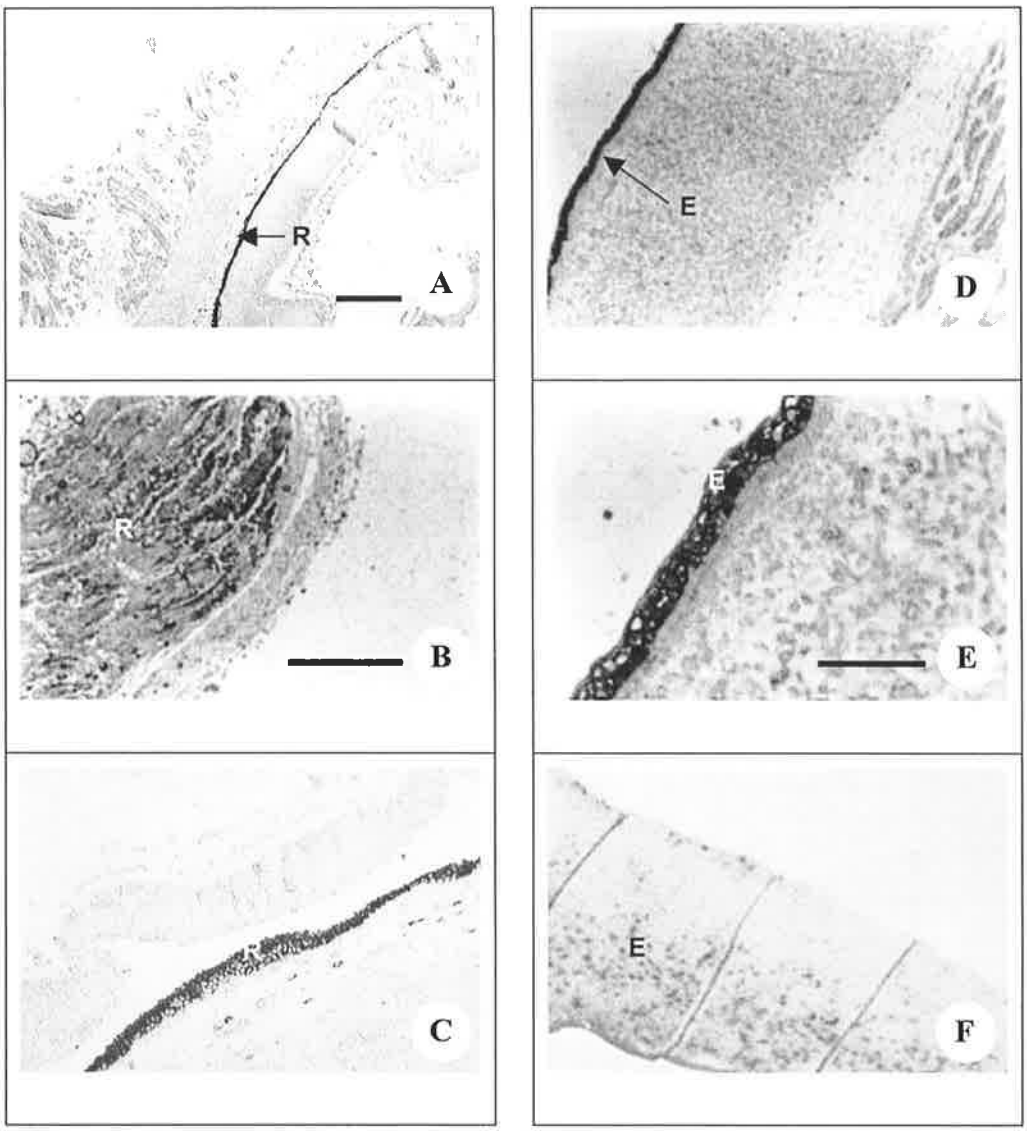

Figure 66 In situ hybridisation to bovine foetaltissue with the HAS 3 probe. Images A, B and C show localisation within the foetaleye (A, B and the sense control (C). Images D, E and F show localisation within the foetalskin (A, B) and the sense control (F). Bar = 150 µm images A, D, C and F, = 50 µm image B, = 25 µm image E. R denotes position of retina, showing cones and rods of the eye containing the retinoid pigment. E shows the position of the epidermal layer in the skin.

5.3.4.5. Follicular Localisation of Hyaluronan Synthase 1 (HAS 1)

The localisation of message for HAS 1 in primordial follicles was seen in approximately 50% of follicles viewed (Figure 70). Close observation showed that this localisation was in the cytoplasm of the granulosa cells. Primary follicles showed weak staining of granulosa cells at approximately 3 times greater than background level and this was noted in 60 - 70% of the follicles (Figure 70). This staining was restricted to the cytoplasm.

In secondary follicles nearly all follicles showed strong positive staining within the cytoplasm of the granulosa cells. In early antral follicles this positive staining pattern was seen in both granulosa cells and theca cells present (Figure 70). It was noted that the endothelial cells of associated blood vessels also stained positively for HAS 1. Healthy follicles of 2 - 4 mm in diameter had very strong staining localising to the granulosa and thecal layers of the follicle (Figure 67). In follicles defined as being healthy columnar, the granulosa cells closest to the basal lamina of columnar appearance showed clear staining within the cytoplasm with apparently no stain of the nucleus. In these cells and those in the two layers above them the staining appeared at its most intense compared with that seen in the rest of the granulosa cells. The basal lamina was clearly visible between the granulosa cell and theca interna layers due to the intense staining pattern of the surrounds and complete absence of stain in the basal lamina. Within the theca interna, patches of intense staining appeared in layers closest to the basal lamina, overall the staining was very strong throughout the theca interna. In the theca externa the pattern of staining was quite different to that of the theca interna with only a proportion of cells (between 20 and 30%) being positively stained. In late atretic follicles of 2 - 4 mm staining was either very weak or completely negative within the theca interna cells. In the granulosa cells the staining remained positive although the level was lower than that recorded in the healthy granulosa cell layers. In granulosa cell layers aligned with the basal lamina the staining was reduced further when compared to that seen in the more antral cells. In early atretic follicles the theca remained positively stained while the granulosa cell layer was weakly stained. Follicles identified as being basally atretic had positive staining within the theca interna and granulosa cells but it was of reduced intensity when compared to that of the healthy follicles. In all cases mentioned above the staining was localised to the cytoplasm with some light staining of the nuclei.

Healthy follicles of 6 - 8 mm in diameter showed staining in both the granulosa cells and theca interna of follicles examined, with the intensity of stain being greatest in the granulosa cell layers and thecal layers closest to the basal lamina and in the layers of the theca interna closest to the theca externa, where it was more patchy (Figure 68). As in the 2 - 4 mm follicles the basal lamina was clearly defined as a clear unstained line separating granulosa from theca cells. In atretic follicles of 6 - 8 mm in diameter showed staining in both the

granulosa cells and theca interna of follicles examined with the intensity of stain being greatest by 2 - 3 fold in the granulosa cells than the theca where the staining appeared to be in only half of cells present. Antral granulosa cell staining was of lower intensity than the more basally situated granulosa cells.

In the healthy follicles of the 12 - 15 mm diameter range the healthy follicles displayed varying patterns of localisation of message (Figure 69). In most follicles the 80 - 100% granulosa cells were stained positively with the intensity of stain being markedly reduced compared to that seen in the theca interna. However in some of these large follicles the granulosa cells were completely devoid of stain while the theca interna remained strongly stained. In most cases approximately 50% of the theca externa also showed some degree of staining. There appeared to be no difference in health status of the follicle between these two types of staining pattern. In atretic follicles of the same size 100% of granulosa cells and theca interna were stained strongly as seen in the healthy follicles but the intensity of staining within the theca interna was slightly less than that seen in their healthy compatriots. Minimal theca externa staining was noted. All localisation noted appeared cytoplasmic in nature.

Additionally it was noted that the endothelial cells of blood vessels were stained positively as were corpora lutea.

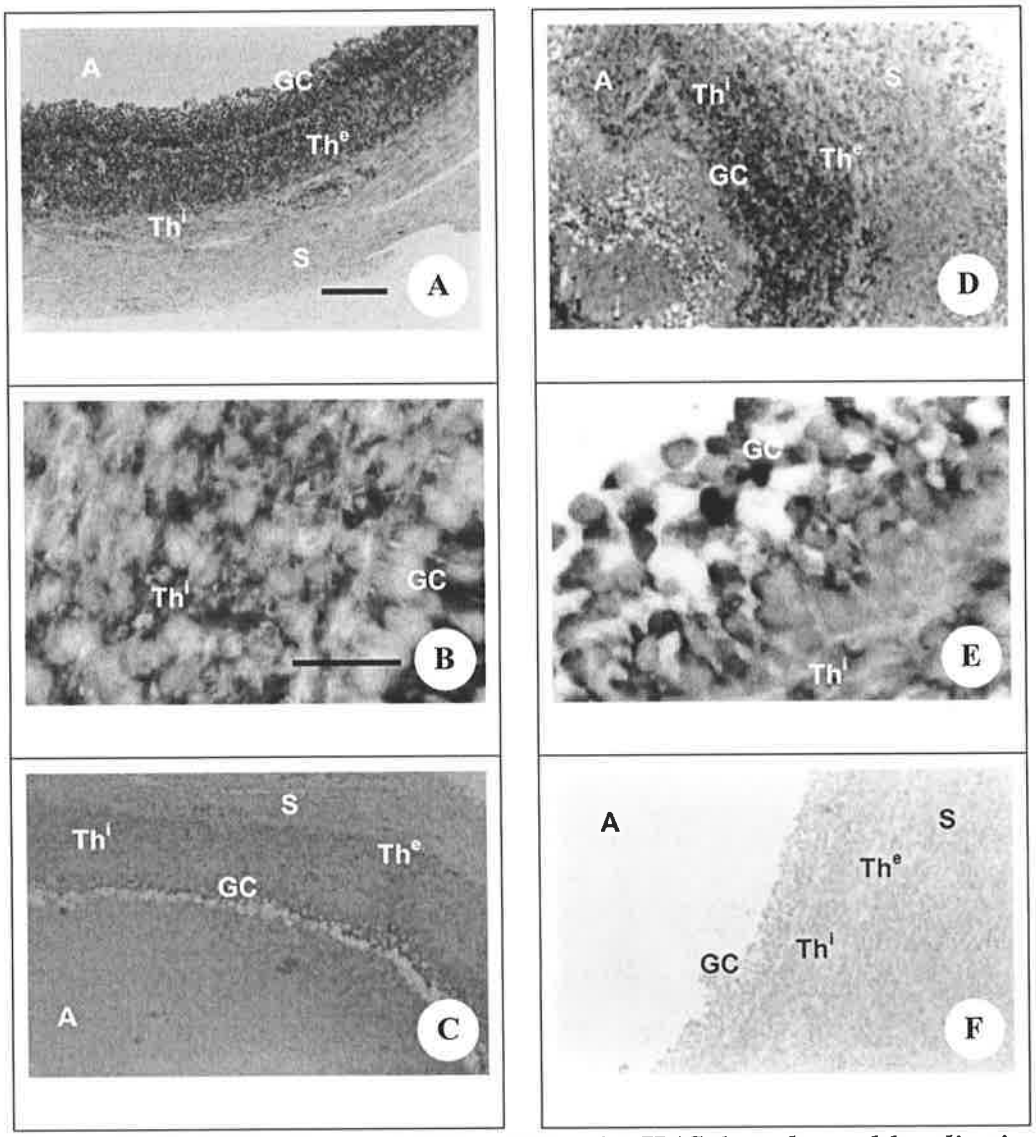

Figure 67 In situ hybridisation to follicles using the HAS 1 probe and localisation of the HAS 1 message. A and B show the result of in situ hybridisation to healthy 2 - 4 mm follicles. C: sense control. D and E show the localisation to atretic 2 - 4 mm follicles. F: sense control. Bar = 150 µm images A, D, C and F, = 25 µm images B and E. A denotes the antrum, S denotes the stroma, GC denotes granulosa cell, Th denotes the thecal layers, Th^i denotes theca interna layer, Th^e denotes theca externa layer. NB: sense controls were not counterstained.

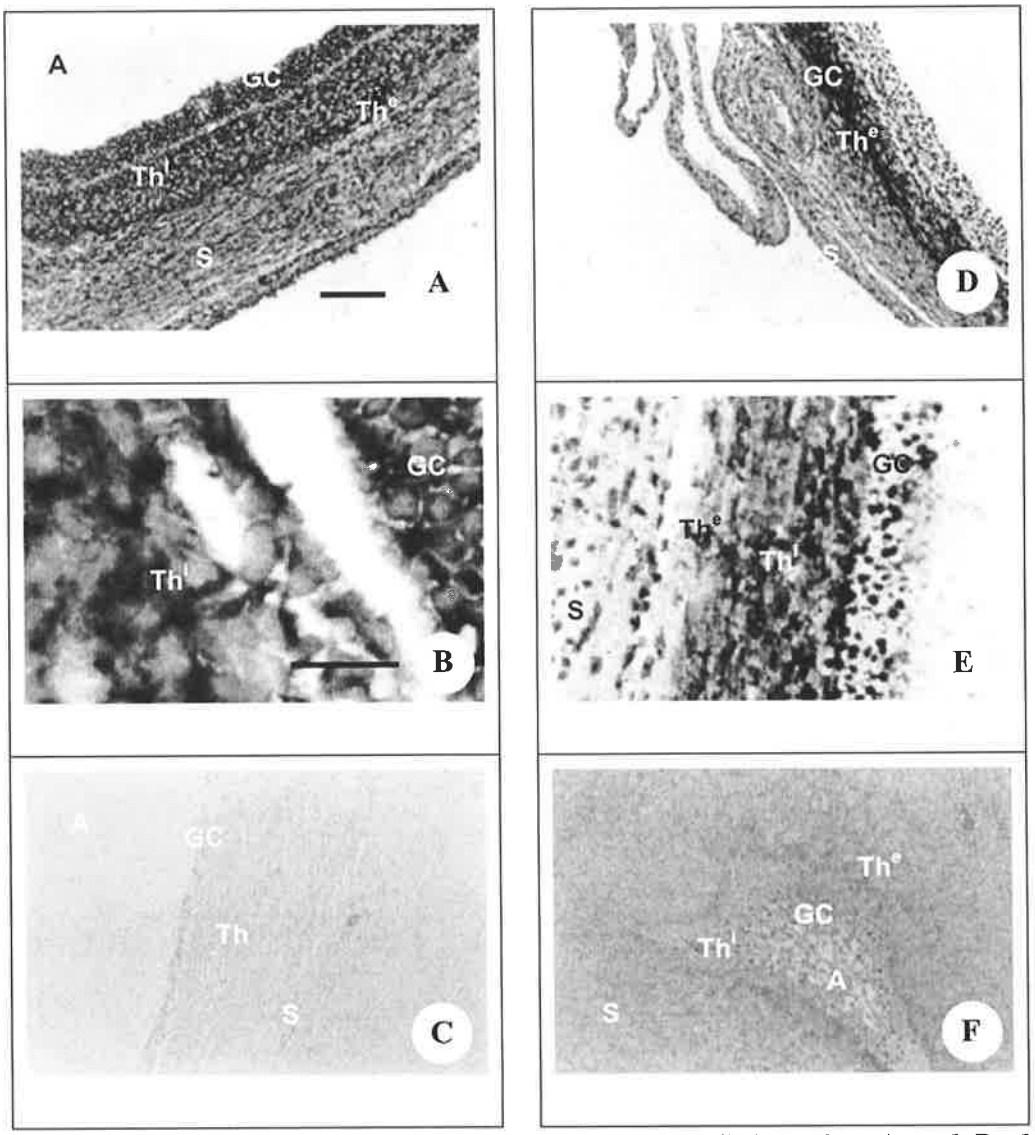

Figure 68 In situ hybridisation to follicles using the HAS 1 probe. A and B show the localisation to healthy 6 - 8 mm. C: sense control. D and E show the localisation to atretic 6 - 8 mm. F: sense control. Bar = 150 µm images A, D, C and F, = 25 µm images B and E. A denotes the antrum, S denotes the stroma, GC denotes granulosa cell, Th denotes the thecal layers, Th^i denotes theca interna layer, Th^e denotes theca externa layer. NB: sense controls were not counterstained.

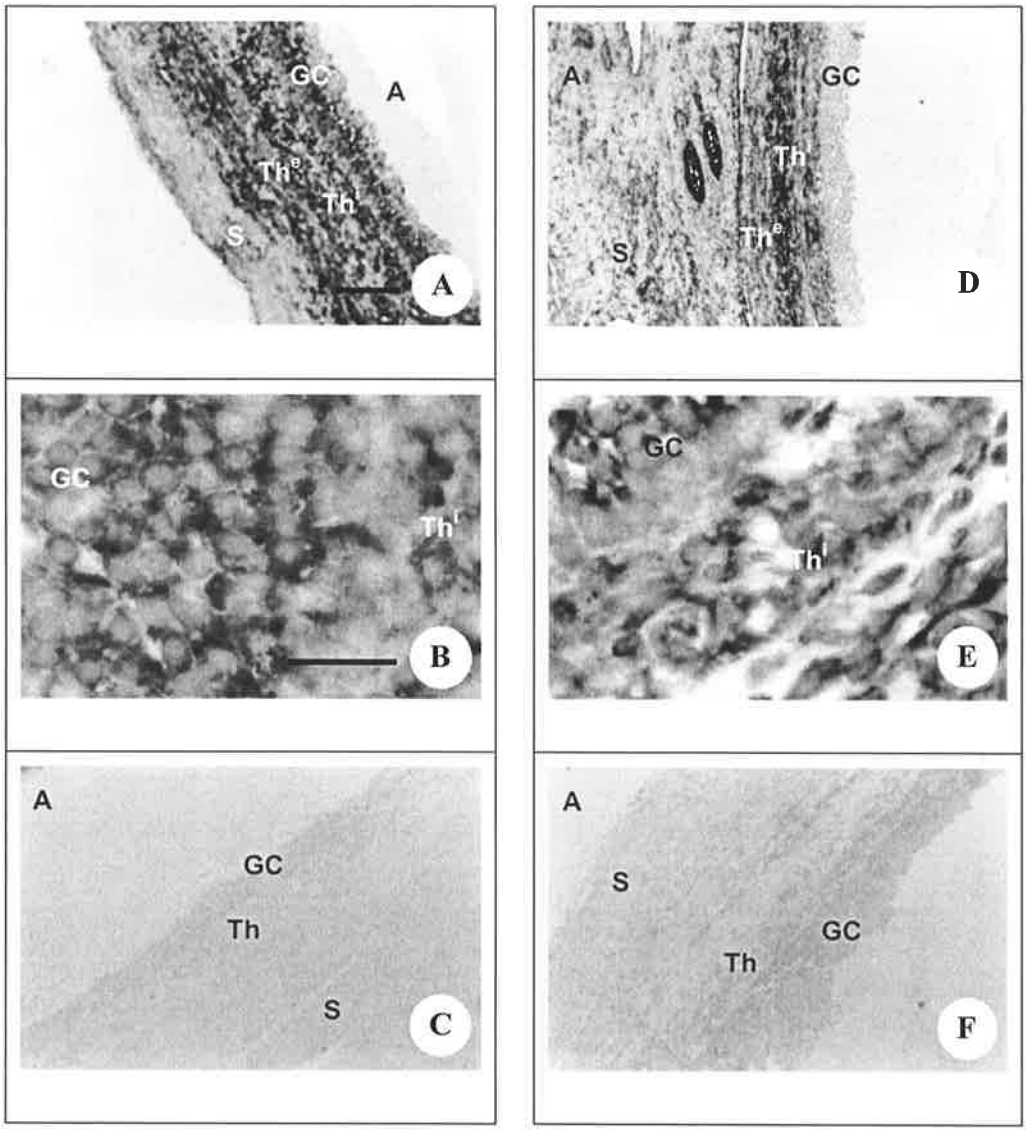

Figure 69 In situ hybridisation to follicles using the HAS 1 probe. A and B show the localisation to healthy 12 - 15 mm follicles. C: is the sense control. D and E show the localisation to atretic 12 - 15 mm follicles. F: sense control. Bar = 150 µm images A, D, C and F, = 25 µm images B and E. A denotes the antrum, S denotes the stroma, GC denotes granulosa cell, Th denotes the thecal layers, Th^i denotes theca interna layer, Th^e denotes theca externa layer. NB: sense controls were not counterstained.

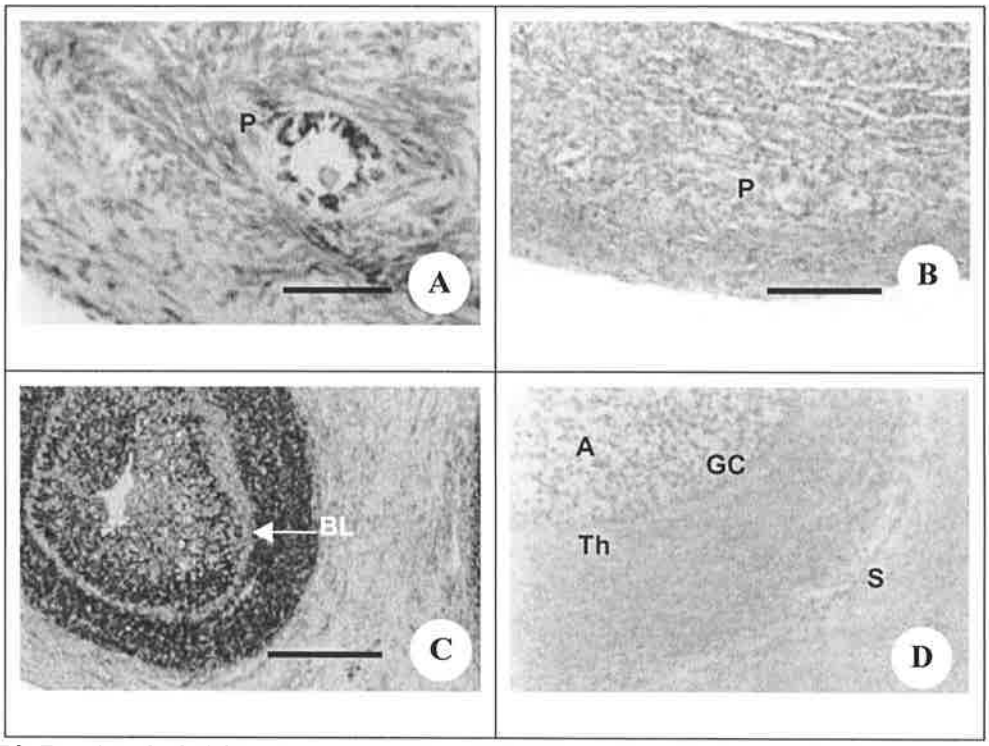

Figure 70 In situ hybridisation using the HAS 1 probe. A shows the localisation within primary follicles. C shows the localisation to an early antral follicle. B and D are the sense controls. The basal lamina (BL) can be seen as a clear line around the follicle between the granulosa and theca cells in C. Bar = 50 µm images B, C and D = 25 µm image A. A denotes the antrum, S denotes the stroma, GC denotes granulosa cell, Th denotes the thecal layers, Th^i denotes theca interna layer, Th^e denotes theca externa layer, P denotes position of primordial follicle. NB: sense controls were not counterstained.

5.3.4.6. Follicular Localisation of Hyaluronan Synthase 2 (HAS 2)

The message for HAS 2 was assayed in the same group of follicles used in the HAS 1 in situ hybridisations. In primordial follicles the message was present in the early granulosa cells of only 11% of follicles with the localisation being cytoplasmic (Figure 74). In primary follicles, again just 11% of follicles displayed a positive staining pattern, with 2 - 3 times background staining seen in the granulosa cells. In large secondary follicles granulosa cells were strongly stained in 42% of follicles examined, the localisation of the staining was cytoplasmic (Figure 74).

In early antral follicles staining was located within the granulosa cell layers of 72% of follicles with some weak staining noted in the theca interna of approximately 20% of follicles. The intensity of the staining within the cytoplasm was approximately two thirds of that seen in later stage follicles (Figure 74). Healthy follicles of 2 - 4 mm in diameter were strongly stained within both the granulosa cell layers and the theca interna, additional staining was noted within approximately 30% of the theca externa cells in most follicles (Figure 71). The staining of the granulosa cell layers was more evenly distributed than that seen with the HAS 1 probe, with the 2 layers of granulosa cell closest to the basal lamina stained more strongly than the more antral cells. In the theca there was an even distribution of staining with no one layer appearing more intense than another. The intensity of stain localised in the cytoplasm of the theca externa was less than that observed in the other two cell types mentioned above.

In basal atretic follicles of 2 - 4 mm the granulosa cells were positively stained in a similar pattern to that displayed by the healthy follicles however; the staining of the theca interna was weaker than seen in healthy follicles with the staining in the layers furthest from the basal lamina being more strongly stained than those aligning the basal lamina (Figure 71). The theca externa had no apparent staining within the cells. In antral atretic follicles of the same size the granulosa cell and theca cell layers were both positively stained to the same degree and were more heavily stained than the equivalent cells within basal atretic follicles.

Healthy follicles 6 - 8 mm displayed positive staining within the granulosa and theca cell layers, with the number of cells staining within the theca externa being approximately 50%. In all cases the pattern of staining was cytoplasmic (Figure 72).

In atretic follicles 6 - 8 mm in diameter the pattern was similar to that noted with the 2 - 4 mm antral atretic follicles although the total number of positively stained cells within the theca interna appeared reduced (Figure 72).

Large healthy follicles of 12 - 15 mm had very strong staining within the granulosa cell layers with 80% of theca interna cells showing strong staining within the cytoplasm with the localisation appearing to be within small "pockets" on the cell membrane (Figure 73). In large atretic follicles the granulosa and theca cell layers were again stained positively as seen in the

healthy follicles though the theca signal was reduced with respect to that seen in the healthy follicles.

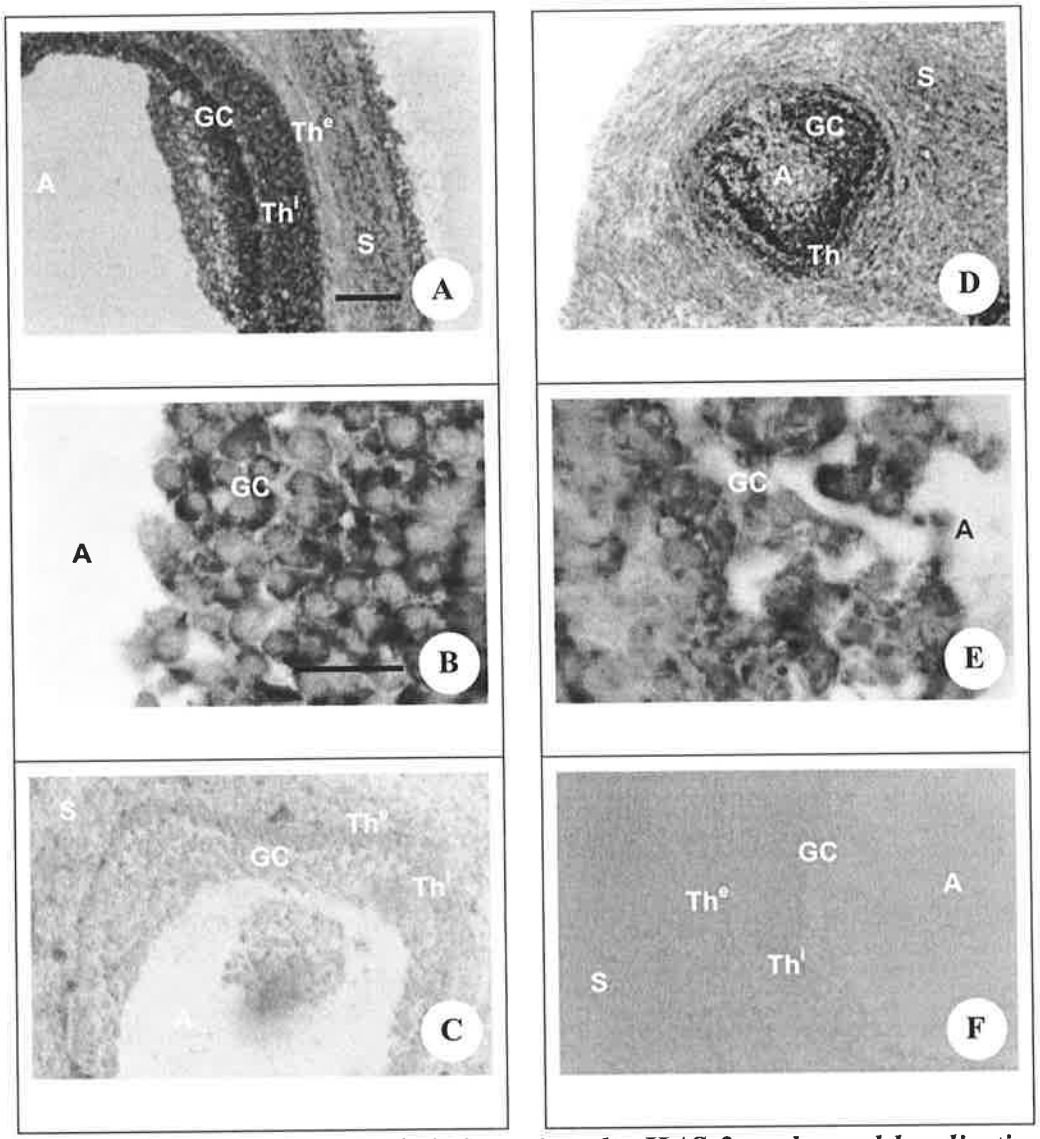

Figure 71 In situ hybridisation to follicles using the HAS 2 probe and localisation of the HAS 2 message. A and B show the localisation to healthy 2 - 4 mm follicles respectively. C: sense control. D and E show the localisation to atretic 2 - 4 mm follicles. F: sense control. Bar = 150 µm images A, D, C and F, = 25 µm images B and E. A denotes the antrum, S denotes the stroma, GC denotes granulosa cell, Th denotes the thecal layers, Th^i denotes theca interna layer, Th^e denotes theca externa layer. NB: sense controls were not counterstained.

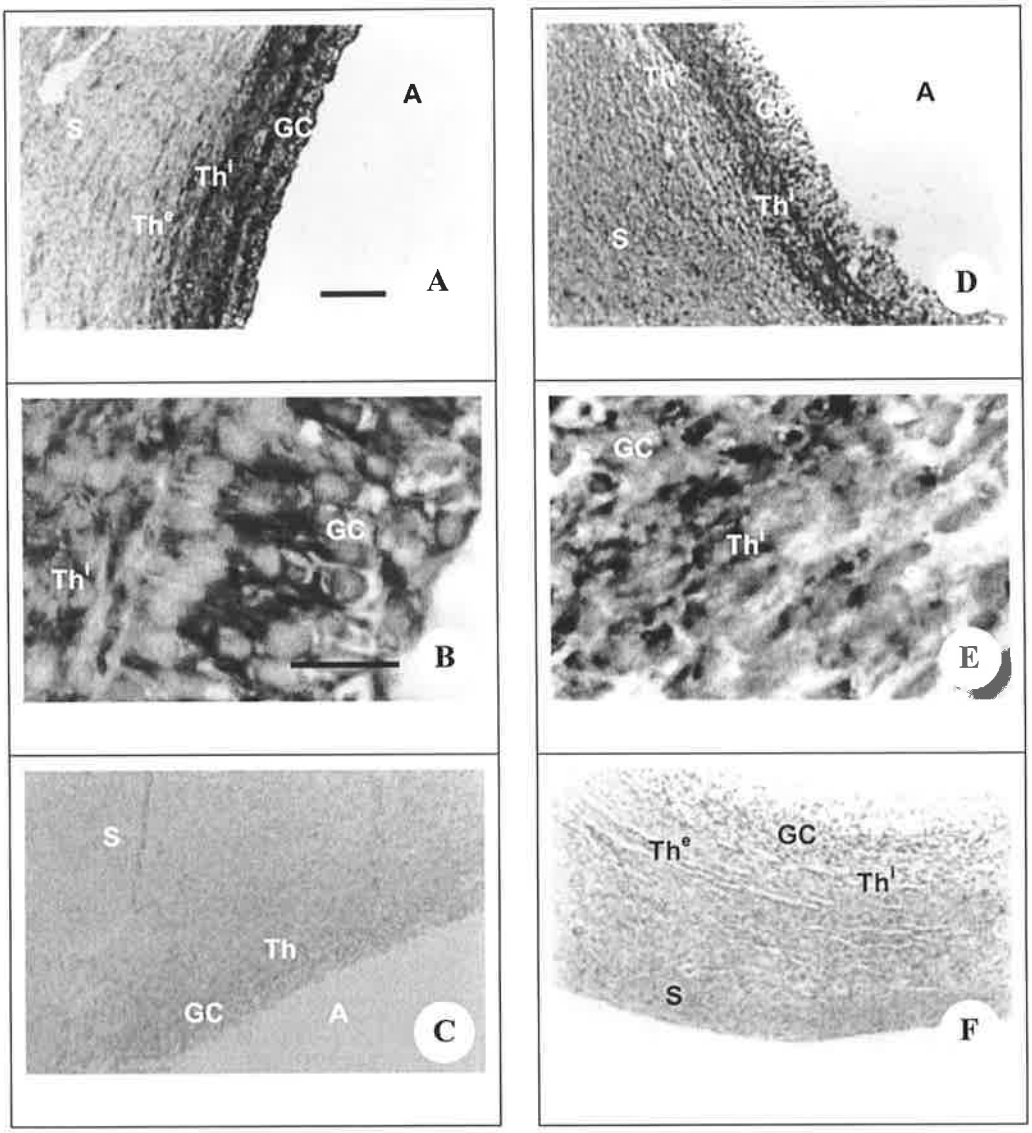

Figure 72 In situ hybridisation to follicles using the HAS 2 probe. A and B show the localisation to healthy 6 - 8 mm follicles respectively. C: sense control. D and E show the localisation to atretic 6 - 8 mm follicles respectively. F: sense control. Bar = 150 µm images A, D, C and F, = 25 µm images B and E. A denotes the antrum, S denotes the stroma, GC denotes granulosa cell, Th denotes the thecal layers, Th^i denotes theca interna layer, Th^e denotes theca externa layer. NB: sense controls were not counterstained.

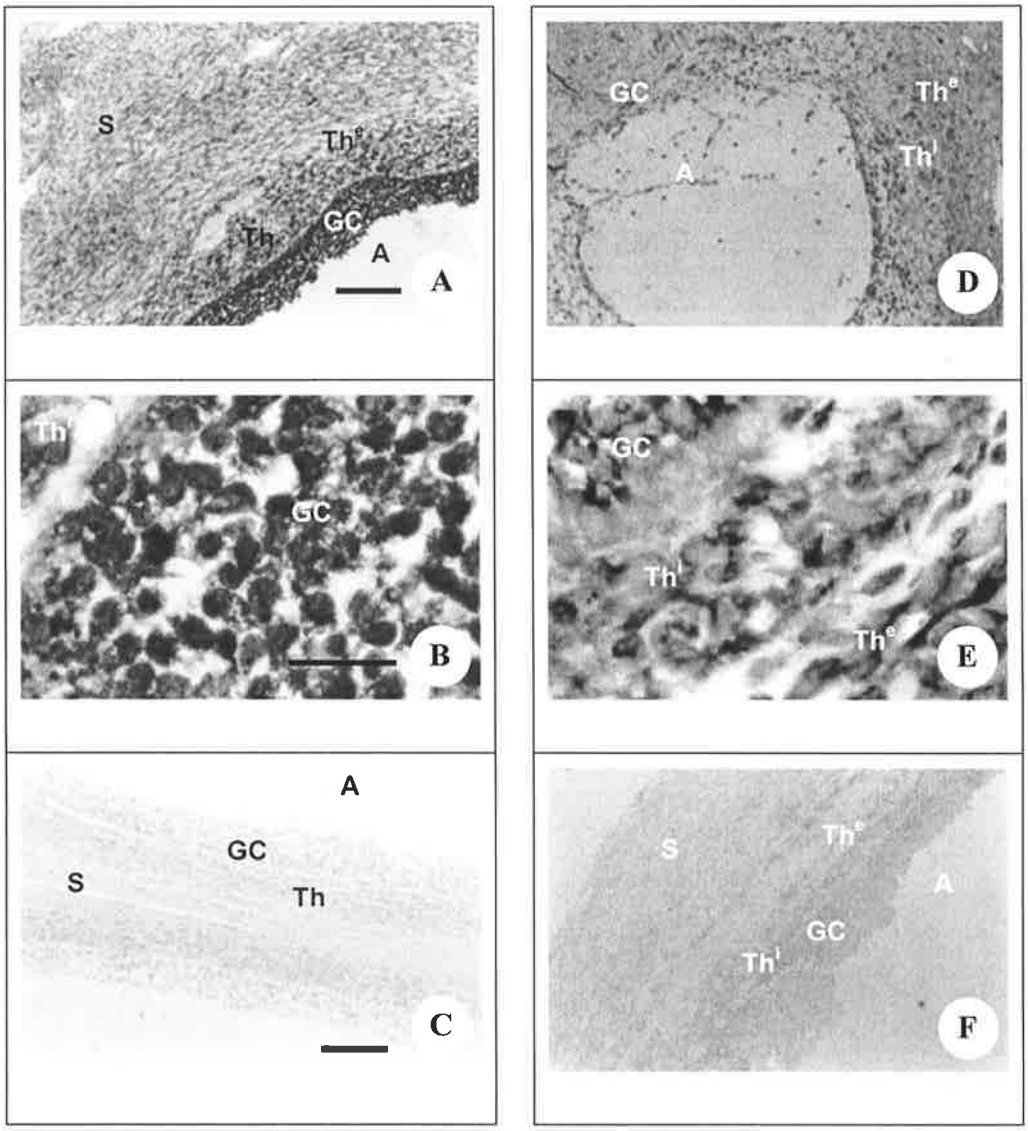

Figure 73 In situ hybridisation to follicles using the HAS 2 probe. A and B show the localisation to healthy 12 - 15 mm follicles respectively. C: sense control. D and E show the localisation to atretic 12 - 15 mm follicles. F: sense control. Bar = 300 µm image A, = 150 µm images C, D and F, = 25 µm images B and E. A denotes the antrum, S denotes the stroma, GC denotes granulosa cell, Th denotes the thecal layers, Th^i denotes theca interna layer, Th^e denotes theca externa layer. NB: sense controls were not counterstained.

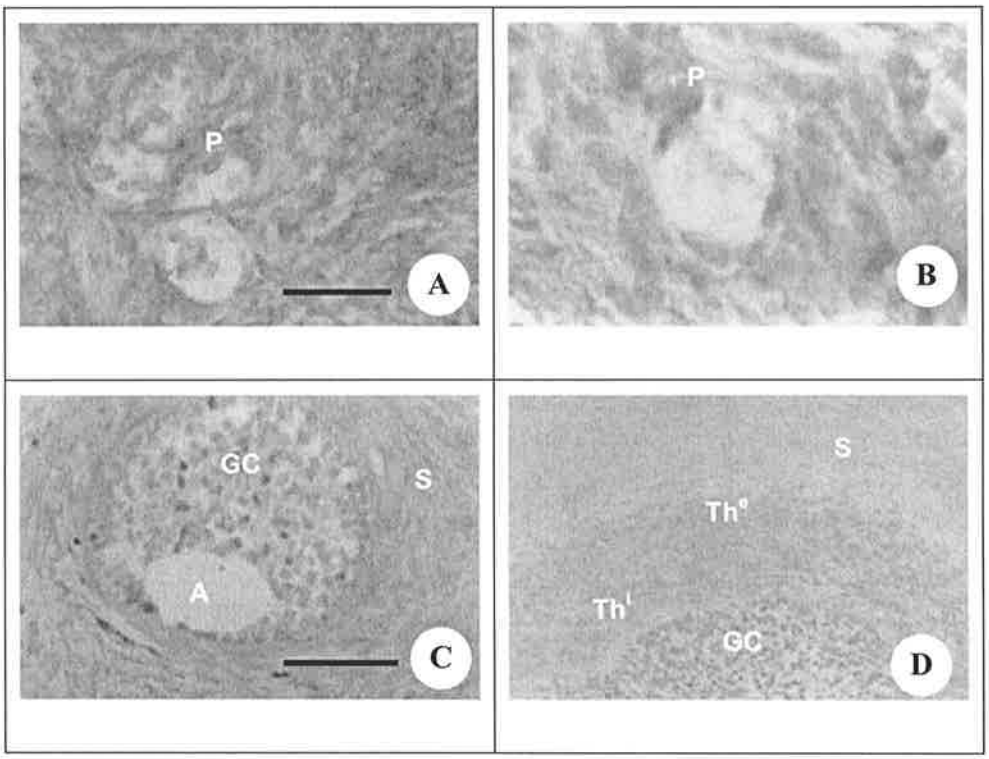

Figure 74 In situ hybridisation using the HAS 2 probe. A and B show the result of in situ hybridisation to primary follicle and primordial follicles. C and D result of in situ hybridisation to an early antral follicle and the sense control respectively. Bar = 50 µm images C and D = 25 µm images A and C. A denotes the antrum, S denotes the stroma, GC denotes granulosa cell, Th denotes the thecal layers, Th^i denotes theca interna layer, Th^e denotes theca externa layer, P denotes position of primordial follicle. NB: sense controls were not counterstained.

5.3.4.7. Follicular Localisation of Hyaluronan Synthase 3 (HAS 3)

Localisation of the message for HAS 3 was found in > 60% of primordial follicles examined (Figure 78). The level of the cytoplasmic staining observed was 2 - 3 times greater than background staining. In primary follicles the number of follicles staining positively was between 50% and 60% again the staining was cytoplasmic (Figure 78). In secondary follicles the granulosa cells were positively stained with the level of staining being very strong. In early antral follicles again the staining observed was intense in the granulosa cells and this was localised within the cytoplasm with weak nuclear staining observed (Figure 78).

In healthy 2 - 4 mm follicles the granulosa and theca cell layers were strongly stained with the theca externa showing weak staining in 50 - 60% of cells examined (Figure 75). In the antral granulosa cell layers of the follicle the intensity of stain was approximately 50% of that seen throughout the rest of the layers, in the theca interna the staining was consistently strong with small patches of accumulated stain noted throughout. In atretic follicles of the same size the intensity of stain was reduced by approximately 20% compared to that of the healthy follicles and the pattern of staining was more irregular, in that groups of granulosa cells appeared positive next to other groups which were apparently negative (Figure 75). This same pattern was observed in the theca layers.

In follicles 6 - 8 mm judged to be healthy all cell layers were strongly stained (Figure 76). In these follicles the most intense stain was observed within the granulosa and theca cell layers closest to the basal lamina. In all cases the staining was noted within the cytoplasm with some weaker localisation within the nucleus. In atretic follicles the theca interna and theca externa layers remained positively stained (Figure 76). The staining noted in the granulosa cell layers was much reduced in a small proportion of follicles, this resulted from the fact that not all granulosa cells in some follicles were stained positively and these cells were stained solely within the cytoplasm with no obvious nuclear staining.

In large healthy follicles of 12 - 15 mm the staining pattern was consistently strong in both granulosa cells and cells within the theca interna, additionally some theca externa cells appeared to be positively stained (Figure 77). This staining as with that of the granulosa and theca interna cells was cytoplasmic with some contribution from the nucleus. In atretic follicles of 12 - 15 mm the staining within the theca externa had gone while that within the theca interna was reduced (Figure 77). The granulosa cells of these follicles remained positively stained. Interestingly the endothelial cells associated with capillary walls were also stained positively as were the corpora lutea, which were very strongly positive for HAS 3 message (data not shown). As above the localisation appeared to be cytoplasmic and nucleic although the staining within the nucleus was reduced compared to that seen in healthy follicles of the same size.

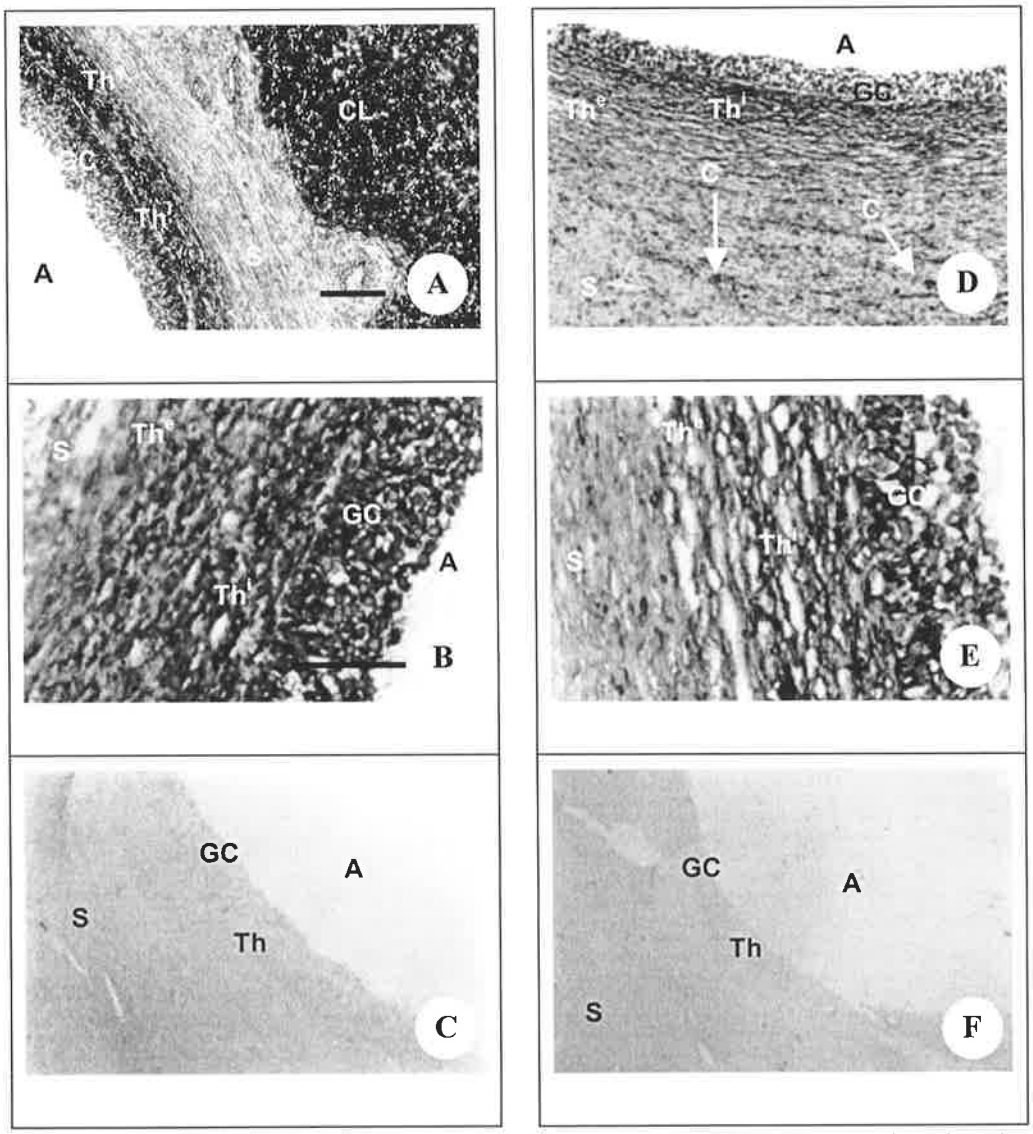

Figure 75 In situ hybridisation to follicles using the HAS 3 probe and localisation of the HAS 3 message. A and B show the localisation to healthy 2 - 4 mm follicles. Note the dark staining of a corpora lutea to the right of the healthy follicle in A. C: sense control. D and E show the localisation to atretic 2 - 4 mm follicles. F: sense control. Bar = 150 µm images A, D, C and F, = 50 µm images B and E. A denotes the antrum, S denotes the stroma, GC denotes granulosa cell, Th denotes the thecal layers, Th^i denotes theca interna layer, Th^e denotes theca externa layer. NB: sense controls were not counterstained. CL denotes corpora lutea. C/White arrows indicate capillaries.

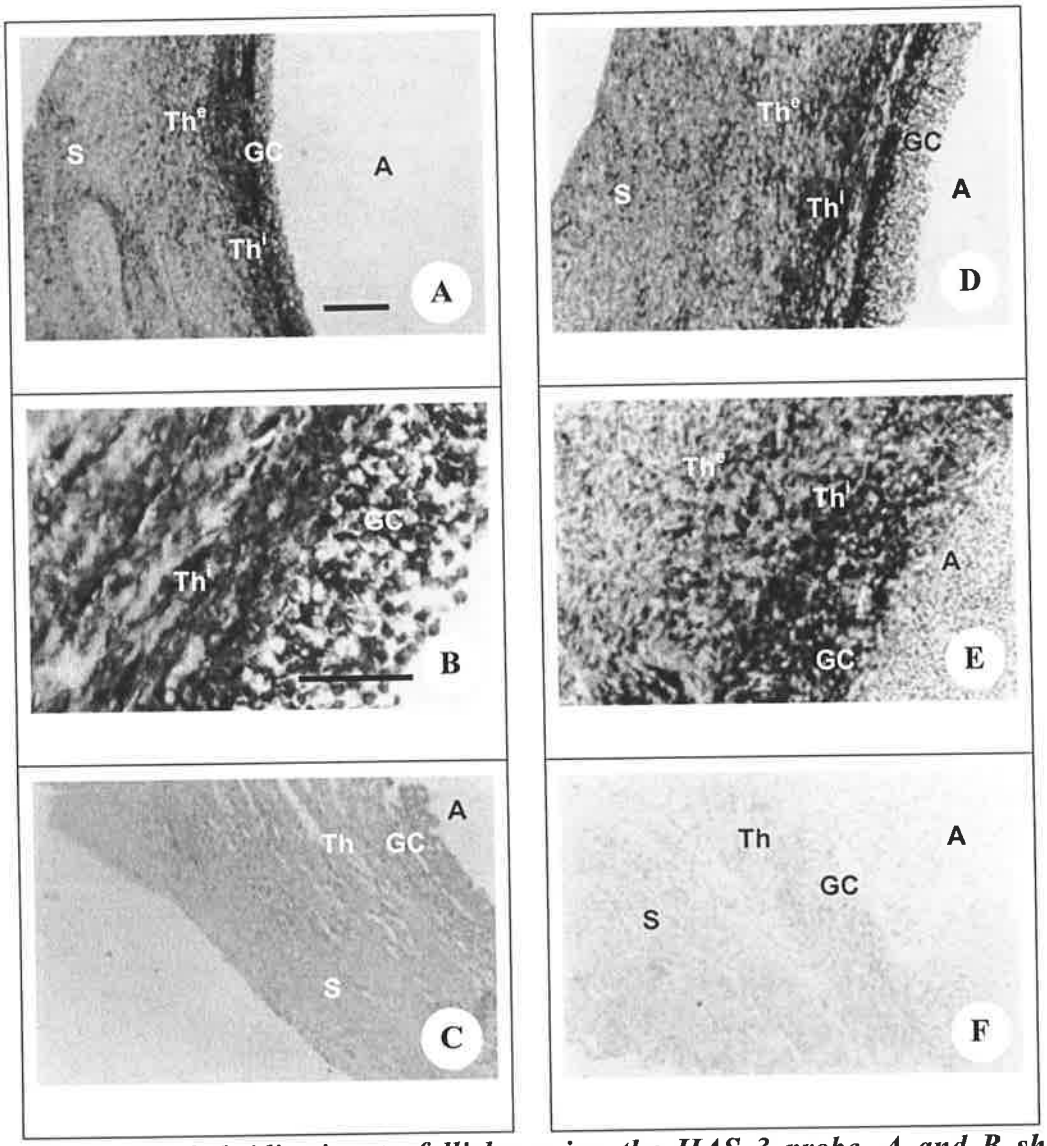

Figure 76 In situ hybridisation to follicles using the HAS 3 probe. A and B show the localisation to healthy 6 - 8 mm follicles respectively. C: sense control. D and E show the localisation to atretic 6 - 8 mm follicles respectively. F: sense control. Bar = 150 µm images A, D, C and F, = 50 µm images B and E. A denotes the antrum, S denotes the stroma, GC denotes granulosa cell, Th denotes the thecal layers, Th^i denotes theca interna layer, Th^e denotes theca externa layer. NB: sense controls were not counterstained.

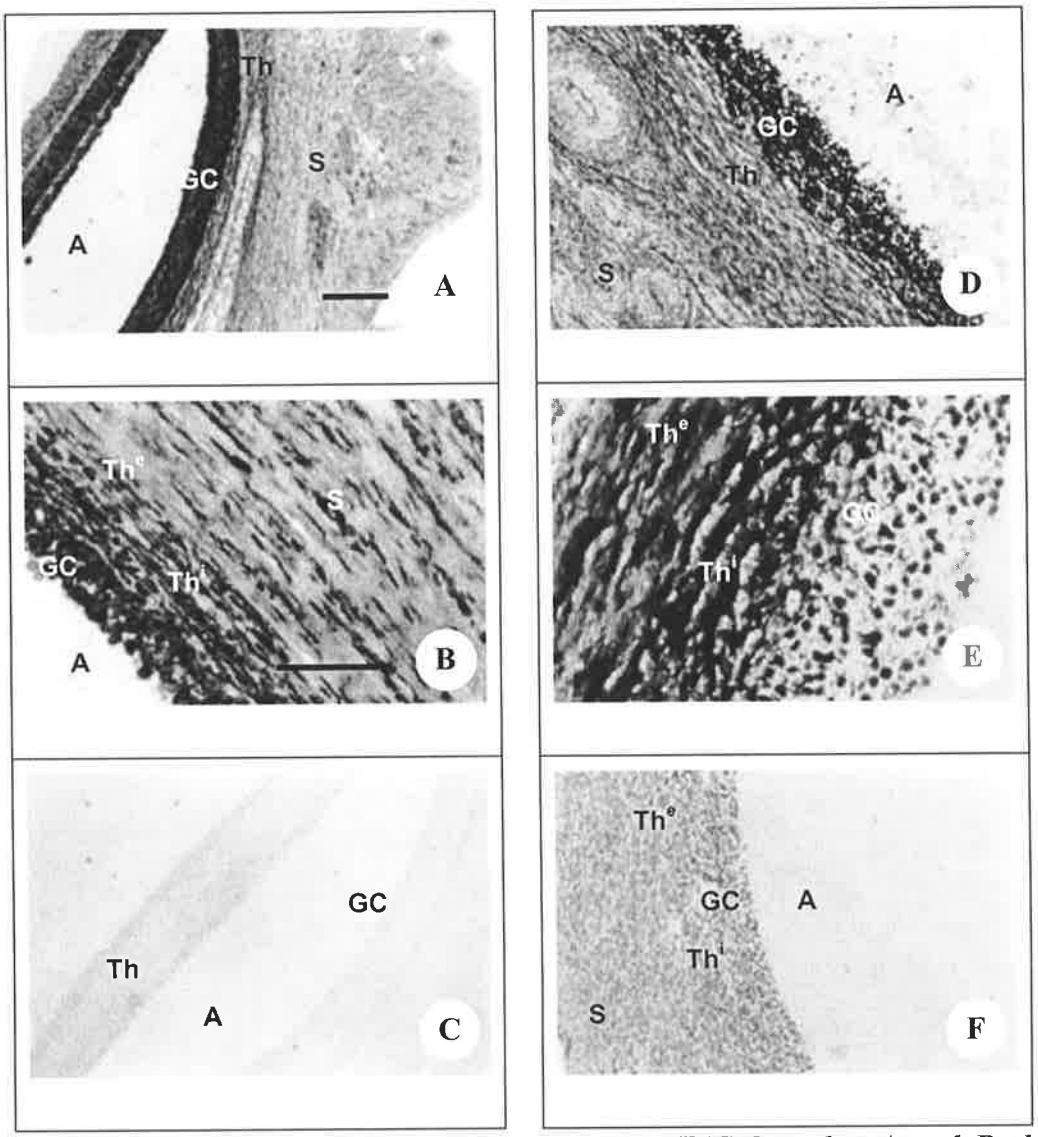

Figure 77 In situ hybridisation to follicles using the HAS 3 probe. A and B show the localisation to healthy 12 - 15 mm follicles respectively. C: sense control. D and E show the localisation to atretic 12 - 15 mm follicles respectively. F: sense control. Bar = 300 µm images A, D, C and F, = 50 µm B and E. A denotes the antrum, S denotes the stroma, GC denotes granulosa cell, Th denotes the thecal layers, Th^i denotes theca interna layer, Th^e denotes theca externa layer. NB: sense controls were not counterstained.

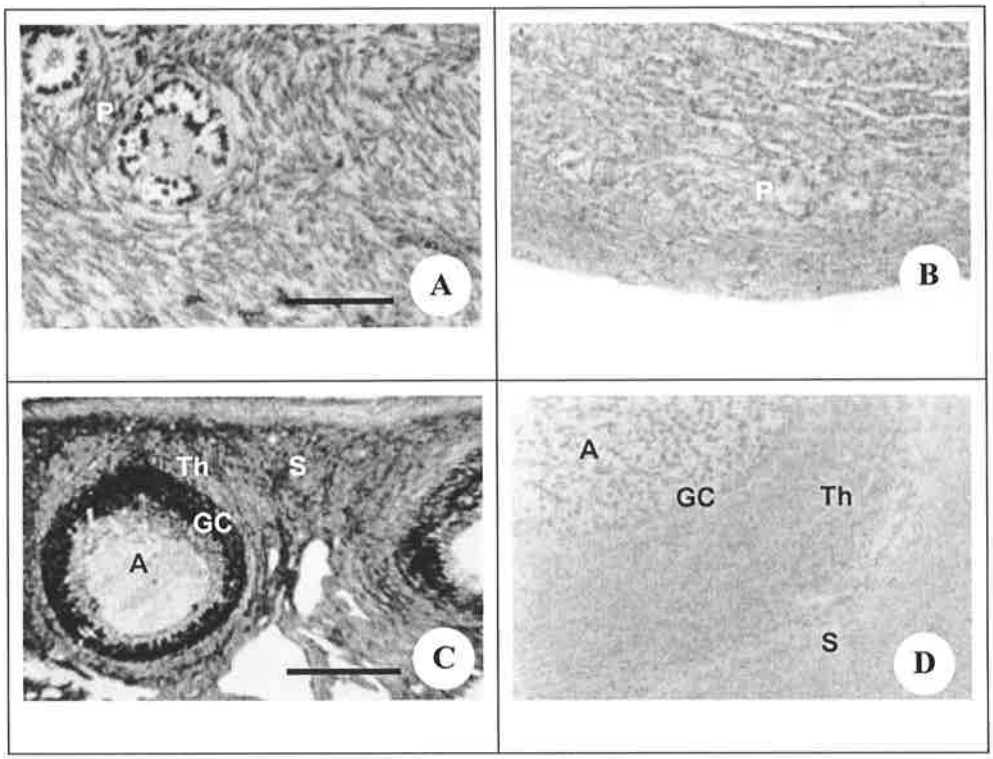

Figure 78 In situ hybridisation using the HAS 3 probe. A and B show the result of in situ hybridisation within primary follicle and primordial follicles. C and D show the localisation to an early antral follicle and the sense control. Bar = 50 µm image C and D, = 25 µm images A and B. A denotes the antrum, S denotes the stroma, GC denotes granulosa cell, Th denotes the thecal layers, Th^i denotes theca interna layer, Th^e denotes theca externa layer, P denotes position of primordial follicle. NB: sense controls were not counterstained.

5.3.4.8. Staining of Corpora Lutea for P450scc, Inhibin βA and HAS mRNA.

All the corpora lutea examined in this study had positive staining for all the hyaluronan synthases (data not shown). The intensity of this staining varied between synthases with that for HAS 3 being much higher than for HAS 2 and HAS 1 which were similar. P450scc message was positively localised to the corpora lutea examined. Positive staining for the inhibin/activin βA message was noted in some corpora lutea with the level of intensity being approximately 50% of that of P450scc

5.3.4.9. Analysis of the Hyaluronan Synthase In Situ Data

Analysis of the data obtained from the in situ assays was done by comparing total numbers of positively stained follicles with the total number of follicles present in that size range (see Table 11). The data showed that in >2 – 4 mm follicles there was no difference in the percentage of follicles displaying a positive signal for any of the HAS isoforms indicating that follicles of >2 – 4 mm were all producing hyaluronan synthesised by the three synthases. Neither was there any difference between the number of positive follicles of healthy and atretic status in the follicles of these sizes. There were though differences in number of positive follicles seen with each hyaluronan synthase in the smaller developing follicles, late stage corpora lutea and regressing follicles with HAS 2 having very few positively stained follicles <2 – 4 mm. The staining in the corpora lutea was very low for HAS 1 and HAS 2 and high for HAS 3.

Table 11 Number of follicles displaying a positive signal in the granulosa cells for each HAS isoform, as a proportion of the total number assessed for that size of follicle with % positive stained follicles calculated.

Follicle type	HAS 1 (+) granulosa cells	% HAS1 positive follicles	HAS 2 (+) granulosa cells	% HAS2 positive follicles	HAS 3 (+) granulosa cells	% HAS3 positive follicles
Primordial	595/1158	51.1	117/1031	11.3	689/1077	64
Primary	161/244	66	19/162	11.7	126/236	54
Secondary	55/64	85.9	63/147	42.8	70/112	62
Early antral	43/52	82.7	71/98	72.4	54/94	57
2 –4 mm	72/74	97	72/74	97	73/75	97
6 – 8 mm	28/32	88	30/32	94	42/42	93
12 – 15 mm	33/34	97	33/34	97	33/34	97
Total No counted	1658		1578		1670	

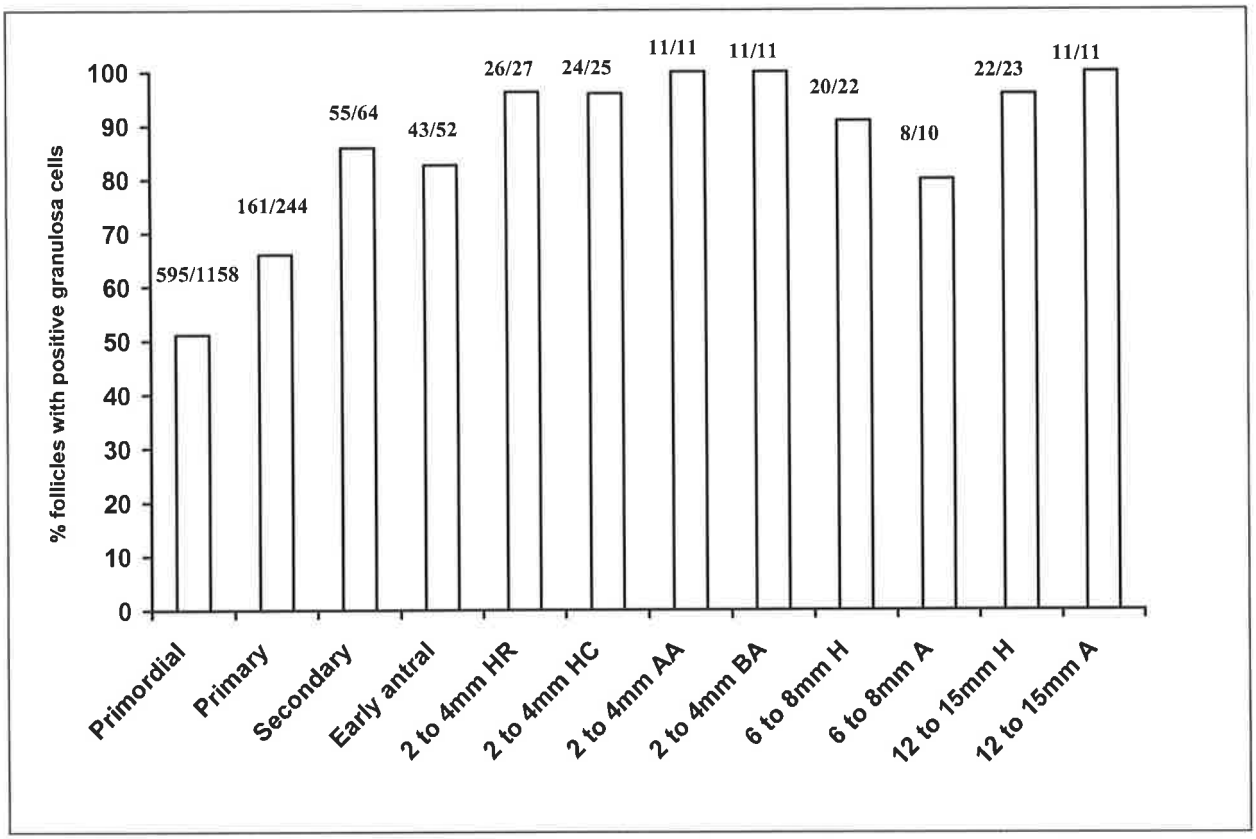

Figure 79 % HAS 1 positive follicles with respect to stage of development as determined by follicular diameter. Number of positive follicles / total number of follicles counted for that size range is indicated above each box. Follicles with healthy rounded granulosa cells – HR, healthy columnar granulosa cells – HC, antral atretic granulosa cells – AA, basal atretic granulosa cells – BA, Healthy follicle – H, Atretic follicle – A.

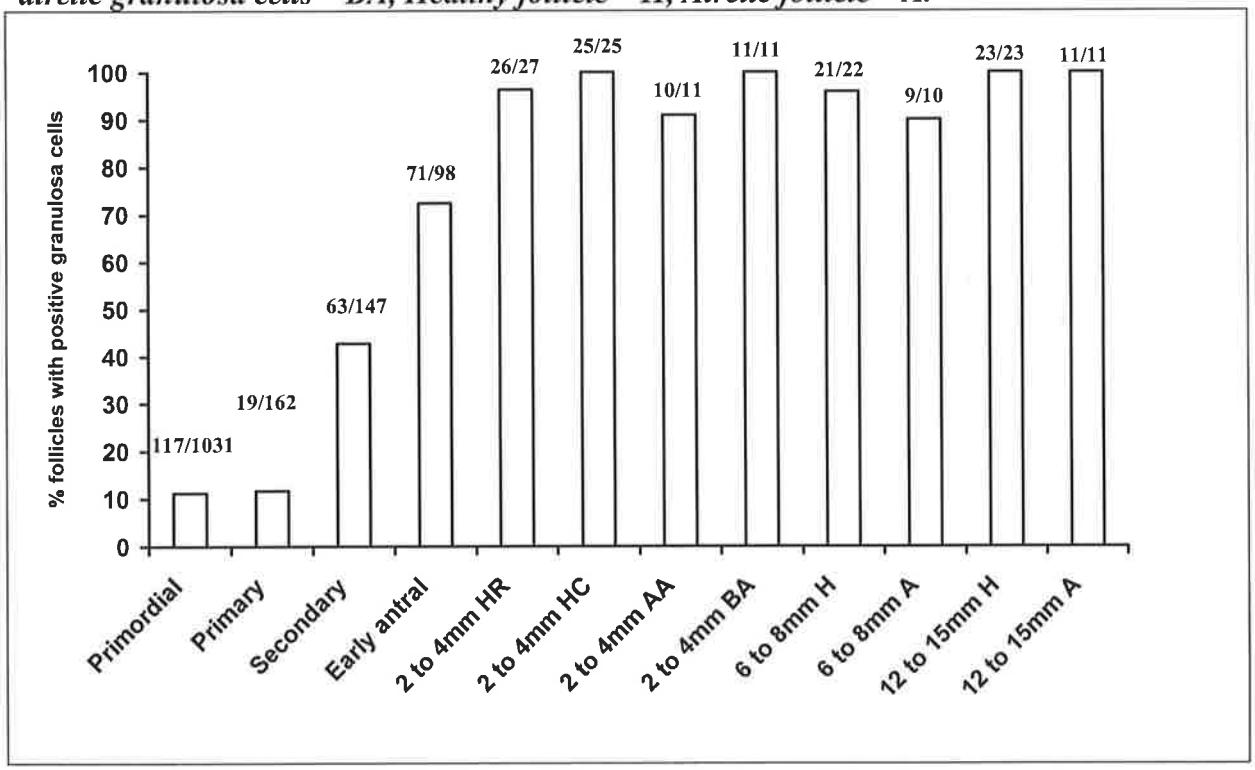

Figure 80 % HAS 2 positive follicles with respect to stage of development as determined by follicular diameter. Number of positive follicles / total number of follicles counted for that size range is indicated above each box. Follicles with healthy rounded granulosa cells – HR, healthy columnar granulosa cells – HC, antral atretic granulosa cells – AA, basal atretic granulosa cells – BA, Healthy follicle – H, Atretic follicle – A.

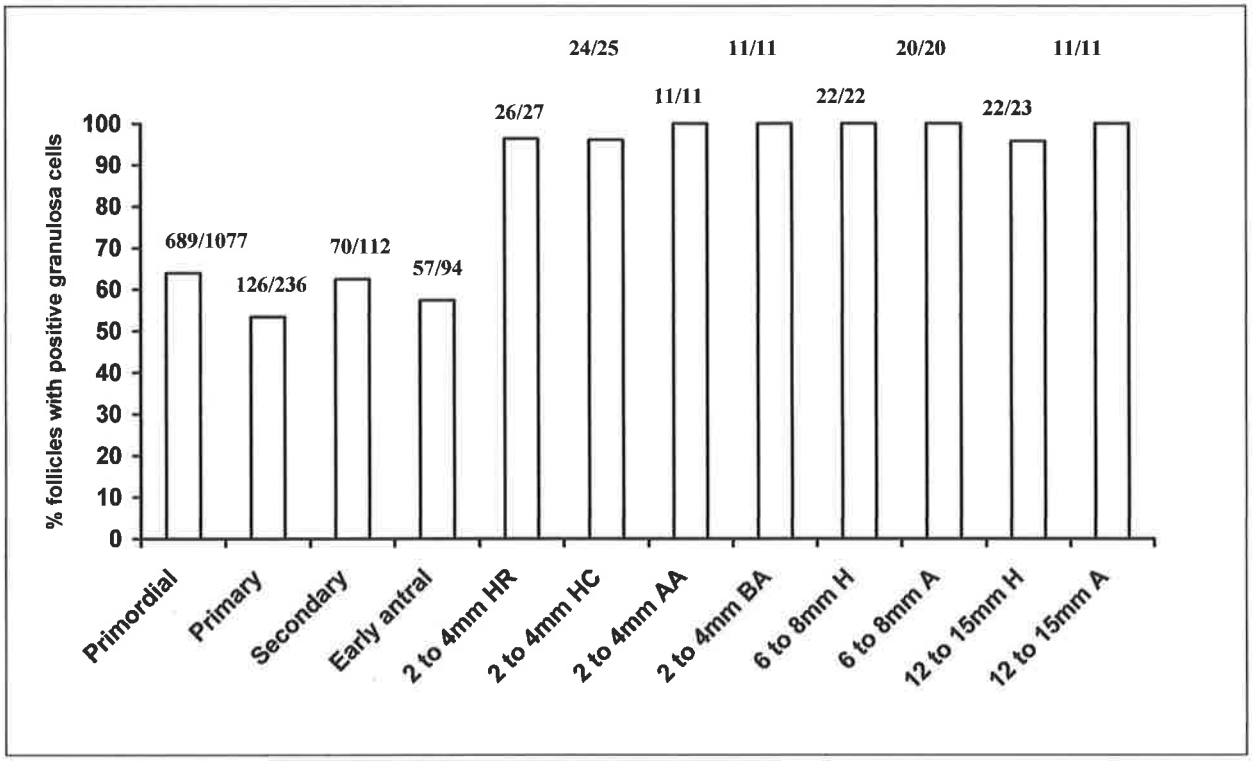

Figure 81 % HAS 3 positive follicles with respect to stage of development as determined by follicular diameter. Number of positive follicles / total number of follicles counted for that size range is indicated above each box. Follicles with healthy rounded granulosa cells – HR, healthy columnar granulosa cells – HC, antral atretic granulosa cells – AA, basal atretic granulosa cells – BA, Healthy follicle – H, Atretic follicle – A.

Statistical analysis was performed using a general linear model to analyse the mean % of positive follicles with respect to stage of development. Results indicated that for follicles > 2 – 4 mm there was no significant difference between the numbers of positively stained follicles obtained for the three-hyaluronan synthases. However, for the smaller follicles (< 2 mm) the results showed differences in the actual and predicted scores for a positive in situ result. The results indicated that HAS 1 expression did not change significantly throughout follicular development. HAS 2 data showed that when compared to the numbers of positively stained follicles obtained with the HAS 1 and 3 probes the number of positively stained follicles were significantly lower ($p < 0.001$) in the primordial through to primary stages of development than those obtained with the other two probes and significantly different to those of the secondary to early antral stages of growth. This indicated that HAS 2 expression varied during follicular growth and that this variation might be linked to stage of development. In the case of HAS 3 the result suggested that HAS 3 expression might be weakly related to the stage of development with its production reduced slightly at a time when HAS 2 production was increased. The percentage of positively stained follicles at different developmental stages for each of the HAS enzymes can be seen in Figure 79, Figure 80 and Figure 81.

5.3.5. Northern Blots

Total RNA was used for Northern blot assays. RNA was prepared from pooled granulosa cells and pooled theca cells taken from follicles of 2 – 4 mm, 6 – 8 mm and 12 – 15 mm to mimic those used in the in situ experiments. The tissues used were collected from a 100-day foetus with the exception of the eye tissue, which was sourced from a 3-year old heifer. The RNA preparation was purified using the RNeasy clean up kit from Qiagen and 10 μg of RNA sample was loaded per lane. The results obtained can be seen in Figure 82 through Figure 88.

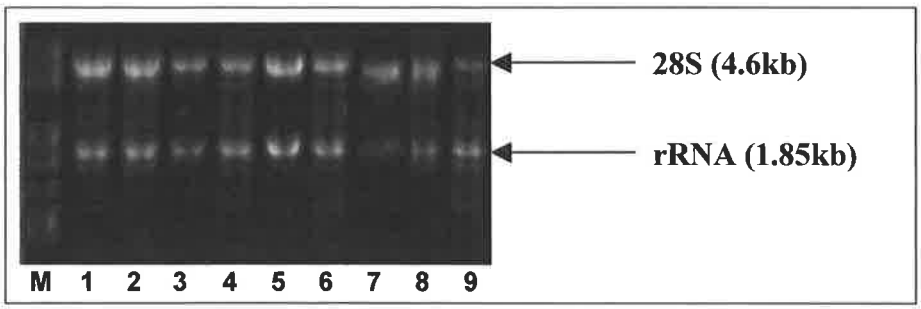

Figure 82 Typical RNA blot used for Northern blots, 1% agarose gel containing formaldehyde stained with ethidium bromide (see materials and methods), 10 ug of RNA loaded in each lane from left to right M: RNA millennium molecular weight marker, lane 1: 2 - 4 mm granulosa cells (gc), lane 2: 6 - 8 mm gc, lane 3: 12 - 15 mm gc, lane 4:2 - 4 mm theca, lane 5: 6 - 8 mm theca, lane 6: 12 - 15 mm theca, lane 7: eye, lane 8: colon, lane 9: heart.

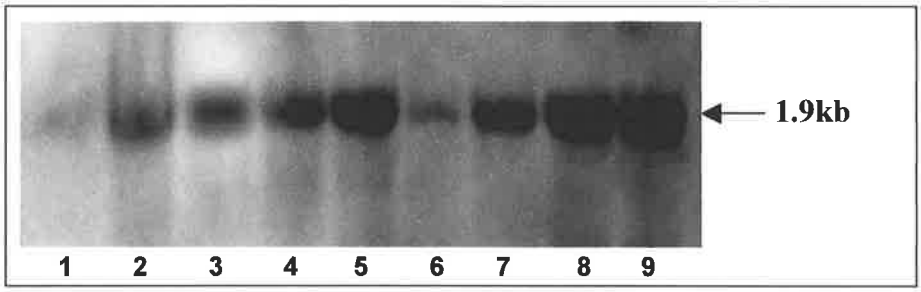

Figure 83 Northern blot using the P450scc probe from left to right lane 1: 2 - 4 mm granulosa cells (gc), lane 2: 6 - 8 mm gc, lane 3: 12 - 15 mm gc, lane 4:2 - 4 mm theca, lane 5: 6 - 8 mm theca, lane 6: 12 - 15 mm theca, lane 7: eye, lane 8: colon, lane 9: heart.

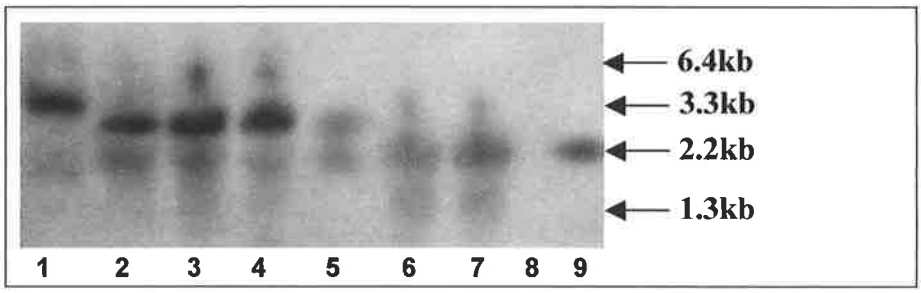

Figure 84 Northern blot using the inhibin/activin βA probe from left to right lane 1: 2 - 4 mm granulosa cells (gc), lane 2: 6 - 8 mm gc, lane 3: 12 - 15 mm gc, lane 4:2 - 4 mm theca, lane 5: 6 - 8 mm theca, lane 6: 12 - 15 mm theca, lane 7: colon, lane 8: eye, lane 9: heart.

5.3.5.1. P450 Side Chain Cleavage (P450scc)

Expression levels of P450scc were confirmed by Northern blot analysis (Figure 83). A 1.9 kb transcript was present in both the follicles and tissues examined. The amount of detectable transcript seen in the granulosa cell preparations increased with increasing size of follicle, with minimal transcript detected in the 2 – 4 mm follicles. In the thecal tissues extracted, strong signals were noted in the 2 – 4 mm and 6 – 8 mm follicles with a reduction in signal intensity noted in the 12 – 15 mm follicles. Strong signals were obtained from the eye, colon and heart tissues.

5.3.5.2. Inhibin/Activin βA

Expression levels of inhibin/activin βA were confirmed by Northern blot analysis (Figure 84). Several transcripts were present in both follicles and tissue samples examined. The transcript sizes were 1.3 kb, 2.2 kb, 3.3 kb and 6.4 kb. The granulosa cells from 2 – 4 mm follicles had 3 transcripts of 2.2 kb, 3.3 kb and 6.4 kb, with the 3.3 kb transcript being the most dominant. The 6 – 8 mm follicular granulosa cells had no apparent 6.4 kb transcript but did exhibit the 2.2 kb and 3.3 kb forms with the 3.3 kb form again being the most abundant. The granulosa cell preparation from 12 – 15 mm follicles indicated all four transcripts were present. The theca cells from 2 – 4 mm follicles appeared to have a very weak signal for the 1.3 kb transcript and a weak signal for the 2.2 kb size. The 3.3 kb and 6.4 kb transcripts were both present with the 3.3 kb size the abundant one seen. Thecal cells from 6 – 8 mm follicles showed a moderate signal for both the 2.2 kb and 3.3 kb transcripts. In addition to these a 1.3 kb transcript seen in the 12 – 15 mm follicular thecal cell blot. Colon tissue displayed the 1.3, 2.2 and 3.3 kb transcripts. No signal was obtained from the eye tissue, in this blot (lane 8), and a sole transcript of 2.2 kb was obtained from heart tissue.

5.3.5.3. GAPDH

The GAPDH transcript obtained by Northern blotting to RNA from follicles and tissues showed the GAPDH transcript to be 1.35 kb in the follicles and tissues selected (Figure 85). The intensity of the band varied with tissue type with a very strong signal obtained in the heart tissue and colon tissue and a slightly weaker one seen in the tissue from whole eye. The intensity of the signal from each of the follicular preparations appeared approximately equal with the exception of the 2 – 4 mm follicle result, which appeared weaker than expected.

5.3.5.4. HAS 1

The expression of HAS 1 in follicles and selected tissues was confirmed by Northern blot (Figure 86). Two transcripts were seen at 4.4 kb and 2.1 kb. The signal from the theca cells from the 2 – 4 mm follicle was weak compared to that of the larger follicles and this supports the data seen with the in situ hybridisation results (see Image C Figure 67, Figure 68 and Figure 69). The HAS 1 transcripts were also seen in two of the three tissues tested (eye and heart) although little signal was seen in the eye tissue examined by in situ the sample. The RNA used in the Northern blots was derived from whole eye tissue and therefore would contain reduced amounts of corneal and ciliary tissue known to contain this isoform compared to a specific preparation of these tissues and so one might expect a reduced signal intensity.

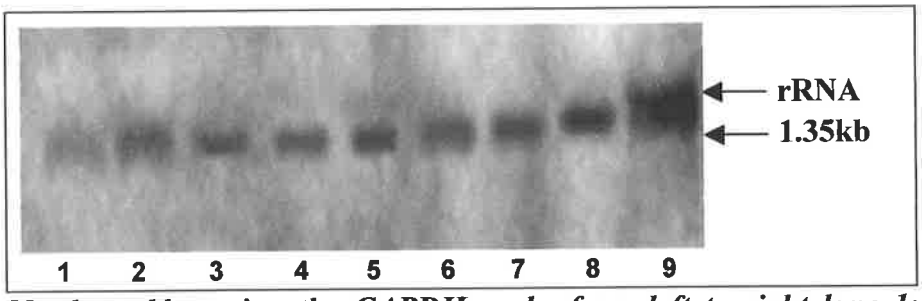

Figure 85 Northern blot using the GAPDH probe from left to right lane 1: 2 - 4 mm granulosa cells (gc), lane 2: 6 - 8 mm gc, lane 3: 12 - 15 mm gc, lane 4:2 - 4 mm theca, lane 5: 6 - 8 mm theca, lane 6: 12 - 15 mm theca, lane 7: eye, lane 8: colon, lane 9: heart.

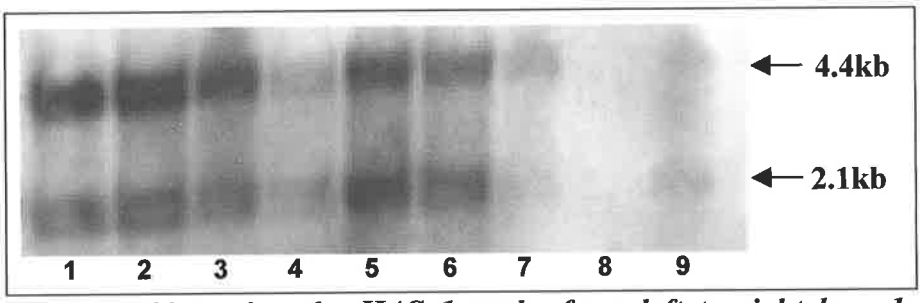

Figure 86 Northern blot using the HAS 1 probe from left to right lane 1: 2 - 4 mm granulosa cells (gc), lane 2: 6 - 8 mm gc, lane 3: 12 - 15 mm gc, lane 4:2 - 4 mm theca, lane 5: 6 - 8 mm theca, lane 6: 12 - 15 mm theca, lane 7: eye, lane 8: colon, lane 9: heart.

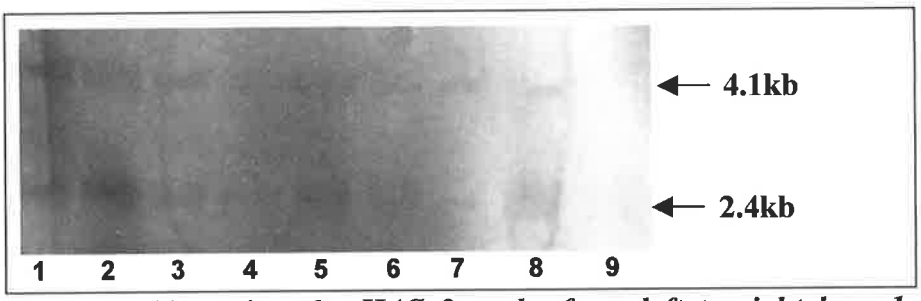

Figure 87 Northern blot using the HAS 2 probe from left to right lane 1: 2 - 4 mm granulosa cells (gc), lane 2: 6 - 8 mm gc, lane 3: 12 - 15 mm gc, lane 4:2 - 4 mm theca, lane 5: 6 - 8 mm theca, lane 6: 12 - 15 mm theca, lane 7: eye, lane 8: colon, lane 9: heart.

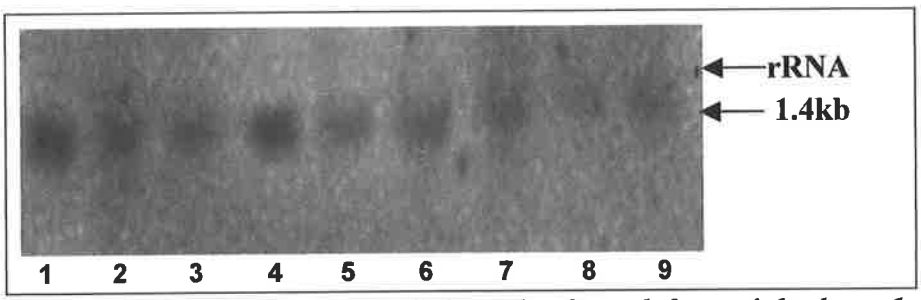

Figure 88 Northern blot using the HAS 3 probe from left to right lane 1: 2 - 4 mm granulosa cells (gc), lane 2: 6 - 8 mm gc, lane 3: 12 - 15 mm gc, lane 4:2 - 4 mm theca, lane 5: 6 - 8 mm theca, lane 6: 12 - 15 mm theca, lane 7: eye, lane 8: colon, lane 9: heart.

5.3.5.5. HAS 2

Two transcripts for HAS 2 were seen in the follicles and tissues examined (Figure 87). They were 4.1 kb and 2.4 kb respectively. The signal obtained with this probe was not very strong when used for Northern blotting and no signal could be obtained from the heart tissue tested. Since the expected signal from this tissue was much less than that for follicular tissue and less than that expected in eye or colon, this was not surprising. The result observed in follicular tissue showed that the signal for the smaller transcript was slightly greater than that for the large. The signal obtained from the granulosa cell and thecal tissues showed an increase in signal in the 6 – 8 mm follicles and a reduction in total signal in the 12 – 15 mm follicles, specifically of the smaller transcript.

5.3.5.6. HAS 3

Northern blotting with the HAS 3 probe produced a single transcript in the tissues examined of approximately 1.4 kb (Figure 88). The strongest signal obtained was seen in the granulosa cell and thecal tissue of follicles 2 – 4 mm, and the weakest signal was given by the colon tissue sample. The two transcripts seen in the colon and heart tissue appeared to be slightly larger than those in follicular tissue.

5.3.6. HAS 2 Protein in the Follicle

The follicular localisation of the HAS 2 enzyme was achieved using the affinity purified human anti-HAS 2 polyclonal antibody kindly provided by P Heldin Ludwig Institute for Cancer Research, Uppsala, Sweden. This antibody showed the presence of the HAS 2 enzyme in the whole of the ovary section used with higher levels of staining detected in the follicular fluid, granulosa cells and theca interna cells of follicles, with the highest levels detected in the granulosa cells and cumulus cells (Figure 89).

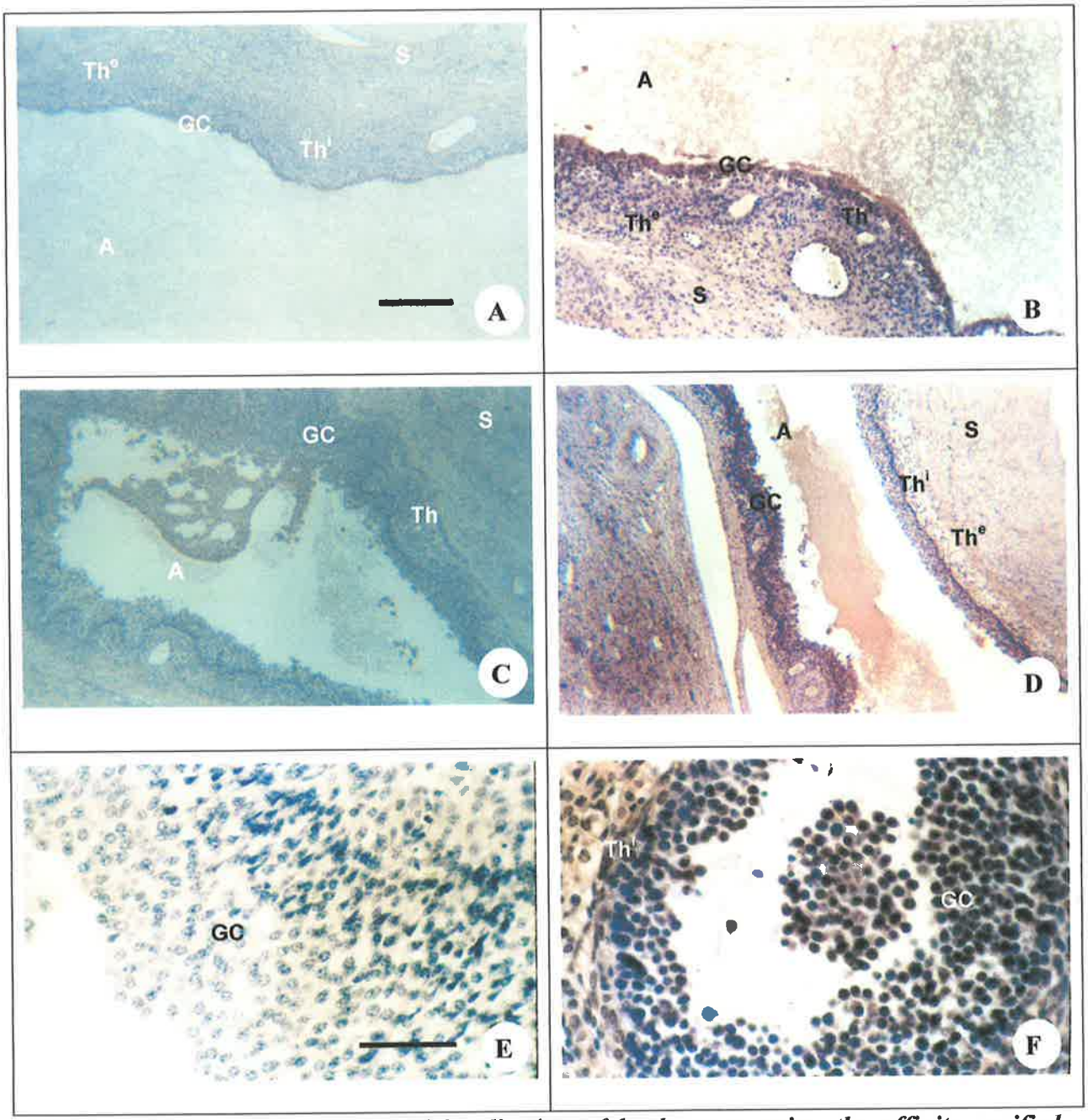

Figure 89 Immuno-histochemical localisation of hyaluronan using the affinity purified human anti-HAS 2 polyclonal antibody at 10 ug/ml supplied by P Heldin conjugated to showing localisation with increased intensity of staining to granulosa cell layers, theca interna and follicular fluid, with some staining of the stromal tissue, Image B, D and F. Images A, C and E are negative controls obtained using a non-immunised serum IgG control. Bar = 150 µm images A, B, C and D, = 50 µm images E and F. A denotes the antrum, S the stroma, GC denotes granulosa cell, Th^i denotes theca interna layer, Th^e denotes theca externa layer, Th shows the position of thecal cells.

5.4. Discussion

Hyaluronan is a ubiquitous molecule of the mammalian body and its presence is associated with matrix structure and plasma proteins. Its high negative charge results in an ability to attract water and therefore rapidly hydrate tissues on demand. It has also been associated with regulation of cell behaviour and has been linked with cell proliferation, angiogenesis inflammation, cell recognition and migration (Laurent T. C. & Fraser, 1992).

Hyaluronan is exclusively synthesised at the plasma membrane by one of three hyaluronan synthases HAS 1, HAS 2 and HAS 3 (Prehm, 1984). The bovine HAS genes are highly conserved and sequence alignment of the bovine HAS enzymes performed here showed that amino acid and nucleotide homology is approximately 60 % with the homology between HAS 2 and 3 being 84 %. Spicer et al (1999) suggested that the potential differences in the function of each of the HAS proteins is related to the length of the hyaluronan chain synthesised, the rate of hyaluronan synthesis, the ability to interact with cell type-specific accessory proteins, and whether or not the hyaluronan is preferentially secreted or retained by the cell in the form of a pericellular coat (Spicer & Nguyen, 1999).

In vitro, the catalytic stability of HAS 1, HAS 2 and HAS 3 has been estimated at 1 h, 4 h, and 8 h respectively. The size of the pericellular coat created by the three enzymes varies, with that of HAS 1 being distinctly smaller than that created by HAS 2 and HAS 3 (Itano *et al.*, 1999) suggesting distinct roles and functions exist for each hyaluronan generated by the respective HAS genes.

The majority of studies of HAS enzymes within the ovarian follicle, describe their roles in the cumulus oocyte expansion process. This study was solely interested in the role of hyaluronan in the osmotic regulation and fluid accumulation processes within the follicle and its potential role in the control of antrum formation. It is accepted that this control is likely to result from a delicate balance between hyaluronan production and matrix formation and its degradation, since this system is common in the control of fluid influx in many other tissues of the body (Fraser J. R. *et al.*, 1997, Toole, 2001).

The understanding of fluid accumulation in the follicle becomes important when considering what a fluid filled antrum provides to that follicle. A follicle requires the correct amount of fluid be present in order to maintain follicular turgidity, whilst providing renewed supplies of nutrients and buffers The granulosa cells of the cumulus oocyte complex have been shown to produce HAS 2 and HAS 3 during the expansion process in response to FSH and LH (Schoenfelder & Einspanier, 2003). Since antrum formation occurs well in advance of cumulus oocyte complex expansion, the cumulus cells are unlikely to be the source of the hyaluronan involved in antrum expansion. Thus it appears likely that since mural granulosa can also produce hyaluronan (Elvin *et al.*, 1999b) that they and/or thecal cells are responsible.

It is hypothesised that the mural granulosa cells are responsible for hyaluronan production in the follicle and this takes place under regulated control. If the hypothesis is true one would expect to find that the expression of one or more of the HAS genes is increased at antrum formation.

With this in mind RT PCR experiments were conducted using primers designed to the known Bovine HAS 1, 2 and 3 sequences and used these to amplify specific HAS DNA from mural granulosa and theca cell preparations. These amplicons were then cloned in to the pGEM T Easy™ vector and sequenced to confirm their identity. Probes prepared from the plasmids were subsequently used in in situ hybridisation assays and Northern blot analyses of RNA extracted from non-follicular tissues known to contain one or more of the synthase enzymes, controls, whole ovaries and granulosa and theca cells collected from follicles of 2 mm – 15 mm in diameter. In addition two probes for follicular tissue quality control were prepared, these were inhibin/activin βA for the granulosa cells and cytochrome P450scc for the theca cells.

One-tube RTPCR (http://www.roche-applied-science.com/fst/amplification.html) experiments revealed that 18S rRNA and GAPDH could be amplified from the tissue samples used. The amplification was consistent between the follicles and control tissues confirming the integrity of the RNA used in the RT PCR and subsequent Northern blots. Northern blot results obtained for these genes were also consistent with those reported for other tissues (Spicer *et al.*, 1996) with an intense signal seen for GAPDH from heart tissue, which was again consistent with the results of other authors (Kako *et al.*, 2000). These data confirmed that the tissues used were in appropriate condition for the analyses to be performed.

RT PCR results obtained with the inhibin/activin βA, showed that inhibin/activin βA could be amplified from all granulosa and theca cell extracts and its presence in these tissues was supported by Northern blot and in situ data. The result obtained from the Northern blots revealed multiple transcripts of inhibin/activin βA at 1.3 kb, 2.2 kb, 3.3 kb, and 6.4 and this data is similar to that of Ireland and Ireland (1994), who found transcripts of similar sizes in small medium and large bovine follicles (Ireland J. L. & Ireland, 1994). The results achieved with these probes therefore appear credible. Having provided proof of the credibility of the inhibin/activin βA probe the viability of the granulosa cells from the follicular tissues used in the in situ assays was demonstrated. Inhibin/activin βA mRNA could not be detected in primordial follicles and was only weakly positive in primary follicles. In follicles of larger size the mRNA could clearly be detected in the granulosa cells with the intensity being reduced in atretic follicles. These localisation patterns are similar to those previously reported (Braw-Tal, 1994) and the positive results obtained for the inhibin/activin βA Northern

analyses and in situ hybridisation proved the integrity of the follicles used in insitu analyses and granulosa cell RNA obtained.

P450scc was chosen as a control for theca cell integrity. RT PCR confirmed that P450scc could be amplified from the selected tissues. Northern blotting confirmed expression of the 1.9kb P450scc transcript in granulosa cells and the theca interna of follicles of 2 – 15 mm and non-follicular tissues. The size of the transcript was comparable to the transcript described by Pescador et al (Pescador *et al.*, 1996). Confirmation of its expression within the follicle was achieved by in situ hybridisation. P450scc was localised to the theca interna of healthy and atretic follicles of 2 – 15 mm diameter. Expression varied with the developmental stage of the follicle. That only a proportion of theca interna cells were stained positively was no surprise, since the thecal layers also contain many non-steroidogenic cells such as fibroblasts and endothelial cells. The expression pattern observed was comparable to that obtained by others (Xu *et al.*, 1995). Together these data provided evidence that the thecal tissue quality was good.

Interestingly there were high levels of expression observed in the colon and heart tissues. Localisation of P450scc has been previously reported in the primitive gut of rats and the mitochondria of heart tissue (Keeney *et al.*, 1995, Novikova *et al.*, 1995).

The positive results obtained in this study for the inhibin/activin βA and cytochrome P450scc probes demonstrated that the viability of the granulosa and theca cells was not compromised by collection, fixation, handling or extraction of RNA from the tissue sections and that RT PCR, Northern blot and in situ methodologies were reliable.

Hyaluronan has been localised previously in bovine reproductive tissue using hyaluronic acid binding protein (Laurent C. *et al.*, 1995a). Their study showed that hyaluronan could be detected in the theca of small and large follicles but made no comment as to the localisation within the mural granulosa cells. This work used bovine HAS specific primers and probes for use in RT PCR, Northern blots and in situ hybridisation to non-follicular tissues and follicular tissues. The non-follicular tissues were used to provide confidence in the bovine specific HAS probes, and the follicular tissues were used to localise HAS expression at known stages of follicular development. Amplicons of the expected size for all the HAS genes of interest were obtained from all non-follicular and follicular tissues and were subsequently cloned. Sequencing of the plasmid constructs confirmed the HAS specificity of all probes used in subsequent analyses.

The transcripts observed with the HAS 1, 2 and 3 probes were in agreement with those previously reported for each of the non-follicular tissues tested and in situ localisation gave further credence to the specificity of the probes.

The non-follicular tissue blot had two transcripts at 2.1 kb and 4.4 kb and in situ localisation showed that HAS 1 mRNA could be detected in the mucosal smooth muscle cells of the colon, growth plate region of the hoof and epithelial cells of foetal skin. All these tissues reportedly express HAS 1 (Kaya *et al.*, 2005, Laurich *et al.*, 2004, Sayo *et al.*, 2004, Yoshida M. *et al.*, 2004). The HAS 2 Northern blot for non-follicular tissue identified transcripts at 2.4 kb and 4.1 kb and in situ analyses showed localisation detected HAS 2 mRNA in the foetal growth plate and ciliary process of the eye, with weaker localisation to mucin cells of the colon and skin epithelial cells. These tissues are documented to contain significant hyaluronan and some reports have shown HAS 2 localisation in these areas (Sugiyama *et al.*, 1998, Usui *et al.*, 1999). Hyaluronan has also been localised to corneal endothelium epithelium and conjunctiva (Rittig *et al.*, 1992, Usui *et al.*, 1999, Usui *et al.*, 2000, Usui *et al.*, 2003). The HAS 2 localisation reported here within the mucus secreting cells of the colon was not unexpected (Jacobson *et al.*, 2002). The HAS 3 Northern blot identified a single transcript at 1.4 kb in the non-follicular tissue samples, this was consistent with the findings of other authors (Bullard 2003; Sayo 2002). In situ analysis of these same tissues localised Has 3 in mucin cells of the colon and skin similar to that previously reported by others (Kim *et al.*, 2004).

The data obtained from the non-follicular tissue Northern blots and in situ localisations together with the inhibin/activin βA and cytochrome P450scc data gave credence to all data obtained from subsequent investigations with good tissue quality, reliable techniques and specific probes established.

RT PCR showed that HAS 1, 2 and 3 could be amplified from pooled extracts of granulosa and theca cells obtained from follicles > 2 – 15 mm confirming their presence in both cell types. While RT PCR showed that the HAS genes were present in these follicles it did not give any indication of the relative abundance or activity of the enzyme present.

Reports by Spicer et al (1999) and Monslow et al (2003) have suggested that the relative abundance of the HAS genes is related to the relative abundance of the protein produced (Monslow *et al.*, 2003, Spicer & Nguyen, 1999). If this is true then it can be assumed that the expression level detected in the analyses of the follicular tissues, as detected by Northern blot and in situ hybridisation, can be related to the actual production hyaluronan type produced by that enzyme.

With respect to the HAS 1 enzyme, the HAS 1 Northern blots showed that the signal for the transcript present in the granulosa cells of small antral follicles was increased over that of the larger follicles. Assuming Monslow et al are correct, this indicated that the mRNA for the least stable form of high molecular weight hyaluronan was being produced maximally in smaller follicles and declined with follicular maturation. HAS 1 transcripts were also obtained

from the thecal tissue suggesting that production of large amounts of unstable, high molecular weight hyaluronan was also occurring in these cells.

In situ data revealed that the HAS 1 signal was present in half of all primordial follicles examined. This number increased in the primary follicles and was approximately 90 % in secondary and early antral follicles. HAS 1 was localised in the granulosa and theca cells of all follicles > 2 mm and this was most intense in the layers aligning the basal lamina of healthy follicles suggesting that the synthesis of hyaluronan by HAS 1 was maximal in this area. Not all cells within the theca interna were stained but in those that were, the staining was intense. The HAS 1 negative cells may be steroidogenic cells within the theca interna, as in hens, these produce only minimal amounts of matrix molecules for structural purposes and a similar situation may be present here (Jackson R. J. *et al.*, 1998). As the follicle increases in size the steroidogenic cells become more prevalent and this is presumably the cause of the reduced HAS 1 message noted in the follicles examined.

Since HAS 1 expression could be detected in high numbers of pre-antral follicles and hence not obviously temporally linked to the initiation of antrum formation, the authors feel that it is unlikely to be directly linked to this process. In addition, its stability as an enzyme is poor and thus it is unlikely to be under the tight intraovarian, autocrine and paracrine regulatory control of folliculogenesis (Monniaux *et al.*, 1997, Monslow *et al.*, 2003). Hence its role might be linked with another function of hyaluronan, that of facilitation of cell division and follicular growth. During the early stages of antrum formation the follicle undergoes rapid expansion requiring rapid cell division (Rodgers R. J. *et al.*, 2001). The intensity of the signal seen in the cells aligning the basal lamina indicated that maximal production of hyaluronan was occurring in this area. In the follicle, hyaluronan synthesis has been documented to increase during mitosis in the dividing cells of in vitro matured cumulus oocyte complex (Salustri *et al.*, 1989). Specifically, HAS 1 has been identified as a critical enzyme for the increased hyaluronan synthesis seen in highly malignant cells, where pericellular hyaluronan is critical for carcinoma cell invasion. This supports an active role during cell division and migration, its invasive capability dependent on its interaction with CD44 (Casey & Skubitz, 2000, Csoka *et al.*, 1997, Itano *et al.*, 2002, Kim *et al.*, 2004, Misra *et al.*, 2003, Wang *et al.*, 1996). HAS 1 is stimulated by growth factors such as TGFβ1 (Knight & Glister, 2003, Magoffin *et al.*, 1989, Morales & Roberts, 1988, Stuhlmeier & Pollaschek, 2004, Tanimoto *et al.*, 2004, Usui *et al.*, 2003). TGFβ1 may stimulate HAS 1 production of hyaluronan in the growing healthy follicle aiding the cell division, migration and signalling processes. A second role for the hyaluronan produced by HAS 1 may lie in its viscoelastic properties. These properties provide lubrication and structural support for organs or structures during rapid growth or shape change such as that encountered with the rapidly

expanding follicle. Perhaps this secondary property allows a follicle to grow and change shape as required by allowing cells to "slide over" one another without friction (Balazs, 1968). It is of interest to note that in atretic follicles HAS 1 signal was decreased in both the granulosa and theca cells when compared to that of healthy follicles. If as HAS 1 were involved in the facilitation of cell division and migration, then it would seem reasonable to assume that a reduced signal would be observed in atretic follicles where these processes are much reduced. The reduced levels of HAS 1 recorded in the atretic follicles would be consistent with this hypothesis.

HAS 2 could be amplified from pooled extracts of granulosa and theca cells from follicles 2 – 15 mm indicating that the message was present in these tissues and confirms the findings of Schoenfelder and Einspanier (2003) in whole ovarian follicle tissue (Schoenfelder & Einspanier, 2003). HAS 2 Northern blot analyses identified transcripts in follicular tissues examined at 2.4 kb and 4.1 kb. The bands appeared strongest in the granulosa cells and theca cells collected from follicles of 6 – 8 mm implying that production was likely to be maximal in these follicles.

Data from in situ hybridisation to follicular tissue showed HAS 2 mRNA could be detected in the granulosa cells of few primordial and primary follicles and less than half of the secondary follicles. However, a marked increase in the number of follicles displaying a positive signal for HAS 2 mRNA was observed in follicles where antrum formation had just begun. By the time fluid pockets had begun to merge to form a single antrum, a positive HAS 2 signal could be detected in the granulosa cells of the majority of follicles examined and in follicles of > 2 mm diameter, 96 % of follicles had a positive signal for HAS 2 in their granulosa and theca cells. This indicated that an up regulation of HAS 2 message in these cells had occurred at a time when antrum formation was beginning. The evenly distributed HAS 2 staining seen among the granulosa and theca cells of smaller follicles indicated that the message was similar in these cell types, this data was supported by the information from the Northern blots. The increased intensity of signal detected in the mural granulosa cells of small and medium healthy follicles of 2 - 8 mm diameter implied that there was further up regulation of the message within the granulosa cells of these follicles. The strongest signal was localised toward the apical surface of granulosa cells suggesting that the hyaluronan was being made specifically within these cells for apical extrusion in to the antrum. The additional information provided by the localisation of HAS 2 protein with the HAS 2 antibody confirmed its presence in these cells. The antibody used appeared to have high background staining regardless of pre-treatment of the sections for endogenous peroxidases. In retrospect pre-digestion with hyaluronidase of the samples may have provided a more significant result

although similar results have been achieved with this antibody in other trials (P. Heldin personal communication).

The HAS 2 signal in the theca cells of large follicles was reduced indicating some down regulation was occurring here, this decrease was confirmed by the Northern data.

These data suggest that HAS 2 is the principle enzyme driving hyaluronan synthesis during antrum formation and fluid accumulation, since an apparent up regulation was detected just prior to antrum formation and increased with increasing follicle size.

The HAS 2 signal in medium and large atretic follicles was much reduced while the signal from the small follicles was only slightly less than that of the healthy follicles. On close inspection, the signal was diffusely located within the cytoplasm of the atretic follicles, unlike the clear apical cytoplasmic membrane staining seen in the healthy follicles. This diffuse staining pattern has been noted with a number of hyaluronan histochemical stains and has been related to reduced hyaluronan synthesis and breakdown of the nuclear membrane (Evanko & Wight, 1999), known to occur during atresia. This is the first report of a diffuse staining pattern following in situ localisation of HAS 2 message to atretic bovine follicles. If the HAS 2 signal localisation and intensity are related to the production of the protein as suggested by Monslow et al (2003) then these results are indicative of reduced hyaluronan production in atretic follicles. If hyaluronan synthesised by the HAS 2 enzyme is responsible for fluid accumulation, the reduction of HAS 2 expression seen in these dying follicles is not unexpected. These follicles no longer undergo antrum expansion therefore there is no reason for the hyaluronan levels to be maintained.

That HAS 2 appeared to be involved in antrum formation was not surprising. HAS 2 is responsible for the production of stable, high molecular weight hyaluronan that can be produced rapidly and its molecular structure suggests it is sensitive to cell specific effects and hence likely to be a under tighter regulatory control than the other HAS genes (Monslow *et al.*, 2003).

In support of a regulated expression of HAS 2, Elvin et al reported that recombinant GDF-9 was able to exert control on mural granulosa cells prior to antrum formation. They found that recombinant GDF-9 stimulated the expression of HAS 2, cyclooxygenase 2, and steroidogenic acute regulator protein mRNA (Elvin *et al.*, 1999b). Granulosa cells produce PGE_2 and therefore have their own substitute for the FSH required for the stimulation seen in the cumulus cells (Salustri *et al.*, 1990b). HAS 2 is known to be developmentally regulated and to be regulated by a number of cytokines and growth factors. Recently, up-regulation of HAS 2 has been recorded in response to gonadotrophins, cytokines and growth factors including FSH, transforming growth factor (TGF) super-family members, platelet derived growth factor (PDGF) epidermal growth factor (EGF), fibroblast growth factor (FGF) and

insulin-like growth factor (IGF) (Fulop *et al.*, 1997a, Knight & Glister, 2003, Laitinen *et al.*, 1998, McGrath *et al.*, 1995, Salustri *et al.*, 1999, Stock A. E. *et al.*, 2002). Oocyte granulosa cell communication has been well established in recent years (Ackert *et al.*, 2001, Nagyova *et al.*, 2000, Vanderhyden *et al.*, 1997) and an as yet unidentified signalling process may stimulate the mural granulosa cells to up-regulate HAS 2 production of hyaluronan.

In 2001 Salamonsen et al suggested that production of hyaluronan might be steroid dependent (Salamonsen *et al.*, 2001). Steroidal regulation of transcription occurs when steroid receptors mediate transcription effects by recruiting transcriptional co-regulators to target promoters. Steroid receptor co-regulators are involved in RNA processing by binding target DNA response elements and promoting recruitment of co-regulators involved in transcription, ensuring co-ordination between RNA production and the final product. Depending on the promoter and the cell context, it is possible that some transcription factors could recruit different co-regulators in different cell types and thus mediate different effects on transcription and processing. A great deal of data pertaining to the expression of HAS genes has been provided by researchers in the ocular field. Usui et al (2000) have shown that both TGFβ1 and PDGF are capable of stimulating HAS 2 expression and suggest some form of steroidal regulation might be involved (Usui *et al.*, 2000). HAS 2 is significantly more active than HAS 1 and the production of large amounts of hyaluronan appears to have significant effects on tissue structure and volume in the eye (Usui *et al.*, 1999, Usui *et al.*, 2000). Thus, HAS 2-dependent hyaluronan biosynthesis has already been demonstrated to affect fluid accumulation within the eye and might be predicted to play important role in follicular tissue expansion and growth. The results indicated that there was a difference in the temporal activation of HAS 2 in mural granulosa cells compared to that of HAS 1 and HAS 3 and clearly it is activated at a different time to that in the cumulus oocyte complex. This suggests that different co-regulators may exist or be recruited by mural cells, which provide fine control of hyaluronan production and hence have the potential to affect follicular fluid osmotic potential and fluid accumulation rates.

Since the results from the HAS 2 in situ results suggested that the signal for the granulosa cells increased many fold during the initial stages of antrum formation, it would have been advantageous to look at expression levels in pre-antral to early antral follicles via Northern blot and RT PCR however; it was not possible to obtain sufficient tissue for these analyses in the given time frame.

RT PCR of HAS 3 indicated that HAS 3 could be amplified in all follicular tissue tested. The Northern blot of follicular tissue identified a single transcript of 1.4 kb and the signal intensity obtained for this transcript was greatest in granulosa and theca cells from 2 – 4 mm follicles. The in situ localisation was similar to that of HAS 1 but with increased

intensity of stain. The increased intensity of stain may have been a result of increased specificity/sensitivity of the probe or indicative of the presence of increased amounts of HAS 3 present. Since the RNA probes used were all species and gene specific it is assumed that the increase in intensity of stain indicated that there was increased amounts of HAS 3 present. In atretic follicles the intensity of stain was marginally reduced. Since the timing of up regulation was not obviously related to the onset of antrum formation, it is thought that again the role of hyaluronan produced by HAS 3 is not primarily associated with this process and that perhaps it may be involved in cell signalling and structural support. The reasons for this are outlined below.

HAS 3 is the most active and stable of the three HAS proteins, synthesising short hyaluronan chains of low-molecular-weight hyaluronan. This form of hyaluronan forms pericellular matrices of comparable size to those created by HAS 2 and can interact with cell surface hyaluronan receptors such as CD44 triggering signalling cascades which lead to changes in cell behaviour (Brinck & Heldin, 1999, Schoenfelder & Einspanier, 2003, Ulbrich *et al.*, 2004). In studies on cell migration HAS 3 and HAS 2 were up regulated by the action of EGF and down regulated by TGFβ in cultured rat keratinocytes, the increase in hyaluronan in these cultures was associated with increased cell migration rates. Down-regulation of synthesis was achieved with hydrocortisone and a significant drop in cell mobility was observed (Pasonen-Seppanen *et al.*, 2003). This same work demonstrated that a similar regulatory effect occurred with CD44 in line with the degree of hyaluronan production. CD44 is involved in the formation of a pericellular matrix, internalisation of hyaluronan (Knudson W. *et al.*, 2002, Tammi *et al.*, 2001), mediation of hyaluronan induced signals, proliferation and migration (Ahrens *et al.*, 2001, Ichikawa *et al.*, 1999).

As with HAS 1, the HAS 3 data do not support a primary role in fluid accumulation. Cells with up-regulated HAS 3 expression assemble a cell surface hyaluronan matrix, which can promote adhesion. Decreases in pericellular hyaluronan concentration have been reported to promote the initiation of cell interactions essential for differentiation (Evanko 1999). If granulosa cells possess such a matrix then the decrease in pericellular concentration might signal the differentiation process required after oocyte expulsion, namely that of the luteal progression of the follicle and formation of a corpora lutea. A strong signal to the HAS 3 message was noted in early stage corpora lutea and this is perhaps indicative of the differentiation processes occurring at this time. Hyaluronan is also known to facilitate cell migration by creation of hydrated pathways. These pathways allow cellular barriers to be penetrated by other cells (Casey & Skubitz, 2000, Itano *et al.*, 2002, Karvinen *et al.*, 2003b). Formation of hydrated pericellular matrices may also facilitate cell rounding during mitosis and perhaps the similar localisation patterns noted from the HAS 1 and HAS 3 in situ data

indicate the cooperation of these enzymes during follicular growth via facilitation of cell division, migration and signalling. Further support for the role of HAS 3 in cellular migration and proliferation roles comes from data relating to its up regulation in colon and prostate cancers (Bullard *et al.*, 2003, Itano *et al.*, 2004, Itano *et al.*, 2002, Karvinen *et al.*, 2003b, Kimura *et al.*, 2002, Monslow *et al.*, 2003, Tienthai *et al.*, 2003) where invasiveness of the tumour can be reduced with inhibition of anti-HAS 3 constructs in vitro resulting in a decrease of the pericellular matrix and inhibition of anchorage independence (Bullard *et al.*, 2003).

Since it is clearly being expressed at all stages of follicle development and in both healthy and atretic follicles it is reasonable to assume that the role of HAS 3 within the follicle is indeed related to cell division, proliferation and migration.

Hyaluronan is known to provide structural stability and elasticity to blood vessels during the increased blood flow and is likely to be important in the control of perivascular flux due to its osmotic buffering capabilities (Rosengren *et al.*, 2001, Sabaratnam *et al.*, 2003, Scott D. *et al.*, 2000(a)). The localisation of all three HAS genes to the endothelial cells of the blood vessels is interesting and appears to provide evidence to support the production of hyaluronan in these areas and suggests that it may be performing these roles. It would be interesting to observe whether changes in strength and localisation of signal occur during follicular growth as this may indicate whether increased or decreased flow is occurring during follicle expansion and following the FSH surge. A preliminary assessment of this within the follicle collection indicated that an increase in the numbers of vessels was present but that there was no increase in intensity of stain (data not shown). The role of hyaluronan surrounding the blood vessels may be important with respect to the filtering effects of the circulating serum.

The blood flow supplied by follicular circulation contains serum albumin. The combination of hyaluronan and albumin has been reported to increase the fluid accumulation capabilities of hyaluronan by synergistic action, forcing the opposition-versus-potential relation upward (Scott D. *et al.*, 2000(a)). If true this would reduce the total amount of hyaluronan required.

A change in hyaluronan concentration will affect the size of molecules able to enter the antrum. Any decrease in hyaluronan concentration such as that seen in the theca interna of large follicles with HAS 2 may lead to decreased filtering capabilities and an increase in the size of molecule able to enter a follicular space. If the molecules able to enter the follicle were larger i.e. proteoglycans and if these were able to bind to hyaluronan, the follicular fluid would have an increased exclusion space over and above that already proposed to occur with

albumin alone leading to increased potential and renewed potential differential and fluid influx to the follicle.

Despite the claims of Spicer and Monslow (Monslow *et al.*, 2003, Spicer & Nguyen, 1999) relating to signal intensity and hyaluronan production the results relating to increases and decreases in hyaluronan production must be tempered by consideration of the as yet unknown action of the hyaluronidases in the follicle. Yoshida et al (2004) reported that decreased expression of the messages for HAS1 and 2 and/or the increased expression of the message for hyaluronidase 2 could be correlated with reduced concentration and decreased average molecular weight of hyaluronan in the joint fluids of patients with osteoarthritis and rheumatoid arthritis (Yoshida M. *et al.*, 2004). Given this report one must expect similar scenarios to occur within the follicle and that fluid accumulation and antrum expansion rely on the interplay of both enzyme groups.

5.5. Summary

In summary HAS 2 production of hyaluronan appeared to produce large amounts of hyaluronan at the start of antrum formation. It is assumed that this occurs in response to either oocyte derived or circulating growth factors. Increased concentrations of hyaluronan would be released in to the follicular fluid by the mural granulosa cells following this signal, where it might be able to form matrices with proteoglycans and collagen. This in turn might lead to an increase in internal follicular osmotic potential over that of the circulating serum causing fluid to flow in to the follicle down a concentration gradient. In the theca similar mechanisms although perhaps dictated by different signalling molecules appear to increase and then decrease the production of hyaluronan. It is likely that this would have some effect on the exclusion barrier firstly maintaining fluid within the follicle by blocking its escape in addition to aiding structural integrity and turgidity. Then following the observed decrease in signal it appears that this barrier is reduced allowing rapid fluid accumulation to occur as the follicle tends towards ovulation.

It is suggested that the primary roles of HAS 1 in the mural granulosa cells and theca are the maintenance of low levels of hyaluronan biosynthesis in order to provide structural stability and hydrated layers for cell proliferation, it may also play some role in the exclusion of larger molecules from the antrum. HAS 3 appears to have a similar role but its inherent stability creates stable pericellular matrix around each cell promoting cellular proliferation, migration and adhesion and perhaps interacting with hyaluronan binding proteins and receptors involved in cell signalling in the ovary. Finally, the as yet unidentified actions of the hyaluronidases must temper this data.

Chapter 6 Final Discussion

The function of the ovary is to produce oocytes and hormones that communicate with the organs involved in reproduction. Ovaries control, or are at least an integral part of many reproductive phases of life, in humans this includes puberty, menstruation, pregnancy and parturition, and menopause (Coutts, 1976). Importantly ovaries do not always function normally and this often results in infertility.

Oocytes mature within ovarian follicles, which undergo complex processes of tissue differentiation, growth and remodelling before ovulation.

During this maturation process follicular fluid accumulates (3-4 ml human, (Wittmaack *et al.*, 1994)) within an antral cavity formed at the avascular centre of the follicle. The functions of this fluid include provision nutrition and protection of the oocyte and follicular cells, transport of the oocyte in to the oviduct at ovulation and structural support of the follicle (Gosden R. G. *et al.*, 1988).

The accumulation of fluid in follicles is thus very important. It comes as a surprise then that there has been no investigation in to how follicular fluid forms.

In women the commonest cause of anovulation, polycystic ovarian disease (PCO), results from the apparent halting of follicular growth at about 5mm diameter. The cause of this is not known, but if the mechanism underlying fluid accumulation could be identified it may be possible to determine the aetiology of PCO syndrome. The rapid expansion of the follicle is considered the signal to ovulation, and yet despite several hypotheses there is no absolute data or clear understanding of what the physical causes are and what molecules are involved.

In the body, fluid movement is controlled by the hydrostatic pressure provided; by active physical pumps (heart), chemical/ ionic pumps (kidney) and osmosis (vasculature). Plasma proteins are an important part of the osmotic regulation of this system. If the protein levels are low then tissue oedema can occur (Negrini *et al.*, 2003).

To cross from the plasma to the cells or vice versa, substances must either cross both membranes of the endothelial cells or travel between the cells and then cross the basement membrane. Proteins that cannot cross the capillary walls exert an osmotic pressure in the capillaries and it is this fluid potential that provides the majority of the forces driving fluid accumulation.

Osmotic pressure equates to osmotic potential when the forces driving the water in to a system are in equilibrium with those driving it out. In general the osmotic pressure of a system is described in terms then of the potential of the fluid or the pressure caused by the fluid.

Current data on the colloid osmotic pressure of follicular fluid has been obtained from studies conducted in human, cow and rat (Edwards, 1974, Shalgi *et al.*, 1972a, Zachariae, 1958). Due to the availability and ease of access to fluid samples the majority of these data have been obtained from the fluid of artificially stimulated pre-ovulatory follicles, with no studies considering the osmotic pressure of fluid from smaller follicles. There is a large discrepancy in the literature as to the colloid osmotic pressure of follicular fluids ranging from them being less than, to equal to, or greater than that of serum (Edwards, 1974, Shalgi *et al.*, 1972a, Zachariae, 1958) and hence a number of hypotheses have been generated as to how fluid accumulation in the follicle may occur.

Additionally, the majority of these data were reported as secondary findings obtained from experiments designed to investigate different primary research initiatives. Thus the experiments were not specifically designed to identify the colloid osmotic pressure of the fluids from different developmental stages or the molecules responsible for that potential. Consequently, there is no data set available for the colloid osmotic pressure of fluid from a range of follicle sizes from a single species, nor has there been any attempt to identify the key molecules responsible.

To understand antrum formation a detailed knowledge of changes in the physiology of the follicle during maturation is required. Changes in the extracellular matrix, steroid and cytokine signals and the structural and physiochemical properties of the molecules in follicular fluid, are all likely to impact on its movement and accumulation, and as such are all critical factors involved.

Good reviews are available on cellular changes in the follicle (Armstrong *et al.*, 2003, Fraser H. M. & Wulff, 2001, Moley & Schreiber, 1995, Patino *et al.*, 2001) and there is some limited research identifying changes in basal lamina constitution and permeability throughout follicular development. Similar data exists for the theca layers surrounding the follicle (Rodgers R. J. *et al.*, 2003, Rodgers R. J. *et al.*, 1999a, Rodgers R. J. *et al.*, 1999b).

Follicle stimulating hormone stimulates the formation of the antrum and follicular fluid accumulation, (Edwards, 1974, Fortune *et al.*, 2001, Ginther *et al.*, 1999, Gosden R. G. *et al.*, 1988, Rondell P, 1964, Shalgi *et al.*, 1972a, Wise & Maurer, 1994, Zachariae, 1958). Fluid accumulation rates are initially steady and then increase following the surge in LH (Kemeter & Feichtinger, 1991, Marion *et al.*, 1968b) via increases in the number of blood vessels, the permeability of the basal lamina and the arterial tension (Mattioli *et al.*, 2001).

The follicle is separated from the general circulation by a diffuse blood-follicle barrier created by the granulosa cells, basal lamina and theca cell layers (Rodgers R. J. *et al.*, 2003). The basal lamina acts as a semi-permeable membrane with a nominal molecular weight cut off at approximately 100 kDa, following the LH surge it becomes more permeable. Follicular

fluid accumulates as pockets between the granulosa cells, which coalesce to form the fluid filled antrum (Gosden R. G. & Hunter, 1988). Changes in the permeability of the blood-follicle barrier provide some control over fluid movement and volume regulation in the follicle. These changes will most likely also affect local concentrations of cell signalling and expression, critical to oocyte development (Gosden R. G. & Hunter, 1988, Gosden R. G. *et al.*, 1988).

Proteoglycans and glycosaminoglycans are large osmotically active molecules involved in several fluid accumulation systems in the body such as wound healing, the temporomandibular joint and the eye (Aukland *et al.*, 1997, Brown *et al.*, 1991, Eriksen *et al.*, 1994, Fraser J. R. *et al.*, 1997). It has been proposed by several authors that they are also active in the follicle (Boushehri *et al.*, 1996, Grimek *et al.*, 1984, Monget & Monniaux, 1995, Rodgers H. F. *et al.*, 1995a, Yanagishita *et al.*, 1979), having been previously identified in whole follicle extracts, follicular fluid and to be produced by granulosa cells (Boushehri *et al.*, 1996, Grimek *et al.*, 1984, McArthur *et al.*, 2000). The available data on proteoglycan and glycosaminoglycan activity in other fluid accumulation scenarios suggests they should be considered as candidates involved in the osmo-regulation of the fluid in the antrum. However, no one has attempted to demonstrate specific effects in the follicular fluid until now.

If the osmotic potential of follicular fluid can be demonstrated to be higher than serum, it would appear reasonable to assume that directional flow would occur from the vascular theca in to the avascular antrum along an osmotic gradient. So the principal driving force behind follicular fluid accumulation could then be attributable in part to the osmotic potential of the fluid itself.

The fine-tuning of the osmotic potential of follicular fluid controls this gradient.

At the outset of this work it was hypothesised that granulosa cells secrete large macromolecules in to the fluid, where on being too large to escape the follicular basal lamina they create an increase in osmotic potential of follicular fluid over that of serum, creating an osmotic gradient. The ability of the follicular fluid to draw more fluid in to the follicular antrum is dependent on the permeability of the follicular wall and the formation and permeability of the vasculature. In addition directional flow was assumed to occur in order to prevent stromal oedema on the appearance of the follicular vasculature.

The experiments carried out in this thesis were specifically designed to provide a data set to demonstrate the existence of an osmotic gradient and identify some of the molecules involved. In addition localisation of the time and point of synthesis of the most osmotically active of these was assessed. Since existing data relates primarily to pre-ovulatory follicles this thesis aimed to provide a data set for a range of developmental stages and health status. In

recognition of a void in the literature the studies described in this thesis form the basis of a project designed to answer some of the following questions:

1. Does an osmotic gradient exist between serum and follicular fluid above molecules 100 kDa ?
2. What sizes and class of molecule contribute the most to the colloid osmotic pressure of follicular fluid and what is their identity?
3. Are these molecules synthesised within the follicle and if so by which cells?
4. Is there sufficient evidence to suggest they have a significant role in antrum development?

To begin with follicular fluid from individual follicles (8 – 30 mm) was collected and the volumes of fluid aspirated from each follicle recorded. The results demonstrated that there was an unbiased sampling of fluid across the size range of follicles used. Increases in follicular diameter and fluid volume indicated that in the early antral stages of growth fluid accumulation rates are slow and this corroborated previous reports (Marion *et al.*, 1968b, Paesi, 1949(a), 1949(b)).

To ascertain whether the colloid osmotic pressure of follicular fluid from increasing size of follicles was different to that of serum, the potential of pooled undiluted follicular fluids from follicles of 2 – 16 mm diameter was measured and compared to that of whole serum. The ratio of fluid colloid osmotic pressure to serum potential, changed during the period of antrum growth, moving from a positive to a negative relationship. This indicated that the colloid osmotic pressure of follicular fluid was indeed different to that of serum and supported the osmotic gradient hypothesis. In addition it suggested that previous reports showing contradictory data, might all have been correct, the contradictions arising from the different developmental stages sampled and species variation and not necessarily from the experimental regimen.

The differences between fluid and serum potentials observed were within the range required to drive directed fluid movement along a gradient (+ 2 cm water) in to the follicle (Miserocchi *et al.*, 1992, Miserocchi *et al.*, 1984, Negrini *et al.*, 1990). This gradient appeared to be developmentally dependent since the measured potential changed with size of follicle.

These data suggested that fluid movement and accumulation is probably driven by osmosis, caused by the osmotic differential between fluid and serum. The change in osmotic potential from a positive relationship to a negative one that is from fluid osmotic potential being greater than serum to less than serum coincided with the period when the rate of fluid

accumulation was at its greatest. The reduction in potential may well have resulted from hydrolysis and degradation of larger molecules (Zachariae, 1960) and although not within the scope of this work, further investigation of this process may resolve this issue.

If hydrolysis occurs during the latter stages of antrum growth, one would expect to see an initial increase in total colloid osmotic pressure, as noted in the 16mm follicles, caused by an increase in a total number of molecules. As these molecules became degraded they would be able to escape the basal lamina and the potential effect would be reduced.

It is probable that the rapid influx of fluid during the later pre-ovulatory stages occurs by osmosis driven peri-cellular flux, but is assisted by the increased capacity for flow offered by aquaporins (McConnell *et al.*, 2002, Sui *et al.*, 2001) and greatly increased permeability of the follicle. Further investigation of the composition of fluid from the pre-ovulatory follicles would be required to confirm this.

The identification of the molecules responsible for the greatest fluid potential measured was achieved by a series of experiments designed to determine what size of molecules were responsible, such that it could be determined with some degree of accuracy as to whether the molecules had been synthesised by granulosa cells in the follicle or imported from serum. Dialysis removed the molecules, which might be prevented from entering or leaving the follicle by the blood-follicle barrier, starting at 100 kDa and differences between the follicular fluids from healthy and atretic follicles were identified. The results indicated that removal of molecules <100 kDa had little effect on the total potential measured from either fluid source. This indicated that salts and small molecules were free to cross the "barrier" and not likely to regulate the osmotic potential in the ovarian follicle as in the kidney (Lever & Kriz, 1966), suggesting difference in the mechanisms of fluid movement.

Molecules >300 kDa contributed 65% of healthy and 71% of atretic fluid potential. Molecules >500 kDa contributed 40% of healthy and 20% of atretic fluid colloid osmotic pressure. Subtle differences between the constitutions of follicular fluid from each existed. The subtle differences observed between the fluids of healthy and atretic follicles may be reflective of a follicular progression to atresia. These differences perhaps result from an inability of the cells of the atretic follicles to synthesise or an increased degradation of, these larger molecules. The data obtained in subsequent in situ experiments suggested that degradation of larger molecules might be occurring in the atretic follicles. This will be discussed later.

This data indicated that molecules of a size not easily able to escape the follicle were the main contributors to the colloid osmotic pressure of follicular fluid and of a size to suggest they were synthesised locally.

The classes of molecule contributing to the colloid osmotic pressure of fluid from healthy and atretic follicles was identified by differential enzyme digestion followed by dialysis at 100 kDa or 300 kDa.

Identification of the classes of molecule contributing to the colloid osmotic pressure of fluid from healthy follicles revealed that hyaluronan, CS/DS proteoglycans, collagen and DNA or their aggregates were responsible for the majority of the fluid potential. DNA, protein and collagen were responsible for the colloid osmotic pressure recorded from the fluid from atretic follicles. The identification of these classes of molecule in follicular fluid was not unexpected since hyaluronan and proteoglycans have previously been isolated from pre-ovulatory fluid (Boushehri *et al.*, 1996, Eriksen *et al.*, 1999, Grimek *et al.*, 1984, Yanagishita *et al.*, 1979) and all these molecules are osmotically active in other fluid recruitment systems, where hyaluronan and proteoglycans provide the negative charge required for osmotic activity.

Terminal follicular maturation occurs by the action of FSH on the granulosa and theca cells. Granulosa cells have been shown to synthesise proteoglycans and glycosaminoglycans in response to FSH (Ax & Ryan, 1979, Ball *et al.*, 1982, Bellin *et al.*, 1983, Eppig & Ward-Bailey, 1984, Schweitzer *et al.*, 1981, Yanagishita *et al.*, 1981).

Evidence supplied by Bellin showed that small follicles were responsible for producing the lager proteoglycans while the larger follicles produced smaller ones, with proteoglycan production inhibited by the LH surge (Bellin *et al.*, 1983). Individual modulation of the components of the matrix that might be required to service follicular needs have been noted i.e. bronchial wall, wound repair and certain tumours (Eikenes *et al.*, 2004, Gapski *et al.*, 2004, Yuan *et al.*, 2003). In these cases differential control of matrix components alters the amount of fluid present and the strength of the matrix. Similar control mechanisms might be expected in follicular fluid.

DNA was observed to contribute to the colloid osmotic pressure of follicular fluid. The contribution of DNA to the colloid osmotic pressure was interesting. DNA can create an osmotic potential in its own right by entanglement with other macromolecules present in a matrix, thus minimising the loss of DNA or macromolecule such as hyaluronan (Turner *et al.*, 1988). The DNA found in follicular fluid was likely to be derived from granulosa cells aligning the follicular antrum, which upon their death, release their DNA in to the follicular fluid (Van Wezel *et al.*, 1999). DNA, whilst contributing to the colloid osmotic pressure of follicular fluid, is unlikely to be a regulated contributor.

The osmotic data also revealed that collagen contributed to fluid colloid osmotic pressure. That collagen contributed to fluid colloid osmotic pressure was worthy of note since granulosa cells are known to produce collagen in culture (Zhao Y. & Luck, 1995). Some

collagens are known to bind and carry glycosaminoglycans and proteoglycans, and are therefore referred to as part time proteoglycans (Dong S. *et al.*, 2003, Halfter *et al.*, 1998). Increases in extra-fibrillar space result in excluded volumes and increased colloid osmotic pressure. Analysis of the digestion products of collagen indicated that none were large or osmotic enough to affect fluid osmotic potential. The extra-fibrillar space surrounding whole collagen is increased by the negative charges associated with the glycosaminoglycan chains of the attached proteoglycans surrounding the collagen. This increase would increase the excluded volume and result in and raise the overall colloid osmotic pressure. Thus the effect on colloid osmotic pressure noted by the removal of collagen was solely related to the collagen itself and its effect on associated matrices and not its digestion products.

Finally, the colloid osmotic pressure data identified that hyaluronan contributed the greatest proportion of the potential recorded. The hyaluronan species present ranged in size from 400 kDA to 2 x 10^6 Da by gel electrophoresis. From the experiments conducted, enzyme digestion and removal of molecules >300 kDa indicated that hyaluronan contributed 58% of the measured colloid osmotic pressure in follicular fluid from healthy follicles. That hyaluronan contributed so much to fluid osmotic potential was not surprising. One of the effects of hyaluronan is that it can greatly increase the osmotic potential of a fluid or gel. This is possible because hyaluronan can take on water of hydration resulting in a solvent domain 10, 000 times its original polymer volume (Scott J. E., 1998). This results in the ability to rapidly hydrate tissues if required (Fraser J. R. *et al.*, 1997, Itano *et al.*, 1999, Knudson C. B. & Knudson, 1993, Laurent T. C. & Fraser, 1986, 1992, Laurent T. C. *et al.*, 1995b, Scott D. *et al.*, 1998b). Conversely, regulation of its production to produce low levels and or hyaluronan fragmentation by hyaluronidases can result in slow and progressive hydration (Itano *et al.*, 1999). Interestingly, it has been reported that high levels of hyaluronan are present during rapid cell proliferation and wound repair, while enhanced but lower levels are recorded during swelling and wound fluid accumulation. This suggests that levels of hyaluronan required for fluid accumulation processes need not be high.

In addition to their existence as separate entities that in the follicle, hyaluronan may form some large complex matrices with proteoglycans and collagen such as those that occur in the eye (Bishop, 2000). These matrices have the ability to significantly increase exclusion volumes and osmotic potentials of any matrix without requiring large increases in concentration of either proteoglycans or hyaluronan.

FSH stimulates the formation of the antrum (Johnson Martin H. & Everitt, 2000) and it is likely that this signal also stimulates hyaluronan and proteoglycan synthesis in the follicle.

The individual contributions to the colloid osmotic pressure, when added together of hyaluronan (43%), CS/DS proteoglycans (53%) and collagen (20%) as a percentage of the

total implied that the overall potential of follicular fluid was greater than 100%. The reason for this is that if, some of these molecules are involved in matrices with each other, the contribution of each of these molecules is not mutually exclusive. Removal of any one of these molecules would affect the osmotic potential created by those that remain, since its removal may also disrupt any aggregate or matrix of which it is a part. An example of this occurs in arthritis. In arthritis, hyaluronan and albumin act together at normal concentrations to conserve synovial fluid in the presence of raised drainage potentials. Hyaluronan acts osmotically by concentration polarisation of the boundary layer. Attenuation of this effect by degradation of the hyaluronan affects the albumin structure within the matrix causing degradation of the whole matrix. This affects the osmotic capabilities of that matrix by a greater amount than removal of hyaluronan alone (Scott D. *et al.*, 1997).

Specific identification of some of the chondroitin sulphate proteoglycans and characterisation of hyaluronan present was required to determine the constituents and nature of the fluid matrix. Since the colloid osmotic pressures of healthy and atretic fluids were not statistically different and hyaluronan was the major contributor to the potential of both fluids, the analysis of follicular fluid was continued using pooled fluids from healthy and atretic follicles of comparable size to those used in previous analyses. CS/DS proteoglycans were isolated and a number were identified using a bank of antibodies to proteoglycans previously reported in the ovary.

The proteoglycans identified were versican V_0 and V_1, the inter-alpha trypsin inhibitor heavy chains and bikunin. The hyaluronan present was found in a range of sizes from 400 kDa to $> 2 \times 10^6$ Da the latter being present in the fluid collected from follicles 10 – 14 mm from which the measured colloid osmotic pressure was highest. The existence of other chondroitin/dermatan sulphate proteoglycans is acknowledged but they could not be detected without specific antibodies or further exhaustive testing.

The identification of versican confirmed previous reports from extracts of whole bovine follicles (McArthur *et al.*, 2000, Russell *et al.*, 2003), human follicular fluid of ovulating follicles (Eriksen *et al.*, 1999), and follicular membrana granulosa (McArthur *et al.*, 2000). Versican and ITI are involved in expansion of the cumulus oocyte complex (Camaioni *et al.*, 1996, Carrette *et al.*, 2001), whereby the heavy chains of ITI become covalently cross-linked to hyaluronan, stabilising the expanding cumulus matrix (Carrette *et al.*, 2001, Eriksen *et al.*, 1997, Kimura *et al.*, 2002, Laurent C. *et al.*, 1995a, Saito *et al.*, 2000). In the case of follicular fluid a similar but more fluid matrix exists and that the versican contributes to the potential of the fluid via its chondroitin sulphate side. Differential expression of versican splice variants is believed to control the hydration properties of the pericellular hyaluronan environment (Dours-Zimmermann & Zimmermann, 1994). If true, variation in the isoforms expressed in

the matrix of the mural granulosa cell might also modulate the interactions with the extracellular matrices of neighbouring cells during maturation. Further investigation of splice variant expression in mural and cumulus associated granulosa cells would be required to establish this.

Of particular interest was the apparent uneven distribution of versican localisation noted by immunohistochemistry. If some of it is linked in a matrix with hyaluronan then this suggests an uneven distribution of hyaluronan might also exist. Schoenfelder and Einspanier (Schoenfelder & Einspanier, 2003) have reported sporadic distribution of hyaluronan in granulosa cells previously. The in situ hybridisation data supported that report, as hyaluronan synthase expression was not detected in a uniform pattern in some follicles.

Uneven tissue distribution of chondroitin sulphate proteoglycans and glycosaminoglycans in some matrices has also been noted. This non-uniform distribution has been linked to the provision of migratory pathways for growth factors with non-uniform binding to molecules providing a local distortion of otherwise helical glycosaminoglycans, in order to present specific motifs to protein for binding (Perissinotto *et al.*, 2000, Soto-Suazo *et al.*, 2002). Whether versican is providing cell migratory pathways or presenting specific binding motifs as either a primary or secondary role in this matrix is unknown.

In bovine follicular fluid ITI was observed in follicular fluids prior to the LH surge and this is in direct contradiction to the data reported by Chen et al (Chen L. *et al.*, 1992) who observed it in fluid only after the LH surge in mice. The data although contradictory to that published in the mouse, was in agreement with that of the porcine data reported by Nagyova et al (Nagyova *et al.*, 2004). The presence of ITI in follicles of a non-ovulatory size indicated that it might have additional roles in the bovine and porcine systems.

This may be related to the need to form an extended hyaluronan matrix early in follicular development. If, follicular hyaluronan binds to ITI, hyaluronan would have an increased capacity to raise the osmotic potential of the fluid to provide a sufficient osmotic differential between serum and fluid, to drive the osmotic recruitment of increased fluid volumes required by the significantly larger follicles of these animals. In this thesis the data has shown that the colloid osmotic pressure of follicular fluid in small follicles is greater than that of serum and sufficiently different to create an osmotic gradient.

Since ITI is not seen in the mouse prior to cumulus oocyte expansion one might assume that it is not necessary for the small amounts of fluid accumulated in the mouse follicle (20% fluid to follicle ratio as opposed to 90% in the cow (Rodgers R. J. *et al.*, 2001)) and that hyaluronan alone is not sufficient to recruit the larger fluid volumes required by the bovine follicle.

Western blotting and immunohistochemistry revealed that ITI was in high concentrations in the fluid of healthy follicles and could be co-localised around the granulosa cells with versican, while atretic follicles had reduced levels of both and no staining was observed in the fluid. These data suggested that the granulosa cells might also be a source of the ITI in the fluid, in addition to that sequestered from the serum. The reduction noted within the atretic follicles was interesting. Since it is unlikely that the atretic follicle could physically exclude ITI and ITI were free to cross the follicular barrier from serum to follicle it would have been detected in equal amounts in the atretic follicles. Why then is ITI not seen in the same high levels in atretic follicles? The answer may lie in the fact that in healthy follicles it is either developmentally regulated or actively destroyed, and that expression studies of ITI components may solve this dilemma.

Hyaluronan, versican and ITI were identified as significant contributors to the maintenance of follicular fluid colloid osmotic pressure. It is interesting to note that the same molecules appear to be active in both fluid accumulation in the follicular antrum and cumulus oocyte expansion process however, the timing and location of their appearance and fluidity of the matrix formed is quite different and therefore are probably differentially regulated.

There are several groups worldwide investigating the roles of ITI and versican in the cumulus oocyte matrix in the mouse and pig and it is likely their control mechanisms will be elucidated in the future. The focus of this thesis was to provide information on the molecule with the greatest effect on osmotic potential of follicular fluid and evaluate whether its production was developmentally regulated. Thus the investigations continued in to the production of hyaluronan.

Hyaluronan has been identified in follicular fluid (Hamamah *et al.*, 1996, Jessen & Odum, 2003, Jessen *et al.*, 1994, Odum L. & Jessen, 2002, Saito *et al.*, 2000, Sato *et al.*, 1987a, Suchanek *et al.*, 1994, Tempel *et al.*, 2000) but the cellular origin, characterisation of the nature of the hyaluronan produced and the timing of its production had not been investigated.

The sizes and stabilities of the hyaluronan produced by the three HAS enzymes, the cells in which the synthesis occurs, environmental conditions present and hyaluronan clearance mechanisms are key to the actual levels and functions of hyaluronan in the follicle.

Hyaluronan synthesis is triggered by gonadotrophins, cytokines and growth factors (Fulop *et al.*, 1997a, Knight & Glister, 2003, Laitinen *et al.*, 1998, McGrath *et al.*, 1995, Salustri *et al.*, 1999, Stock A. E. *et al.*, 2002) and it is likely a delicate balance between these and hyaluronan degradation and clearance mechanisms control local follicular hyaluronan levels. The size of hyaluronan produced and its ability to interact with proteins in solution provide hyaluronan with the opportunity to change its conformation and thus the physicality

of any hyaluronan rich matrix of which it is a part. This is probably the key to its functional diversity within a matrix.

A series of experiments was designed to characterise hyaluronan expression in the follicle and investigate whether its synthesis could be correlated with antrum formation.

In order to determine where and by which cells in the follicle the hyaluronan was being produced, and whether this was developmentally linked, existing molecular and histochemical technologies were used. Bovine specific, HAS specific RNA probes to the three synthases were made and ovaries with healthy and atretic follicles collected for in situ hybridisation analysis. The follicles used in these analyses incorporated the sizes of follicle, which had previously recorded significant changes in colloid osmotic pressure. At the same time three pools of granulosa and theca cells from uncharacterised small medium and large follicles were collected and RNA extracted for PCR and Northern blot analyses for detection of the levels of the HAS forms present.

The in situ hybridisation, Northern blotting and RT PCR data showed that HAS 2 expression was linked to the visualisation of an antrum. HAS 1 and HAS 3 were expressed in all follicles in the granulosa and theca cells throughout follicular development. Roles for each of the HAS genes is proposed below.

HAS 1 was present in the granulosa cells of up to 70% of primordial and primary follicles and in both cell types of approximately 90% of secondary and early antral follicles. HAS 1 was present in both cell types of nearly all healthy antral follicles examined. The signal from the atretic follicles examined was noticeably reduced. Whether this reduction was indicative of the atretic process is not known. The reduced signal for hyaluronan in atretic follicles supported the data obtained by immunohistochemistry. If hyaluronan is a key contributor to either the cell or fluid matrices, that reduced presence or absence would be detrimental to follicular health and viability.

The detection of HAS 1 and HAS 3 expression by granulosa cells was interesting in the light of the work published by Schoenfelder and Einspanier (Schoenfelder & Einspanier, 2003). While there is no data on cumulus cell synthesis presented here, we disagree with their report stating that HAS 1 mRNA was "not detectable" in granulosa cells and that HAS3 expression was limited. There were clear differences between that work and this. Schoenfelder and Einspanier used FSH and LH stimulated granulosa cell cultures. They showed that HAS 1 expression could not be induced by either of the above whereas HAS 3 expression could be increased. They also reported that cultured granulosa cells expression of HAS 2 and 3 could not be maintained beyond 24 h with either FSH or LH. These data suggest that stimulation of HAS 1 in cultured granulosa cells may require a different factor to that of HAS 2 and 3 and that granulosa cells cultures are not good models for long-term studies of

hyaluronan synthesis. It is interesting to note that in their control tissues (whole ovary extracts) HAS 1 and 3 were clearly detectable, while perhaps considered derived from stromal tissue, Schoenfelder and Einspanier make no comment on their presence.

In several body systems hyaluronan is the key regulator of fluid accumulation. In the follicle, the data obtained here did not suggest that HAS 1 production of hyaluronan was temporally linked to antrum formation, despite evidence suggesting HAS 1 is active in synovial fluid production (rabbit) (Tanimoto *et al.*, 2004) and known to be stimulated by TGFβ, present in the developing follicle (McNatty *et al.*, 2000). HAS1 expression was detected in advance of antrum formation and its expression level did not change in line with expected increases in fluid requirements. Thus, it is necessary to consider some of the other functions of the polymer produced by this enzyme. As mentioned earlier, hyaluronan levels are high in tissues undergoing proliferation, migration (Tempel *et al.*, 2000) and those involved in fluid accumulation. As such it is not unreasonable to expect that the synthases responsible for these processes show equivalent elevations of their expression. The Northern blot data indicated that the expression of both HAS 1 and HAS 3 was greater than that of HAS 2. It is more likely therefore that the primary role of HAS 1 in the follicle is related to cell division and migration and the creation of cell migration "highways" by the hyaluronan rich extracellular space (Ichikawa *et al.*, 1999). Such a matrix would allow granulosa and theca cells to migrate and or pass over one another during follicular growth. One study has shown that the size of the hyaluronan pericellular coat produced by HAS 1 is small and that this promotes cell growth (Itano *et al.*, 2002). Moreover, HAS 1 is known to be critical in the disease progression of cancer, having an active role in migration and cell division (Yabushita *et al.*, 2004). The reduced HAS 1 signal detected in atretic follicles supports the cell division premise, since cell division and migration are reduced in these follicles and the requirement for migration highways in these follicles is reduced.

The signal for HAS 3 was strong in the granulosa cells of the small healthy follicles and granulosa and theca cells of large healthy follicles. Approximately 65% of primordial to early antral follicles expressed HAS 3. The signal was also detected in the majority of follicles > 2 mm diameter and these data were confirmed by Northern blot and RT-PCR. The data showed that HAS 3 expression was occurring in most of the follicles prior to antrum formation but was expressed in all follicles only after the antrum had already formed. As such it could not be temporally linked to antrum formation and is unlikely to be directly involved in fluid accumulation at this time.

Studies in inflammatory migratory cells have shown that HAS 3 does not contribute to the fluid of the synovium since the hyaluronan it synthesises is retained in a pericellular

matrix and does not diffuse in to the joint cavity (Yoshida M. *et al.*, 2004). Again, alternative reasons must be suggested for the presence of HAS 3 in granulosa cells.

HAS 3 is known to promote cell adhesion, proliferation and migration and to be involved in tumour invasion in the colon and prostate and therefore it is not unreasonable to suppose it might facilitate cell division, proliferation and migration in the follicle. During the rapid growth phase associated with the expanding antrum, the granulosa and theca cells replicate rapidly in order to accommodate the expanding antrum (Rodgers R. J. *et al.*, 2001). This process would require maximal production of the molecules assisting these processes to occur. If the primary roles of HAS 3 are to assist cell division and proliferation, a maximal signal for this synthase located in these cells would be expected. The data obtained from the in situ analyses appears to support this proposal, with the most intense staining observed in those cells aligning the basal lamina. With HAS 1, where support of division and migration appear to be the primary roles, a similar staining pattern to that of HAS 3 would be expected.

The results obtained for HAS 2 appear to provide the greatest insight in to the role of hyaluronan in fluid accumulation. The HAS 2 enzyme is responsible for the rapid production of high molecular weight hyaluronan that has the ability to rapidly hydrate tissues. This function alone would suggest that it is a suitable candidate for a role in fluid accumulation in the follicle, being able to provide rapid increases in fluid hyaluronan levels and hence osmotic potential and fluid uptake.

In situ hybridisation data showed that HAS 2 expression could be correlated with the visualisation of a follicular antrum. The HAS 2 signal was noticeably reduced in the atretic follicles observed and the contribution of hyaluronan to atretic fluid colloid osmotic pressure was also reduced. The lower levels of HAS 2 detected in the smaller follicles by in situ hybridisation appeared to provide some explanation of why fluid accumulation is slow in small follicles even though the surface area to volume ratio is higher than at later stages. Whether a lower fluid potential is created by hyaluronan alone in these small follicles or whether there is a reduced hyaluronan matrix or increased hyaluronan degradation is not known at this stage. The presence of ITI in the fluid from follicles of 2 mm suggests that some of the components for an extended hyaluronan matrix do exist.

Fluid from follicles < 2 mm was not collected, as it was not feasible to collect the volumes required for colloid osmotic pressure measurement. If a method of potential measurement could be devised whereby minute volumes of fluid could have been tested it would be interesting to see whether the change in HAS 2 expression at antrum formation could be detected by a concurrent change in colloid osmotic pressure of the fluid. Since fluid could not be collected this phenomenon could not be investigated further.

In situ hybridisation and Northern blot data showed that maximal expression of HAS 2 occurred in 6 – 8 mm diameter and some smaller follicles of the 12 mm – 15 mm group. The fluid colloid osmotic pressure data recorded for this group was also the maximum recorded. Maximal hyaluronan production by HAS 2 is reportedly responsible for rapid wound fluid accumulation in burns victims and appears to be the standard mechanism used by the body when large fluid volumes are required. In these cases hyaluronan represented an entirely separate entity where it acted purely as a volume expander (Onarheim *et al.*, 1991).

The decrease in HAS 2 expression observed in the granulosa cells of large preovulatory follicles (16 mm diameter – general observation - data not shown) corresponded with the drop in measured colloid osmotic pressure of that fluid. It is not surprising that a decreased production, in conjunction with probable degradation of hyaluronan and increased fluid flow in to the follicle would result in a lowered colloid osmotic pressure of the fluid.

The molecular structure of HAS 2 gene suggests it is sensitive to cell specific effects and under tight regulatory control from steroids or growth factors (Monslow *et al.*, 2003). Regulatory control of hyaluronan synthesis has been shown in the past by several authors and suggested by many, but results from the few experiments conducted have indicated that more than one factor is capable of stimulating production depending on the cell type, location and signal received (Dragovic *et al.*, 2005, Juengel & McNatty, 2005, McNatty *et al.*, 2005a, b, Thomas *et al.*, 2005). The recent suggestion by Salamonsen et al (Salamonsen *et al.*, 2001) that differential steroid signalling controlled hyaluronan synthesis certainly appears an attractive hypothesis. Promoters and cell dependency are the probable keys to transcription factor recruitment of co-regulators and the mediation of transcription and processing of the HAS 2 gene. The expression of each HAS enzyme in mural granulosa cells was temporally different and this suggests that different co-regulators exist. In order to complete this preliminary study and elucidate the complete mechanism behind fluid accumulation in the follicle it will be necessary to conduct a full investigation in to the regulatory control of HAS 2 in the follicle. At the very least an evaluation of the regulation of transcription of HAS 2 by each of the growth factors and cytokines known to be involved in its stimulation i.e. FSH, TGF super-family members, PDGF, EGF, FGF and IGF must be completed in mural granulosa and theca cells (Fulop *et al.*, 1997a, Knight & Glister, 2003, Laitinen *et al.*, 1998, McGrath *et al.*, 1995, Salustri *et al.*, 1999, Stock A. E. *et al.*, 2002).

The diffuse signal for hyaluronan obtained from some atretic follicles during in situ hybridisation experiments may be indicative of hyaluronan degradation and breakdown of the nuclear membrane (Evanko 1999; Evanko 2004). Degradation of hyaluronan results in an increase in the number of smaller fragments of hyaluronan (300 kDa to 500 kDa) and may

partially explain the slight increase in the proportion of this size of molecule detected in fluid from atretic follicles.

HAS expression in the theca was interesting since its presence in this tissue does not appear to result in any oedema of the stroma. Hence, different roles for hyaluronan may exist in the theca to those of the granulosa cells. Northern blot and in situ hybridisation data using the HAS1 and HAS 3 probes showed their expression in the theca was strong and that localisation changed over time. A role for HAS 1 in the theca may be linked to the provision of structural stability and elasticity to the blood vessels, required in conditions of increased blood during antrum formation (Balazs, 1968, Rondell P., 1970, Swartz *et al.*, 1999). The intense staining found in the endothelial cells surrounding the blood vessels supports this hypothesis. The hyaluronan produced by HAS 1 in this location may have some filtering capability by increasing the resistance to flow (McDonald & Levick, 1994, Rosengren *et al.*, 2001) and aid in the regulation of blood flow around the follicle.

Any degradation of the hyaluronan in this area would create a more open structure, allowing freer flow of molecules in to and out of the follicle depending on their size and charge.

Monslow et al (Monslow, Williams et al. 2003) showed that HAS expression levels could be directly linked to hyaluronan production. If this is true the higher levels of expression of all the HAS genes detected in the granulosa cells over that of the theca cells in small follicles may be representative of a higher concentration of hyaluronan in granulosa cells over that of theca cells. If the degradation of hyaluronan was equal in both cell types, the data might represent a visualisation of a hyaluronan gradient. Assuming this exists it would provide a means of directional flow of fluid in to the follicle, although whether hyaluronan gradients exist in the interstitium, as have been proposed for electrolyte gradients is yet to be determined (Schwartz, Kaipainen et al 1999).

The decrease in HAS 2 expression seen in the theca cells of the large follicles corresponded with the drop in measured colloid osmotic pressure of the fluid. It is likely that this drop was assisted by the proposed decrease in filtering capabilities of the follicle at this time. This reduction would result in a decreased resistance to flow in to the follicle. An increase in fluid flux would result from the initial increase in colloid osmotic pressure differential caused by probable hydrolysis of the proteoglycans and hyaluronan in the fluid (Saito *et al.*, 2000, Salustri *et al.*, 1990b, Salustri *et al.*, 1992, Salustri *et al.*, 1999, Scott D. *et al.*, 2000(a), Zachariae, 1958).

Hyaluronan appears to be the most osmotically active molecule in follicular fluid. The turnover of hyaluronan in the follicle is no doubt a key factor in the regulation of fluid osmotic potential. Hyaluronan degradation or depolymerisation is achieved by two

mechanisms, enzymatic and non-enzymatic. Hyaluronidases, chondroitinases and hexosaminidases degrade hyaluronan (Laurent U. B. *et al.*, 1992). The six mammalian hyaluronidases like the hyaluronan synthases are presumed ancient genes. The major hyaluronidase found in serum is a 57kDa protein, hyaluronidase 1 (Hyal-1). Degradation of hyaluronan occurs by sequential endolytic cleavage, which generates increasing numbers of smaller fragments of hyaluronan within a solution or fluid. The different sized fragments have differential effects on the behaviour of certain cell types. In vitro these effects have included inflammatory gene expression, cell migration and proliferation and angiogenesis (Ahrens *et al.*, 2001, McKee *et al.*, 1996, Noble *et al.*, 1996, West *et al.*, 1985), with the function of fragmented hyaluronan proven to be different to different to that of the native molecule.

It is believed that the hyaluronidases reside in an inactive form in many cell/fluid matrices because if they were active, the matrix would break down. Efficient in vivo activation provides a more rapid response mechanism for altering local levels of hyaluronan, than relying on its synthesis alone.

A second method of modulating hyaluronan concentrations is provided by receptor-mediated pathways, which facilitate hyaluronan removal from the lymph and vasculature. The local receptor for such activity is CD44. It is thought that CD44 aids in the clearing of small fragments of hyaluronan by binding it at the cell surface and internalising it delivering it to the lysosomes however; the mechanism for this is as yet unknown (Aguiar *et al.*, 1999, Knudson W. *et al.*, 2002). The structure and function of CD44 are covered in some excellent reviews (Lesley & Hyman, 1998, Lesley *et al.*, 1993).

Of particular relevance to this study and the comments made on hyaluronan turnover above is the work of Yoshida et al in 2004 (Yoshida M. *et al.*, 2004) who found that the expression of HAS genes and hyaluronidases in arthritic knee joint synovium changed with disease status. Yoshida et al (2004) showed that reduced fluid in diseased synovium could be correlated with decreased expression of hyaluronan synthases and increased expression of hyaluronidases, compared to that of controls. This resulted in a reduced concentration of hyaluronan and decreased amount of joint fluid. It appeared that hyaluronan turnover in the knee was regulated in part by a differential expression of the two enzyme types. It is possible therefore that the osmotic potential of the follicular fluid and resultant fluid accumulation in the antrum is controlled by the regulation of a hyaluronan rich matrix synthesised in the granulosa cells and the action of hyaluronidases in the antrum.

In relation to follicular fluid in the follicle, in addition to the steroid/growth factor stimulation of the HAS enzymes, fluidity, accumulation and volume are also controlled by the depolymerisation of hyaluronan by the hyaluronidases.

In order to shed more light on the process of follicular fluid accumulation, detailed studies of hyaluronan turnover in the follicle are required. The regulation of this HA-rich matrix should be examined by studying the effects of differential signalling or receptor activity of one or more of the cytokines and growth factors mentioned earlier on HAS 2 stimulation. In addition thorough investigation of the regulation of hyaluronan turnover by the hyaluronidases is warranted.

In summary it appears that in the growing follicle, the primary roles of HAS 1 in the mural granulosa and theca cells might be linked to maintenance of low levels of hyaluronan biosynthesis for the provision of structural stability and hydrated layers for cell proliferation and migration. It may also play some role in the exclusion of larger molecules from the antrum by increasing the filtering capabilities of the theca. HAS 3 appears to play a similar role but its inherent stability provides conditions of low molecular weight hyaluronan environment, which may promote cellular proliferation, migration and adhesion. In addition it may interact with hyaluronan binding proteins and receptors involved in cell signalling in the ovary. Finally, the high molecular weight polymer synthesised by HAS 2 in response to either oocyte derived or circulating growth factors is responsible for an increased concentration of hyaluronan being released in to the follicular antrum by the mural granulosa cells. In follicular fluid some of this hyaluronan appears to form hyaluronan-rich matrices with versican, ITI heavy chains and collagen providing a fluid matrix with an osmotic potential greater than that of circulating serum. This leads to the creation of an osmotic gradient down which fluid flows in to the follicle. Regulation of hyaluronan is probably achieved by differential synthesis by the HAS genes and degradation by the hyaluronidases.

The HAS data obtained in these experiments may or may not support the hypothesis that a hyaluronan gradient is the driving force behind fluid accumulation in the follicle. Without real-time PCR data of hyaluronan synthesis and degradation, the HAS data obtained cannot support the hypothesis. They do not disprove it.

Concluding Remarks

The studies described in this thesis have attempted to address the issue of how follicular fluid forms and accumulates during folliculogenesis. Using bovine follicles it was identified that the fluid contains large osmotic molecules that have the capacity to exert an osmotic potential. These were sufficiently larger than the reported cut off in size of molecules that can cross the nominal blood follicle barrier. Enzymatic digestion identified which classes of compounds these were from, and then went on to identify some individual components in these classes. Hyaluronan and the hyaluronan binding proteins versican and ITI were some of the molecules in follicular fluid that could contribute to its colloid osmotic pressure. If one or all of these were to contribute to colloid osmotic pressure inside a follicle and then attract the flow of fluid in to the follicle across the follicular basal lamina it would be expected that one or other of these compounds be made locally by the granulosa cells during the time of follicular antrum formation. Since hyaluronan is well known to be an osmotically active molecule the three enzymes that synthesise hyaluronan, namely HAS 1-3 were investigated further. HAS enzyme expression was observed in granulosa cells, but the expression was not confined to the antral stage of folliculogenesis, nor was it confined to the membrana granulosa. Expression also occurred in the thecal layers. Thus the studies of the HAS expression do not negate our hypothesis but they do not provide any definitive support for it either. If hyaluronan production by granulosa cells is involved in generating osmotic potential at the time of antrum formation and expansion, then for us to demonstrate this would require a full examination of its production and net destruction in both thecal and granulosa cell layers. This was not possible during the course of this PhD project. However, this is the first viable hypothesis on how follicular fluid accumulates and some evidence to support that hypothesis has been provided.

7. References

Ackert CL, Gittens JE, O'Brien MJ, Eppig JJ & Kidder GM 2001 Intercellular communication via connexin43 gap junctions is required for ovarian folliculogenesis in the mouse. *Dev Biol* **233** 258-270.

Acosta TJ, Hayashi KG, Ohtani M & Miyamoto A 2003 Local changes in blood flow within the preovulatory follicle wall and early corpus luteum in cows. *Reproduction* **125** 759-767.

Adams GP, Matteri RL, Kastelic JP, Ko JC & Ginther OJ 1992 Association between surges of follicle-stimulating hormone and the emergence of follicular waves in heifers. *J Reprod Fertil* **94** 177-188.

Aguiar DJ, Knudson W & Knudson CB 1999 Internalization of the hyaluronan receptor CD44 by chondrocytes. *Exp Cell Res* **252** 292-302.

Ahrens T, Assmann V, Fieber C, Termeer C, Herrlich P, Hofmann M & Simon JC 2001 CD44 is the principal mediator of hyaluronic-acid-induced melanoma cell proliferation. *J Invest Dermatol* **116** 93-101.

Albertini DF & Anderson E 1974 The appearance and structure of intercellular connections during the ontogeny of the rabbit ovarian follicle with particular reference to gap junctions. *J Cell Biol* **63** 234-250.

Alberts B, Bray D, Lewis J, Raff RA, Roberts K & Watson JD 1989 *Molecular Biology of The Cell*, p.^pp Pages, edn 2nd. Ed.^Eds New York: Garland Publishing Inc.

Amselgruber WM, Schafer M & Sinowatz F 1999 Angiogenesis in the bovine corpus luteum: an immunocytochemical and ultrastructural study. *Anat Histol Embryol* **28** 157-166.

Andersen MM, Kroll J, Byskov AG & Faber M 1976 Protein composition in the fluid of individual bovine follicles. *J Reprod Fertil* **48** 109-118.

Anderson E & Albertini DF 1976 Gap junctions between the oocyte and companion follicle cells in the mammalian ovary. *J Cell Biol* **71** 680-686.

Anderson E, Lee G, Letourneau R, Albertini DF & Meller SM 1976 Cytological observations of the ovarian epithelium in mammals during the reproductive cycle. *J Morphol* **150** 135-165.

Andrade-Gordon P, Wang SY & Strickland S 1992 Heparin-like activity in porcine follicular fluid and rat granulosa cells. *Thromb Res* **66** 475-487.

Armstrong DG, Gong JG & Webb R 2003 Interactions between nutrition and ovarian activity in cattle: physiological, cellular and molecular mechanisms. *Reprod Suppl* **61** 403-414.

Aukland K, Wiig H, Tenstad O & Renkin EM 1997 Interstitial exclusion of macromolecules studied by graded centrifugation of rat tail tendon. *Am J Physiol* **273** H2794-2803.

Austin EJ, Mihm M, Evans AC, Knight PG, Ireland JL, Ireland JJ & Roche JF 2001 Alterations in intrafollicular regulatory factors and apoptosis during selection of follicles in the first follicular wave of the bovine estrous cycle. *Biol Reprod* **64** 839-848.

Aviles M, Okinaga T, Shur BD & Ballesta J 2000 Differential expression of glycoside residues in the mammalian zona pellucida. *Mol Reprod Dev* **57** 296-308.

Ax RL & Ryan RJ 1979 FSH stimulation of 3H-glucosamine-incorporation into proteoglycans by porcine granulosa cells in vitro. *J Clin Endocrinol Metab* **49** 646-648.

Bagavandoss P, Midgley AR, Jr. & Wicha M 1983 Developmental changes in the ovarian follicular basal lamina detected by immunofluorescence and electron microscopy. *J Histochem Cytochem* **31** 633-640.

Balazs EA 1968 Viscoelastic properties of hyaluronic acid and biological lubrication. *Univ Mich Med Cent J* 255-259.

Ball GD, Bellin ME, Ax RL & First NL 1982 Glycosaminoglycans in bovine cumulus-oocyte complexes: morphology and chemistry. *Mol Cell Endocrinol* **28** 113-122.

Bao B & Garverick HA 1998 Expression of steroidogenic enzyme and gonadotropin receptor genes in bovine follicles during ovarian follicular waves: a review. *J Anim Sci* **76** 1903-1921.

Bao B, Garverick HA, Smith GW, Smith MF, Salfen BE & Youngquist RS 1997 Expression of messenger ribonucleic acid (mRNA) encoding 3beta-hydroxysteroid dehydrogenase delta4,delta5 isomerase (3beta-HSD) during recruitment and selection of bovine ovarian follicles: identification of dominant follicles by expression of 3beta-HSD mRNA within the granulosa cell layer. *Biol Reprod* **56** 1466-1473.

Bassett WL 1943 The changes in vascular pattern of the ovary of the albino rat during hte oestrous cycle. *Am J Anat.* **73** 251-259.

Battaglia C, Aumailley M, Mann K, Mayer U & Timpl R 1993 Structurl basis of B1 integrin-mediated cell adhesion to a large heparan sulphate proteoglycan from basement membrane. *Eur J Cell Biology* **61** 92-99.

Bellin ME & Ax RL 1984 Chondroitin sulfate: an indicator of atresia in bovine follicles. *Endocrinology* **114** 428-434.

Bellin ME & Ax RL 1987a Purification of glycosaminoglycans from bovine follicular fluid. *J Dairy Sci* **70** 1913-1919.

Bellin ME & Ax RL 1987b Chemical characteristics of follicular glycosaminoglycans. *Adv Exp Med Biol* **219** 731-735.

Bellin ME, Veldhuis JD & Ax RL 1987 Follicular fluid glycosaminoglycans inhibit degradation of low-density lipoproteins and progesterone production by porcine granulosa cells. *Biol Reprod* **37** 1179-1184.

Bellin ME, Lenz RW, Steadman LE & Ax RL 1983 Proteoglycan production by bovine granulosa cells in vitro occurs in response to fsh. *Mol Cell Endocrinol* **29** 51-65.

Bellin ME, Ax RL, Laufer N, Tarlatzis BC, DeCherney AH, Feldberg D & Haseltine FP 1986 Glycosaminoglycans in follicular fluid from women undergoing in vitro fertilization and their relationship to cumulus expansion, fertilization, and development. *Fertil Steril* **45** 244-248.

Bercegeay S, Allaire F, Jean M, L'Hermite A, Bruyas JF, Renard N, Tainturier D & Barriere P 1993 [The bovine zona pellucida: differences in macromolecular composition between oocytes, pre-treated with A-23187 or not, and embryos]. *Reprod Nutr Dev* **33** 567-576.

Bergfelt DR, Kulick LJ, Kot K & Ginther OJ 2000 Follicular and hormonal response to experimental suppression of FSH during follicle deviation in cattle. *Theriogenology* **54** 1191-1206.

Bishop PN 2000 Structural macromolecules and supramolecular organisation of the vitreous gel. *Prog Retin Eye Res* **19** 323-344.

Bjersing L, Cajander S, Damber JE, Janson PO & Kallfelt B 1981 The isolated perfused rabbit ovary-a model for studies of ovarian function. Ultrastructure after perfusion with different media. *Cell Tissue Res* **216** 471-479.

Bleil JD & Wassarman PM 1980 Mammalian sperm-egg interaction: identification of a glycoprotein in mouse egg zonae pellucidae possessing receptor activity for sperm. *Cell* **20** 873-882.

Blumenkrantz N & Asboe-Hansen G 1973 New Method for Quantitative Determination of Uronic Acids. *Anal Biochem* **54** 484-489.

Bodensteiner KJ, McNatty KP, Clay CM, Moeller CL & Sawyer HR 2000 Expression of growth and differentiation factor-9 in the ovaries of fetal sheep homozygous or heterozygous for the inverdale prolificacy gene (FecX(I)). *Biol Reprod* **62** 1479-1485.

Borkakoti N 1998 Matrix metalloproteases: variations on a theme. *Prog Biophys Mol Biol* **70** 73-94.

Bortolussi M, Zanchetta R, Doliana R, Castellani I, Bressan GM & Lauria A 1989 Changes in the organization of the extracellular matrix in ovarian follicles during the preovulatory phase and atresia. An immunofluorescence study. *Basic Appl Histochem* **33** 31-38.

Borum K 1961 Oogenesis in the mouse. A study of the meiotic prophase. *Exp Cell Res* **24** 495-507.

Bost F, Diarra-Mehrpour M & Martin JP 1998 Inter-alpha-trypsin inhibitor proteoglycan family--a group of proteins binding and stabilizing the extracellular matrix. *Eur J Biochem* **252** 339-346.

Boushehri I, Yadav MC & Meur SK 1996 Characteristics of proteoglycans of buffalo ovarian follicular fluid during maturation of follicles. *Indian J Biochem Biophys* **33** 213-217.

Bradford MM 1976 A rapid and sensitive method for the quantitation of microgram quantities of protein utilizing the principle of protein-dye binding. *Anal Biochem* **72** 248-254.

Brambell FWR 1928 The development and morphology of the gonads of the mouse.part III The growth of the foliicles. *Proc. R. Soc. Lond., Ser. B,* **103** 258-272.

Braw-Tal R 1994 Expression of mRNA for follistatin and inhibin/activin subunits during follicular growth and atresia. *J Mol Endocrinol* **13** 253-264.

Braw-Tal R 2002 The initiation of follicle growth: the oocyte or the somatic cells? *Mol Cell Endocrinol* **187** 11-18.

Braw-Tal R & Yossefi S 1997 Studies in vivo and in vitro on the initiation of follicle growth in the bovine ovary. *J Reprod Fertil* **109** 165-171.

Brinck J & Heldin P 1999 Expression of recombinant hyaluronan synthase (HAS) isoforms in CHO cells reduces cell migration and cell surface CD44. *Exp Cell Res* **252** 342-351.

Brown TJ, Laurent UB & Fraser JR 1991 Turnover of hyaluronan in synovial joints: elimination of labelled hyaluronan from the knee joint of the rabbit. *Exp Physiol* **76** 125-134.

Bullard KM, Kim HR, Wheeler MA, Wilson CM, Neudauer CL, Simpson MA & McCarthy JB 2003 Hyaluronan synthase-3 is upregulated in metastatic colon carcinoma cells and manipulation of expression alters matrix retention and cellular growth. *Int J Cancer* **107** 739-746.

Buschmann MD & Grodzinsky AJ 1995 A molecular model of proteoglycan-associated electrostatic forces in cartilage mechanics. *J Biomech Eng* **117** 179-192.

Bushmeyer SM, Bellin ME, Brantmeier SA, Boehm SK, Kubajak CL & Ax RL 1985 Relationships between bovine follicular fluid glycosaminoglycans and steroids. *Endocrinology* **117** 879-885.

Byskov AG 1974 Cell kinetic studies of follicular atresia in the mouse ovary. *J Reprod Fertil* **37** 277-285.

Cahill LP & Mauleon P 1981 A study of the population of primordial and small follicles in the sheep. *J Reprod Fertil* **61** 201-206.

Camaioni A, Hascall VC, Yanagishita M & Salustri A 1993 Effects of exogenous hyaluronic acid and serum on matrix organization and stability in the mouse cumulus cell-oocyte complex. *J Biol Chem* **268** 20473-20481.

Camaioni A, Salustri A, Yanagishita M & Hascall VC 1996 Proteoglycans and proteins in the extracellular matrix of mouse cumulus cell-oocyte complexes. *Arch Biochem Biophys* **325** 190-198.

Campbell BK, Souza C, Gong J, Webb R, Kendall N, Marsters P, Robinson G, Mitchell A, Telfer EE & Baird DT 2003 Domestic ruminants as models for the elucidation of the mechanisms controlling ovarian follicle development in humans. *Reprod Suppl* **61** 429-443.

Canipari R, Epifano O, Siracusa G & Salustri A 1995 Mouse oocytes inhibit plasminogen activator production by ovarian cumulus and granulosa cells. *Dev Biol* **167** 371-378.

Carrette O, Nemade RV, Day AJ, Brickner A & Larsen WJ 2001 TSG-6 is concentrated in the extracellular matrix of mouse cumulus oocyte complexes through hyaluronan and inter-alpha-inhibitor binding. *Biol Reprod* **65** 301-308.

Casey RC & Skubitz AP 2000 CD44 and beta1 integrins mediate ovarian carcinoma cell migration toward extracellular matrix proteins. *Clin Exp Metastasis* **18** 67-75.

Caterson B, Baker JR, Christner JE, Lee Y & Lentz M 1985 Monoclonal antibodies as probes for determining the microheterogeneity of the link proteins of cartilage proteoglycan. *J Biol Chem* **260** 11348-11356.

Chapman SC & Woodruff TK 2003 Betaglycan localization in the female rat pituitary: implications for the regulation of follicle-stimulating hormone by inhibin. *Endocrinology* **144** 5640-5649.

Cheifetz S & Massague J 1989 Transforming growth factor-beta (TGF-beta) receptor proteoglycan. Cell surface expression and ligand binding in the absence of glycosaminoglycan chains. *J Biol Chem* **264** 12025-12028.

Chen HL, Marcinkiewicz JL, Sancho-Tello M, Hunt JS & Terranova PF 1993a Tumor necrosis factor-alpha gene expression in mouse oocytes and follicular cells. *Biol Reprod* **48** 707-714.

Chen L, Mao SJ & Larsen WJ 1992 Identification of a factor in fetal bovine serum that stabilizes the cumulus extracellular matrix. A role for a member of the inter-alpha-trypsin inhibitor family. *J Biol Chem* **267** 12380-12386.

Chen L, Russell PT & Larsen WJ 1993b Functional significance of cumulus expansion in the mouse: roles for the preovulatory synthesis of hyaluronic acid within the cumulus mass. *Mol Reprod Dev* **34** 87-93.

Chen L, Mao SJ, McLean LR, Powers RW & Larsen WJ 1994 Proteins of the inter-alpha-trypsin inhibitor family stabilize the cumulus extracellular matrix through their direct binding with hyaluronic acid. *J Biol Chem* **269** 28282-28287.

Chen L, Zhang H, Powers RW, Russell PT & Larsen WJ 1996 Covalent linkage between proteins of the inter-alpha-inhibitor family and hyaluronic acid is mediated by a factor produced by granulosa cells. *J Biol Chem* **271** 19409-19414.

Choi-Miura NH, Yoda M, Saito K, Takahashi K & Tomita M 2001 Identification of the substrates for plasma hyaluronan binding protein. *Biol Pharm Bull* **24** 140-143.

Chong H, Pangas SA, Bernard DJ, Wang E, Gitch J, Chen W, Draper LB, Cox ET & Woodruff TK 2000 Structure and expression of a membrane component of the inhibin receptor system. *Endocrinology* **141** 2600-2607.

Clark LJ, Irving-Rodgers HF, Dharmarajan AM & Rodgers RJ 2004 Theca Interna: The Other Side of Bovine Follicular Atresia. *Biol Reprod.*

Coleman PJ, Scott D, Mason RM & Levick JR 1999 Characterization of the effect of high molecular weight hyaluronan on trans-synovial flow in rabbit knees. *J Physiol* **514 (Pt 1)** 265-282.

Comper WD 1994 The thermodynamic and hydrodynamic properties of macromolecules that influence the hydrodynamics of porous systems. *J Theor Biol* **168** 421-427.

Comper WD 1996 *Extracellular matrix*, p.^pp Pages, edn. Ed.^Eds WD Comper. Harwood Academic Publishers.

Comper WD & Preston BN 1974 Model connective-tissue systems. A study of polyion-mobile ion and of excluded-volume interactions of proteoglycans. *Biochem J* **143** 1-9.

Comper WD & Laurent TC 1978 Physiological function of connective tissue polysaccharides. *Physiol Rev* **58** 255-315.

Comper WD & Williams RP 1987 Hydrodynamics of concentrated proteoglycan solutions. *J Biol Chem* **262** 13464-13471.

Comper WD & Zamparo O 1989 Hydraulic conductivity of polymer matrices. *Biophys Chem* **34** 127-135.

Comper WD & Williams RP 1990 Osmotic flow caused by chondroitin sulfate proteoglycan across well-defined nuclepore membranes. *Biophys Chem* **36** 215-222.

Comper WD, Williams RP & Zamparo O 1990 Water transport in extracellular matrices. *Connect Tissue Res* **25** 89-102.

Cooke DJ, Crowe MA & Roche JF 1997 Circulating FSH isoform patterns during recurrent increases in FSH throughout the oestrous cycle of heifers. *J Reprod Fertil* **110** 339-345.

Coutts JR 1976 Hormone production by the ovary. *Clin Obstet Gynaecol* **3** 63-87.

Csoka TB, Frost GI & Stern R 1997 Hyaluronidases in tissue invasion. *Invasion Metastasis* **17** 297-311.

Culav EM, Clark CH & Merrilees MJ 1999 Connective tissues: matrix composition and its relevance to physical therapy. *Phys Ther* **79** 308-319.

Dalin AM 1987 Ovarian follicular activity during the luteal phase in gilts. *Zentralbl Veterinarmed A* **34** 592-601.

David G 1991 Biology and pathology of the pericellular heparan sulphate proteoglycans. *Biochem Soc Trans* **19** 816-820.

Day A 2001 Understanding HA protein interactions, vol. 2001: Glycoforum.

de la Sota RL, Simmen FA, Diaz T & Thatcher WW 1996 Insulin-like growth factor system in bovine first-wave dominant and subordinate follicles. *Biol Reprod* **55** 803-812.

DeAngelis PL, Jing W, Graves MV, Burbank DE & Van Etten JL 1997 Hyaluronan synthase of chlorella virus PBCV-1. *Science* **278** 1800-1803.

Deed R, Rooney P, Kumar P, Norton JD, Smith J, Freemont AJ & Kumar S 1997 Early-response gene signalling is induced by angiogenic oligosaccharides of hyaluronan in endothelial cells. Inhibition by non-angiogenic, high-molecular-weight hyaluronan. *Int J Cancer* **71** 251-256.

Dembczynski R & Jankowski T 2001 Determination of pore diameter and molecular weight cut-off of hydrogel-membrane liquid-core capsules for immunoisolation. *J Biomater Sci Polym Ed* **12** 1051-1058.

Dick DAT 1966 *Cell water*, p.^pp Pages, edn. Ed.^Eds London: Butterworths.

Dong J, Albertini DF, Nishimori K, Kumar TR, Lu N & Matzuk MM 1996 Growth differentiation factor-9 is required during early ovarian folliculogenesis. *Nature* **383** 531-535.

Dong S, Cole GJ & Halfter W 2003 Expression of collagen XVIII and localization of its glycosaminoglycan attachment sites. *J Biol Chem* **278** 1700-1707.

Dong Z, Patel Y, Saikumar P, Weinberg JM & Venkatachalam MA 1998 Development of porous defects in plasma membranes of adenosine triphosphate-depleted Madin-Darby canine kidney cells and its inhibition by glycine. *Lab Invest* **78** 657-668.

Dours-Zimmermann MT & Zimmermann DR 1994 A novel glycosaminoglycan attachment domain identified in two alternative splice variants of human versican. *J Biol Chem* **269** 32992-32998.

Dragovic RA, Ritter LJ, Schulz SJ, Amato F, Armstrong DT & Gilchrist RB 2005 Role of oocyte-secreted growth differentiation factor 9 in the regulation of mouse cumulus expansion. *Endocrinology*.

Drahorad J, Tesarik J, Cechova D & Vilim V 1991 Proteins and glycosaminoglycans in the intercellular matrix of the human cumulus-oophorus and their effect on conversion of proacrosin to acrosin. *J Reprod Fertil* **93** 253-262.

Draper LB, Matzuk MM, Roberts VJ, Cox E, Weiss J, Mather JP & Woodruff TK 1998 Identification of an inhibin receptor in gonadal tumors from inhibin alpha-subunit knockout mice. *J Biol Chem* **273** 398-403.

Driancourt MA 2001 Regulation of ovarian follicular dynamics in farm animals. Implications for manipulation of reproduction. *Theriogenology* **55** 1211-1239.

Driancourt MA & Thuel B 1998 Control of oocyte growth and maturation by follicular cells and molecules present in follicular fluid. A review. *Reprod Nutr Dev* **38** 345-362.

Driancourt MA, Gibson WR & Cahill LP 1985 Follicular dynamics throughout the oestrous cycle in sheep. A review. *Reprod Nutr Dev* **25** 1-15.

Driancourt MA, Fevre J, Martal J & Al-Gubory KH 2000 Control of ovarian follicular growth and maturation by the corpus luteum and the placenta during pregnancy in sheep. *J Reprod Fertil* **120** 151-158.

Dube JL, Wang P, Elvin J, Lyons KM, Celeste AJ & Matzuk MM 1998 The bone morphogenetic protein 15 gene is X-linked and expressed in oocytes. *Mol Endocrinol* **12** 1809-1817.

Duke KL 1966 Histological observations on the ovary of the white-tailed mole, Parascaptor leucurus. *Anat Rec* **154** 527-531.

Dunbar BS, Prasad S, Carino C & Skinner SM 2001 The ovary as an immune target. *J Soc Gynecol Investig* **8** S43-48.

Edwards RG 1974 Follicular fluid. *J Reprod Fertil* **37** 189-219.

Ehrlich S, Wolff N, Schneiderman R, Maroudas A, Parker KH & Winlove CP 1998 The osmotic pressure of chondroitin sulphate solutions: experimental measurements and theoretical analysis. *Biorheology* **35** 383-397.

Eikenes L, Bruland OS, Brekken C & Davies Cde L 2004 Collagenase increases the transcapillary pressure gradient and improves the uptake and distribution of monoclonal antibodies in human osteosarcoma xenografts. *Cancer Res* **64** 4768-4773.

Eissa HM 1996 Concentrations of steroids and biochemical constituents in follicular fluid of buffalo cows during different stages of the oestrous cycle. *Br Vet J* **152** 573-581.

Elenius K, Vainio S, Laato M, Salmivirta M, Thesleff I & Jalkanen M 1991 Induced expression of syndecan in healing wounds. *J Cell Biol* **114** 585-595.

Elvin JA, Yan C, Wang P, Nishimori K & Matzuk MM 1999a Molecular characterization of the follicle defects in the growth differentiation factor 9-deficient ovary. *Mol Endocrinol* **13** 1018-1034.

Elvin JA, Clark AT, Wang P, Wolfman NM & Matzuk MM 1999b Paracrine actions of growth differentiation factor-9 in the mammalian ovary. *Mol Endocrinol* **13** 1035-1048.

Eppig JJ & Ward-Bailey PF 1984 Sulfated glycosaminoglycans inhibit hyaluronic acid synthesizing activity in mouse cumuli oophori. *Exp Cell Res* **150** 459-465.

Eppig JJ, Pendola FL & Wigglesworth K 1998 Mouse oocytes suppress cAMP-induced expression of LH receptor mRNA by granulosa cells in vitro. *Mol Reprod Dev* **49** 327-332.

Eppig JJ, Wigglesworth K, Pendola F & Hirao Y 1997 Murine oocytes suppress expression of luteinizing hormone receptor messenger ribonucleic acid by granulosa cells. *Biol Reprod* **56** 976-984.

Erickson GF 1978 Normal ovarian function. *Clin Obstet Gynecol* **21** 31-52.

Erickson GF & Shimasaki S 2001 The physiology of folliculogenesis: the role of novel growth factors. *Fertil Steril* **76** 943-949.

Ericson AC & Spring KR 1982 Coupled NaCl entry into Necturus gallbladder epithelial cells. *Am J Physiol* **243** C140-145.

Eriksen GV, Malmstrom A & Uldbjerg N 1997 Human follicular fluid proteoglycans in relation to in vitro fertilization. *Fertil Steril* **68** 791-798.

Eriksen GV, Malmstrom A, Uldbjerg N & Huszar G 1994 A follicular fluid chondroitin sulfate proteoglycan improves the retention of motility and velocity of human spermatozoa. *Fertil Steril* **62** 618-623.

Eriksen GV, Carlstedt I, Morgelin M, Uldbjerg N & Malmstrom A 1999 Isolation and characterization of proteoglycans from human follicular fluid. *Biochem J* **340** 613-620.

Espey LL 1994 Current status of the hypothesis that mammalian ovulation is comparable to an inflammatory reaction. *Biol Reprod* **50** 233-238.

Espey LL & Lipner H 1963 Measurements of Intrafollicular Pressures in the Rabbit Ovary. *Am J Physiol* **205** 1067-1072.

Evanko SP & Wight TN 1999 Intracellular localization of hyaluronan in proliferating cells. *J Histochem Cytochem* **47** 1331-1342.

Evans AC & Fortune JE 1997 Selection of the dominant follicle in cattle occurs in the absence of differences in the expression of messenger ribonucleic acid for gonadotropin receptors. *Endocrinology* **138** 2963-2971.

Evans AC, Adams GP & Rawlings NC 1994 Endocrine and ovarian follicular changes leading up to the first ovulation in prepubertal heifers. *J Reprod Fertil* **100** 187-194.

Fair T, Hyttel P & Greve T 1995 Bovine oocyte diameter in relation to maturational competence and transcriptional activity. *Mol Reprod Dev* **42** 437-442.

Fair T, Hulshof SC, Hyttel P, Greve T & Boland M 1997 Oocyte ultrastructure in bovine primordial to early tertiary follicles. *Anat Embryol (Berl)* **195** 327-336.

Fessler JH & Fessler LI 1966 Electron microscopic visualization of the polysaccharide hyaluronic acid. *Proc Natl Acad Sci U S A* **56** 141-147.

Findlay JK 1993 An update on the roles of inhibin, activin, and follistatin as local regulators of folliculogenesis. *Biol Reprod* **48** 15-23.

Fitz TA, Mayan MH, Sawyer HR & Niswender GD 1982 Characterization of two steroidogenic cell types in the ovine corpus luteum. *Biol Reprod* **27** 703-711.

Forabosco A, Sforza C, De Pol A, Vizzotto L, Marzona L & Ferrario VF 1991 Morphometric study of the human neonatal ovary. *Anat Rec* **231** 201-208.

Fortune JE, Kito S & Byrd DD 1999 Activation of primordial follicles in vitro. *J Reprod Fertil Suppl* **54** 439-448.

Fortune JE, Sirois J, Turzillo AM & Lavoir M 1991 Follicle selection in domestic ruminants. *J Reprod Fertil Suppl* **43** 187-198.

Fortune JE, Rivera GM, Evans AC & Turzillo AM 2001 Differentiation of dominant versus subordinate follicles in cattle. *Biol Reprod* **65** 648-654.

Franchimont P, Hazee-Hagelstein MT, Hazout A, Gysen P, Salat-Baroux J, Schatz B & Demerle F 1990 Correlation between follicular fluid content and the results of in vitro fertilization and embryo transfer. III. Proteoglycans. *Biol Reprod* **43** 183-190.

Fraser HM & Wulff C 2001 Angiogenesis in the primate ovary. *Reprod Fertil Dev* **13** 557-566.

Fraser JR, Laurent TC & Laurent UB 1997 Hyaluronan: its nature, distribution, functions and turnover. *J Intern Med* **242** 27-33.

Fraser JR, Kimpton WG, Laurent TC, Cahill RN & Vakakis N 1988 Uptake and degradation of hyaluronan in lymphatic tissue. *Biochem J* **256** 153-158.

Fulop C, Salustri A & Hascall VC 1997a Coding sequence of a hyaluronan synthase homologue expressed during expansion of the mouse cumulus-oocyte complex. *Arch Biochem Biophys* **337** 261-266.

Fulop C, Kamath RV, Li Y, Otto JM, Salustri A, Olsen BR, Glant TT & Hascall VC 1997b Coding sequence, exon-intron structure and chromosomal localization of murine TNF-stimulated gene 6 that is specifically expressed by expanding cumulus cell-oocyte complexes. *Gene* **202** 95-102.

Gapski R, Barr JL, Sarment DP, Layher MG, Socransky SS & Giannobile WV 2004 Effect of systemic matrix metalloproteinase inhibition on periodontal wound repair: a proof of concept trial. *J Periodontol* **75** 441-452.

Gebauer H, Lindner HR & Amsterdam A 1978 Synthesis of heparin-like glycosaminoglycans in rat ovarian slices. *Biol Reprod* **18** 350-358.

Gelety TJ & Magoffin DA 1997 Ontogeny of steroidogenic enzyme gene expression in ovarian theca-interstitial cells in the rat: regulation by a paracrine theca-differentiating factor prior to achieving luteinizing hormone responsiveness. *Biol Reprod* **56** 938-945.

Ghosh S, Li X, Reed C & Reed W 1990 Apparent persistence lenghts and diffusion behaviour of high molecular weight hyaluronate. *Biopolymers* **30** 1101-1112.

Ginther OJ 2000 Selection of the dominant follicle in cattle and horses. *Anim Reprod Sci* **60-61** 61-79.

Ginther OJ, Knopf L & Kastelic JP 1989 Ovarian follicular dynamics in heifers during early pregnancy. *Biol Reprod* **41** 247-254.

Ginther OJ, Bergfelt DR, Kulick LJ & Kot K 1999 Selection of the dominant follicle in cattle: establishment of follicle deviation in less than 8 hours through depression of FSH concentrations. *Theriogenology* **52** 1079-1093.

Ginther OJ, Bergfelt DR, Kulick LJ & Kot K 2000 Selection of the dominant follicle in cattle: role of two-way functional coupling between follicle-stimulating hormone and the follicles. *Biol Reprod* **62** 920-927.

Ginther OJ, Wiltbank MC, Fricke PM, Gibbons JR & Kot K 1996 Selection of the dominant follicle in cattle. *Biol Reprod* **55** 1187-1194.

Girard N, Delpech A & Delpech B 1986 Characterization of hyaluronic acid on tissue sections with hyaluronectin. *J Histochem Cytochem* **34** 539-541.

Goldstein LA, Zhou DF, Picker LJ, Minty CN, Bargatze RF, Ding JF & Butcher EC 1989 A human lymphocyte homing receptor, the hermes antigen, is related to cartilage proteoglycan core and link proteins. *Cell* **56** 1063-1072.

Gomez-Alejandre S, de la Blanca ES, de Usera CA, Rey-Stolle MF & Hernandez-Fuentes I 2000 Partial specific volume of hyaluronic acid in different media and conditions. *Int J Biol Macromol* **27** 287-290.

Gosden R & Bownes M 1995 *Gametes- The Oocyte - Cellular and molecular aspects of oocyte development*, p.^pp Pages, edn. Ed.^Eds J Grudzinskas & JL Yovich. Cambridge: Cambridge University Press.

Gosden RG 1987 Follicular status at the menopause. *Hum Reprod* **2** 617-621.

Gosden RG & Hunter RH 1988 Electrophysiological properties of the follicle wall in the pig ovary. *Experientia* **44** 212-214.

Gosden RG, Hunter RH, Telfer E, Torrance C & Brown N 1988 Physiological factors underlying the formation of ovarian follicular fluid. *J Reprod Fertil* **82** 813-825.

Gotting C, Kuhn J, Tinneberg HR, Brinkmann T & Kleesiek K 2002 High xylosyltransferase activities in human follicular fluid and cultured granulosa-lutein cells. *Mol Hum Reprod* **8** 1079-1086.

Gougeon A 1993 Oocyte amturation in the human. *Acta Eur Fertil* **89** 4.

Gougeon A 1996 Regulation of ovarian follicular development in primates: facts and hypotheses. *Endocr Rev* **17** 121-155.

Gougeon A & Chainy GB 1987 Morphometric studies of small follicles in ovaries of women at different ages. *J Reprod Fertil* **81** 433-442.

Gougeon ML & Theze J 1987 Participation of L3T4 in the avidity, activation and interactions of TH-cell clones. *Ann Inst Pasteur Immunol* **138** 144-147.

Grant ME & Ayad S 1988 The collagens of skin: structure and assembly. *Biochem Soc Trans* **16** 663-666.

Grebner EE, Hall CW & Neufeld EF 1966 Glycosylation of serine residues by a uridine diphosphate-xylose: protein xylosyltransferase from mouse mastocytoma. *Arch Biochem Biophys* **116** 391-398.

Gribbon P, Heng BC & Hardingham TE 2000 The analysis of intermolecular interactions in concentrated hyaluronan solutions suggest no evidence for chain-chain association. *Biochem J* **350** 329-335.

Grimek HJ & Ax RL 1982 Chromatographic comparison of chondroitin-containing proteoglycan from small and large bovine ovarian follicles. *Biochem Biophys Res Commun* **104** 1401-1406.

Grimek HJ, Bellin ME & Ax RL 1984 Characteristics of proteoglycans isolated from small and large bovine ovarian follicles. *Biol Reprod* **30** 397-409.

Grimshaw J, Kane A, Trocha-Grimshaw J, Douglas A, Chakravarthy U & Archer D 1994 Quantitative analysis of hyaluronan in vitreous humor using capillary electrophoresis. *Electrophoresis* **15** 936-940.

Grippo AA, Henault MA, Anderson SH & Killian GJ 1992 Cation concentrations in fluid from the oviduct ampulla and isthmus of cows during the estrous cycle. *J Dairy Sci* **75** 58-65.

Grondahl C, Hyttel P, Grondahl ML, Eriksen T, Gotfredsen P & Greve T 1995 Structural and endocrine aspects of equine oocyte maturation in vivo. *Mol Reprod Dev* **42** 94-105.

Gu WY, Lai WM & Mow VC 1993 Transport of fluid and ions through a porous-permeable charged-hydrated tissue, and streaming potential data on normal bovine articular cartilage. *J Biomech* **26** 709-723.

Halfter W, Dong S, Schurer B & Cole GJ 1998 Collagen XVIII is a basement membrane heparan sulfate proteoglycan. *J Biol Chem* **273** 25404-25412.

Hamamah S, Wittemer C, Barthelemy C, Richet C, Zerimech F, Royere D & Degand P 1996 Identification of hyaluronic acid and chondroitin sulfates in human follicular fluid and their effects on human sperm motility and the outcome of in vitro fertilization. *Reprod Nutr Dev* **36** 43-52.

Hammel HT 1999 Evolving ideas about osmosis and capillary fluid exchange. *Faseb J* **13** 213-231.

Hardingham TE & Fosang AJ 1992 Proteoglycans: many forms and many functions. *Faseb J* **6** 861-870.

Hardingham TE & Fosang AJ 1995 The structure of aggrecan and its turnover in cartilage. *J Rheumatol Suppl* **43** 86-90.

Hasan S, Hosseini G, Princivalle M, Dong JC, Birsan D, Cagide C & de Agostini AI 2002 Coordinate expression of anticoagulant heparan sulfate proteoglycans and serine protease inhibitors in the rat ovary: a potent system of proteolysis control. *Biol Reprod* **66** 144-158.

Hascall VC, Majors AK, De La Motte CA, Evanko SP, Wang A, Drazba JA, Strong SA & Wight TN 2004 Intracellular hyaluronan: a new frontier for inflammation? *Biochim Biophys Acta* **1673** 3-12.

Hasty KA, Hibbs MS, Kang AH & Mainardi CL 1984 Heterogeneity among human collagenases demonstrated by monoclonal antibody that selectively recognizes and inhibits human neutrophil collagenase. *J Exp Med* **159** 1455-1463.

Haussinger D 1996 The role of cellular hydration in the regulation of cell function. *Biochem J* **313** 697-710.

Hayashi M, McGee EA, Min G, Klein C, Rose UM, van Duin M & Hsueh AJ 1999 Recombinant growth differentiation factor-9 (GDF-9) enhances growth and differentiation of cultured early ovarian follicles. *Endocrinology* **140** 1236-1244.

Hedrick JL & Wardrip NJ 1987 On the macromolecular composition of the zona pellucida from porcine oocytes. *Dev Biol* **121** 478-488.

Henderson KM, McNeilly AS & Swanston IA 1982 Gonadotrophin and steroid concentrations in bovine follicular fluid and their relationship to follicle size. *J Reprod Fertil* **65** 467-473.

Hering TM 1999 Regulation of chondrocyte gene expression. *Front Biosci* **4** D743-761.

Hertan R, Farnworth PG, Fitzsimmons KL & Robertson DM 1999 Identification of high affinity binding sites for inhibin on ovine pituitary cells in culture. *Endocrinology* **140** 6-12.

Herz Z, Northey D, Lawyer M & First NL 1985 Acrosome reaction of bovine spermatozoa in vivo: sites and effects of stages of the estrous cycle. *Biol Reprod* **32** 1163-1168.

Hess KA, Chen L & Larsen WJ 1998 The ovarian blood follicle barrier is both charge- and size-selective in mice. *Biol Reprod* **58** 705-711.

Hess KA, Chen L & Larsen WJ 1999 Inter-alpha-inhibitor binding to hyaluronan in the cumulus extracellular matrix is required for optimal ovulation and development of mouse oocytes. *Biol Reprod* **61** 436-443.

Hildebrand A, Romaris M, Rasmussen LM, Heinegard D, Twardzik DR, Border WA & Ruoslahti E 1994 Interaction of the small interstitial proteoglycans biglycan, decorin and fibromodulin with transforming growth factor beta. *Biochem J* **302** 527-534.

Hirashima Y, Kobayashi H, Gotoh J & Terao T 1997 Inter-alpha-trypsin inhibitor is concentrated in the pericellular environment of mouse granulosa cells through hyaluronan-binding. *Eur J Obstet Gynecol Reprod Biol* **73** 79-84.

Hirshfield AN 1991 Development of follicles in the mammalian ovary. *Int Rev Cytol* **124** 43-101.

Hirshfield AN 1997 Overview of ovarian follicular development: considerations for the toxicologist. *Environ Mol Mutagen* **29** 10-15.

Hoffman P, Mashburn TA, Jr. & Meyer K 1967 Proteinpolysaccharide of bovine cartilage. II. The relation of keratan sulfate and chondroitin sulfate. *J Biol Chem* **242** 3805-3809.

Hosseini G, Liu J & Agostini AI 1996 Characterization and hormonal modulation of anticoagulant heparan sulfate proteoglycans synthesized by rat ovarian granulosa cells. *J Biol Chem* **271** 22090-22099.

Huet C, Monget P, Pisselet C & Monniaux D 1997 Changes in extracellular matrix components and steroidogenic enzymes during growth and atresia of antral ovarian follicles in the sheep. *Biol Reprod* **56** 1025-1034.

Huet C, Monget P, Pisselet C, Hennequet C, Locatelli A & Monniaux D 1998 Chronology of events accompanying follicular atresia in hypophysectomized ewes. Changes in levels of steroidogenic enzymes, connexin 43, insulin-like growth factor II/mannose 6 phosphate receptor, extracellular matrix components, and matrix metalloproteinases. *Biol Reprod* **58** 175-185.

Humphries DE, Nicodemus CF, Schiller V & Stevens RL 1992 The human serglycin gene. Nucleotide sequence and methylation pattern in human promyelocytic leukemia HL-60 cells and T-lymphoblast Molt-4 cells. *J Biol Chem* **267** 13558-13563.

Ichikawa T, Itano N, Sawai T, Kimata K, Koganehira Y, Saida T & Taniguchi S 1999 Increased synthesis of hyaluronate enhances motility of human melanoma cells. *J Invest Dermatol* **113** 935-939.

Iozzo RV 1998 Matrix proteoglycans: from molecular design to cellular function. *Annu Rev Biochem* **67** 609-652.

Iozzo RV & Murdoch AD 1996 Proteoglycans of the extracellular environment: clues from the gene and protein side offer novel perspectives in molecular diversity and function. *Faseb J* **10** 598-614.

Iozzo RV, Cohen IR, Grassel S & Murdoch AD 1994 The biology of perlecan: the multifaceted heparan sulphate proteoglycan of basement membranes and pericellular matrices. *Biochem J* **302** 625-639.

Ireland JJ & Roche JF 1983a Growth and differentiation of large antral follicles after spontaneous luteolysis in heifers: changes in concentration of hormones in follicular fluid and specific binding of gonadotropins to follicles. *J Anim Sci* **57** 157-167.

Ireland JJ & Roche JF 1983b Development of nonovulatory antral follicles in heifers: changes in steroids in follicular fluid and receptors for gonadotropins. *Endocrinology* **112** 150-156.

Ireland JJ, Fogwell RL, Oxender WD, Ames K & Cowley JL 1984 Production of estradiol by each ovary during the estrous cycle of cows. *J Anim Sci* **59** 764-771.

Ireland JL & Ireland JJ 1994 Changes in expression of inhibin/activin alpha, beta A and beta B subunit messenger ribonucleic acids following increases in size and during different stages of differentiation or atresia of non-ovulatory follicles in cows. *Biol Reprod* **50** 492-501.

Irving-Rodgers HF & Rodgers RJ 2000 Ultrastructure of the basal lamina of bovine ovarian follicles and its relationship to the membrana granulosa. *J Reprod Fertil* **118** 221-228.

Irving-Rodgers HF, Krupa M & Rodgers RJ 2003 Cholesterol side-chain cleavage cytochrome P450 and 3beta-hydroxysteroid dehydrogenase expression and the concentrations of steroid hormones in the follicular fluids of different phenotypes of healthy and atretic bovine ovarian follicles. *Biol Reprod* **69** 2022-2028.

Irving-Rodgers HF, Mussard ML, Kinder JE & Rodgers RJ 2002 Composition and morphology of the follicular basal lamina during atresia of bovine antral follicles. *Reproduction* **123** 97-106.

Irving-Rodgers HF, van Wezel IL, Mussard ML, Kinder JE & Rodgers RJ 2001 Atresia revisited: two basic patterns of atresia of bovine antral follicles. *Reproduction* **122** 761-775.

Ishihara H, Warensjo K, Roberts S & Urban JP 1997 Proteoglycan synthesis in the intervertebral disk nucleus: the role of extracellular osmolality. *Am J Physiol* **272** C1499-1506.

Isnard N, Legeais JM, Renard G & Robert L 2001 Effect of hyaluronan on MMP expression and activation. *Cell Biol Int* **25** 735-739.

Isobe N, Nakao T & Yoshimura Y 2003 Distribution of cytochrome P450-side chain cleavage in the theca interna layers of bovine small antral and cystic follicles. *Reprod Domest Anim* **38** 405-409.

Itano N, Sawai T, Atsumi F, Miyaishi O, Taniguchi S, Kannagi R, Hamaguchi M & Kimata K 2004 Selective expression and functional characteristics of three mammalian hyaluronan synthases in oncogenic malignant transformation. *J Biol Chem* **279** 18679-18687.

Itano N, Sawai T, Yoshida M, Lenas P, Yamada Y, Imagawa M, Shinomura T, Hamaguchi M, Yoshida Y, Ohnuki Y *et al.* 1999 Three isoforms of mammalian hyaluronan synthases have distinct enzymatic properties. *J Biol Chem* **274** 25085-25092.

Itano N, Kimata K, Atsumi F, Sawai T, Yamada Y, Miyaishi O, Senga T, Hamaguchi M, Yoshida M, Narimatsu H *et al.* 2002 Mammalian hyaluronan synthases. *IUBMB Life* **54** 195-199.

Iwata M & Carlson SS 1993 A large chondroitin sulfate proteoglycan has the characteristics of a general extracellular matrix component of adult brain. *J Neurosci* **13** 195-207.

Iwata M, Wight TN & Carlson SS 1993 A brain extracellular matrix proteoglycan forms aggregates with hyaluronan. *J Biol Chem* **268** 15061-15069.

Jackson DG 2003 The lymphatics revisited: new perspectives from the hyaluronan receptor LYVE-1. *Trends Cardiovasc Med* **13** 1-7.

Jackson RJ, Maguire DJ, Hinds LA & Ramshaw IA 1998 Infertility in mice induced by a recombinant ectromelia virus expressing mouse zona pellucida glycoprotein 3. *Biol Reprod* **58** 152-159.

Jacobson A, Rahmanian M, Rubin K & Heldin P 2002 Expression of hyaluronan synthase 2 or hyaluronidase 1 differentially affect the growth rate of transplantable colon carcinoma cell tumors. *Int J Cancer* **102** 212-219.

Jessen TE & Odum L 2003 Role of tumour necrosis factor stimulated gene 6 (TSG-6) in the coupling of inter-alpha-trypsin inhibitor to hyaluronan in human follicular fluid. *Reproduction* **125** 27-31.

Jessen TE, Odum L & Johnsen AH 1994 In vivo binding of human inter-alpha-trypsin inhibitor free heavy chains to hyaluronic acid. *Biol Chem Hoppe Seyler* **375** 521-526.

Jiang JY, Macchiarelli G, Tsang BK & Sato E 2003 Capillary angiogenesis and degeneration in bovine ovarian antral follicles. *Reproduction* **125** 211-223.

Jimenez-Krassel F, Winn ME, Burns D, Ireland JL & Ireland JJ 2003 Evidence for a negative intrafollicular role for inhibin in regulation of estradiol production by granulosa cells. *Endocrinology* **144** 1876-1886.

Jinga VV, Bogdan I & Fruchter J 1986 Experimental model for the quantitative estimation of transendothelial transport in vitro; a two-compartment system. *Physiologie* **23** 227-236.

John ME, John MC, Ashley P, MacDonald RJ, Simpson ER & Waterman MR 1984 Identification and characterization of cDNA clones specific for cholesterol side-chain cleavage cytochrome P-450. *Proc Natl Acad Sci U S A* **81** 5628-5632.

Johnson A, Mishkin GJ, Lew SQ, Mishkin M, Abramson F & Lecchi P 2003 In vitro performance of hemodialysis membranes after repeated processing. *Am J Kidney Dis* **42** 561-566.

Johnson J, Canning J, Kaneko T, Pru JK & Tilly JL 2004 Germline stem cells and follicular renewal in the postnatal mammalian ovary. *Nature* **428** 145-150.

Johnson MH & Everitt BJ 2000 *Essential Reproduction*, p.^pp Pages, edn 5. Ed.^Eds B Science. Oxford UK: Blackwell.

Juengel JL & Niswender GD 1999 Molecular regulation of luteal progesterone synthesis in domestic ruminants. *J Reprod Fertil Suppl* **54** 193-205.

Juengel JL & McNatty KP 2005 The role of proteins of the transforming growth factor-beta superfamily in the intraovarian regulation of follicular development. *Hum Reprod Update* **11** 143-160.

Kako K, Tsumori K, Ohmasa Y, Takahashi Y & Munekata E 2000 The expression of Cox17p in rodent tissues and cells. *Eur J Biochem* **267** 6699-6707.

Karvinen S, Kosma VM, Tammi MI & Tammi R 2003a Hyaluronan, CD44 and versican in epidermal keratinocyte tumours. *Br J Dermatol* **148** 86-94.

Karvinen S, Pasonen-Seppanen S, Hyttinen JM, Pienimaki JP, Torronen K, Jokela TA, Tammi MI & Tammi R 2003b Keratinocyte growth factor stimulates migration and hyaluronan synthesis in the epidermis by activation of keratinocyte hyaluronan synthases 2 and 3. *J Biol Chem* **278** 49495-49504.

Kaya G, Grand D, Hotz R, Augsburger E, Carraux P, Didierjean L & Saurat JH 2005 Upregulation of CD44 and hyaluronate synthases by topical retinoids in mouse skin. *J Invest Dermatol* **124** 284-287.

Keeney DS, Ikeda Y, Waterman MR & Parker KL 1995 Cholesterol side-chain cleavage cytochrome P450 gene expression in the primitive gut of the mouse embryo does not require steroidogenic factor 1. *Mol Endocrinol* **9** 1091-1098.

Keikhoffer W, Holmer GJ & Peckham B 1962 Some chemical characteristics of ovarian and parovarian cystic fluids. *Obstet. Gynecol.* **20** 471-483.

Kemeter P & Feichtinger W 1991 [Ultrasound monitoring of follicle growth in IVF]. *Wien Med Wochenschr* **141** 9-13.

Kerin JF, Edmonds DK, Warnes GM, Cox LW, Seamark RF, Matthews CD, Young GB & Baird DT 1981 Morphological and functional relations of Graafian follicle growth to ovulation in women using ultrasonic, laparoscopic and biochemical measurements. *Br J Obstet Gynaecol* **88** 81-90.

Khalsa PS & Eisenberg SR 1997 Compressive behavior of articular cartilage is not completely explained by proteoglycan osmotic pressure. *J Biomech* **30** 589-594.

Kim HR, Wheeler MA, Wilson CM, Iida J, Eng D, Simpson MA, McCarthy JB & Bullard KM 2004 Hyaluronan facilitates invasion of colon carcinoma cells in vitro via interaction with CD44. *Cancer Res* **64** 4569-4576.

Kimura N, Konno Y, Miyoshi K, Matsumoto H & Sato E 2002 Expression of hyaluronan synthases and CD44 messenger RNAs in porcine cumulus-oocyte complexes during in vitro maturation. *Biol Reprod* **66** 707-717.

Kjellen L & Lindahl U 1991 Proteoglycans: structures and interactions. *Annu Rev Biochem* **60** 443-475.

Klagsbrun M 1991 Regulators of angiogenesis: stimulators, inhibitors, and extracellular matrix. *J Cell Biochem* **47** 199-200.

Knepper PA & McLone DG 1985 Glycosaminoglycans and outflow pathways of the eye and brain. *Pediatr Neurosci* **12** 240-251.

Knight PG & Glister C 2003 Local roles of TGF-beta superfamily members in the control of ovarian follicle development. *Anim Reprod Sci* **78** 165-183.

Knight PG, Feist SA, Tannetta DS, Bleach EC, Fowler PA, O'Brien M, Groome NP, Kohyama K, Ohnishi J, Murata M *et al.* 1998 Measurement of inhibin-A (alpha beta A dimer) during the oestrous cycle, after manipulation of ovarian activity and during pregnancy in ewes. *J Reprod Fertil* **113** 159-166.

Knudson CB & Knudson W 1993 Hyaluronan-binding proteins in development, tissue homeostasis, and disease. *Faseb J* **7** 1233-1241.

Knudson CB & Knudson W 2001 Cartilage proteoglycans. *Semin Cell Dev Biol* **12** 69-78.

Knudson W, Chow G & Knudson CB 2002 CD44-mediated uptake and degradation of hyaluronan. *Matrix Biol* **21** 15-23.

Ko JC, Kastelic JP, Del Campo MR & Ginther OJ 1991 Effects of a dominant follicle on ovarian follicular dynamics during the oestrous cycle in heifers. *J Reprod Fertil* **91** 511-519.

Kobayashi H, Sun GW, Hirashima Y & Terao T 1999 Identification of link protein during follicle development and cumulus cell cultures in rats. *Endocrinology* **140** 3835-3842.

Kobe B & Deisenhofer J 1994 The leucine-rich repeat: a versatile binding motif. *Trends Biochem Sci* **19** 415-421.

Kolle S, Sinowatz F, Boie G & Palma G 1998 Differential expression of ZPC in the bovine ovary, oocyte, and embryo. *Mol Reprod Dev* **49** 435-443.

Kolset SO, Vuong TT & Prydz K 1999 Apical secretion of chondroitin sulphate in polarized Madin-Darby canine kidney (MDCK) cells. *J Cell Sci* **112 (Pt 11)** 1797-1801.

Koster KL, Maddocks KJ & Bryant G 2003 Exclusion of maltodextrins from phosphatidylcholine multilayers during dehydration: effects on membrane phase behaviour. *Eur Biophys J* **32** 96-105.

Kotsuji F, Kubo M & Tominaga T 1994 Effect of interactions between granulosa and thecal cells on meiotic arrest in bovine oocytes. *J Reprod Fertil* **100** 151-156.

Kovach IS 1995 The importance of polysaccharide configurational entropy in determining the osmotic swelling pressure of concentrated proteoglycan solution and the bulk compressive modulus of articular cartilage. *Biophys Chem* **53** 181-187.

Kresse H & Schonherr E 2001 Proteoglycans of the extracellular matrix and growth control. *J Cell Physiol* **189** 266-274.

Krusius T, Gehlsen KR & Ruoslahti E 1987 A fibroblast chondroitin sulfate proteoglycan core protein contains lectin-like and growth factor-like sequences. *J Biol Chem* **262** 13120-13125.

Kuettner KE & Kimura JH 1985 Proteoglycans: an overview. *J Cell Biochem* **27** 327-336.

Kulick LJ, Kot K, Wiltbank MC & Ginther OJ 1999 Follicular and hormonal dynamics during the first follicular wave in heifers. *Theriogenology* **52** 913-921.

Laemmli UK 1970 Cleavage of structural proteins during the assembly of the head of bacteriophage T4. *Nature* **227** 680-685.

Laitinen M, Vuojolainen K, Jaatinen R, Ketola I, Aaltonen J, Lehtonen E, Heikinheimo M & Ritvos O 1998 A novel growth differentiation factor-9 (GDF-9) related factor is co-expressed with GDF-9 in mouse oocytes during folliculogenesis. *Mech Dev* **78** 135-140.

Lam X, Gieseke C, Knoll M & Talbot P 2000 Assay and importance of adhesive interaction between hamster (Mesocricetus auratus) oocyte-cumulus complexes and the oviductal epithelium. *Biol Reprod* **62** 579-588.

Landolt RM, Vaughan L, Winterhalter KH & Zimmermann DR 1995 Versican is selectively expressed in embryonic tissues that act as barriers to neural crest cell migration and axon outgrowth. *Development* **121** 2303-2312.

Larsen WJ, Chen L, Powers R, Zhang H, Russell PT, Chambers C, Hess K & Flick R 1996 Cumulus expansion initiates physical and developmental autonomy of the oocyte. *Zygote* **4** 335-341.

Laurent C, Hellstrom S, Engstrom-Laurent A, Wells AF & Bergh A 1995a Localization and quantity of hyaluronan in urogenital organs of male and female rats. *Cell Tissue Res* **279** 241-248.

Laurent T 1998 *The Chemistry, Biology and Medical Applications of Hyaluronan and its Derivatives*, p.^pp Pages, edn. Ed.^Eds L TC. Portland Press, London.

Laurent TC 1987 Biochemistry of hyaluronan. *Acta Otolaryngol Suppl* **442** 7-24.

Laurent TC & Ogston AG 1963 The Interaction between Polysaccharides and Other Macromolecules. 4. The Osmotic Pressure of Mixtures of Serum Albumin and Hyaluronic Acid. *Biochem J* **89** 249-253.

Laurent TC & Fraser JR 1986 The properties and turnover of hyaluronan. *Ciba Found Symp* **124** 9-29.

Laurent TC & Fraser JR 1992 Hyaluronan. *Faseb J* **6** 2397-2404.

Laurent TC, Ryan M & Pietruszkiewicz A 1960 Fractionation of hyaluronic acid. The polydispersity of hyaluronic acid from the bovine vitreous body. *Biochim Biophys Acta* **42** 476-485.

Laurent TC, Laurent UB & Fraser JR 1995b Functions of hyaluronan. *Ann Rheum Dis* **54** 429-432.

Laurent TC, Laurent UB & Fraser JR 1996 The structure and function of hyaluronan: An overview. *Immunol Cell Biol* **74** A1-7.

Laurent UB & Granath KA 1983 The molecular weight of hyaluronate in the aqueous humour and vitreous body of rabbit and cattle eyes. *Exp Eye Res* **36** 481-492.

Laurent UB, Fraser JR, Engstrom-Laurent A, Reed RK, Dahl LB & Laurent TC 1992 Catabolism of hyaluronan in the knee joint of the rabbit. *Matrix* **12** 130-136.

Laurich C, Wheeler MA, Iida J, Neudauer CL, McCarthy JB & Bullard KM 2004 Hyaluronan mediates adhesion of metastatic colon carcinoma cells. *J Surg Res* **122** 70-74.

Lebaron RG 1996 Versican. *Perspect Dev Neurobiol* **3** 261-271.

LeBaron RG, Zimmermann DR & Ruoslahti E 1992 Hyaluronate binding properties of versican. *J Biol Chem* **267** 10003-10010.

Lefevre B, Gougeon A & Testart J 1990 Primates in the study of oocyte maturation. *Pathol Biol (Paris)* **38** 166-169.

Lemire JM, Merrilees MJ, Braun KR & Wight TN 2002 Overexpression of the V3 variant of versican alters arterial smooth muscle cell adhesion, migration, and proliferation in vitro. *J Cell Physiol* **190** 38-45.

Lenz RW, Ax RL, Grimek HJ & First NL 1982 Proteoglycan from bovine follicular fluid enhances an acrosome reaction in bovine spermatozoa. *Biochem Biophys Res Commun* **106** 1092-1098.

Leroy JL, Vanholder T, Delanghe JR, Opsomer G, Van Soom A, Bols PE & de Kruif A 2004 Metabolite and ionic composition of follicular fluid from different-sized follicles and their relationship to serum concentrations in dairy cows. *Anim Reprod Sci* **80** 201-211.

Lesley J & Hyman R 1998 CD44 structure and function. *Front Biosci* **3** d616-630.

Lesley J, Hyman R & Kincade PW 1993 CD44 and its interaction with extracellular matrix. *Adv Immunol* **54** 271-335.

Lever AF & Kriz W 1966 Countercurrent exchange between the vasa recta and the loop of Henle. *Lancet* **1** 1057-1060.

Lindahl U & Hook M 1978 Glycosaminoglycans and their binding to biological macromolecules. *Annu Rev Biochem* **47** 385-417.

Lindahl U & Kjellen L 1991 Heparin or heparan sulfate--what is the difference? *Thromb Haemost* **66** 44-48.

Lindqvist U, Chichibu K, Delpech B, Goldberg RL, Knudson W, Poole AR & Laurent TC 1992 Seven different assays of hyaluronan compared for clinical utility. *Clin Chem* **38** 127-132.

Lintern-Moore S & Moore GP 1979 The initiation of follicle and oocyte growth in the mouse ovary. *Biol Reprod* **20** 773-778.

Logan KA, Juengel JL & McNatty KP 2002 Onset of steroidogenic enzyme gene expression during ovarian follicular development in sheep. *Biol Reprod* **66** 906-916.

Longley WH 1911 The maturation of the egg and ovulation in the domestic cat. *Am J Anat.* **12** 139-172.

Lopez-Casillas F, Wrana JL & Massague J 1993 Betaglycan presents ligand to the TGF beta signaling receptor. *Cell* **73** 1435-1444.

Lord RC 1999 Osmosis, osmometry, and osmoregulation. *Postgrad Med J* **75** 67-73.

Luck MR & Zhao Y 1993 Identification and measurement of collagen in the bovine corpus luteum and its relationship with ascorbic acid and tissue development. *J Reprod Fertil* **99** 647-652.

Luck MR, Zhao Y & Silvester LM 1995 Identification and localization of collagen types I and IV in the ruminant follicle and corpus luteum. *J Reprod Fertil Suppl* **49** 517-521.

Luck MR, Griffiths S, Gregson K, Watson E, Nutley M & Cooper A 2001 Follicular fluid responds endothermically to aqueous dilution. *Hum Reprod* **16** 2508-2514.

Lundy T, Smith P, O'Connell A, Hudson NL & McNatty KP 1999 Populations of granulosa cells in small follicles of the sheep ovary. *J Reprod Fertil* **115** 251-262.

Lunenfeld B, Kraiem Z & Eshkol A 1976 Structure and function of the growing follicle. *Clin Obstet Gynaecol* **3** 27-42.

Lyons KM, Pelton RW & Hogan BL 1989 Patterns of expression of murine Vgr-1 and BMP-2a RNA suggest that transforming growth factor-beta-like genes coordinately regulate aspects of embryonic development. *Genes Dev* **3** 1657-1668.

Macchiarelli G, Vizza E, Nottola SA, Familiari G & Motta PM 1992 Cellular and microvascular changes of the ovarian follicle during folliculogenesis: a scanning electron microscopic study. *Arch Histol Cytol* **55** 191-204.

Magoffin DA, Gancedo B & Erickson GF 1989 Transforming growth factor-beta promotes differentiation of ovarian thecal-interstitial cells but inhibits androgen production. *Endocrinology* **125** 1951-1958.

Makris A, Ryan KJ, Yasumizu T, Hill CL & Zetter BR 1984 The nonluteal porcine ovary as a source of angiogenic activity. *Endocrinology* **115** 1672-1677.

Mallya SK, Mookhtiar KA, Gao Y, Brew K, Dioszegi M, Birkedal-Hansen H & Van Wart HE 1990 Characterization of 58-kilodalton human neutrophil collagenase: comparison with human fibroblast collagenase. *Biochemistry* **29** 10628-10634.

Manarang-Pangan S & Menge AC 1971 Immunologic studies on human follicular fluid. *Fertil Steril* **22** 367-372.

Manova K, Huang EJ, Angeles M, De Leon V, Sanchez S, Pronovost SM, Besmer P & Bachvarova RF 1993 The expression pattern of the c-kit ligand in gonads of mice supports a role for the c-kit receptor in oocyte growth and in proliferation of spermatogonia. *Dev Biol* **157** 85-99.

Maravei DV, Trobovich AM, Perez GI, Tilly kI, Talanian RV, Banach D, Wong WW & Tilly JL 1997 Cleavage of cytoskeletal proteins by caspases during ovarian cell death: evidence that cell free systems do not always mimic apoptopic events in intact cells. *Cell Death Differ* **4** 707-712.

Marion GB, Norwood JS & Gier HT 1968a Uterus of the cow after parturition: factors affecting regression. *Am J Vet Res* **29** 71-75.

Marion GB, Gier HT & Choudary JB 1968b Micromorphology of the bovine ovarian follicular system. *J Anim Sci* **27** 451-465.

Matikainen T, Perez GI, Zheng TS, Kluzak TR, Rueda BR, Flavell RA & Tilly JL 2001 Caspase-3 gene knockout defines cell lineage specificity for programmed cell death signaling in the ovary. *Endocrinology* **142** 2468-2480.

Matousek M, Carati C, Gannon B & Brannstrom M 2001 Novel method for intrafollicular pressure measurements in the rat ovary: increased intrafollicular pressure after hCG stimulation. *Reproduction* **121** 307-314.

Mattioli M, Barboni B, Turriani M, Galeati G, Zannoni A, Castellani G, Berardinelli P & Scapolo PA 2001 Follicle activation involves vascular endothelial growth factor production and increased blood vessel extension. *Biol Reprod* **65** 1014-1019.

McArthur ME, Irving-Rodgers HF, Byers S & Rodgers RJ 2000 Identification and immunolocalization of decorin, versican, perlecan, nidogen, and chondroitin sulfate proteoglycans in bovine small-antral ovarian follicles. *Biol Reprod* **63** 913-924.

McConnell NA, Yunus RS, Gross SA, Bost KL, Clemens MG & Hughes FM, Jr. 2002 Water permeability of an ovarian antral follicle is predominantly transcellular and mediated by aquaporins. *Endocrinology* **143** 2905-2912.

McDonald JN & Levick JR 1994 Hyaluronan reduces fluid escape rate from rabbit knee joints disparately from its effect on fluidity. *Exp Physiol* **79** 103-106.

McGee EA & Hsueh AJ 2000 Initial and cyclic recruitment of ovarian follicles. *Endocr Rev* **21** 200-214.

McGee EA, Hsu SY, Kaipia A & Hsueh AJ 1998 Cell death and survival during ovarian follicle development. *Mol Cell Endocrinol* **140** 15-18.

McGrath SA, Esquela AF & Lee SJ 1995 Oocyte-specific expression of growth/differentiation factor-9. *Mol Endocrinol* **9** 131-136.

McKee CM, Penno MB, Cowman M, Burdick MD, Strieter RM, Bao C & Noble PW 1996 Hyaluronan (HA) fragments induce chemokine gene expression in alveolar macrophages. The role of HA size and CD44. *J Clin Invest* **98** 2403-2413.

McNatty KP, Dobson C, Gibb M, Kieboom L & Thurley DC 1981 Accumulation of luteinizing hormone, oestradiol and androstenedione by sheep ovarian follicles in vivo. *J Endocrinol* **91** 99-109.

McNatty KP, Heath DA, Lundy T, Fidler AE, Quirke L, O'Connell A, Smith P, Groome N & Tisdall DJ 1999 Control of early ovarian follicular development. *J Reprod Fertil Suppl* **54** 3-16.

McNatty KP, Fidler AE, Juengel JL, Quirke LD, Smith PR, Heath DA, Lundy T, O'Connell A & Tisdall DJ 2000 Growth and paracrine factors regulating follicular formation and cellular function. *Mol Cell Endocrinol* **163** 11-20.

McNatty KP, Juengel JL, Reader KL, Lun S, Myllymaa S, Lawrence SB, Western A, Meerasahib MF, Mottershead DG, Groome NP *et al.* 2005a Bone morphogenetic protein 15 and growth differentiation factor 9 co-operate to regulate granulosa cell function in ruminants. *Reproduction* **129** 481-487.

McNatty KP, Juengel JL, Reader KL, Lun S, Myllymaa S, Lawrence SB, Western A, Meerasahib MF, Mottershead DG, Groome NP *et al.* 2005b Bone morphogenetic protein 15 and growth differentiation factor 9 co-operate to regulate granulosa cell function. *Reproduction* **129** 473-480.

Meng N, Nakashima N, Nagasaka T, Fukatsu T, Nara Y, Yoshida K, Kawaguchi T & Takeuchi J 1994 Immunohistochemical characterization of extracellular matrix components of granulosa cell tumor of ovary. *Pathol Int* **44** 205-212.

Mihm M & Bleach EC 2003 Endocrine regulation of ovarian antral follicle development in cattle. *Anim Reprod Sci* **78** 217-237.

Mihm M, Crowe MA, Knight PG & Austin EJ 2002 Follicle wave growth in cattle. *Reprod Domest Anim* **37** 191-200.

Mihm M, Good TE, Ireland JL, Ireland JJ, Knight PG & Roche JF 1997 Decline in serum follicle-stimulating hormone concentrations alters key intrafollicular growth factors involved in selection of the dominant follicle in heifers. *Biol Reprod* **57** 1328-1337.

Milas M, Rinaudo M, Roure I, Al-Assaf S, Phillips GO & Williams PA 2001 Comparative rheological behavior of hyaluronan from bacterial and animal sources with cross-linked hyaluronan (hylan) in aqueous solution. *Biopolymers* **59** 191-204.

Miserocchi G, Venturoli D, Negrini D, Gilardi MC & Bellina R 1992 Intrapleural fluid movements described by a porous flow model. *J Appl Physiol* **73** 2511-2516.

Miserocchi G, Pistolesi M, Miniati M, Bellina CR, Negrini D & Giuntini C 1984 Pleural liquid pressure gradients and intrapleural distribution of injected bolus. *J Appl Physiol* **56** 526-532.

Misra S, Ghatak S, Zoltan-Jones A & Toole BP 2003 Regulation of multidrug resistance in cancer cells by hyaluronan. *J Biol Chem* **278** 25285-25288.

Miyake K, Underhill CB, Lesley J & Kincade PW 1990 Hyaluronate can function as a cell adhesion molecule and CD44 participates in hyaluronate recognition. *J Exp Med* **172** 69-75.

Moley KH & Schreiber JR 1995 Ovarian follicular growth, ovulation and atresia. Endocrine, paracrine and autocrine regulation. *Adv Exp Med Biol* **377** 103-119.

Monget P & Monniaux D 1995 Growth factors and the control of folliculogenesis. *J Reprod Fertil Suppl* **49** 321-333.

Monget P, Besnard N, Huet C, Pisselet C & Monniaux D 1996 Insulin-like growth factor-binding proteins and ovarian folliculogenesis. *Horm Res* **45** 211-217.

Monniaux D, Huet C, Besnard N, Clement F, Bosc M, Pisselet C, Monget P & Mariana JC 1997 Follicular growth and ovarian dynamics in mammals. *J Reprod Fertil Suppl* **51** 3-23.

Monslow J, Williams JD, Norton N, Guy CA, Price IK, Coleman SL, Williams NM, Buckland PR, Spicer AP, Topley N *et al.* 2003 The human hyaluronan synthase genes:

genomic structures, proximal promoters and polymorphic microsatellite markers. *Int J Biochem Cell Biol* **35** 1272-1283.

Morales TI & Roberts AB 1988 Transforming growth factor beta regulates the metabolism of proteoglycans in bovine cartilage organ cultures. *J Biol Chem* **263** 12828-12831.

Mossman HW & Duke KL 1973 *Comparative Morphology of the Mammalian ovary.*, p.^pp Pages, edn. Ed.^Eds Madison: University of Winsconsin Press.

Motro B & Bernstein A 1993 Dynamic changes in ovarian c-kit and Steel expression during the estrous reproductive cycle. *Dev Dyn* **197** 69-79.

Mueller PL, Schreiber JR, Lucky AW, Schulman JD, Rodbard D & Ross GT 1978 Follicle-stimulating hormone stimulates ovarian synthesis of proteoglycans in the estrogen-stimulated hypophysectomized immature female rat. *Endocrinology* **102** 824-831.

Nagyova E, Vanderhyden BC & Prochazka R 2000 Secretion of paracrine factors enabling expansion of cumulus cells is developmentally regulated in pig oocytes. *Biol Reprod* **63** 1149-1156.

Nagyova E, Camaioni A, Prochazka R & Salustri A 2004 Covalent Transfer of Heavy Chains of Inter-{alpha}-Trypsin Inhibitor Family Proteins to Hyaluronan in In Vivo and In Vitro Expanded Porcine Oocyte-Cumulus Complexes. *Biol Reprod* **71** 1838-1843.

Naso MF, Zimmermann DR & Iozzo RV 1994 Characterization of the complete genomic structure of the human versican gene and functional analysis of its promoter. *J Biol Chem* **269** 32999-33008.

Neame PJ & Barry FP 1994 The link proteins. *Exs* **70** 53-72.

Negrini D, Tenstad O & Wiig H 2003 Interstitial exclusion of albumin in rabbit lung during development of pulmonary oedema. *J Physiol* **548** 907-917.

Negrini D, Gonano C, Del Fabbro M & Miserocchi G 1990 Transperitoneal fluid dynamics in rabbit liver. *J Appl Physiol* **69** 625-629.

Nekola MV & Nalbandov AV 1971 Morphological changes of rat follicular cells as influenced by oocytes. *Biol Reprod* **4** 154-160.

Netti PA, Berk DA, Swartz MA, Grodzinsky AJ & Jain RK 2000 Role of extracellular matrix assembly in interstitial transport in solid tumors. *Cancer Res* **60** 2497-2503.

Nishida Y, Knudson CB, Kuettner KE & Knudson W 2000 Osteogenic protein-1 promotes the synthesis and retention of extracellular matrix within bovine articular cartilage and chondrocyte cultures. *Osteoarthritis Cartilage* **8** 127-136.

Noble PW, McKee CM, Cowman M & Shin HS 1996 Hyaluronan fragments activate an NF-kappa B/I-kappa B alpha autoregulatory loop in murine macrophages. *J Exp Med* **183** 2373-2378.

Noonan DM, Fulle A, Valente P, Cai S, Horigan E, Sasaki M, Yamada Y & Hassell JR 1991 The complete sequence of perlecan, a basement membrane heparan sulfate proteoglycan, reveals extensive similarity with laminin A chain, low density lipoprotein-receptor, and the neural cell adhesion molecule. *J Biol Chem* **266** 22939-22947.

Novikova LA, Savel'ev AS, Zviagil'skaia RA & Luzikov VN 1995 [Import of a modified form of a cytochrome P450scc precursor into mitochondria from various sources]. *Biokhimiia* **60** 995-1004.

Odum L & Jessen TE 2002 Characterisation of a coupling activity for the binding of ITI to hyaluronidase in follicular fluid. *?*

Odum L, Andersen CY & Jessen TE 2002 Characterization of the coupling activity for the binding of inter-alpha-trypsin inhibitor to hyaluronan in human and bovine follicular fluid. *Reproduction* **124** 249-257.

Onarheim H, Missavage AE, Gunther RA, Kramer GC, Reed RK & Laurent TC 1991 Marked increase of plasma hyaluronan after major thermal injury and infusion therapy. *J Surg Res* **50** 259-265.

O'Shea JD 1981 Structure-function relationships in the wall of the ovarian follicle. *Aust J Biol Sci* **34** 379-394.

O'Shea JD, Hay MF & Cran DG 1978 Ultrastructural changes in the theca interna during follicular atresia in sheep. *J Reprod Fertil* **54** 183-187.

Ostgaard G & Reed RK 1994 Increased lymphatic hyaluronan output and preserved hyaluronan content of the rat small intestine in prolonged hypoproteinaemia. *Acta Physiol Scand* **152** 51-56.

Otsuka F, Yamamoto S, Erickson GF & Shimasaki S 2001 Bone morphogenetic protein-15 inhibits follicle-stimulating hormone (FSH) action by suppressing FSH receptor expression. *J Biol Chem* **276** 11387-11392.

Otsuka F, Yao Z, Lee T, Yamamoto S, Erickson GF & Shimasaki S 2000 Bone morphogenetic protein-15. Identification of target cells and biological functions. *J Biol Chem* **275** 39523-39528.

Paesi FJ 1949(a) The influence of hypophysectomy and of subsequent treatment with chorionic gonadotrophin on follicles of different size in the ovary of the rat. *Acta Endocrinol (Copenh)* **3** 89-104.

Paesi FJ 1949(b) The influence of pituitary gonadotrophin and of mixtures of pituitary and chorionic gonadotrophin on the follicles in the ovary of the hypophysectomized rat and the normal mouse. *Acta Endocrinol (Copenh)* **3** 156-172.

Parillo F, Stradaioli G & Verini-Supplizi A 1998 Glycoconjugates in small antral ovarian follicles of the river buffalo (Bubalus bubalis L.). *Acta Histochem* **100** 229-243.

Pasonen-Seppanen S, Karvinen S, Torronen K, Hyttinen JM, Jokela T, Lammi MJ, Tammi MI & Tammi R 2003 EGF upregulates, whereas TGF-beta downregulates, the hyaluronan synthases Has2 and Has3 in organotypic keratinocyte cultures: correlations with epidermal proliferation and differentiation. *J Invest Dermatol* **120** 1038-1044.

Patino R, Yoshizaki G, Thomas P & Kagawa H 2001 Gonadotropic control of ovarian follicle maturation: the two-stage concept and its mechanisms. *Comp Biochem Physiol B Biochem Mol Biol* **129** 427-439.

Paulus W, Baur I, Dours-Zimmermann MT & Zimmermann DR 1996 Differential expression of versican isoforms in brain tumors. *J Neuropathol Exp Neurol* **55** 528-533.

Pedersen T 1970 Follicle kinetics in the ovary of the cyclic mouse. *Acta Endocrinol (Copenh)* **64** 304-323.

Pepling ME & Spradling AC 1998 Female mouse germ cells form synchronously dividing cysts. *Development* **125** 3323-3328.

Perissinotto D, Iacopetti P, Bellina I, Doliana R, Colombatti A, Pettway Z, Bronner-Fraser M, Shinomura T, Kimata K, Morgelin M *et al.* 2000 Avian neural crest cell migration is diversely regulated by the two major hyaluronan-binding proteoglycans PG-M/versican and aggrecan. *Development* **127** 2823-2842.

Perloff WH, Schultz J, Farris EJ & Balin H 1955 Some aspects of the chemical nature of human ovarian follicular fluid. *Fertil Steril* **6** 11-16.

Pescador N, Soumano K, Stocco DM, Price CA & Murphy BD 1996 Steroidogenic acute regulatory protein in bovine corpora lutea. *Biol Reprod* **55** 485-491.

Peters H 1969 The development of the mouse ovary from birth to maturity. *Acta Endocrinol (Copenh)* **62** 98-116.

Picton HM 2001 Activation of follicle development: the primordial follicle. *Theriogenology* **55** 1193-1210.

Poltorak Z, Cohen T & Neufeld G 2000 The VEGF splice variants: properties, receptors, and usage for the treatment of ischemic diseases. *Herz* **25** 126-129.

Potter-Perigo S, Baker C, Tsoi C, Braun KR, Isenhath S, Altman GM, Altman LC & Wight TN 2004 Regulation of proteoglycan synthesis by leukotriene d4 and epidermal growth factor in bronchial smooth muscle cells. *Am J Respir Cell Mol Biol* **30** 101-108.

Powers RW, Chen L, Russell PT & Larsen WJ 1995 Gonadotropin-stimulated regulation of blood-follicle barrier is mediated by nitric oxide. *Am J Physiol* **269** E290-298.

Prehm P 1984 Hyaluronate is synthesized at plasma membranes. *Biochem J* **220** 597-600.

Preston GM, Carroll TP, Guggino WB & Agre P 1992 Appearance of water channels in Xenopus oocytes expressing red cell CHIP28 protein. *Science* **256** 385-387.

Price FM, Levick JR & Mason RM 1996 Glycosaminoglycan concentration in synovium and other tissues of rabbit knee in relation to synovial hydraulic resistance. *J Physiol* **495 (Pt 3)** 803-820.

Princivalle M, Hasan S, Hosseini G & de Agostini AI 2001 Anticoagulant heparan sulfate proteoglycans expression in the rat ovary peaks in preovulatory granulosa cells. *Glycobiology* **11** 183-194.

Rahe CH, Owens RE, Fleeger JL, Newton HJ & Harms PG 1980 Pattern of plasma luteinizing hormone in the cyclic cow: dependence upon the period of the cycle. *Endocrinology* **107** 498-503.

Ramsden CA, Bankier A, Brown TJ, Cowen PS, Frost GI, McCallum DD, Studdert VP & Fraser JR 2000 A new disorder of hyaluronan metabolism associated with generalized folding and thickening of the skin. *J Pediatr* **136** 62-68.

Reardon A, Heinegard D, McLeod D, Sheehan JK & Bishop PN 1998 The large chondroitin sulphate proteoglycan versican in mammalian vitreous. *Matrix Biol* **17** 325-333.

Reyes R, Carranco A, Hernandez O, Rosado A, Merchant H & Delgado NM 1984 Glycosamineglycan sulfate as acrosomal reaction-inducing factor of follicular fluid. *Arch Androl* **12** 203-209.

Risbridger GP, Robertson DM & de Kretser DM 1990 Current perspectives of inhibin biology. *Acta Endocrinol (Copenh)* **122** 673-682.

Rittig M, Lutjen-Drecoll E & Prehm P 1992 Immunohistochemical localization of hyaluronan synthase in cornea and conjunctive of cynomolgus monkey. *Exp Eye Res* **54** 455-460.

Robertson DM, Klein R, de Vos FL, McLachlan RI, Wettenhall RE, Hearn MT, Burger HG & de Kretser DM 1987 The isolation of polypeptides with FSH suppressing activity from bovine follicular fluid which are structurally different to inhibin. *Biochem Biophys Res Commun* **149** 744-749.

Robinson A 1918 The formation, rupture, and closure of ovarian follicles in ferrets and ferret-polecat hybrids amnd some associated phenomena. *Trans. Roy. Soc. Edinburgh* **52**.

Rodbard D 1968 Mechanics of ovulation. *J Clin Endocrinol Metab* **28** 849-861.

Rodgers HF, Lavranos TC, Vella CA & Rodgers RJ 1995a Basal lamina and other extracellular matrix produced by bovine granulosa cells in anchorage-independent culture. *Cell Tissue Res* **282** 463-471.

Rodgers RJ, O'Shea JD & Findlay JK 1985 Do small and large luteal cells of the sheep interact in the production of progesterone? *J Reprod Fertil* **75** 85-94.

Rodgers RJ, Mitchell MD & Simpson ER 1988 Secretion of progesterone and prostaglandins by cells of bovine corpora lutea from three stages of the luteal phase. *J Endocrinol* **118** 121-126.

Rodgers RJ, Irving-Rodgers HF & Russell DL 2003 Extracellular matrix of the developing ovarian follicle. *Reproduction* **126** 415-424.

Rodgers RJ, Lavranos TC, van Wezel IL & Irving-Rodgers HF 1999a Development of the ovarian follicular epithelium. *Mol Cell Endocrinol* **151** 171-179.

Rodgers RJ, Lavranos TC, Rodgers HF, Young FM & Vella CA 1995b The physiology of the ovary: maturation of ovarian granulosa cells and a novel role for antioxidants in the corpus luteum. *J Steroid Biochem Mol Biol* **53** 241-246.

Rodgers RJ, Irving-Rodgers HF, van Wezel IL, Krupa M & Lavranos TC 2001 Dynamics of the membrana granulosa during expansion of the ovarian follicular antrum. *Mol Cell Endocrinol* **171** 41-48.

Rodgers RJ, van Wezel IL, Irving-Rodgers HF, Lavranos TC, Irvine CM & Krupa M 1999b Roles of extracellular matrix in follicular development. *J Reprod Fertil Suppl* **54** 343-352.

Rondell P 1964 Follicular pressure and distensibility in ovulation. *Am J Physiol* **207** 590-594.

Rondell P 1970 Biophysical aspects of ovulation. *Biol Reprod* **2** 64-89.

Rosenberg LC, Choi HU, Poole AR, Lewandowska K & Culp LA 1986 Biological roles of dermatan sulphate proteoglycans. *Ciba Found Symp* **124** 47-68.

Rosengren BI, Carlsson O & Rippe B 2001 Hyaluronan and peritoneal ultrafiltration: a test of the "filter-cake" hypothesis. *Am J Kidney Dis* **37** 1277-1285.

Rouet P, Daveau M & Salier JP 1992 Electrophoretic pattern of the inter-alpha-inhibitor family proteins in human serum, characterized by chain-specific antibodies. *Biol Chem Hoppe Seyler* **373** 1019-1024.

Rowlands IW, Tam WH & Kleiman DG 1970 Histological and biochemical studies on the ovary and of progesterone levels in the systemic blood of the green acouchi (Myoprocta pratti). *J Reprod Fertil* **22** 533-545.

Ruoslahti E & Yamaguchi Y 1991 Proteoglycans as modulators of growth factor activities. *Cell* **64** 867-869.

Russe I 1983 Oogenesis in cattle and sheep. *Bibl Anat* **24** 77-92.

Russell DL, Ochsner SA, Hsieh M, Mulders S & Richards JS 2003 Hormone-regulated expression and localization of versican in the rodent ovary. *Endocrinology* **144** 1020-1031.

Sabaratnam S, Mason RM & Levick JR 2003 Molecular sieving of hyaluronan by synovial interstitial matrix and lymphatic capillary endothelium evaluated by lymph analysis in rabbits. *Microvasc Res* **66** 227-236.

Saito H, Kaneko T, Takahashi T, Kawachiya S, Saito T & Hiroi M 2000 Hyaluronan in follicular fluids and fertilization of oocytes. *Fertil Steril* **74** 1148-1152.

Sajdera SW & Hascall VC 1969 Proteinpolysaccharide complex from bovine nasal cartilage. A comparison of low and high shear extraction procedures. *J Biol Chem* **244** 77-87.

Sakata M, Kobayashi H, Sun GW, Mochizuki O, Takagi A & Kojima T 2000 Ryudocan expression by luteinized granulosa cells is associated with the process of follicle atresia. *Fertil Steril* **74** 1208-1214.

Salamonsen LA, Shuster S & Stern R 2001 Distribution of hyaluronan in human endometrium across the menstrual cycle. Implications for implantation and menstruation. *Cell Tissue Res* **306** 335-340.

Salier JP, Diarra-Mehrpour M, Sesboue R, Bourguignon J, Benarous R, Ohkubo I, Kurachi S, Kurachi K & Martin JP 1987 Isolation and characterization of cDNAs encoding the heavy chain of human inter-alpha-trypsin inhibitor (I alpha TI): unambiguous evidence for multipolypeptide chain structure of I alpha TI. *Proc Natl Acad Sci U S A* **84** 8272-8276.

Salustri A, Yanagishita M & Hascall VC 1989 Synthesis and accumulation of hyaluronic acid and proteoglycans in the mouse cumulus cell-oocyte complex during follicle-stimulating hormone-induced mucification. *J Biol Chem* **264** 13840-13847.

Salustri A, Yanagishita M & Hascall VC 1990a Mouse oocytes regulate hyaluronic acid synthesis and mucification by FSH-stimulated cumulus cells. *Dev Biol* **138** 26-32.

Salustri A, Camaioni A & D'Alessandris C 1996 Endocrine and paracrine regulation of cumulus expansion. *Zygote* **4** 313-315.

Salustri A, Ulisse S, Yanagishita M & Hascall VC 1990b Hyaluronic acid synthesis by mural granulosa cells and cumulus cells in vitro is selectively stimulated by a factor produced by oocytes and by transforming growth factor-beta. *J Biol Chem* **265** 19517-19523.

Salustri A, Yanagishita M, Underhill CB, Laurent TC & Hascall VC 1992 Localization and synthesis of hyaluronic acid in the cumulus cells and mural granulosa cells of the preovulatory follicle. *Dev Biol* **151** 541-551.

Salustri A, Camaioni A, Di Giacomo M, Fulop C & Hascall VC 1999 Hyaluronan and proteoglycans in ovarian follicles. *Hum Reprod Update* **5** 293-301.

Sato E, Ishibashi T & Koide SS 1987a Prevention of spontaneous degeneration of mouse oocytes in culture by ovarian glycosaminoglycans. *Biol Reprod* **37** 371-376.

Sato E, Izumi T & Ishibashi T 1987b Hen ovarian factors influencing neovascularization in mice. *Poult Sci* **66** 1053-1058.

Sato E, Kawamura N & Ishibashi T 1988 Chemicals influencing maturation, activation, and degeneration of bovine oocytes in culture. *J Dairy Sci* **71** 3482-3488.

Sato E, Miyamoto H & Koide SS 1990 Glycosaminoglycans in porcine follicular fluid promoting viability of oocytes in culture. *Mol Reprod Dev* **26** 391-397.

Savio JD, Thatcher WW, Morris GR, Entwistle K, Drost M & Mattiacci MR 1993 Effects of induction of low plasma progesterone concentrations with a progesterone-releasing intravaginal device on follicular turnover and fertility in cattle. *J Reprod Fertil* **98** 77-84.

Savolainen H 1999 Isolation and separation of proteoglycans. *J Chromatogr B Biomed Sci Appl* **722** 255-262.

Sayo T, Sakai S & Inoue S 2004 Synergistic effect of N-acetylglucosamine and retinoids on hyaluronan production in human keratinocytes. *Skin Pharmacol Physiol* **17** 77-83.

Sayo T, Sugiyama Y, Takahashi Y, Ozawa N, Sakai S, Ishikawa O, Tamura M & Inoue S 2002 Hyaluronan synthase 3 regulates hyaluronan synthesis in cultured human keratinocytes. *J Invest Dermatol* **118** 43-48.

Scaramuzzi RJ, Adams NR, Baird DT, Campbell BK, Downing JA, Findlay JK, Henderson KM, Martin GB, McNatty KP, McNeilly AS *et al.* 1993 A model for follicle selection and the determination of ovulation rate in the ewe. *Reprod Fertil Dev* **5** 459-478.

Schmalfeldt M, Dours-Zimmermann MT, Winterhalter KH & Zimmermann DR 1998 Versican V2 is a major extracellular matrix component of the mature bovine brain. *J Biol Chem* **273** 15758-15764.

Schmid P, Cox D, van der Putten H, McMaster GK & Bilbe G 1994 Expression of TGF-beta s and TGF-beta type II receptor mRNAs in mouse folliculogenesis: stored maternal TGF-beta 2 message in oocytes. *Biochem Biophys Res Commun* **201** 649-656.

Schneyer AL, Hall HA, Lambert-Messerlian G, Wang QF, Sluss P & Crowley WF, Jr. 1996 Follistatin-activin complexes in human serum and follicular fluid differ immunologically and biochemically. *Endocrinology* **137** 240-247.

Schochet SS 1916 A Suggestion as to the process of ovulation and ovarian cyst formation. *Anat. Record* **10** 447-457.

Schoenfelder M & Einspanier R 2003 Expression of hyaluronan synthases and corresponding hyaluronan receptors is differentially regulated during oocyte maturation in cattle. *Biol Reprod* **69** 269-277.

Schultz G & G L 2005 Extracellular matrix: review of its roles in acute and chronic wounds. In *World Wide Wounds*, vol. 2005: obgyn.ufl.edu.

Schweitzer M, Jackson JC & Ryan RJ 1981 The porcine ovarian follicle. VII. FSH stimulation of in vitro [3H]-glucosamine incorporation into mucopolysaccharides. *Biol Reprod* **24** 332-340.

Scott D, Coleman PJ, Mason RM & Levick JR 1997 Glycosaminoglycan depletion greatly raises the hydraulic permeability of rabbit joint synovial lining. *Exp Physiol* **82** 603-606.

Scott D, Coleman PJ, Mason RM & Levick JR 1998a Direct evidence for the partial reflection of hyaluronan molecules by the lining of rabbit knee joints during trans-synovial flow. *J Physiol* **508 (Pt 2)** 619-623.

Scott D, Coleman PJ, Mason RM & Levick JR 2000(a) Concentration dependence of interstitial flow buffering by hyaluronan in synovial joints. *Microvasc Res* **59** 345-353.

Scott D, Coleman PJ, Abiona A, Ashhurst DE, Mason RM & Levick JR 1998b Effect of depletion of glycosaminoglycans and non-collagenous proteins on interstitial hydraulic permeability in rabbit synovium. *J Physiol* **511 (Pt 2)** 629-643.

Scott JE 1998 Secodar and tertiary structures of Hyaluronan in aqueous solutions. Some Biological consequences, vol. 2002: Glycoforum.

Screaton GR, Bell MV, Jackson DG, Cornelis FB, Gerth U & Bell JI 1992 Genomic structure of DNA encoding the lymphocyte homing receptor CD44 reveals at least 12 alternatively spliced exons. *Proc Natl Acad Sci U S A* **89** 12160-12164.

Seppala PO 1969 Viscoelastic properties of synovial fluid. *Duodecim* **85** 1137-1143.

Shalgi R, Kraicer PF & Soferman N 1972a Human follicular fluid. *J Reprod Fertil* **31** 515-516.

Shalgi R, Kraicer PF & Soferman N 1972b Gases and electrolytes of human follicular fluid. *J Reprod Fertil* **28** 335-340.

Shalgi R, Kraicer P, Rimon A, Pinto M & Soferman N 1973 Proteins of human follicular fluid: the blood-follicle barrier. *Fertil Steril* **24** 429-434.

Shapiro SD 2000 A concise yet informative stroll through matrix metalloproteinases and TIMPs. *J Cell Sci* **113** 3355-3356.

Shibata S, Midura RJ & Hascall VC 1992 Structural analysis of the linkage region oligosaccharides and unsaturated disaccharides from chondroitin sulfate using CarboPac PA1. *J Biol Chem* **267** 6548-6555.

Shibata S, Kaneko S, Yanagishita M & Yamashita Y 1999 Histochemical localization of hyaluronan and versican in the rat molar dental pulp. *Arch Oral Biol* **44** 373-376.

Shibata S, Fukada K, Suzuki S, Ogawa T & Yamashita Y 2001 Histochemical localisation of versican, aggrecan and hyaluronan in the developing condylar cartilage of the fetal rat mandible. *J Anat* **198** 129-135.

Shimada H, Kasakura S, Shiotani M, Nakamura K, Ikeuchi M, Hoshino T, Komatsu T, Ihara Y, Sohma M, Maeda Y *et al.* 2001 Hypocoagulable state of human preovulatory ovarian follicular fluid: role of sulfated proteoglycan and tissue factor pathway inhibitor in the fluid. *Biol Reprod* **64** 1739-1745.

Short RV 1962 Steroids present in the follicular fluid of the cow. *J.Endocrinol.* **23** 401-411.

Smith JT & Ketteringham RT 1937 Rupture of the Graafian follicle. *J. Obstet. Gynaecol.* **36** 453-446-.

Smith MF, McIntush EW & Smith GW 1994 Mechanisms associated with corpus luteum development. *J Anim Sci* **72** 1857-1872.

Snashall PD 1977 Mucopolysaccharide osmotic pressure in the measurement of interstitial pressure. *Am J Physiol* **232** H608-616.

Sonal D 2001 Prevention of IGF-1 and TGFbeta stimulated type II collagen and decorin expression by bFGF and identification of IGF-1 mRNA transcripts in articular chondrocytes. *Matrix Biol* **20** 233-242.

Sorrell JM, Carrino DA, Baber MA & Caplan AI 1999 Versican in human fetal skin development. *Anat Embryol (Berl)* **199** 45-56.

Soto-Suazo M, San Martin S, Ferro ES & Zorn TM 2002 Differential expression of glycosaminoglycans and proteoglycans in the migratory pathway of the primordial germ cells of the mouse. *Histochem Cell Biol* **118** 69-78.

Spears N, Murray AA, Allison V, Boland NI & Gosden RG 1998 Role of gonadotrophins and ovarian steroids in the development of mouse follicles in vitro. *J Reprod Fertil* **113** 19-26.

Spicer AP & McDonald JA 1998 Characterization and molecular evolution of a vertebrate hyaluronan synthase gene family. *J Biol Chem* **273** 1923-1932.

Spicer AP & Nguyen TK 1999 Mammalian hyaluronan synthases: investigation of functional relationships in vivo. *Biochem Soc Trans* **27** 109-115.

Spicer AP, Augustine ML & McDonald JA 1996 Molecular cloning and characterization of a putative mouse hyaluronan synthase. *J Biol Chem* **271** 23400-23406.

Stagg K, Spicer LJ, Sreenan JM, Roche JF & Diskin MG 1998 Effect of calf isolation on follicular wave dynamics, gonadotropin and metabolic hormone changes, and interval to first ovulation in beef cows fed either of two energy levels postpartum. *Biol Reprod* **59** 777-783.

Stewart RE, Spicer LJ, Hamilton TD, Keefer BE, Dawson LJ, Morgan GL & Echternkamp SE 1996 Levels of insulin-like growth factor (IGF) binding proteins, luteinizing hormone and IGF-I receptors, and steroids in dominant follicles during the first follicular wave in cattle exhibiting regular estrous cycles. *Endocrinology* **137** 2842-2850.

Stock AE, Bouchard N, Brown K, Spicer AP, Underhill CB, Dore M & Sirois J 2002 Induction of hyaluronan synthase 2 by human chorionic gonadotropin in mural granulosa cells of equine preovulatory follicles. *Endocrinology* **143** 4375-4384.

Stock CE & Fraser LR 1989 Divalent cations, capacitation and the acrosome reaction in human spermatozoa. *J Reprod Fertil* **87** 463-478.

Stone D & Hechter O 1954 Studies on ACTH action in perfused bovine adrenals: failure of cholestenone to act as a corticosteroid precursor. *Arch Biochem Biophys* **51** 246-250.

Stouffer R, Martinez-Chequer J, Molskness T, Xu F & Hazzard T 2001 Regulation and action of angiogenic factors in the primate ovary. *Arch Med Res* **32** 567-575.

Stuhlmeier KM & Pollaschek C 2004 Differential effect of transforming growth factor beta (TGF-beta) on the genes encoding hyaluronan synthases and utilization of the p38 MAPK pathway in TGF-beta-induced hyaluronan synthase 1 activation. *J Biol Chem* **279** 8753-8760.

Suchanek E, Simunic V, Juretic D & Grizelj V 1994 Follicular fluid contents of hyaluronic acid, follicle-stimulating hormone and steroids relative to the success of in vitro fertilization of human oocytes. *Fertil Steril* **62** 347-352.

Sugiyama Y, Shimada A, Sayo T, Sakai S & Inoue S 1998 Putative hyaluronan synthase mRNA are expressed in mouse skin and TGF-beta upregulates their expression in cultured human skin cells. *J Invest Dermatol* **110** 116-121.

Sui HX, Han BG, Kee JK, Walian P & Jap BK 2001 Structural basis od water-specific transport through the a-q1 water channel. *Nature* **414** 872-878.

Sun GW, Kobayashi H & Terao T 1999 Expression of link protein during mouse follicular development. *J Histochem Cytochem* **47** 1433-1442.

Sun GW, Kobayashi H, Suzuki M, Kanayama N & Terao T 2002 Production of cartilage link protein by human granulosa-lutein cells. *J Endocrinol* **175** 505-515.

Swartz MA, Kaipainen A, Netti PA, Brekken C, Boucher Y, Grodzinsky AJ & Jain RK 1999 Mechanics of interstitial-lymphatic fluid transport: theoretical foundation and experimental validation. *J Biomech* **32** 1297-1307.

Tadano Y & Yamada K 1978 The histochemistry of complex carbohydrates in the ovarian follicles of adult mice. *Histochemistry* **57** 203-215.

Takagi J, Dobashi M, Araki Y, Imai Y, Hiroi M, Tonosaki A & Sendo F 1989 The development of porcine zona pellucida using monoclonal antibodies: II. Electron microscopy. *Biol Reprod* **40** 1103-1108.

Tammi R, Rilla K, Pienimaki JP, MacCallum DK, Hogg M, Luukkonen M, Hascall VC & Tammi M 2001 Hyaluronan enters keratinocytes by a novel endocytic route for catabolism. *J Biol Chem* **276** 35111-35122.

Tanimoto K, Suzuki A, Ohno S, Honda K, Tanaka N, Doi T, Yoneno K, Ohno-Nakahara M, Nakatani Y, Ueki M *et al.* 2004 Effects of TGF-beta on hyaluronan anabolism in fibroblasts derived from the synovial membrane of the rabbit temporomandibular joint. *J Dent Res* **83** 40-44.

Telfer E, Ansell JD, Taylor H & Gosden RG 1988 The number of clonal precursors of the follicular epithelium in the mouse ovary. *J Reprod Fertil* **84** 105-110.

Tempel C, Gilead A & Neeman M 2000 Hyaluronic acid as an anti-angiogenic shield in the preovulatory rat follicle. *Biol Reprod* **63** 134-140.

Terranova PF & Rice VM 1997 Review: cytokine involvement in ovarian processes. *Am J Reprod Immunol* **37** 50-63.

Thomas FH, Ethier JF, Shimasaki S & Vanderhyden BC 2005 Follicle-stimulating hormone regulates oocyte growth by modulation of expression of oocyte and granulosa cell factors. *Endocrinology* **146** 941-949.

Tienthai P, Kimura N, Heldin P, Sato E & Rodriguez-Martinez H 2003 Expression of hyaluronan synthase-3 in porcine oviducal epithelium during oestrus. *Reprod Fertil Dev* **15** 99-105.

Tombs M & Peacocke A 1974 *The osmotic pressure of biological macromolecules*, p.^pp Pages, edn 1. Ed.^Eds Ou press. Clarendon press Oxford.

Toole BP 1990 Hyaluronan and its binding proteins, the hyaladherins. *Current Opinions in Cell Biology* **2** 839-844.

Toole BP 2000 Hyaluronan in morphogenesis and tissue remodelling, vol. 2000: Glycoforum.

Toole BP 2001 Hyaluronan in morphogenesis. *Semin Cell Dev Biol* **12** 79-87.

Topper EK, Kruijt L, Calvete J, Mann K, Topfer-Petersen E & Woelders H 1997 Identification of bovine zona pellucida glycoproteins. *Mol Reprod Dev* **46** 344-350.

Torney AH, Hodgson YM, Forage R & de Kretser DM 1989 Cellular localization of inhibin mRNA in the bovine ovary by in-situ hybridization. *J Reprod Fertil* **86** 391-399.

Towbin H, Staehelin T & Gordon J 1979 Electrophoretic transfer of proteins from polyacrylamide gels to nitrocellulose sheets: procedure and some applications. *Proc Natl Acad Sci U S A* **76** 4350-4354.

Tsafriri A 1995 Ovulation as a tissue remodelling process. Proteolysis and cumulus expansion. *Adv Exp Med Biol* **377** 121-140.

Tsafriri A & Reich R 1999 Molecular aspects of mammalian ovulation. *Exp Clin Endocrinol Diabetes* **107** 1-11.

Tsafriri A, Popliker M, Nahum R & Beyth Y 1998 Effects of ketoconazole on ovulatory changes in the rat: implications on the role of a meiosis-activating sterol. *Mol Hum Reprod* **4** 483-489.

Tsuiki A, Preyer J & Hung TT 1988 Fibronectin and glycosaminoglycans in human preovulatory follicular fluid and their correlation to follicular maturation. *Hum Reprod* **3** 425-429.

Tufvesson E & Westergren-Thorsson G 2000 Alteration of proteoglycan synthesis in human lung fibroblasts induced by interleukin-1beta and tumor necrosis factor-alpha. *J Cell Biochem* **77** 298-309.

Turley EA 1984 Proteoglycans and cell adhesion. Their putative role during tumorigenesis. *Cancer Metastasis Rev* **3** 325-339.

Turner RE, Lin PY & Cowman MK 1988 Self-association of hyaluronate segments in aqueous NaCl solution. *Arch Biochem Biophys* **265** 484-495.

Turzillo AM & Fortune JE 1993 Effects of suppressing plasma FSH on ovarian follicular dominance in cattle. *J Reprod Fertil* **98** 113-119.

Ujita M, Shinomura T, Ito K, Kitagawa Y & Kimata K 1994 Expression and binding activity of the carboxyl-terminal portion of the core protein of PG-M, a large chondroitin sulfate proteoglycan. *J Biol Chem* **269** 27603-27609.

Ulbrich SE, Schoenfelder M, Thoene S & Einspanier R 2004 Hyaluronan in the bovine oviduct--modulation of synthases and receptors during the estrous cycle. *Mol Cell Endocrinol* **214** 9-18.

Underhill CB, Nguyen HA, Shizari M & Culty M 1993 CD44 positive macrophages take up hyaluronan during lung development. *Dev Biol* **155** 324-336.

Urban JP & Maroudas A 1981 Swelling of the intervertebral disc in vitro. *Connect Tissue Res* **9** 1-10.

Usui T, Suzuki K, Kaji Y, Amano S, Miyata K, Heldin P & Yamashita H 1999 Hyaluronan synthase expression in bovine eyes. *Invest Ophthalmol Vis Sci* **40** 563-567.

Usui T, Amano S, Oshika T, Suzuki K, Miyata K, Araie M, Heldin P & Yamashita H 2000 Expression regulation of hyaluronan synthase in corneal endothelial cells. *Invest Ophthalmol Vis Sci* **41** 3261-3267.

Usui T, Nakajima F, Ideta R, Kaji Y, Suzuki Y, Araie M, Miyauchi S, Heldin P & Yamashita H 2003 Hyaluronan synthase in trabecular meshwork cells. *Br J Ophthalmol* **87** 357-360.

Valve E, Penttila TL, Paranko J & Harkonen P 1997 FGF-8 is expressed during specific phases of rodent oocyte and spermatogonium development. *Biochem Biophys Res Commun* **232** 173-177.

van Wezel IL & Rodgers RJ 1996 Morphological characterization of bovine primordial follicles and their environment in vivo. *Biol Reprod* **55** 1003-1011.

Van Wezel IL, Dharmarajan AM, Lavranos TC & Rodgers RJ 1999 Evidence for alternative pathways of granulosa cell death in healthy and slightly atretic bovine antral follicles. *Endocrinology* **140** 2602-2612.

Vanderboom RJ, Carroll DJ, Bellin ME, Schneider DK, Miller DJ, Grummer RR & Ax RL 1989 Binding of bovine follicular fluid glycosaminoglycans to fibronectin, laminin and low-density lipoproteins. *J Reprod Fertil* **87** 81-87.

Vanderhyden BC & Macdonald EA 1998 Mouse oocytes regulate granulosa cell steroidogenesis throughout follicular development. *Biol Reprod* **59** 1296-1301.

Vanderhyden BC, Telfer EE & Eppig JJ 1992 Mouse oocytes promote proliferation of granulosa cells from preantral and antral follicles in vitro. *Biol Reprod* **46** 1196-1204.

Vanderhyden BC, Macdonald EA, Merchant-Larios H, Fernandez A, Amleh A, Nasseri R & Taketo T 1997 Interactions between the oocyte and cumulus cells in the ovary of the B6.Y(TIR) sex-reversed female mouse. *Biol Reprod* **57** 641-646.

Van't-Hoff HH 1887 The role of osmotic pressure in the analogy between solutions and gasses. *Zeitschrift fur physikalische Chemie.* **1** 481-508.

Varner DD, Forrest DW, Fuentes F, Taylor TS, Hooper RN, Brinsko SP & Blanchard TL 1991 Measurements of glycosaminoglycans in follicular, oviductal and uterine fluids of mares. *J Reprod Fertil Suppl* **44** 297-306.

Waddington RJ, Embery G & Samuels RH 1994 Characterization of proteoglycan metabolites in human gingival crevicular fluid during orthodontic tooth movement. *Arch Oral Biol* **39** 361-368.

Wagenen V & M.E S 1965 *Embryology of the ovary and testis in Homo sapiens and Macaca mulatta*, p.^pp Pages, edn. Ed.^Eds: Yale University Press.

Wandji SA, Srsen V, Voss AK, Eppig JJ & Fortune JE 1996 Initiation in vitro of growth of bovine primordial follicles. *Biol Reprod* **55** 942-948.

Wang C, Tammi M, Guo H & Tammi R 1996 Hyaluronan distribution in the normal epithelium of esophagus, stomach, and colon and their cancers. *Am J Pathol* **148** 1861-1869.

Wassarman PM & Alberton GM 1994 The Mammalian ovum. In *The Physiology of Reproduction*, pp 79-122, edn. Ed.^Eds E Knobil & J Neill.

Watanabe H, Cheung SC, Itano N, Kimata K & Yamada Y 1997 Identification of hyaluronan-binding domains of aggrecan. *J Biol Chem* **272** 28057-28065.

Weissman B & Meyer K 1954 The structure of hyalobiuronic acid and of hyaluronic acid from umbilical cord. *J. Am. Chem. Soc* **76** 1753-1757.

Welling LW & Welling DJ 1988 Theoretical models of cyst formation and growth. *Scanning Microsc* **2** 1097-1102.

Wen DZ, Dittman WA, Ye RD, Deaven LL, Majerus PW & Sadler JE 1987 Human thrombomodulin: complete cDNA sequence and chromosome localization of the gene. *Biochemistry* **26** 4350-4357.

West DC, Hampson IN, Arnold F & Kumar S 1985 Angiogenesis induced by degradation products of hyaluronic acid. *Science* **228** 1324-1326.

Wiederhielm CA & Black LL 1976 Osmotic interaction of plasma proteins with interstitial macromolecules. *Am J Physiol* **231** 638-641.

Wiltbank MC, Diskin MG, Flores JA & Niswender GD 1990 Regulation of the corpus luteum by protein kinase C. II. Inhibition of lipoprotein-stimulated steroidogenesis by prostaglandin F2 alpha. *Biol Reprod* **42** 239-245.

Wise T & Maurer RR 1994 Follicular development, oocyte viability and recovery in relation to follicular steroids, prolactin and glycosaminoglycans throughout the estrous period in superovulated heifers with a normal LH surge, no detectable LH surge, and progestin inhibition of LH surge. *Domest Anim Endocrinol* **11** 35-58.

Wisniewski HG, Naime D, Hua JC, Vilcek J & Cronstein BN 1996 TSG-6, a glycoprotein associated with arthritis, and its ligand hyaluronan exert opposite effects in a murine model of inflammation. *Pflugers Arch* **431** R225-226.

Wittmaack FM, Kreger DO, Blasco L, Tureck RW, Mastroianni L, Jr. & Lessey BA 1994 Effect of follicular size on oocyte retrieval, fertilization, cleavage, and embryo quality in in vitro fertilization cycles: a 6-year data collection. *Fertil Steril* **62** 1205-1210.

Xu Z, Garverick HA, Smith GW, Smith MF, Hamilton SA & Youngquist RS 1995 Expression of messenger ribonucleic acid encoding cytochrome P450 side-chain cleavage, cytochrome p450 17 alpha-hydroxylase, and cytochrome P450 aromatase in bovine follicles during the first follicular wave. *Endocrinology* **136** 981-989.

Yabushita H, Noguchi M, Kishida T, Fusano K, Noguchi Y, Itano N & Kimata K 2004 Hyaluronan synthase expression in ovarian cancer. *Oncol Rep* **12** 739-743.

Yamaguchi Y & Ruoslahti E 1988 Expression of human proteoglycan in Chinese hamster ovary cells inhibits cell proliferation. *Nature* **336** 244-246.

Yanagimachi R 1984 Fertilization in mammals. *Tokai J Exp Clin Med* **9** 81-85.

Yanagishita M 1994 Proteoglycans and hyaluronan in female reproductive organs. *Exs* **70** 179-190.

Yanagishita M & Hascall VC 1979 Biosynthesis of proteoglycans by rat granulosa cells cultured in vitro. *J Biol Chem* **254** 12355-12364.

Yanagishita M & Hascall VC 1983a Characterization of heparan sulfate proteoglycans synthesized by rat ovarian granulosa cells in culture. *J Biol Chem* **258** 12857-12864.

Yanagishita M & Hascall VC 1983b Characterization of low buoyant density dermatan sulfate proteoglycans synthesized by rat ovarian granulosa cells in culture. *J Biol Chem* **258** 12847-12856.

Yanagishita M & Hascall VC 1984a Metabolism of proteoglycans in rat ovarian granulosa cell culture. Multiple intracellular degradative pathways and the effect of chloroquine. *J Biol Chem* **259** 10270-10283.

Yanagishita M & Hascall VC 1984b Proteoglycans synthesized by rat ovarian granulosa cells in culture. Isolation, fractionation, and characterization of proteoglycans associated with the cell layer. *J Biol Chem* **259** 10260-10269.

Yanagishita M, Rodbard D & Hascall VC 1979 Isolation and characterization of proteoglycans from porcine ovarian follicular fluid. *J Biol Chem* **254** 911-920.

Yanagishita M, Hascall VC & Rodbard D 1981 Biosynthesis of proteoglycans by rat granuloma cells cultured in vitro: modulation by gonadotropins, steroid hormones, prostaglandins, and a cyclic nucleotide. *Endocrinology* **109** 1641-1649.

Ying SY 1987 Inhibins and activins: chemical properties and biological activity. *Proc Soc Exp Biol Med* **186** 253-264.

Yong VW, Krekoski CA, Forsyth PA, Bell R & Edwards DR 1998 Matrix metalloproteinases and diseases of the CNS. *Trends Neurosci* **21** 75-80.

Yoshida H, Takakura N, Kataoka H, Kunisada T, Okamura H & Nishikawa SI 1997 Stepwise requirement of c-kit tyrosine kinase in mouse ovarian follicle development. *Dev Biol* **184** 122-137.

Yoshida M, Sai S, Marumo K, Tanaka T, Itano N, Kimata K & Fujii K 2004 Expression analysis of three isoforms of hyaluronan synthase and hyaluronidase in the synovium of knees in osteoarthritis and rheumatoid arthritis by quantitative real-time reverse transcriptase polymerase chain reaction. *Arthritis Res Ther* **6** R514-520.

Yoshimatsu N, Yanagimachi R & Lopata A 1988 Zonae pellucidae of salt-stored hamster and human eggs: their penetrability by homologous and heterologous spermatozoa. *Gamete Res* **21** 115-126.

Yoshioka S, Ochsner S, Russell DL, Ujioka T, Fujii S, Richards JS & Espey LL 2000 Expression of tumor necrosis factor-stimulated gene-6 in the rat ovary in response to an ovulatory dose of gonadotropin. *Endocrinology* **141** 4114-4119.

Yuan Y, Wang Z & Dong B 2003 Modulation of matrix metalloproteinase by dexamethasone in airway remodeling in asthmatic rats. *Sichuan Da Xue Xue Bao Yi Xue Ban* **34** 680-683.

Zachariae F 1958 Studies on the mechanism of ovulation. Permeability of the blood -liquor barrier. *Acta Endocrinol* **27** 339-342.

Zachariae F 1960 Acid mucopolysaccharides in the femaile genital system and their role in the mechanism of ovulation. *Acta.Endocrinol.* **33** 13-64.

Zachariae F & Jensen CE 1958 Studies on the mechanism of ovulation. Histochemical and physio-chemical investigations on genuine follicular fluids. *Acta Endocrinol* **27** 343-355.

Zamparo O & Comper WD 1989 Hydraulic conductivity of chondroitin sulfate proteoglycan solutions. *Arch Biochem Biophys* **274** 259-269.

Zhao M, Yoneda M, Ohashi Y, Kurono S, Iwata H, Ohnuki Y & Kimata K 1995 Evidence for the covalent binding of SHAP, heavy chains of inter-alpha-trypsin inhibitor, to hyaluronan. *J Biol Chem* **270** 26657-26663.

Zhao Y & Luck MR 1995 Gene expression and protein distribution of collagen, fibronectin and laminin in bovine follicles and corpora lutea. *J Reprod Fertil* **104** 115-123.

Zhuo L & Kimata K 2001 Cumulus oophorus extracellular matrix: its construction and regulation. *Cell Struct Funct* **26** 189-196.

Zhuo L, Yoneda M, Zhao M, Yingsung W, Yoshida N, Kitagawa Y, Kawamura K, Suzuki T & Kimata K 2001 Defect in SHAP-hyaluronan complex causes severe female infertility. A study by inactivation of the bikunin gene in mice. *J Biol Chem* **276** 7693-7696.

Zimmermann DR, Dours-Zimmermann MT, Schubert M & Bruckner-Tuderman L 1994 Versican is expressed in the proliferating zone in the epidermis and in association with the elastic network of the dermis. *J Cell Biol* **124** 817-825.

8. Appendix A

8.1. Chemical and Supplier details

Products	Supplier	Catalog No.
10mM dNTPs	Invitrogen	280-00
Aff-Gel Blue Gel	Biorad	153-7301
Amersham hyperfilm	Amersham	RPN 3103K
Amplitaq gold	Applied biosystems	4311806
Anti DIG antibody	Roche	1093274
APES	Sigma	A3648
Biotin-16-dUTP	Roche	1093070
CDP-star	Roche	1685627
DIG RNA labelling kit	Roche	1277073
DIG wash buffer kit	Roche	1585762
DNA free	Geneworks	AM-1906
Gel code blue stain reagent	Pierce chemicals	24950
HEPES	Sigma	H3662
Oligonucleotides	Sigma	
Polyacrylamide gels	Gradipore	NG21-010
PCR clean-up kit	Mo Bio laboratories	125-250
pGem-T Easy vector system1	Promega	1360
Plasmid midi-kit	Qiagen	12243
Precision stained protein markers	Biorad	161-0318
Primers	Sigma	
Protein assay reagent	Biorad	500-0006
Puc19/HpaII DNA markers	Geneworks/Ambion	DMW-P1
Random hexamers	Geneworks/Ambion	RP-6
RNA Bee	Geneworks/Ambion	BL-104
RNA later	Geneworks/Ambion	AM-7020
RNA milennium markers	Geneworks/Ambion	7785
RNAsin (RNAse inhibitor)	Promega	N2511
Siver stain kit	Biorad	161-0449
SP6 RNA polymerase	Roche	810274
Superscript reverse transcriptase	Invitrogen	18064-041
T7 RNA polymerase	Roche	881767

Taq polymerase	Invitrogen	10342-020
Transfection kit	Qiagen	
Trizol®-LS reagent	GibcoBRL	10296-010
X-gal	Roche	651745
SDS gels	Gradipore	NG21-010,NG21-0420
Slowfade	Molecular Probes	
Uronic acid standards	Sigma	
Hybond N (PVDF)	Amersham	RPN 203N
Hybond C+	Amersham	RPN 303E
Scintillation fluid Wallac optiphase Hisafe3	Perkin – Elmer Life Sciences	
Paraplast	Brunswick Co	

8.2. Supplier Details

Supplier	**Address**
Ambion/Geneworks	Adelaide, Australia,
Amersham Pharmacia Biotech	Piscataway, NJ, USA.
Amrad Pharmacia Biotech	Melbourne, Vic, Australia
Analar	Merck Pty Ltd, Kilsyth, Vic, Australia
BDH/AnalaR/Merck	Merck Pty Ltd, Kilsyth, Vic, Australia
BIO-RAD laboratories,	Hercules, CA,
Boehringer Mannheim	Mannheim, Germany,
Brunswick Co	St Louis, MO
Crown Scientific	SA, Australia
Developmental Studies Hybridoma Bank	The University of Iowa, Iowa City, IA, USA
Difco	Detroit, Michigan, USA
Dr. Larry Fisher,	Bone Research Branch, NIH, Bethesda, MD
Geneworks/Ambion	Adelaide, Australia,
Gonotec	GmbH, Berlin, Germany.
Gradipore	Frenchs Forest, NSW, Australia
ICN Biomedicals,	Seven Hills, NSW, Australia.
Interpath	W. Hiedelberg, Vic, Australia
Invitrogen Life Technologies	Mt Waverley, Vic, Australia

Millipore Corporation,	Bedford, USA.
Mo Bio laboratories Inc.	Solana Beach, CA 92075
Molecular Probes	Eugene Oregon, USA
Pierce chemicals	Rockford, MA, USA
Progen	Darra, QLD, Australia
Promega	Annadale, NSW, Australia
Qiagen	Clifton Hill, Vic, Australia
Perkin – Elmer Life Sciences	Walac OY Turku Finland
Roche	GmbH, Mannheim, Germany.
Siekagaku America,	MA, USA.
Sigma chemical Company	St Louis, MO.
Silenus Laboratories	Victoria, Australia
Spencer American Optical Co.	Buffalo, Colorado, USA
Unilab	Ajax Chemicals Pty Ltd, Auburn, NSW
Univar	Ajax Chemicals Pty Ltd, Sydney, NSW

8.3. Enzyme Details

Enzyme	**Supplier**	**Catalog No.**
Streptomyces hyaluronidase	Seikagaku	100740
Chondroitinase ABC	Seikagaku	100332
Keratanase	Seikagaku	100810
Proteinase K	Sigma	P2308
Collagenase 1	Sigma	M1802
DNase 1	Sigma	AMP-D1
Heparinase	Sigma	51534

8.4. Kits

Kit	**Supplier**	**Catalog No.**
BCA protein assay	Pierce,	
Superscript reverse transcriptase	Invitrogen	18064-041

8.5. Film

	Supplier	Catalog No.
Hyperfilm ECL	Amersham	

9. Appendix B: Recipes

9.1. Tissue Collection and Processing

9.1.1. Tissue Collection

9.1.1.1. Earles Balanced Salt Solution (EBSS)

pH7.4 Sigma # E6132

EBSS	8.7g
Sodium hydrogen carbonate	2.2g
Sodium azide	1:1000

Make up to 1L with distilled water

9.1.2. Processing

9.1.2.1. Buffered Formalin

Formaldehyde	100 ml
Disodium hydrogen phosphate (anhydrous)	6.5 g
Sodium dihydrogen phosphate (hydrated)	4.0 g
Distilled H_2O	900 ml

9.1.2.2. Bouin's Fixative

Saturated picric acid	300 ml
Formaldehyde	100 ml
Glacial acetic acid	20 ml

Mix ingredients together overnight

9.2. Proteoglycan and Glycosaminoglycan analysis

9.2.1. Proteoglycan Extraction Buffer

4M Guanidine -HCl

50mM sodium acetate

10mM disodium EDTA

0.1M aminocaproic acid

pH 6.0

9.2.2. CL-2B-300 Size Exclusion Column Buffer

Sigma cross linked 2% beads fraction range globular proteins 70,000-40,000,000 wet bead diameter 60-200 μm

2M Guanidine	191.06g
0.1M Sodium acetate	8.2g
0.05M Tris	6.05g

pH 7.5 make up to 1 litre

9.2.3. DEAE Column Buffers

9.2.3.1. DEAE Column Buffer pH 5

4M Urea
0.05M sodium acetate
Make up to 1L with distilled water

9.2.3.2. DEAE Column Elution Buffer

4M Urea
0.05M sodium acetate
2M sodium chloride
Make up to 1L with distilled water

9.2.4. Dyes and Stains

9.2.4.1. Stains-All®

0.0125g in 250ml of 50% Methanol

9.2.4.2. Coomassie Stain

Coomassie blue r250	1g (0.1%)
Methanol	400ml (40%)
Acetic acid	100ml (10%)

Make up to 1L with distilled water
Stir ingredients together until dissolved and filter through a Whatman No 1 filter paper.

9.2.4.3. Tracking Dye (Agarose gels)

2M Sucrose
0.02% bromophenol blue

Dissolve in 10 ml 1 X TAE

9.2.5. Enzymes

9.2.5.1. Chondroitinase ABC

0.01M Tris acetate pH 7.5-8.0

0.1U Chondroitinase ABC/100 μg uronic acid in sample

9.2.5.2. Streptomyces Hyaluronidase

0.1M Sodium acetate pH5.0

0.1U streptomycin hyaluronidase/100µg hyaluronic acid

9.2.5.3. Streptomyces Hyaluronidase Buffer

0.1M sodium phosphate

0.15M sodium chloride pH5.3

9.3. ELISA

9.3.1. ELISA solutions

9.3.1.1. ABTS Substrate

Acetate buffer

0.1M sodium acetate

0.05M Sodium dihydrogen orthophosphate

pH 4.0

9.3.1.2. Citrate Buffer

5.25mg sodium citrate

50 ml distilled water

Use 10ml of citrate buffer

200 μl 2,2'–azino-di- (3-ethylbenzthioazoline-6-sulphonic acid) (ABTS)

20 μl hydrogen peroxide

9.3.1.3. ABTS

ABTS 0.219g

Make up to 10 ml with distilled water

Final substrate:

Acetate buffer	2 ml
Hydrogen peroxide	20 μl
ABTS	100 μl

9.3.1.4. 10 X ELISA Wash Buffer

Disodium hydrogen phosphate	10.7g
Sodium dihydrogen phosphate	3.9g
Sodium chloride	85g
Tween 20	500 μl

Make up to 1L with distilled water

NB: ELISA Sample Diluting Buffer 1 X Elisa wash buffer containing 1% non-fat milk powder

9.3.1.5. ELISA Coating Buffer

14mM Disodium carbonate	1.5g
35mM Sodium hydrogen carbonate-	2.9g

Make up to 1L with distilled water

9.3.1.6. Carbonate Buffer pH 9.8 (1L)

0.1M Sodium hydrogen carbonate

0.001M Magnesium chloride

Make up to 1L with distilled water

9.4. Agarose Gels, PAGE and Western Blotting

9.4.1. Gels

9.4.1.1. Agarose

Diluted in TAE or TBE (see 9.4.3.3 or 9.8.1.4)

9.4.2. Tris/Glycine SDS-PAGE

9.4.2.1. Separating Gel (10% gel/10ml)

Water	4.0 ml
30% Acrylamide mix	3.30 ml
1.5M Tris pH 8.8	2.50 ml

10% Sodium dodecyl sulphate	0.10 ml
10% Ammonium persulphate	0.10 ml
N',N',N',N, tetramethylethylenediamine (TEMED) Sigma #9128	0.0040 ml

9.4.2.2. Stacking Gel (2 ml)

Water	1.4 ml
30% Acrylamide mix	0.33 ml
1.5M Tris pH 8.8	0.25 ml
10% Sodium dodecyl sulphate	0.02 ml
10% A mmonium persulphate	0.02 ml
N',N',N',N, tetramethylethylenediamine (TEMED)	0.002 ml

9.4.3. Buffers

9.4.3.1. SDS glycine Running Buffer (10X)

125mM Trisma Base	29g
0.96M Glycine	144g
0.25% SDS	10g
Distilled water	1.0l

9.4.3.2. Tris/Glycine Running Buffer for PAGE (10 X)

Tris-HCl	29g
Glycine	144g
SDS	10g

Make up to 1L with distilled water

9.4.3.3. TAE Buffer (50X)

Tris base	242g
Glacial acetic acid	57.1 ml
0.05M EDTA	100 ml

Make up to 1L with distilled water

9.4.3.4. Western Transfer Buffer

Tris ultra pure	6.06g
Glycine	28.8g

Methanol	200 ml

Make up to 1L with distilled water

9.4.3.5. 10 X Tris Buffered Saline (TBS) pH 8.0

0.1M Tris-HCl	12.11g
1.5M Sodium chloride	87.66g

Make up to 1L with distilled water

NB for blocking buffer add 5% skim milk, for washing add 0.1% Tween 20 (TBST)

9.4.3.6. Phosphate Buffered Saline (PBS) 1X

NaCl	16g
Na_2HPO_4	1.15g
KCl	0.2g
KH_2PO_4	0.2g
H_2O	to 1L

NB: for washing membranes or plates 0.1% Tween 20 (PBST)

9.5. 2X CHAPS extraction buffer

10mM benzamidine

1mM Phenyl methyl sulphonyl fluoride (PMSF)

10mM CHAPS

Make up to 10 ml with 40mM Tris 6.8

9.6. 2% SDS extraction buffer

10mM benzamidine

1mM Phenyl methyl sulphonyl fluoride (PMSF)

2% Sodium dodecyl sulphate

Make up to 10 ml with 40mM Tris 6.8

9.7. Gel Drying Solution (PAGE and Agarose)

Water	47%
Glycerol	3%
Methanol	40%
Acetic acid	10%

9.8. Molecular Analyses

9.8.1. Buffers

9.8.1.1. RNAse Buffer

0.5M NaCl	58.44g/200ml of 5M
10mM tris-HCl pH 7.5	20ml 1M
1mM EDTA pH 8.0	4ml 0.5M
DEPC H_2O	to 2L (autoclave)

9.8.1.2. Buffer1

100mM tris-HCl pH 7.5	100ml 1M
150mM NaCl	30ml 5M
DEPC H_2O	to 1L

9.8.1.3. Buffer2

100mM tris-HCl pH 9.5	50ml 1M
100mM NaCl	10ml 5M
50mM $MgCl_2$	25ml 1M
DEPC H_2O	to500ml

9.8.1.4. 5 X TBE

Tris	55g
Boric acid	27.5g
50mM EDTA pH8.0	20ml

Make up to 1L with distilled water

Use at ½ X concentration

9.8.1.5. 1 X Tris/EDTA (10mM: 1mM) (TE) Buffer

1M Tris-HCl pH 8.0	20ml
0.5M EDTA pH 8.0	4ml

Make up to 2L with distilled water

9.8.2. L-Broth

Bacto-tryptone	10g
Yeast extract	5g

Sodium chloride	10g

Make up to 1L with distilled water

9.8.3. L-Broth Agar

Bacto-tryptone	10g
Yeast extract	5g
Sodium chloride	10g
Agar	15g

Make up to 1L with distilled water

Add 1:1000 of 100ug/ml ampicillin to 100ng/ml

9.8.4. RNA Gels and Northern Blot

9.8.4.1. 10 X MOPS ((3-[N-Morpholino] propanesulphonic acid)

MOPS	41.86
Sodium acetate (anhydrous)	4.1
EDTA pH 8.0 DEPC treated	20 ml

Dissolve in 800ml DEPC water, adjust to pH 7.0 with sodium hydroxide, Add 1.0 ml DEPC.

Make up to 1 litre. Autoclave

9.8.4.2. Non-Reducing Loading Buffer (for PAGE)

0.5M tris pH 6.8	1.0 ml
Glycerol	0.8 ml
10% sodium dodecyl sulphate (SDS)	1.6 ml
Mix well in 10 ml tube and add 0.1% bromophenol blue (in ethanol)	0.2 ml
Distilled water	4.4 ml

9.8.4.3. Pre-hybridisation Solution (Northern blot)

6 X SSC	15 ml
0.5%SDS	2.5 ml
5 X Denhardts	5 ml
Water	27.5 ml

9.8.4.4. Nitro-blue tetrazolium (NBT)

Dissolve 50mg NBT in 1.0 ml 70% dimethyl fluoride

9.8.4.5. RNA Loading Dye (prepare with DEPC water)

Glycerol	50%
EDTA	1mM
Bromophenol blue	0.25%
Xylene cyanol FF	0.25%

9.8.4.6. RNA Agarose Denaturing Gel

Agarose	2.0g
DEPC water	144 ml
10 X MOPS	20 ml
Formaldehyde	36 ml

9.8.4.7. RNA Cocktail

10X MOPS	50µl
Formaldehyde	87.5µl
Deionised formamide	250µl
Ethidium bromide	50µl
DEPC water	62.5µl

9.8.5. Reverse Transcription Buffer

1M Tris-HCl	25 µl
1M potassium chloride	37.5 µl
0.25M magnesium chloride	6 µl
1M (dithiothreitol) DTT	26.5 µl

Make up to 100µl with distilled water

9.8.6. 20 X SSPE

Sodium chloride	173.5g
Disodium hydrogen orthophosphate	26.7g
EDTA	7.4g

Dissolve in 800 ml adjust pH 7.4 with 10M sodium hydroxide add 1.0 ml DEPC make up to 1 litre and autoclave

9.9. In situ Hybridisation

9.9.1. In Situ Buffers and Solutions

9.9.1.1. 10X Salts

3M NaCl	175.32g
100mM tris-HCl pH 7.5	100ml 1M
50mM EDTA pH 8.0	100ml 0.5M
0.2% Ficoll400	20ml 10%
0.2% polyvinyl pyrolidone	100ml 2%
0.2% BSA	100ml 2%

BSA cannot be autoclaved, therefore following DEPC treatment add the BSA just before the solution is required, make up to 0.2% solution. Make 2% BSA stock in DEPC H_2O and freeze aliquots.

DEPC H_2O is 0.05% diethyl pyrocarbonate (Sigma) (1ml in to 2L) @ 37°C for 2 hrs then autoclave.

9.9.1.2. 4% Formaldehyde

Parafomaldehyde powder	20g/ 500 ml
DEPC treated water	200 ml/ 500 ml
Sodium hydroxide	15 drops/ 500 ml
Phosphate buffer (*)	250 ml/ 500 ml

*Heat to 60C to dissolve paraformaldehyde cool and add phosphate buffer

02M phosphate buffer =

NaH_2PO_4	1.79g
Na_2HPO_4	5.48g

9.9.1.3. Proteinase K

10mg/ml stock diluted in distilled water

9.9.1.4. 100 X Denhardts

2% ficoll (type 400)

2% polyvinylpyrrolidine (sigma PVP-40)

2%bovine serum albumin

Make up to 100ml with distilled water

Filter through a Whatman no 54 paper and store at 20C

9.9.1.5. Proteinase K Buffer

50mM tris-HCl pH 7.5	12.5ml 1M
5mM EDTA pH 8.0	6.25ml 0.2M
DEPC H_2O	231.25ml

9.9.1.6. Formamide Wash Buffer

100ml 10X salts

400ml DEPC H_2O

500ml formamide (not deionized)

500µl triton-X 100

9.9.1.7. 0.5M EDTA pH8.0

EDTA	93.05g
Ultrapure water	200 ml
Adjust pH 8.0	
DEPC	0.5ml

Make up to 500ml with distilled water and autoclave

9.9.1.8. Hydrolysis Neutralisation Buffer

200mM Sodium acetate

1% w/v Acetic acid

pH 6.0

9.9.1.9. Alkaline Phosphatase Buffer

0.1M Tris –HCl

1M NaCl

pH 9.5

9.9.1.10. BCIP Stock Solution

5-bromo-4-chloro-3-indolyl phosphate p-toluidine salt (BCIP)	15 mg
Dimethy fluoride	1ml

Colour development uses 1μl BCIP stock + 1 μl NBT in carbonate buffer (see appendix 1.9)

9.9.1.11. 20 X SSC pH 7.0

3M Sodium chloride	175.3g
0.3M Sodium citrate	88.2g

Adjust pH with concentrated HCl

Make up to 1L with distilled water

9.9.1.12. Maleic Acid Wash Buffer

100mM maleic acid

150mM sodium chloride

pH 7.5

9.9.1.13. 1M Tris HCl

Tris

Buffer to pH 8.0 with HCl

9.9.1.14. 20 X SCC

3M NaCl	600ml 5M
300mM Na_3citrate	300ml 1M
DEPC H_2O	100ml

pH 7.0

Dilute 1:10 to obtain 2X